AIM & SCOPE

"Technical journal is a multidisciplinary journal in the field of engineering science and technology that offers platform for researchers, engineers and scientists to publish their original and to date research of high scientific value. It is a double blind peer-reviewed open access academic journal, published quarterly by University of Engineering & Technology, Taxila, Pakistan. Articles published in the Journal illustrate innovations, developments and achievements in the field of engineering and technology. The journal is being published electronically as well as in print form."

Technical Journal

A Quarterly Journal of University of Engineering & Technology (UET) Taxila, Pakistan
Recognized by Higher Education Commission (HEC)
Y Category

ISSN: 1813-1786 (Print) ISSN: 2313-7770 (Online)
Volume No. 21 (Quarterly)
No. IV (Oct - Dec)
2016

Phone: 92 - 51 - 9047896 **Fax: 92 - 51 - 9047420** **E-Mail: technical.journal@uettaxila.edu.pk**

EDITORIAL OFFICE:
Editor Technical Journal
Central Library, University of Engineering and Technology (UET) Taxila, Pakistan

EDITORIAL BOARD

CONTENTS

Section A

CIVIL, ENVIRONMENTAL, ARCHITECTURE, TRANSPORTATION ENGINEERING CITY AND REGIONAL PLANNING

Hydrologic Modeling of Khanpur Dam Watershed Using Snowmelt Runoff Model

A. Khan[1], H. N. Hashmi[2], U. A. Naeem[3], M. Q. Fareed[4]

[1,2,3]Department of Civil Engineering, University of Engineering & Technology, Taxila
[4]NESPAK, Lahore
[3]usman.naeem@uettaxila.edu.pk

Abstract-The flow contribution to Haro River is from the three main sources i.e. rainfall, snowfall and groundwater. Certain models like HBV (HydrologiskaByråns Vattenbalansavdelning) model, UBC (University of British Columbia) watershed model and SRM (Snowmelt Runoff Model) are available for the watershed modeling accounting the process of snowmelt. This particular studies utilizes SRM. Khanpur watershed was selected as study area and the watershed was calibrated for the hydrologic year 2005. The daily river discharge and daily precipitation data were used in calibration of the study area. The area was divided into five elevation zones. Moderate Resolution Imaging Spectroradiometer MODIS remote sensing product was used to predict snow cover area of Khanpur dam watershed. The calibration results show high efficiency value of 88% but the validation results were not very encouraging. The poor efficiency of validation results were highly believed to be as result of low snow cover in the watershed. From the results it was concluded that SRM cannot work well for low snow covered watersheds.

Keywords-Snowmelt Runoff Model, MODIS, Model Calibration, Snow Cover

I. Introduction

Snowmelt is main source of water for many rivers in Northwest Pakistan. The rivers of Northern Pakistan play an important role in socio financial development of the country. Normally the flood damages are always severe in this part of the world. Therefore, proper water resource management system is required to check and mitigate the floods. A very vital approach in order to estimate the floods is through watershed modeling. The use of appropriate model is very important for estimation of flood discharge over a watershed. It is desired that the model used must understand the meteorological and climatological aspects of the watershed. Most of the computer watershed models are fairly capable of doing that. Snowmelt Runoff Model (SRM) is also a very useful model for modeling the river discharges over such watersheds where snowmelt runoff adds to the river discharge as a major contributor. The changing climate and global warming phenomenon has caused the glacier of the world to retreat followed by change in precipitation patterns. The continuous decreasing of glacier and snow melting at a higher rate is affecting the climate and such effect can definitely change the dimensions of local and socio economic progress of a country.

The changes in the climate of a region can be estimated from the depletion of glacier and snow present there. For the last 20 years the glaciers are facing the crumple and it is reported that the decrease of glacier extent and snow is an indication of active global warming over that watershed [i-ii]. The SRM has been extensively used to a large number of watersheds of various sizes i.e. (76 - 120,000 km^2) all over the world with elevation range of (305 - 7690 m a.s.l) [iii]. The SRM is very useful for water resources planning and management, hydropower generation and flood warning in those areas having snowmelt contribution [iv]. Simulations for such watershed where snowmelt is a major contributor to the flow need a bit more attention in the case that accurate estimates for snowmelt rate are required for water resource planning and management.

Snowmelt Runoff Model (SRM) is one of the most commonly used models to simulate and estimate the daily stream flows in such mountainous catchments [v]. The model uses the approach of simple degree-day method to account snowmelt runoff. The daily rainfall, daily temperature and daily snow cover area are the major inputs to the model. In addition, the information of catchment features such as basin area, zone area, and the hypsometric (area elevation) curve is also required. The daily water produced from the snowmelt and rainfall is added on the calculated recession flow and converted into day-to-day discharge from the catchment.

In the light of above discussion it is very significant to model a watershed for flood estimation. SRM can be used for such watersheds where there is a contribution from snowmelt by using the dataset as mentioned before. The current research describes the snowmelt modeling for the catchment of Khanpur dam using SRM. In order to achieve the calibration results through SRM techniques of remote sensing (RS) and geographical information system (GIS) were also used.

II. Study Area

Khanpur dam watershed is situated in Khyber Pakhtunkhwa of Haripur district. It is located about 50 kilometers Northwest of Islamabad at River Haro. Haro River drains runoff from western slopes of Murree Hills and southern slopes of Nathiagulli mountain and also receives partial runoff from Margalla Hills. The Khanpur dam is situated in Pakistan with a latitude 33°48' and longitude 72°55' and covers an area of about 308 square mile. The location map of the study area is shown in Fig. 1. Pakistan Meteorological Department PMD has only one station i.e. Khanpur station in the study area. The maximum elevation reaches 2755m in the watershed. The analysis of Moderate Resolution Imaging Spectroradiometer MODIS daily data revealed that around 15 to 20% of Khanpur catchment remains covered with snow in winter season.

III. Litreature Review

The climate impact has been studied by many researchers. In a study Naeem et al., (2013); concluded the reduction in Chitral River flows under assumed reduced glaciated extents by using UBCWM [vi]. River Kunar watershed was modeled by using the data of snowpack water equivalent and total winter rainfall in Kunhar Basin through SRM where it was found that about 65% of flow is generated due to snowmelt in Kunar River measured at Talhatta [vii] . Snow cover of Gilgit catchment was found by using NDSI on MODIS daily images. The images having high cloud cover were excluded for the analysis and the cloud cover days were interpolated linearly by plotting conventional depletion curve. Later on these snow cover depletion values were used in SRM to simulate flows of Gilgit River [viii].

In another study SRM was used for modeling and the results obtained were utilized for flood forecasting in Swat River. The snow cover area was extracted by using MODIS images having free from cloud cover. First the Model was calibrated for the melting season of year 2004 with model efficiency of 0.90 and verified for years 2005 & 2006 with coefficient of model efficiency of 0.95 and 0.080 respectively. After application of Model it was concluded that SRM model can efficiently be used for water resources planning, management and flood forecasting [ix]. Similarly, another study was focused on the reduction in Astore River flows under assumed reduced glaciated extents with the help of Landsat data and UBCWM [x].

SRM Model was also used in Astore catchment to simulate snowmelt runoff. Landsat-TM monthly satellite images data were used to map snow cover area and coefficient of model efficiency remained 0.91 [xi]. Application of temperature index approach along with extracted snow cover data from remote sensing can be successfully applied to Upper Indus basins for snowmelt simulation.

It is stated in an Interim Report that Mangla Basin comprises of catchment area of 33460 km^2 and 50% of the catchment lies outside line of control. Therefore, MODIS daily snow cover product is encouraged to use to extract the snow cover area of huge basins and further use in the hydrological models to simulate and forecast flows of the catchment. In this particular research, SRM was applied on Khanpur dam catchment with a major objective to observe the change in the flows under different climate scenarios. For this purpose, the temperature and precipitations trends of the catchment was observed for the past data.

IV. Snowmelt Runoff Model (SRM)

SRM (snowmelt runoff model) is a temperature index hydrologic model which was used to perform simulation in this study. The Snowmelt Runoff model also called Martinec Rango model was first developed in 1973 at the Federal Institute for snow and Avalanche Research in Davos, Switzerland. The generation of satellite remote sensing data enhanced the possibility of simulating even huge watersheds. SRM has been used to simulate the Gangas River basin with catchment area of 917,444 Km^2. This Model has been used to more than 100 basins located in different 29 countries by universities, self-governing operators and institutes etc. [xii].

The three main variables of the model are daily temperature, precipitation, and daily snow covered area. SRM calculates the daily quantity of water from snowmelt and rainfall, adds it to the calculated recession flow, and transfers it to the daily discharge from the basin. The area has been divided into different elevation zones. Particular basin characteristics include runoff coefficients, degree-day factors and historical recession coefficients and the zonal mean hypsometric elevation.

The strong point of SRM is its primary dependence on snow cover areal degree which is arranged as a depletion curve at the end of snowmelt period. This feature allows the model to work even with limited data, as the snow covered area data can be found today from readily available Remote sensing Snow data by several agencies.

V. Data Acquisition and Pre-Processing

A. Daily Discharge

Daily inflow data at Khanpurstream gauging station was gathered from Khanpur dam WAPDA office for the years 2003 to 2013. This flow data has no role in running the simulations. The flow data is used to find the efficiency of the calibration of the model.

B. Observed Climatological Data

SRM require daily precipitation as well as average daily temperature data as main input to the model. Both

of these parameters are being observed by the glacier Monitoring research Centre of Water and Power Development Authority (WAPDA) at Khanpur Dam Station. Daily precipitations and daily average temperatures for the years 2003 to 2013 were collected from WAPDA.

C. Terrain Elevation

Digital Elevation Model (DEM) model was used to define the catchment boundaries and divide it to different elevation zones. SRTM DEM for Khanpur Dam catchment has been downloaded in tiff format from http://www.cgiar-csi.org/data/srtm-90m-digital-elevation-database-v4-1. For extraction of complete catchment boundary and river system of Khanpur watershed, Arc Hydro Tools; the extension of ArcGIS was used as shown in Fig. 1. Khanpur dam catchment has been divided into different elevation zones having equal elevation difference of 500 meter.

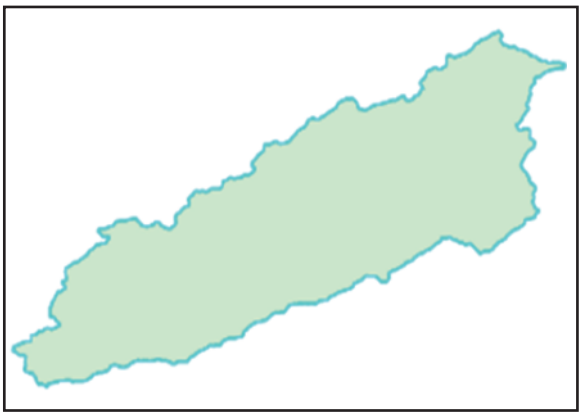

Fig. 1. Catchment area of Khanpur dam

D. Snow Cover Area

The MODIS processed data provides various data which even help to distinguish between various features such as fire [xiii] and clouds [xiv] with a certain degree of accuracy. The MODIS snow product data was used in this study which was downloaded from web of MODIS. Global MODIS data for different features types e.g. snow and vegetation are available in open domain.

The technical team of MODIS continues to develop algorithms to map snow cover over different land use types and revise again and again prior to the launch MODIS snow cover products. As a result of this continuous refinement of algorithms, MODIS daily snow product MOD10A1 is found to be 93-100% accurate [xv]. This daily product has been selected as the source data to map snow cover over Khanpur watershed. MODIS has developed snow cover products such as daily snow cover product (MOD10A1) and weekly snow cover product (MOD10A2).

SRM Model requires snow covered area input on daily basis in the form of Conventional Depletion Curve of snow cover (CDC). Therefore, temporal data is very much important in determining the snow depletion over the watershed. MOD10A1 tile was downloaded, covering Khanpur Dam catchment and was further analyzed by using special analyst tool of ArcGIS software. Figures 2 to 4 show the variation and distribution of snow cover over the Khanpur watershed.

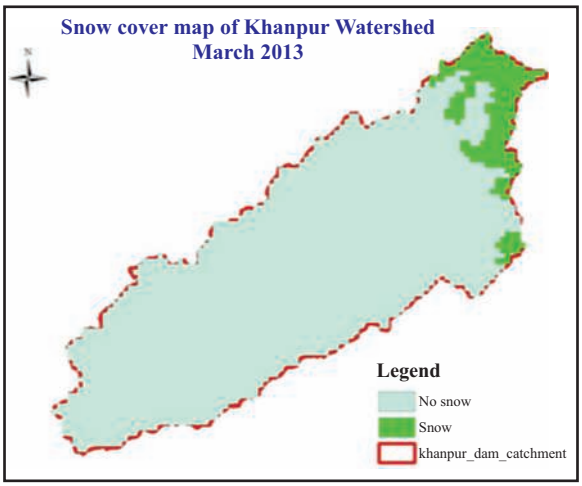

Fig. 2. Snow cover area of Khanpur dam catchment during March 2013

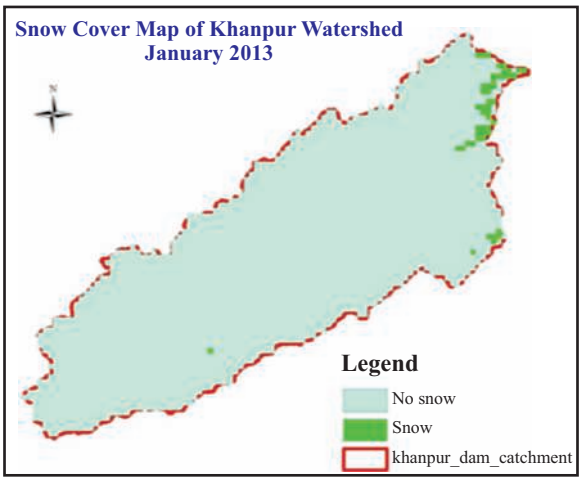

Fig. 3. Snow cover area of Khanpur dam catchment during January 2013

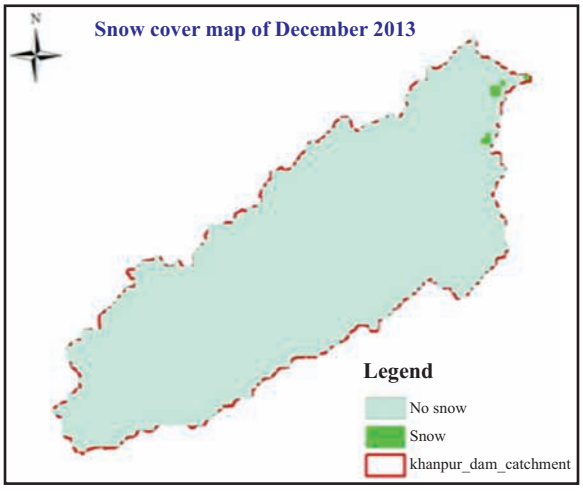

Fig. 4: Snow cover area of Khanpur dam catchment during December 2013

E. Climate Change

The mean annual temperature and mean annual precipitation data trends were analyzed over the past 10 years i.e. (2003-2011) over the Khanpur watershed. The graph were plotted between time and mean annual temperature and also plotted between time and average annual rainfall. The overall trend of the plots were found by introducing trend line. The Fig 5 and Fig 6 below show mean annual change of temperature and precipitation data respectively.

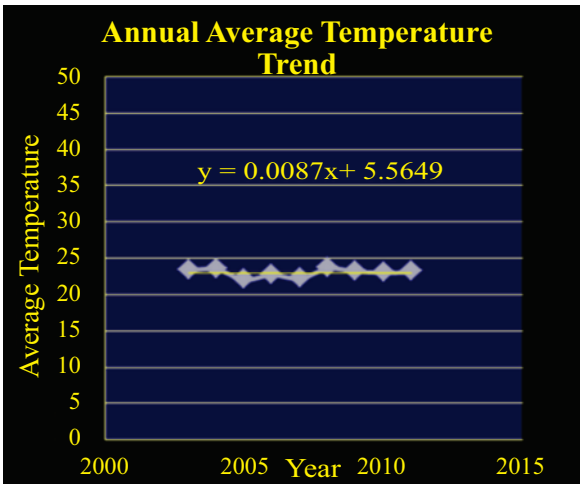

Fig. 5. Average Annual Temperature Trend

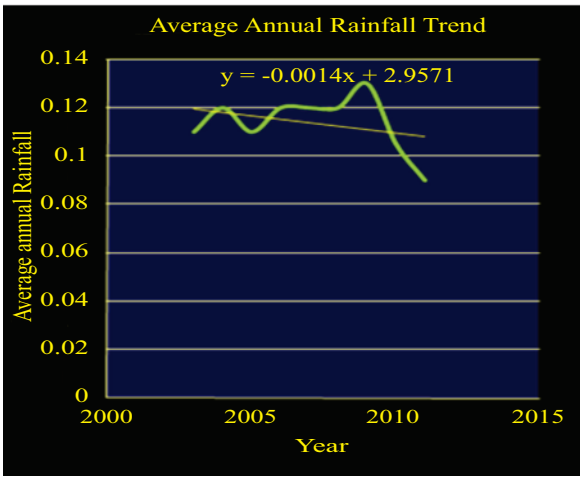

Fig 6: Average Annual Rainfall Trend

VI. Calibration of the Model

Calibration of the model was done by comparing the simulation results with the actual observed data so that the accuracy of the model can be checked. The model was calibrated for the year 2005 as shown in Fig. 7. This is carried out by adjusting the values of various parameters of model again and again to bring the simulated results closer to the actual observed data.

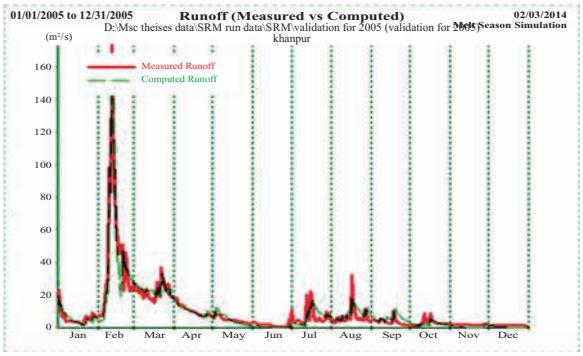

Fig. 7: Calibration of the Model for the year 2005

VII. Assesment of the Model Accuracy

The accuracy of the Snowmelt Runoff Model can be checked by two criteria, one is known as coefficient of determination, R^2, and the second criteria is volume difference, D_V. The R^2 value can be obtained as given in eq (1)

$$[R^2 = 1 - \sum_{i=0}^{n} \frac{(Q_i - Q_s)2}{(Q_i - Q)2}] \quad (1)$$

Where

Q_i is the measured daily discharge

Q_s is the simulated daily discharge

Q is the mean measured discharge for the given year or snowmelt season, n is the number of daily discharge values.

The volume difference between measured and simulated discharge is computed as given in eq (2)

$$[D_v = \frac{(V_R - V_R')}{V_R}] \quad (2)$$

Where

V_R is the measured yearly or seasonal runoff volume

V_R' is the computed yearly or seasonal runoff volume.

VIII. Validation of Model

Validation of the model is carried out by applying the model for any year other than the calibration year while using the same values of model parameters as finalized during the calibration processes. The simulated flows obtained in this way are then compared with the observed flows to verify the model calibration results. It was found that the results obtained from the validation of the model were not healthy. The validation results for year (2007) are shown in Fig. 8.

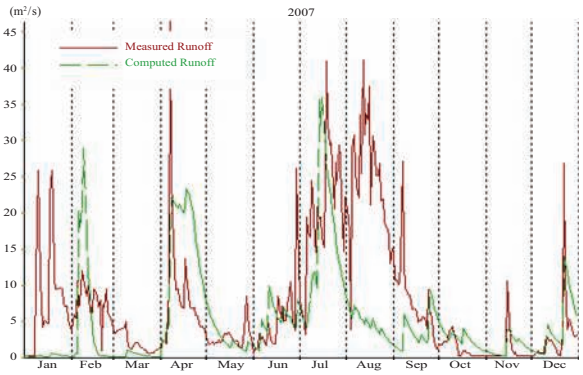

Fig. 8: Validation of the model for year 2007

IX. Results and Discussion

From the simulation results it was found that around 15% of the total flow was from snowmelt. Hence mainly the Haro river flows are from the contribution of rainfall and not because of the snowmelt. Since SRM uses daily degree approach to model the flows and was used to study the hydrology of the study area. It was found that the results of validation were not healthy. The simulated results could have been better if a rainfall runoff model has been used over the watershed. Since the contribution of snow was too low for the watershed hence SRM was not appropriate to use over such watershed.

X. Conclusions

Based on the results the following conclusions were drawn:

1. Snowmelt Runoff Model is well calibrated but not validated good for rest of the years due to very less snow cover area.
2. From above results it is concluded that Snowmelt Runoff Model does not apply in those catchments having snow cover area is very low.
3. On average basis, contribution of snowmelt-runoff in Khanpur dam Catchment at Khanpur gauging station is about 15%.

XI. Recommendations

Following Recommendations have been made depending on the results and conclusions of the study:

1. It is recommended to figure out mandatory minimum Snow Covered Area SCA of a watershed prior to use SRM. Hence in this way some reliable results of calibration and validation can be found.
2. Some rainfall-runoff model e.g. HEC-HMS should also be used to study the hydrology of the watershed.

References

[i] F. Paul, A. Kaab, M. Maisch, T. Kellenberger and W. Haeberli, "Rapid disintegration of Alpine glaciers observed with satellite data," Geophysical research letters 31, L21402. doi: 10.1029/ 2004GL02081, (2004).

[ii] J. T. Houghton, Y. Ding, D. J. Griggs, M. Noguer, P.J. van der Linden, X. Dai, K. Maskell and C.A. Johnson.Climate change, 2001. The scientific basis, Contribution of working group 1 to the third assessment Report of the Intergovernmental Panel on Climate Change, Cambridge university Press, 2001,pp. 88, (2001).

[iii] WMO Inter comparisons of models of snowmelt runoff. Operational report no. 23, WMO, Geneva. (1986).

[iv] T. Nagler, Real time snowmelt runoff forecasting using ERS SAR PRI data, (2006)

[v] A. Rango, J. Martinec and R. Roberts, "Snowmelt Runoff Model User's Manual, 3-25, (2007)

[vi] U. A. Naeem, H. N. Hashmi and A. S. Shakir, (2013). "Flow trends in river Chitral due to different scenarios of glaciated extent." KSCE Journal of Civil Engineering, Vol. 17, No. 1, pp. 244-251, DOI: 10.1007/s12205-013-1978-1.

[vii] F. D. SCALLY, Relative importance of snow accumulation and monsoon rainfall data for estimating annual runoff, Jhelum basin, Pakistan, Hydrological Sciences-journal- des Sciences hydrologiques,39,16-18, (1994)

[viii] Tahir, A. Ahmad, P. Chevallier, Y. Arnaud, and B. Ahmad. Snow cover dynamics

andhydrological regime of the Hunza River basin, Karakoram Range, Northern Pakistan. Hydrol. Earth Syst. Sci., 15,2275–2290, 2011.doi:10.5194/hess-15-2275-2011

[ix] WAPDA (Water & Power Development Authority) Inception Report Upgrading of Tools Water Resources Database, Management Systems and Models under Sub-component B1 of WCAP, 12-20. (2011)

[x] U. A. Naeem, H. N. Hashmi, M. S. Shamim, and N. Ejaz. (2012). "Flow variations in Astore river under assumed glaciated extents due to climate change." Pak J. Engg and Appl. Sci, Vol. 11, pp. 73-81, ISSN 1995-1302

[xi] J. Martinec, A. Rango, R. Roberts, Snowmelt Runoff Model (SRM) User's Manual, Agricultural Experiment Station Special Report 100, College of Agriculture and Home Economics, 2008.

[xii] J. A. Lamadrid, L. K. Macclune, Climate and Hydrological modeling in the Hind-Kush Himalaya region, CICERO, ISET, (2010).

[xiii] K. P. panday. Snowmelt runoff modelling in the tamor river basin in the eastern Nepalese Himalaya.

[xiv] Akhtar, A. Shakil, Romshoo and M. S. Bhat. Estimation of snowmelt runoff using Snowmelt Runoff Model (SRM) in a Himalayan watershed. World journal of science and technology 1(9): 37-42 ISSN: 2231-2587, (2011).

[xv] G. G. Nabi, M. Latif and A. H. Azhar. G. G. Nabi, M. Latif, H. rehman and A. H. Azhar. The role of environmental parameter (degree day) of Snowmelt runoff simulation (2011).

Role of Private Sector in Providing Affordable Housing in Lahore

R. Hameed[1], O. Nadeem[2], G.A. Anjum[3], S. Tabbasum[4]

[1,2,3]City & Regional Planning Department, University of Engineering &Technology, Lahore.
[4]Lahore Development Authority, Lahore.
[1]drrizwanhameed@uet.edu.pk

Abstract-Shortage of affordable housing has become a global issue. The governments in developed and developing countries have initiated various programmes but those have proved inadequate to meet the growing demand of affordable housing. Pakistani metropolitan cities are also facing this issue. Lahore is the second largest city of Pakistan and is an administrative, business, education and recreational hub of the Punjab province. The rapid growth of population has created huge demand for housing in the city. In addition to the Lahore Development Authority (LDA), the principal planning agency in Lahore, the private sector has also been contributing towards housing supply through development of housing schemes. This research mainly attempts to explore how far the small plots/houses in such schemes are affordable to low income people and how many of such plots/houses have actually been occupied by them? The methodology includes: analysis of data on approved private housing schemes, views of the LDA officials, private developers and the residents of selected private housing schemes. The analysis confirms that the small sized plots in private housing schemes are occupied by the high and middle income groups. The housing has become severally unaffordable for the low income people. The government is falling short of providing adequate incentives to the private sector for delivering affordable housing to the low income groups. The study identifies several measures to improve the situation.

Keywords-Affordable Housing, Private Sector, Housing Demand, Low Income People, Lahore, Pakistan.

I. INTRODUCTION

Shelter is globally recognized as a basic need of human being. Under the Universal Declaration of Human Rights and the UN Habitat Conference 1996, all the governments are responsible to make diligent efforts for providing affordable housing to their citizens [i-ii]. Affordable housing means the housing facility that low to median income households can avail within their resources without compromising their other basic necessities for living such as food, clothing, children education and medical facility [iii]. For housing to be affordable in metropolitan areas, it is suggested that, "housing prices should not exceed three times gross annual household earnings" [iv].

Lack of affordable housing is a global problem but it is most sever in Asian, African, Latin and North American as well as some of the European countries. Several factors have contributed to this problem. Those mainly include: rapid increase in population, urbanization, limited tenure choice, shortage of land for affordable housing, high cost of construction, high rate of interest on mortgages, and inadequate supply of social housing etc. [v-vi]. As a corollary to that, "the average floor space of a new dwelling in England and Wales is now the lowest in Europe at 76 sqm (compared with 92 in Japan and 115 in the Netherlands, countries with higher population pressures). For all dwellings (new and existing)the figure was 85 sqm compared with 98 in the Netherlands" [vii].

As a planning instrument to promote affordable housing, diversity in lot sizes is used by planning agencies in some countries. For instance, while discussing housing affordability issues in non-metropolitan coastal Australia, Squires and Gurran [viii] have noted that 36 out of 143 local councils were found to have developed planning instruments and policies specifically aimed at addressing the affordability of housing in the local area. Majority (19) of such councils sought to achieve this aim by promoting diversity of housing types and lot sizes. In Indonesia, the 1:3:6 rule requires private developers to provide 6 units of low income housing, 3 units of mid standard housing against every unit of luxury housing [ix].Likewise, the land disposal policy of the Delhi Development Authority, India provided that the distribution of plots among low middle and high income groups should be in the proportion of 50:30:20 to roughly correspond to their population share [x].

In the case of Asia, the magnitude of the demand for affordable housing can be assessed keeping in view the facts that the urban population in Asian cities in 1950 was 229 million which has reached2.161 billion in 2016(i.e. 48% of 4.453 billion) [xi-xii]. The rate and scale of urban growth in Asian cities is distinctive from others. It is predicted that the major urban centres in Asia will have to accommodate 120,000 new residents every day. This will impose more pressure on

the availability of affordable housing [xiii]. The economic growth in the urban areas of Asian countries is pushing up the land prices and the availability of land at affordable prices is a major constraint towards supply of affordable housing. As in most of the Asian countries, the land is privately owned and development of affordable housing project seems to be less profitable for private sector, therefore the low income families are seem to be pricing out of formal land and housing market.

The situation is no different in case of Pakistan where population growth in cities of the country has also been rapid. It has increased from 58.74 million in 2008 to 74.77 million in 2015 (39% of 191.71 million). If the current pattern of urbanization continues, the urban population of Pakistan will be around 122 million in 2030, which will form 50 % of total population of the country [xiv-xvi]. The rapidly increasing population and economic competition are dominating urban land and housing markets, thus exacerbating the lack of housing of an acceptable standard that the poor can afford. The World Bank has estimated a shortage of 7.6 million housing units in Pakistan, of which two-third is because of the demand from low-income groups, earning less than Rs. 12000 per month [xvii]. According to the National Housing Policy of Pakistan [ii], over 70% of the housing shortage and recurring demand is for low income groups [ii].

Informal settlements house a significant proportion of low income groups in major urban centres. For instance, in Karachi, as many as 80% of city's inhabitants live in plots of 120 square yards or less. Similarly, of the 36.7% of land utilized in Karachi for the residential purposes, 27 percent has been developed formally and 8.1 percent informally. But 62% of the city's population lives on 8.1% of the city's land developed informally for residential purposes. Such informal settlements serve as alternative to affordable housing for the poor marked by below par provision and maintenance of infra structural services [xviii]. Moreover, Sheikh argues: “The emergence of katchiabadis in Islamabad (the federal capital of Pakistan) shows that even the better controlled and managed cities have not been able to extend affordable options for urban poor” [xix].

Similarly, Punjab being the biggest province of the country, is facing cumulative shortage of housing mainly in its urban areas [xx]. As a policy to provide low income housing, the Housing and Physical Planning Department (H &PPD) renamed as Housing, Urban Development and Public Health Engineering Department (HUD &PHE) of the Punjab Government developed several low income housing schemes during 1970s to 1990s providing plots of 3 to 5 Marla. Plots having an area of 5 marla or less are considered to be affordable, since the National Housing Policy provides for exemption of all taxes on construction of houses on plots measuring up to 150 sq. yds (5 marla @272.25 sq. ft./marla.)[ii].Moreover, the Punjab Government does not charge property tax on the house constructed on less than 5 marla plots, provided that it is occupied by its owner. However, author of [xxi] observed significant 'downward raiding' of the middle and high income groups on the small plots, since the housing requirement for these groups were not catered for in the planned sites and services schemes and the poor people soled their plots to these groups at higher prices.

In a recent attempt to facilitate low income people, the Government of Punjab Province has made it mandatory that at least 20% of the plots in every private housing scheme should be of 5 Marla or less in size [xi].

Lahore is a metropolitan city. Its total population in 1951 was 1.13 million with 75.73% urban share. It increased up to 8.83 million with 87% urban share in the year 2010 [xii] and is estimated around 9 million in 2012 [xiii].The increased number of housing schemes played a major role in the expansion of the Lahore city. Major contribution towards development of these schemes was initially made by Lahore Development Authority (LDA). But since 1980s, the private sector is predominantly contributing towards development of private housing schemes in this city. As a result, the urban fringe has now grown to the greater extent along the Multan road, Ferozepur road, Canal road and Raiwind road accommodating most of such schemes [xviii].

Looking beyond different epochs of the city development and expansion, one of the most distinctive factors which can now be observed in case of Lahore is the occupancy of nearly 90% of the housing units already constructed in private housing schemes by high and middle income groups. Although small size plots of 5 Marla or less have also been provided in these approved schemes. But nothing can be said for sure that whether these too have gone in the ownership of high and middle income groups in the absence of any empirical evidence. This paper deals with the role of private sector in the development of approved private housing schemes in Lahore and resultantly its contribution toward affordable housing through provision of small sized plots generally perceived and associated with low income class. In particular, it attempts to explore:

- What is the number of 5 Marla and smaller size residential plots provided in the approved private housing schemes?
- Which income group is actually residing in the houses constructed on plots of 5 Marla and smaller size in those schemes?
- Whether the plots provided by the private developers are really affordable by the low income people?
- How to facilitate the provision housing that is affordable for the low income people?

II. Materials and Methods

The materials and methods for this research include: review of relevant literature, collection of secondary data from LDA and face to face interviews with key stakeholders. There are over 236 approved private housing schemes within the jurisdiction of LDA but only 48 schemes provided 26.1% plots of 5 Marla or less along with 73.9% bigger plots ranging from 8 Marla to 2 Kanal. Of these 48 schemes, 19 were developed by individual developers, 15 by cooperative societies registered under the Co-operative Societies Act 1925, and 14 by groups/companies registered under the companies Ordinance 1984.

Out of the 48 private housing schemes mentioned above, three housing schemes were selected for detailed investigation, namely, River Edge, WAPDA Town, and Pak Arab. The River Edge Scheme represents induvial developer, WAPDA Town represents cooperative societies and Pak Arab Housing Scheme represents groups/companies registered under the companies Ordinance 1984. Although the WAPDA town was launched much earlier as compared to other schemes, however, the houses in this scheme were constructed much later). The construction of houses in the scheme was another underlying criteria to ensure that survey from inhabitants of these schemes could be done.

For the purpose of interviewing, 30 residents/ owners of 5 Marla houses from each of the scheme were chosen randomly using structured interview schedule. This type of sampling is also known as probability sampling where every member of the target population has an equal and independent chance of inclusion [xiv]. The questionnaire for the residents comprised of different sections depending upon the nature of information. It included general information regarding their income level, source of income and plots or house cost, which ever was applicable, since some interviewees bought plot and then constructed the house whilst others directly bought the house Table IV. The second section consisted of questions to know their affordability level and how did they arrange finances for buying the plot etc. Where the respondents/residents were reluctant to provide information regarding income level and the cost of buying plots/house, alternative housing units were selected. It was useless to increase the sample size, since the response trend of 30 interviews from each of the three selected housing schemes showed repetition of similar answers. The Residents' interview data was analysed using the Statistical Package for Social Sciences (SPSS) Version 18. The questions and possible answers were coded and assigned value labels before entering the data. Frequency tables, cross tables and bar charts were then generated to present the results while comparing the views of the key stakeholders.

Face to face interviews of 19 officials of the LDA responsible for land use and building control, and 30 developers of private housing schemes were also conducted. The interview schedules comprised of open ended questions and issues concerning weaknesses in the housing policy/regulations, constraints in implementation, frequency of sale and purchase of small size plots, reasons of the reluctance of developers to provide small plots etc. and possibilities of facilitating or increasing the supply of affordable housing in Lahore.

III. Results and Discussion

The following sections present results and discussion:

A. Contribution of the public (LDA) and private sectors in provision of small plots for housing in Lahore

Small size plots are available in both the public and private housing schemes within the jurisdiction of LDA. The distribution of different sizes of residential plots in both kind of housing schemes is presented in the Table I.

Usual sizes of residential plots found in Lahore are:

3 marla, 5 marla, 7 marla, 8 marla, 10 marla and 1 kanal, whereas, 2 kanal plots are very rare [xxix]. It is evident that out of the total number of plots provided by the public sector, 44% are small size plots and 56% are large size plots (56%). The private sector could provide only 5.4% small sized plots (5 Marla or less) while 94.6% plots are of large size.

TABLE I
Distribution of Residential Plots in the Public and Private Housing Schemes

Type of Housing Schemes	No. and Sizes of Plots		Total
	5 Marla or less	More than 5 Marla	
Public Sector Housing	35164 (44%)	44776 (56%)	79940 (31%)
Private Sector Housing	9476 (5.4%)	168169 (94.6%)	177645 (69%)
Total	44640 (17.4%)	212945 (82.6%)	257585 (100%)

Source: LDA, 2012

Note: Standard area of one marla= 25.33sqm. In Lahore: 21sqm
Standard are of one kanal = 506.51 sqm. In Lahore: 418.60sqm

Further, this analysis reveals that the percentage of small size plots is not according to the demand of housing because, as pointed out earlier, 70% housing demand is from low income sector [ii].It is also clear from the above facts that the public sector is contributing more towards the supply of small size plots as compared to the private sector which is dominated by investors and land speculators. Fig. 1 presents the distribution of plots provided in the 236

approved private housing schemes. It shows that the maximum (62694) plots were provided during the course of 2005-2010 while the minimum (15213) plots were provided during the period 1985-1989. The provision of plots kept on changing during different time periods perhaps due to changing purchasing power of the buyers/investors.

B. Distribution and Inhabitation on plots in three selected private housing schemes

It is important to know the distribution of small (5 Marla) and large size (More than 5 Marla) plots in the three selected private housing schemes. In the Pak Arab and River Edge housing schemes, the distribution of small size plots is 64.4% and 51.9% respectively (Table II), whereas in WAPDA town, the distribution of small size plots is less (19.48%) as compared to large size plots. But the total number of small plots is higher if compared with the other two schemes due to huge size of this scheme.

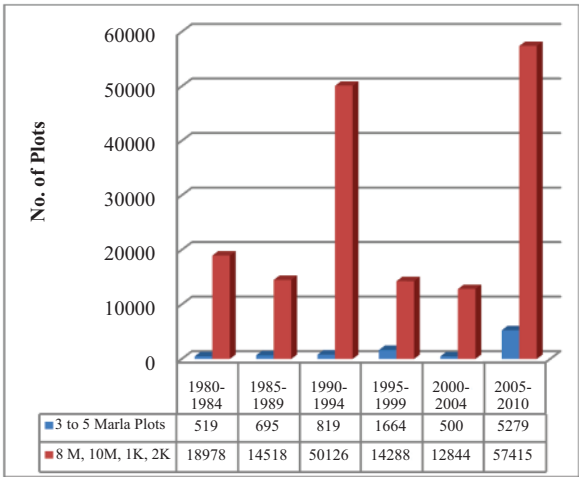

Fig. 1. Plots Distribution in Approved PHSs over the Years
Source: LDA, 2012

Note: The data collected from the Office of the Chief Metropolitan Planner, LDA revealed that in the 48 approved private schemes there was no plot of sizes between 5 and 8 marla.

TABLE II
DISTRIBUTION OF PLOTS IN THE THREE SELECTED PRIVATE HOUSING SCHEMES

Name of Schemes	Distribution of Plots in Case Study Housing Schemes		
	5 Marla	More than 5 Marla	Total
Pak Arab	1485 (64.4%)	818 (35.6%)	2303 (100%)
WAPDA Town	1606 (19.48%)	6637 (80.52%)	8243 (100%)
River Edge	515 (51.9%)	476 (48.1%)	991 (100%)

Source: Field Survey

It is encouraging to note that houses have been constructed on most of the small size plots and people are living in the selected schemes. The Table III shows that 93.74% plots in Pak Arab, 96.51% plots in WAPDA and 76.7% plots in the River Edge scheme are inhabited by either owners or tenants. On the other hand, large size plots (8 Marla and above) are relatively less inhabited except in the case of River Edge scheme. The very reason appear to be that the large size plots were held by some of the owners for speculations purposes.

TABLE III
INHABITATION STATUS ON PLOTS IN THE THREE SELECTED PRIVATE HOUSING SCHEMES

Name of Scheme	Number of Plots Provided		Number of Plots Inhabited	
	5 Marla	More than 5 Marla	5 Marla	More than 5 Marla
Pak Arab	1485	818	1392 (93.74%)	464 (56.72%)
WAPDA Town	1606	6637	1550 (96.51%)	4975 (75%)
River Edge	515	476	395 (76.7%)	397 (83.4%)

Source: Field survey

C. Results of Interviews with the Residents of Small Plots in Three Selected Housing Schemes

i) Occupation, monthly income and price paid by the residents

The importance of exploring the occupation/ income level of the residents is directly related to the main objective of this study that is to determine whether the small size plots are actually acquired by low income people. The Table IV reveals the whole situation.

TABLE IV
OCCUPATION, MONTHLY INCOME AND PRICE OF PLOT PAID BY THE RESIDENTS

Occupation/ Source of Income	No. of Respondents				
	Pak Arab (n)	WAPDA Town (n)	River Edge (n)	N	%age
Personal Business	10	3	9	22	24.4
Government employee	9	18	4	31	34.4
Private employee	11	9	17	37	41.1
Monthly Income (Rs.)					
15000-25000	5	1	2	8	9.8
26000-35000	7	10	9	26	28.6
36000-45000	12	8	7	27	29.7
Above 46000	6	11	12	29	31.9
Plot/House Price Paid (Millions)					

1.0-1.5	7	0	8	15	16.7
1.6-2.0	11	2	10	23	25.6
2.1-2.5	2	3	6	11	12.2
2.6-3.0	1	12	1	14	15.6
2.1-2.5 (House)	7	2	2	11	12.2
2.6-3.0 (House)	2	11	3	16	17.8
Total	63		27	90 (100%)	

Source: Field Survey

The data suggest that 41.1% of residents are private employees, while 34.4% are employed in public sector. Only 24.4% of the residents are having their personal business. The monthly income of only 9.8% of the families interviewed for the study ranges between Rs. 15000-25000. The other three ranges of monthly income are almost evenly distributed, i.e. of 28.6% between Rs. 26000-35000, of 29.7% between Rs. 36000-45000 and of 31.9% above Rs. 46000. The Punjab Private Housing Schemes and Land Sub-Division Rules 2010 define a person as low income whose monthly income does not exceed Rs. 15000. A considerable percentage of interviewed developers and LDA officials revealed that households earning up to Rs. 25000 per month should be considered as low income given the increasing inflation. To account for all possible variations in the definition of low income, the range of Rs 15000-25000 per month has been taken. Thus, the analysis clearly shows that maximum number of residents of small size plot are those with middle and high income level.

Likewise, the maximum number of residents (23) of small size plot in selected three housing schemes had to pay an amount of Rs. 1.6 to 2.0 million. This indicates that the price of small size plots in private housing schemes is severely unaffordable for the low income groups. This observation is further substantiated by the fact that 16 residents purchased the house at a price ranging from Rs. 2.1 to 3.0 million.

In most of the schemes, holding the plots for a few years is generally a common practice to get better price. The residents of small size plots were asked about the year of the purchase of plot and whether they were the first purchaser of this plot or they bought it from previous owner. Most of the interviewees (63%) of the selected schemes purchased plot or house during the years 2010 onwards, 33% purchased during 2007 to 2009 and only 4% purchased during 2004 to 2006. The findings also suggest that 54% of the plots were bought from the previous owners in the form of either land or a house. There are only 46% plots still under the ownership of the first purchasers who bought the plots from the developers of the schemes. About this phenomenon, no study could be found which reports average figures for the city and hence it is not possible to make such a comparison. However, this analysis justifies the above fact that most of the purchasers buy plots to get more profit by re-selling the same at higher prices.

The residents of the selected schemes were also asked about the instalments if paid by them while purchasing the plot/house. The analysis suggests that 23.3% of the respondents paid the price in instalments while the remaining 76.6% of the respondents paid the price in lump sum. It is thus evident that the residents of 5 Marla plots belong to middle income group. It is not possible for a low income family to pay the lump sum amount, as they can hardly manage to make the both ends meet then how they were able to save millions of rupees. Other studies also found similar situation in several private housing schemes of Lahore [xxi], [xxx].

ii) Arrangement of finance to purchase a plot/house

The residents of the selected private housing schemes were also asked how they arranged finance to purchase the plot/house. The analysis shows that most of the residents (50%) used savings for paying the property price. This confirms the findings of reference [xxv]. However, 37.8% of the respondents arranged finance by selling their previously owned or inherited property. Surprisingly, no respondent approached a bank to get loan for buying the property Table V.

TABLE V
ARRANGEMENT OF FINANCE TO PURCHASE A PLOT/HOUSE

Category	Plot	House	Total
Savings	37 (58.7%)	08 (29.6 %)	45 (50%)
Loan from Bank	-	-	-
Selling gold	03 (4.7%)	-	3 (3.3 %)
Selling previous property	15 (23.8%)	19 (70.3 %)	34 (37.8 %)
Any other	08 (12.8%)	-	8 (8.9 %)

Source: Field Survey

iii) Reasons of reluctance to approach banks for loan

The house loan facility is provided by the House Building Finance Corporation of Pakistan and the public as well as private banks, but most of the people hesitate to approach banks for getting loans. The main reasons as stated by the residents of small plots are: complicated procedure, high interest rate and various other conditions of the banks for this purpose. The analysis (Table VI) shows that 32.2% of the residents did not approach bank because of the complicated procedure of getting loan from the banks whereas 31.1% of the residents were not willing to pay high interest rates. Another 30% of the respondents also

showed their dissatisfaction towards several other conditions of the banks for providing loan to customers. Only 6.7% respondents said that they did not require loan for buying plot in private housing schemes.

TABLE VI
REASONS OF RELUCTANCE TO APPROACH BANKS FOR LOAN

Reason of Reluctance	No. of Respondents			Total	%age
	Pak Arab	WAPDA Town	River Edge		
Complicated loan gaining system	11 (36.6%)	12 (40%)	6 (20%)	29	32.2
High interest rate	8 (26.6%)	5 (16.6%)	15 (50%)	28	31.1
Not satisfied with the conditions	9 (30%)	10 (33.3%)	8 (26.6%)	27	30
Loan was not required	2 (6.6%)	3 (10%)	1 (3.3%)	6	6.7
Total	30	30	30	90	100

Source: Field Survey

The respondents were also asked why they didn't approach Islamic Banks where the interest rate is nil. They were of the view that the processing/service charges and other terms and conditions were very strict that is why they did not consider this as a feasible option.

iv) Comparison of prices and affordability of 5 Marla plots in selected housing schemes at the time of their launch and in 2012

The comparison is based on the prices of plots and income level at the time of launch of the scheme and at the time of our field survey during 2012. The Housing Affordability rate is calculated by using the formula of Median Multiple used in the "10th Annual Demographia International Housing Affordability Survey 2014". According to the survey report, this formula is recommended by the World Bank and United Nations. It has also been used by the Harvard University Joint Centre on Housing. It facilitates a transparent comparison of housing affordability in the international context [iv]. The formula is presented below: Median Multiple = Median House Price / Median Annual Income

The Table VII indicates that if the median house price in a housing market is three times the gross annual median income of the households (price to income ratio= 3 or below) , it can be considered as affordable. Whilst a median multiple of 3.1 go 4.0 means the housing is moderately unaffordable, the value of 5.1 and above indicate server unaffordability.

TABLE VII
HOUSING AFFORDABILITY RATING CATEGORIES

Rating	Median Multiple
Affordability	3.0 & below
Moderate Unaffordability	3.1 to 4.0
Serious Unaffordability	4.1 to 5.0
Severe Unaffordability	5.1 & above

Source: [iv]

Using the aforementioned formula, the median multiple/affordability of the interviewed residents of the three selected housing schemes were calculated at the time of the launch of housing scheme and during the year 2012. The results are presented in the Table VIII. It is evident from the Table 8 that the small size plot in WAPDA Town was within the affordability of the low to middle income people (with a median multiple of 1.4) at the time of launch of the scheme, whilst those were severely unaffordable in the Pak Arab and River Edge Housing Schemes.

TABLE VIII
AFFORDABILITY RATING OF THE RESIDENTS OF THE THREE SELECTED HOUSING SCHEMES

Name of Scheme	Year	Average Price of 5 Marla Plot (Rs.)*	Average Annual income of low income household (Rs.)	Median Multiple	Affordability Rating
Pak Arab	2006	950,000	60,000**	15.8	Severely Unaffordable
	2012	1,850,000	240,000***	7.7	Severely Unaffordable
WAPDA Town	1982	8,500	6,000**	1.4	Affordable
	2012	2,950,000	240,000***	12.2	Severely Unaffordable
River Edge	2007	600,000	60,000**	10.0	Severely Unaffordable
	2012	1,250,000	240,000***	5.2	Severely Unaffordable

Source: Authors' own construct
*Based on discussion with estate agents operating in and around the selected housing schemes.
** Based on discussion with estate agents, and LDA officials.
***Based on Government of Punjab criteria of Rs. 20,000/month [xvi].

The median multiple values for these schemes were extremely high (15.8 and 10.0 respectively) because these schemes were launched 24-25 years after the unveiling of WAPDA Town. This indicates that the gross annual median income of the households increased 10 times whilst the plot prices increased 70 to 111 times during this era. Though the international housing markets (e.g. Australia, UK, USA, Canada) reached sever unaffordability level during the past 10 years, their median multiple values did not exceed 6.0 [iv].

The small size plot remained severely unaffordable in all the selected private housing schemes in 2012. However, the 2012 values of median multiple in the cases of Pak Arab and River Edge housing schemes remained relatively lower (7.7 and 5.2) than that of the WAPDA Town (12.2). These values indicate that the plot prices in WAPDA Town increased at much higher rate than the prices in the other two schemes. This is because the WAPDA Town is a project of a Federal Government Agency having much better credibility and high standard/maintenance of infrastructure facilities. The other two schemes are the projects of private developers with relatively lower standard/maintenance of infrastructure facilities. Comparing the median multiple in the case of WAPDA Town with the international housing markets, it is even higher than that in the Vancouver (10.3) which is found to be the second most unaffordable market in the World. The top most unaffordable housing market is that of Hong Kong with a median multiple of 14.9 [iv].

D. Views of the Regulators on How to Facilitate the Provision of Affordable Housing

The Town Planning officials of the LDA were interviewed to seek their opinion on aforementioned issue (Box 1).

BOX I
VIEWS OF OFFICIALS OF LDA CONCERNING AFFORDABLE HOUSING FOR THE LOW INCOME GROUPS

- ✓ Realistic productive incentives should be provided to attract private sector for investment
- ✓ Land for housing should be provided by public sector by entering into partnership with the private developers
- ✓ Scheme plan processing charges should be lowered for the schemes having small size plots
- ✓ Joint problem solving approach should be adopted by all the relevant development sectors/organizations
- ✓ No new scheme should be approved till the habitation of existing schemes
- ✓ Housing finance mechanism should be improved
- ✓ Controlling the corruption by minimizing the bureaucratic role at local level

Source: Field Survey

It was revealed that the absence of any effective policy measures to control the use of plots for speculation purposes has also given land speculators room to acquire maximum number of plots in approved housing schemes without developing them. The speculators create artificial land scarcity and escalate the land prices. Therefore, it has become impossible for low income groups to own a small plot of even 3 Marla (675 sq. ft.). Moreover, the profit margin on small size plots is low as compared to that on large size plots due to more length of utility services required for such plots. It compels the developers to increase the rate of small size plots. Therefore, the low income people are forced to look towards informal land market to gain access to land for shelter.

In order to control speculation phenomenon which contributes to pushing up the land prices artificially, it was suggested that the government should take steps to curb land speculation by imposing taxes on the vacant plots, and by banning sale/purchase of already sold out plots for at least five years. Similarly, majority of the interviewed officials were of the view that, in order to make the affordable housing project profitable, it was important to provide realistic and productive incentives to the private developers. In this regard, provision of land by the Government to the private sector, reduction in taxes on transfer of land and housing scheme processing charges were proposed as necessary measures. Other suggestion included adopting the joint problem solving approach by all the relevant development sectors and concerned organizations, and improvements in housing finance mechanism for facilitating low income groups. Another important viewpoint emerged during the interviews was that the private sector alone cannot contribute towards lowering the backlog of affordable housing. The Government sector should also continue its efforts and initiate more projects for this purpose.

E. Views of the Private Developers on How to Facilitate the Provision of Affordable Housing

The views of the private developers were also sought to identify necessary measures and incentives needed to encourage them for the provision of affordable housing. They insisted that they were already providing 20% plots of 5 Marla or of the smaller size as per the provision of the new rules for private housing schemes. However, they admitted that the plots were not affordable by the low income people due to high cost of land and infrastructure. Necessary measures suggested by the private developers were in line with those suggested by the LDA officials (Box 2). However, they emphasized that the land should preferably be located near the workplace of the target group.

BOX 2
VIEWS OF THE PRIVATE DEVELOPERS CONCERNING AFFORDABLE HOUSING FOR LOW INCOME GROUPS

- Under the new rules, every private housing scheme provides 20% plots of 5 Marla or of the smaller size. Such plots are being sold on the basis of instalments but still the amount is unaffordable for low income people having a salary of Rs.15000-25000 per month.
- Public private partnership can prove to be effective if the land is provided by the government sector preferably near the industrial area/workplace of low income people with access through public transport.
- Public sector should provide incentives in the form of tax reduction on transfer of land for low income housing.

Source: Field Survey

IV. CONCLUSIONS

The private sector has failed in providing adequate and affordable housing/plots for the low income people of Lahore. Compared to the public sector, though the private sector has played a significant role as reflected through 236 housing schemes approved by the LDA, but still it has proved ineffective in catering to the needs of housing for low income people. The plots provided by the private sector remained unaffordable by the target group because of lower supply and high cost of land and infrastructure. The Government will have to come forward and join hands with those private developers who are willing to expedite the pace of providing small but affordable plots for the low income people. This may take the form of equity partnership in terms of land and necessary tax reductions by the public sector and development of infrastructure/project management etc by the private developers.

The 2010 Rules in current state have little potential to help in ensuring provision of affordable housing and hence meeting the housing needs of low income groups. This is because in the absence of any appropriate mechanism, the condition of provision of 20% small sized plots in a housing scheme would never automatically assure that these plots would go in the hands of low income groups. In this regard, the Government will have to devise a mechanism in consultation with private developers.

It may prove useful to ensure that the most of those 20% plots comprise of 3 Marla in size and provided with relatively lower standard of infrastructure services, making them affordable by low income groups. Given the minimum size of a dwelling unit in developed countries (76 sqm or 3 Marla), it can be stated that 3 Marla plot can provide adequate housing or in other words less than 3 Marla plot may not provide adequate housing. Since the cost of plot per Marla in Lahore is increasing day by day, 5 Marla plot would not be affordable by the majority of low income groups. Hence, 3 Marla plot is expected to serve the purpose.

However, the possible locations where such schemes can now be developed in the case of Lahore are far away from the city centre. This in turn will lead to increasing the home to work place distance in case of such schemes in future thus emphasizing the need for effective role of efficient public transport. Finally, like other cities of Punjab, the speculation phenomenon is contributing to pushing up the land prices artificially. The Government should take steps to curb land speculation by imposing taxes on the vacant plots, and by banning sale/purchase of already sold out plots for at least five years. It is good to note that, during the revision of this paper, the Government has recently increased the tax rates on sale/purchase of vacant plots.

REFERENCES

[i]. U. Millennium, "Booklet 10: The right to adequate shelter in international instruments", Special Session of the General Assembly for an Overall Review and Appraisal of the Implementation of the Habitat Agenda, 6-8 June 2001, NewYork. Available at: http://www.un.org/ga/Istanbul+5/booklet10.pdf [accessed March 31, 2015].

[ii]. GOP, "National housing policy 2001". Islamabad: Ministry of Housing and Works, Government of Pakistan, 2001.

[iii]. V. Milligan, P. Phibbs, N. Gurran, and K. Fagan,"Approaches to evaluation of affordable housing initiatives in Australia," National Research Venture 3: Housing affordability for lower income Australians Research Paper No. 7, Australian Housing and Urban Research, 2007.

[iv]. Demographia, "10th annual Demographiainternational housing affordabilitysurvey: 2014- Ratings for Metropolitan Markets", USA: Wendell Cox Consultancy, 2014, [Available at: www.demographia.com/dhi.pdf]

[v]. UN-HABITAT, "Housing for all: Challenges of affordability", Nairobi: United Nations Human Settlements Programme, 2008.

[vi]. UN-HABITAT,"Affordable land and housing in Europe and North America", Vol. 4. Nairobi: United Nations Human Settlements Programme, 2011a.

[vii]. R. Home, "Land ownership in the United Kingdom: Trends, preferences and future Challenges", Land Use Policy 26S, S103–S108, 2009.

[viii]. C. Squires, and N. Gurran, "Planning for affordable housing in coastal sea change communities", In Proceedings of the Building for Diversity National Housing Conference held on 26-28 Oct, 2005 at Perth, Australia.

[ix]. M. C. Hoek-Smit, "Implementing Indonesia's new housing policy: The way forward", Kimpraswil: Government of Indonesia and the World Bank, 2002.

[x]. A. Singh, K. Kapoor and R. Bhattacharyya, eds. "Governance and poverty reduction: Beyond the cage of best practices", New Delhi: PHI Learning Pvt. Ltd., 2009.

[xi]. J. Bredenoord, P.V. Lindert, and P. Smets (eds), "Affordable housing in the urban global south: Seeking sustainable solutions", London: Routledge, 2014.

[xii]. Worldometers, "Asia population", Available at: http://www.worldometers.info/world-population/asia-population/ [accessed November 27, 2016].

[xiii]. UN-HABITAT, "Affordable land and housing in Asia", Vol. 2. Nairobi: United Nations Human Settlements Programme, 2011b.

[xiv]. GOP, "Economic survey of Pakistan 2012-13", Islamabad: Ministry of Finance, 2013.

[xv]. World Bank, "Urban population (% of total)", United Nations, World Urbanization Prospects, Available at: http://data.worldbank.org/indicator/SP.URB.TOTL.IN.ZS[accessed November 15, 2016].

[xvi]. GOP, "Monthly bulletin of statistics", Islamabad: Statistics Division, Statistics Bureau of Pakistan, Feb., 2016.

[xvii]. T. Nenova, "Expanding housing finance to the underserved in South Asia: Market review and forward agenda", The International Bank for Reconstruction and Development / World Bank, Washington DC, 2010.

[xviii].A. Hassan, "Karachi: The housing imperative", Dawn, 16 June 2011. Available at: http://arifhasan.org/articles/karachi-the-housing-imperative, [accessed November 26, 2016].

[xix]. H. Shaikh, "Housing inequality in Pakistan: The case of affordable housing", International Growth Centre Note, February 2016. Available at: http://cdpr.org.pk/wp-content/uploads/2016/02/IGC-Pakistan-2016-Policy-note.pdf [accessed November 26, 2016].

[xx]. GoPb, "Punjab growth strategy 2018 first draft: Accelerating economic growth and social outcomes", Planning and Development Department, Government of Punjab, Lahore, 2013.

[xxi]. S. S. H. Zaidi, "The sites and services schemes and the problem of low-income housing in Lahore, Research Journal, UET, Lahore, 1993.

[xxii]. World Bank, "World development indicators", The International Bank for Reconstruction and Development / World Bank, Washington DC, 2012.

[xxiii]. R. M. Kahloon, "Aashiana housing project", Quarterly Research and News, No. 14-15, Centre for Public Policy and Governance, FC College, (A Chartered University), Lahore, 2011.

[xxiv].GoPb, "Punjab private housing schemes and subdivision rules 2010", Local Government and Community Development Department, Government of the Punjab, Lahore, 2010.

[xxv]. K. Zaman, and A. A. Baloch, "Urbanization of arable land in Lahore city in Pakistan: A case study", Journal of Agricultural Biotechnology and Sustainable Development, 3(7), 126 -135, 2011.

[xxvi].GoPb, "Punjab development statistics 2012", Bureau of Statistics, Government of Punjab, Lahore, 2012.

[xxvii]. G. A. Anjum, and R. Hameed, "The dynamics of colonization of peripheral housing schemes and policy options in case of Lahore", Pak. J. Engg. & Appl. Sci., Vol. 1, pp. 24-30, 2007.

[xxviii]. R. Kumar, "Research methodology: A step by step guide for beginners", Second edition, Pearson Education, India, 2005.

[xxix].NESPAK/LDA, "Integrated master plan for Lahore-2021", Lahore: National Engineering Services (Pvt) Ltd. and Lahore Development Authority, 2004.

[xxx]. GoPb. "Assessment of urban land development and management practices in five large cities of Punjab", Draft Final Report, The Urban Unit, Planning and Development Department, Government of Punjab, Lahore, 2010.

[xxxi].Tabassum, S. (2013), Role of private sector in accommodating low income groups in housing schemes approved by Lahore Development Authority, Lahore, City & Regional Planning Department, University of Engineering & Technology, Lahore.

Development of Stable Channel Design Equations - Using a New Approach

M. Ashiq[1], K. Zahra[2]

[1] Department of Civil Engineering, University of Engineering and Technology, Lahore
[2] Department of Civil Engineering, University of Toronto, Canada
[1]mashiqk@yahoo.come

Abstract-— This study was aimed at the developing a new set of equations for the design of channels involving concentration (ordinary channels) and sinuosity (curved channels). The six well known channel design equations were evaluated with the different data sets before developing the new equations. These existing equations showed huge inconsistencies in results and these inconsistencies varied from equation to equation and method to method. The data used in the development of the new equations were obtained from the North American, European, and Asian continents. The new equations were developed using two approaches, with and without involving the earlier computed variables in the following equations. Performance tests of these equations showed encouraging results.

Keywords- Equations, Stable Channel, Regime Channel, Sinuosity, Performance, Lacey Equation, Tractive Force.

I. Introduction

In efforts of advancing the regime or stable channel design approaches, the investigators have moved from simple empirical equations to complex mathematical, analytical and numerical methods. These mathematical, analytical and numerical methods are questionable due to various assumptions and boundary conditions associated with them and these complex methods do not always guarantee the improved results. For example, authors of [i] developed mathematical models for depth and width of channel cross-sections for the straight sand rivers. However, these mathematical models are based on seven additional assumptions to the basic flow equations. Many methods involve spur correlations and are based on the laboratory studies which used the small width channels/flumes. Therefore, the behavior of these methods is unknown for the real field conditions as mentioned by many investigators such as Reference [ii] in their article "Hans Albert Einstein: Innovation and Compromise in Formulating Sediment Transport by Rivers". They stated that "commonly, the practical design engineer and the scientist in the field have found the empirical approach more practicable and have been more skeptical of sophisticated, predictive methods based on advanced fluid mechanics and data from laboratory flumes."

Seven decades have passed since [iii] developed his regime equations which have been successfully used to design the thousand of miles of channels in the world and these channels are still in good conditions. On the other hand, the tractive force method has its own advantages and it is mostly applied in the USA. In Canada, the regime and tractive force methods have been applied, depending on the prevailing situation. The simplicity, popularity, and significance of these design methods (regime and tractive force) suggest further research for their refinements and applications.

This study was, therefore, designed to test the validity of the existing channel design equations based on the regime and tractive force theories and to develop the new equations involving concentration and sinuosity parameters by using adequate field data obtained from different part of the world.

II. Performance Test of Important Existing Equations

Before developing the new equations for the design of channels in alluvial materials, six well known equations [iii-viii] based on both regime and tractive force methods, were evaluated and tested. These equations are presented in Table I.

To carry out extensive performance tests, a large amount of data were compiled from the different published sources, such as 312 data sets from Canada [ix]; 68 data sets from Ireland [x]; 305 data sets by U.S Army Corps of Engineers [xi]; 33 data sets form Indian canals [xii]; and 55 data sets by [xiii].

Most of the data sets have had large variations for all parameters of discharge, width, depth, slope, bed materials etc. Therefore, the minimum, maximum, average, median and standard deviation for all the data sets were computed to determine the data ranges/limits.

TABLE-I
DIFFERENT SETS OF EQUATIONS SELECTED FOR TESTING

Originator	Equations
Lacey (1929)	$P = 2.67\sqrt{Q}$, $R = 0.474\left(\frac{Q}{f}\right)^{1/3}$, $V = 1.154\sqrt{fR}$, $S = 0.0005423\frac{f^{5/3}}{Q^{1/6}}$
Stevens and Nordin (1990)	$A = 5.63\left(\frac{Q^{5/6}}{C^{1/3}}\right)$, $V = 0.178Q^{1/6}C^{1/3}$, $R = 2.11\left(\frac{Q}{C}\right)^{1/3}$, $P = 2.67Q^{1/2}$, $S = \left(\frac{C^{5/3}}{3{,}340{,}000Q^{1/6}}\right)$
Blench (1970)	$b = \sqrt{\frac{f_b}{f_s}\,x\,Q}$, $d = \sqrt[3]{\frac{f_s Q}{f_b^2}}$, $S = \frac{f_b^{0.83} f_s^{0.08}}{KQ^{0.16}\left(1+\frac{C}{233}\right)}$, $f_b = V^2/d$, $K = \frac{3.63g}{\nu^{0.25}}$, $f_b = 9.6\sqrt{d}\left(1+0.012C\right)$, $f_s = V^3/b$
Julien and Wargadalam (1995)	$W = 1.33Q^{2+4m/(5+6m)}d_s^{-4m/(5+6m)}S^{-1-2m/(5+6m)}$ $h = 0.2Q^{2/(5+6m)}d_s^{6m/(5+6m)}S^{-1/(5+6m)}$ $V = 3.76Q^{1+2m/(5+6m)}d_s^{-2m/(5+6m)}S^{2+2m/(5+6m)}$ $\tau_* = 0.121Q^{2/(5+6m)}d_s^{-5/(5+6m)}S^{4+6m/(5+6m)}$
Schumm (1977)	$P = 0.94M^{0.25}$, $D = 0.6M^{0.342}Q^{0.29}$, $W = 37\frac{Q^{0.38}}{M^{0.39}}$, $S = \frac{60}{M^{0.38}Q^{0.32}}$, $\lambda = 1890\frac{Q^{0.34}}{M^{0.74}}$
Kellerhals (1972)	$W_{sm} = 1.8Q^{0.5}$, $D = 0.256Q^{0.331}\left(D_g(50)\right)^{-0.025}$, $S = 0.096Q^{-0.344}\left\{D_g(50)\right\}^{0.586}$

Note: Please see the cited references for the description of variables in the above equations.

To test the performance of the existing equations, the computed values of width (W), depth (D), and slope (S) were plotted versus the observed values by using the line of perfect agreement (LPA) as a standard (Figures 1-4). The mean of the discrepancy ratios (DR, ratio of computed to observed values) and the standard deviation of the above parameters were determined which are given in Table II. During the tests, with the Canadian data, the performance of Stevens and Nordin equation was found to be the best one which was followed by Blench, Kellerhals and Lacey equations for the width and depth parameters, respectively. This trend was changed while test was conducted with the Irish data, in which Kellerhals equation proved the best one followed by Lacey, Blench and Stevens, and Nordin equations, respectively.

While for the Corps of Engineers, India canals, and Lepold data sets the performance of the Blench equation was the best one, followed by Stevens and Nordin and Lacey's formulas, respectively, for the width and depth parameters. Nonetheless, the performance of all these equations for slope parameter, for all the data sets, was generally found to be very poor. The performance of Julien and Wargadalam's equation was generally better for the 'V' parameter as compared to W and D.

for the Corps of Engineers, India canals and Leopold data sets that were contrary to its performance for Canada and Irish data when it performed better for the H parameter. Based upon all these test results, it can be concluded that the performance of the Blench, and Stevens and Nordin equations was the best and close to each other although Blench's equation has an edge, followed by Lacey and Kellerhals.

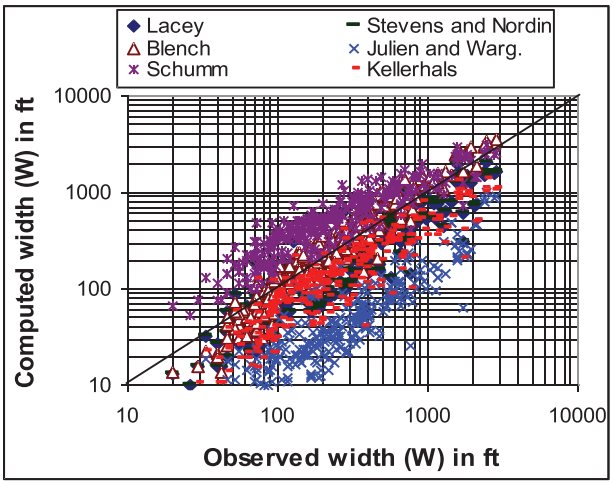

(a)

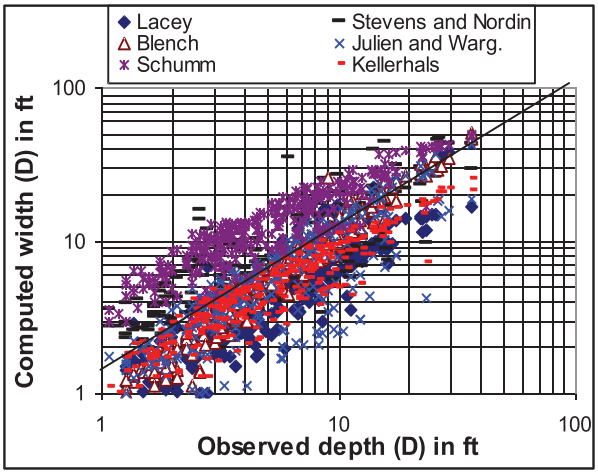

(b)

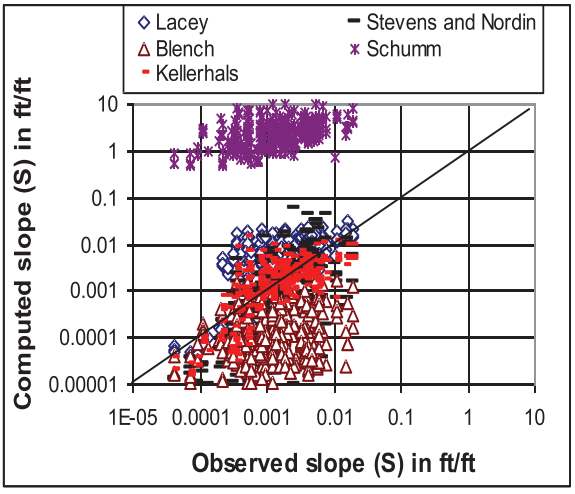

(c)

Fig. 1: Comparison of computed and observed values using Canadian data for: a) width, b) depth, and c) slope parameters.

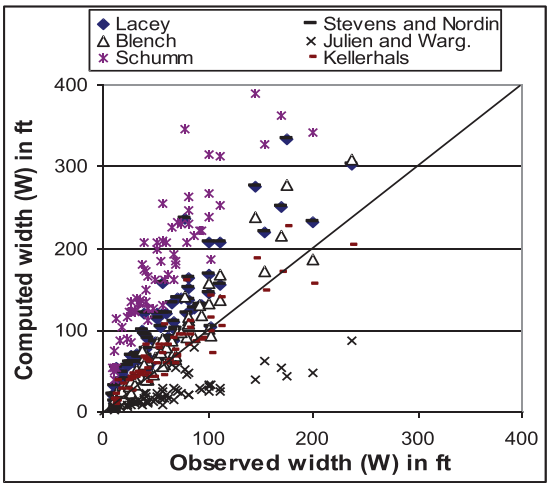

(a)

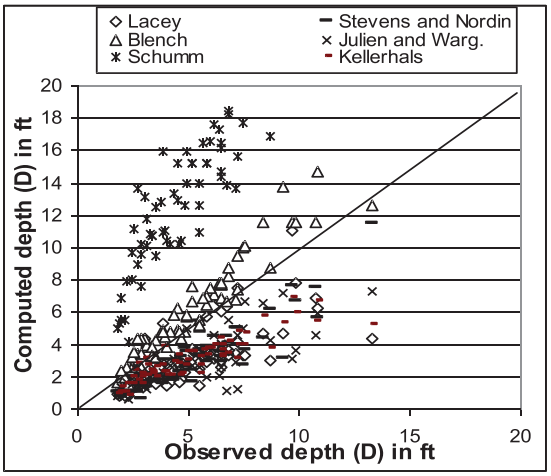

(b)

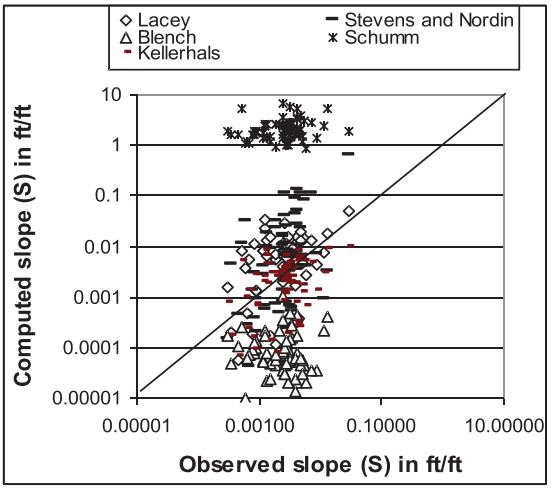

(c)

Fig. 2: Comparison of computed and observed values using Irish data for: a) width, b) depth, and c) slope parameters.

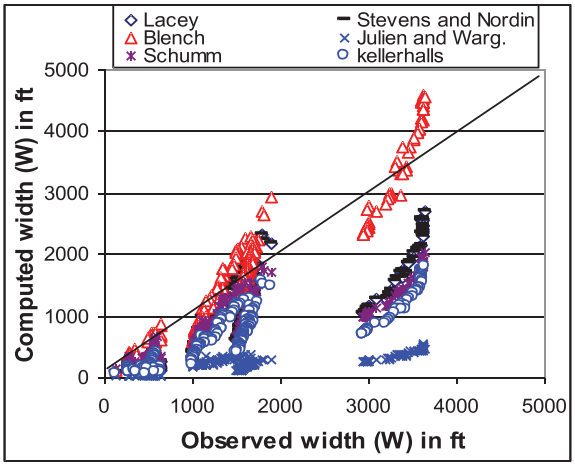

(a)

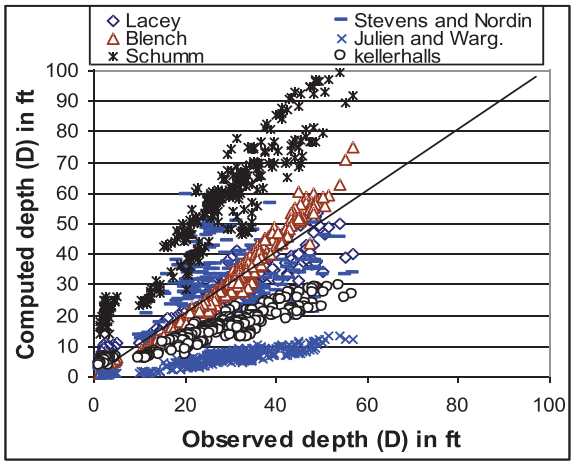

(b)

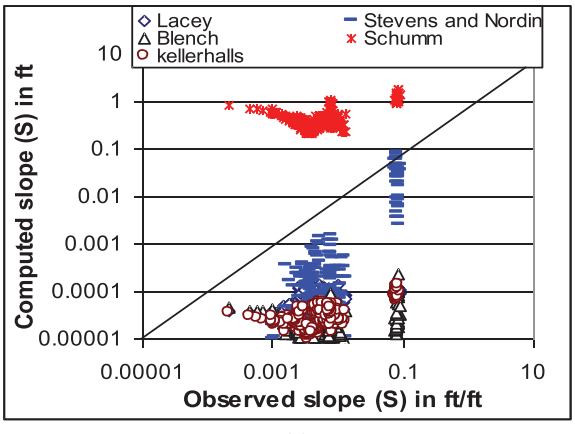

(c)

Fig. 3: Comparison of computed and observed values using Corps of Engineers data for: a) width, b) depth, and c) slope parameters.

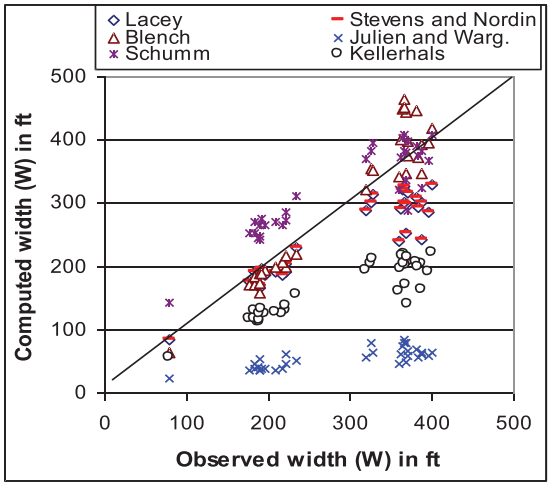

(a)

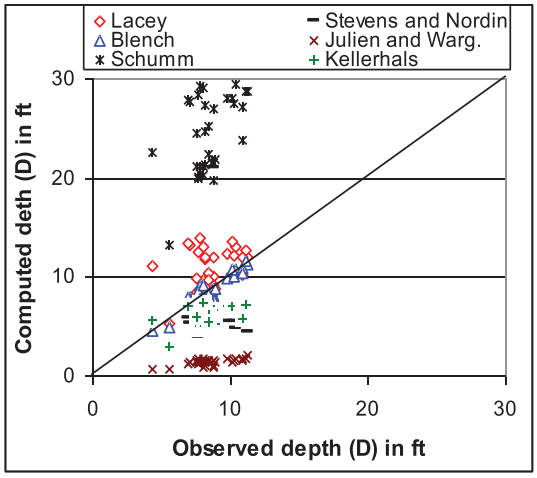

(b)

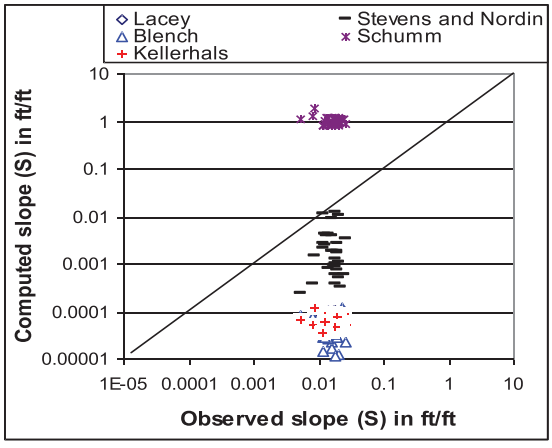

(c)

Fig. 4: Comparison of computed and observed values using Indian Canals data for: a) width, b) depth, and c) slope parameters.

TABLE-II
MEAN DISCREPANCY RATIOS (DR) AND STANDARD DEVIATION (STD) VALUES COMPUTED BY USING DIFFERENT EQUATIONS.

Equations	DR &STD	Canada Data			Irish Data			Corps data			India canals data			Leopold data		
	mean	W	H	S	W	H	S	W	H	S	W	H	S	W	H	S
Lacey	DR Mean	0.8754	0.8605	5.6351	1.9145	0.6036	3.5757	0.6584	1.2541	0.0135	0.8650	1.2897	0.0049	0.6621	1.2539	0.0065
(1929)	DR Standev	0.3875	0.3118	6.5196	0.5812	0.2389	4.5805	0.2129	0.8957	0.0146	0.1193	0.3528	0.0025	0.1311	0.2612	0.0042
Stevens and	DR Mean	0.8754	1.4079	1.1155	1.9145	0.5643	11.9451	0.6584	1.0580	0.0764	0.8650	0.7347	0.1796	0.6621	1.0253	0.0311
Nordin(1990)	DR Standev	0.3875	0.7560	2.1847	0.5812	0.1523	46.1911	0.2129	0.4216	0.1684	0.1193	0.3455	0.2190	0.1311	0.2870	0.0491
Blench(1970)	DR Mean	1.1730	1.1073	0.2211	1.2705	1.1660	0.0683	1.0300	1.0148	0.0067	1.0129	1.0071	0.0036	0.9072	0.9360	0.0051
	DR Standev	0.3521	0.2465	0.4244	0.2893	0.1790	0.1064	0.2104	0.1395	0.0158	0.1110	0.0728	0.0033	0.0845	0.0590	0.0032
Schumm	DR Mean	2.3404	2.5622	3312.3051	3.6168	2.8609	1258.5933	0.6567	2.8089	132.8765	1.1797	2.9420	72.4172	0.8743	3.0038	70.4451
(1977)	DR Standev	1.0156	0.8000	4673.6503	1.3259	0.6378	1435.1723	0.1940	2.3475	279.2557	0.2233	0.6370	44.2149	0.1615	0.5778	41.4366
Kellerhals	DR Mean	0.5902	0.9428	1.5826	1.2907	0.6264	1.2238	0.4438	0.7340	0.0073	0.5831	0.7252	0.0044	0.4463	0.7375	0.0050
(1967)	DR Standev	0.2612	0.2663	2.5958	0.3918	0.1366	1.5186	0.1436	0.5371	0.0117	0.0805	0.1687	0.0027	0.0884	0.1360	0.0030
Julien and	DR Mean	0.1917	1.0898	V = 0.190	0.3942	0.6024	V = 0.145	0.1401	0.2276	V = 1.014	0.1963	0.1689	V =0.899	0.1353	0.1975	V=1.114
Warg.(1995)	DR Standev	0.1305	0.4022	V= 0.097	0.1609	0.1786	V = 0.060	0.0503	0.0709	V = 0.248	0.0420	0.0301	V =0.192	0.0251	0.0361	V=0.253

*For Julien and Wargadalam equation under the S (slope) column the values given are for the velocity, not for slope.

III. DEVELOPMENT OF EQUATIONS

Due to the inconsistent and poor performance of the existing equations, especially for the slope parameter, it was decided to develop new equations comprising of some variables that were not used in the tested equations. The new equations were developed using both linear and non-linear approaches. The different sets of linear and nonlinear equations were developed for determining the channel width, depth, slope, and velocity parameters. In the development of these equations, two approaches were used: i) preceding variables were used in the development of the following equations (here-in-after called as 'with earlier computed variables, WECV'); and ii) preceding variables were not used in the development of the following equations (here-in-after called as 'without earlier computed variables, WOECV'). The equations developed using the former approach showed slightly better values of the correlation coefficients. Among the linear and nonlinear equations, the nonlinear method gave better correlation coefficient values. Therefore, nonlinear equations were selected for further evaluation.

A. The developed equations involving the sediment concentration parameters are given below. In the development of these equations, the data were obtained from 'A Compendium of Solid Transport Data for Mobile Boundary Channels' and comprising of 770 data sets.

WECV Equations:

$$W = 10.68\frac{Q^{0.40}}{d_{50}^{0.18}C^{0.0225}} \quad (1)$$

$$D = 0.513\frac{Q^{0.681}}{d_{50}^{0.183}C^{0.10}W^{0.568}} \quad (2)$$

$$S = 0.203\frac{Q^{0.723}d_{50}^{0.426}C^{0.123}}{W^{0.972}D^{1.474}} \quad (3)$$

WOECV Equations:

$$W = 10.68\frac{Q^{0.40}}{d_{50}^{0.18}C^{0.0225}} \quad (4)$$

$$D = 0.134\frac{Q^{0.454}}{d_{50}^{0.0811}C^{0.0875}} \quad (5)$$

$$S = 0.393\frac{d_{50}^{0.721}C^{0.274}}{Q^{0.335}} \quad (6)$$

Where W, Q, d50, C, D, S, and V represent the channel width (ft), discharge (ft3/s), bed material size (mm), sediment concentration (PPHT), depth (ft), slope (ft/ft), and velocity (ft/s), respectively. The value of C may be determined using the expression, $C = 875.9 - 199.0\ln d_{50}$.

The performance of these equations (Eqs. 1-6) was tested using Portugal data (219 data sets) and Nordge and Bragg Creek data (188 data sets). Among the two types of equations, WECV and WOECV, the latter type (Eqs. 4-6) performed relatively better with mean DR values of 0.845, 1.167, and 0.994 for the Portuagl data and 1.235, 0.928, and 1.198 for the Nordge and Bragg Creek data. While for the former type of equations (Eqs 1-3) the mean DR values were 0.845, 1.162 and 1.28 for the Portugal data and 1.235, 0.925 and 1.524 for the Nordge and Bragg Creek.

B. For channels having sinuous course, the equations were developed using sinuosity parameters and Canadian data from Catalogue of Alluvial Rivers. Similar to the earlier mentioned equations involving concentration (given in 'A'), these equations were also developed both with and without using the preceding variables. The developed equations are given below.

WECV Equations:

$$W = 8.22\frac{Q^{0.424}}{d_{50}^{0.046}s^{0.277}} \quad (7)$$

$$D = 0.498\frac{Q^{0.409}s^{0.302}}{d_{50}^{0.079}W^{0.185}} \quad (8)$$

$$S = 0.0033\frac{Q^{0.852}d_{50}^{0.182}}{s^{0.196}W^{1.025}D^{1.951}} \quad (9)$$

$$V = 1.101\frac{Q^{0.90}d_{50}^{0.0021}S^{0.023}}{s^{0.00572}W^{0.867}D^{0.883}} \quad (10)$$

WOECV Equations:

$$W = 8.22\frac{Q^{0.424}}{d_{50}^{0.046}s^{0.277}} \quad (11)$$

$$D = 0.338\frac{Q^{0.331}}{d_{50}^{0.07}s^{0.354}} \quad (12)$$

$$S = 0.00312\frac{d_{50}^{0.366}}{Q^{0.229}s^{0.602}} \quad (13)$$

$$V = 0.405\frac{Q^{0.235}d_{50}^{0.112}}{s^{0.0914}} \quad (14)$$

Where sinuosity, s, parameter can be determined using the expression;

$$s = 1.72\,Q^{-0.0281}$$

As the results from the performance test for the WECV and WOECV equations in section 'A', the performance of the WOECV type equations (Eqs. 11-14) was relatively better with mean DR values of 1.117, 0.838, 1.333, and 1.028; with the exception of equation 12 (for D parameter) for which mean DR value was smaller than the WECV type equation (Eqs. 8) while the mean DR values were found to be 1.117, 1.032, 1.376 and 1.088 for the WECV type equations (Eqs. 7-10), respectively.

Some of the geomorphic relations obtained in this study are different from those stated by Stevens and Nordin [xiv]. The Stevens and Nordin's geomorphic relations and those obtained in this study are compared in Table III.

IV. Conclusions

Performance of six channel design equations, form the regime and tractive force approaches, was tested using data from various regions of the world and found to be generally inconsistent with each other. These equations predicted the slope parameter poorly. However, the performance of the Blench, and Stevens and Nordin equations was found to be the best.

Two sets of nonlinear equations involving concentration (Eqs. 4-6) and sinuosity (Eqs. 11-14) parameter were developed and suggested. These equations performed well for the prediction of all the four variables of width, depth, slope and velocity when tested with two different data sets from Portugal and Nordge and Bragg Creek.

TABLE-III
GEOMORPHIC RELATIONS OF STEVENS AND NORDIN (1987) AND THOSE OBTAINED DURING THIS STUDY

Sr. No.	Stevens and Nordin		Data from Catalogue of Alluvial Rivers (312 data sets)		Data from Compandium of Solid Transport (800 datasets)	
	Relation	Coefficient	Relation	Coefficient	Relation	Coefficient
1	$W \sim Q^{1/2}$	-----	$W \sim Q^{0.44}$	5.77	$W \sim Q^{1/2}$	3.21
2	$D \sim Q^{1/3}$	-----	$D \sim Q^{1/3}$	0.30	$D \sim Q^{1/2}$	0.062
3	$S \sim Q^{-1/6}$	-----	$S \sim Q^{-1/4}$	0.011	$S \sim Q^{-0.81}$	86.66
4	$V \sim Q^{1/6}$	-----	$V \sim Q^{0.22}$	0.64	-----	-----

REFERENCES

[i] S. Ikeda and N. Izumi (1991). "Stable channel cross sections of straight sand rivers," Water Resources Research, 27(9), pp 2429 - 2438.

[ii] E. Ettema and C. Mutel (2004). "Hans Albert Einstein: innovation and compromise in formulating sediment transport by rivers," Journal of Hydraulic Engineering, ASCE, 130(6), pp 477-487.

[iii] C.Lacey (1929). "Stable channel in alluvium,"Proc. Institution of Civil Engineers, London,Vol. 229

[iv] M.A. Stevens and C.F. Norden (1990). "First step away from Lacey' regime equations," Journal of Hydraulic Engineering, ASCE, 116(11), pp 1422-1425.

[v] T. Blench (1970). "Regime theory design of canals with sand beds," Journal of Irrigation and drainage, ASCE, 96(2), pp 205-213.

[vi] P.Y. Julien and J. Wargadalam (1995)." Alluvial channel geometry: theory and application," Journal of Hydraulic Engineering, ASCE, 121(4), pp 312-325.

[vii] S.A. Schumm (1977). The Fluvial Systems. John Wiley & Sons Ltd, New York.

[viii] R. Kellerhals (1972). "Stables channels with gravel-paved beds.," Journal of the Waterways and Harbors Divisions, ASCE, pp 63-84.

[ix] M. Church and R. Rood (1983). "Catalogue of alluvial river channel regime data," Rep., Dept. of Geography, Univ. of British Columbia, Vancouver, Canada.

[x] R.D. Hey and G.L. Heritage (1988). "Dimensional and dimensionless regime equations for gravel bed rivers," Proc. International Conference on River Regime. John Wiley and Sons. Ltd. (UK), Paper A1, May 18-20.

[xi] F.B. Toffaleti (1968). "A procedure for computation of the total river sand discharge and detailed distribution, bed to surface," Technical Report No.5, Committee of Channel Stabilization, Corps of Engineers, U.S. Army.

[xii] H.M. Chaudhry, K.V.H. Smith and H. Vigil (1970). "Computation of sediment transport in irrigation canals," Proc. Institution of Civil Engineers, Vol. 45, Paper 7241, pp 79-101.

[xiii] L.B. Leopold (1969). "Personal Communication, "Sediment Transport data for various U.S. Rivers (adopted from Peterson and Howells 1978).

[xiv] M.A. Stevens and C.F. Norden (1987). "Critique of the regime theory for alluvial channels," Journal of Hydraulic Engineering, ASCE, 113 (11), pp 1359-1380.

Geometrically Optimum Design of Steel Portal Frames

S. N. R. Shah[1], Muhammad Aslam[2], N H R Sulong[3]

[1]Civil Engineering Department, Mehran University of Engineering & Technology, SZAB Campus, Khairpur Mir's, Pakistan
[2-3]Civil Engineering Department, University of Malaya, Kuala Lumpur, Malaysia
naveedshah@muetkhp.edu.pk

Abstract-Portal frames cover a high percentage of steel construction and demand flexible optimum cost solutions for design and construction purposes. This study determines the effects of change in geometry of portal frames on overall cost of the structure in terms of self-weight and will help practical designers to choose a quick economical bay spacing. The total width of portal frame was kept constant and change of bay width between portals and influence of shorter and larger span on portal design were the parameters under investigation. Initially, a 2D plastic analysis was performed on six different pinned base portal frames with varied span and bay spacing. The optimization was performed on the basis of member sizes and total weight of the frames. The most effective geometry was found to be the least selected bay width with shorter span. A 2D non-linear Finite Element (FE) model, reflecting actual lateral load field conditions, was then developed to validate the design of achieved optimal geometry of portal frames.

Keywords-Steel portal frames, geometrical optimization; bay spacing; strength-to-weight, finite element analysis

I. INTRODUCTION

In recent years, portal frames have become a must-to-adopt option to use as an industrial building. These structures offer sufficient open space and effective use of allocated land available in the building for industrial and storage purposes [i]. The versatility of these frames also lies in the facility of providing different eaves levels and openings in the same structure [i]. Moreover, internal columns can be easily replaced by valley beams in the case of multi-span portal frames. To support the future construction, built-in provisions for the building can be made at the design stage. Additionally, the excellent strength-to-weight ratio enables these frame in carrying

sufficient load and required spanning, satisfactorily. 'I' and 'H' sections are mainly used for columns and rafters in portal frames, however, for long span multi-bay portal frames, a few researchers focused to execute other types of cold-formed steel sections [i]. Portal frames carry high imposed loads and support the application of plastic analysis method in steel structures. If an elastic design is desired to be carried out, a torsional restraint must be provided under the haunch to maintain column stability. For the rafters, high bending moment in the plane of frame is the point of concentration for design process [ii]. A sagging moment near apex travels to the junction of rafter and column to create a high value hogging bending moment. In addition, rafters also sustain global compression due to the frame action [ii]. The behaviour of connections constituting the portal frame is significantly important [i]. These connections are the rafter-apex connection, column-base and the column-rafter connections and the connection between bracing members [i]. The connections either may be welded or bolted using gusset plates connected with the web of sections. Mainly, the column-rafter connections are designed to be moment-resisting in order to transfer bending moment from rafters to columns. This helps to reduce the size of rafter and to increase the span of frame with similar rafter size.

The use of cold-formed steel in several unique types of steel construction is widely recognized [ii-iv]. Further, the growing number of portal frame buildings with steel frames clearly shows the ability of structural steelwork to comfortably meet all of the requirements including minimum possible design and construction expenditures. For instance, the United Kingdom consumes 50% of the produced hot-rolled steel in single-storey buildings, mainly in portal frames [v]. A few studies have also brought to light more benefits of using cold-formed steel sections instead of traditional hot-rolled steel [vi, vii]. The major advantage of using cold-formed steel is that the weight and cost of a portal frame structure can be estimated precisely by the manufacturer which may pave the way for better structural optimization of portal frames.

The optimization of portal frames by analysing the effect of different geometries has not been discussed in the past. This research follows a simple approach and examines the influence of geometrical shapes on overall weight of structure by performing a plastic analysis using Quicksoft software. The model building

was assumed to be located in Kuala Lumpur, Malaysia. BS5950 was referred to apply loading combinations and selection of member sizes. The total width of portal frame was kept constant and change of bay width between portals and influence of shorter and larger span on portal design was observed. Later, a non-linear FE model using Abaqus 6.13.4 [viii] was prepared based on the most optimal geometry. The model was prepared based on accurate field conditions and the results of linear analysis were validated. The effects of design decision, fabrication and erection on overall cost of whole project are also discussed.

II. Literature Review

The cost of material plays less than 50% role in optimizing a project [v]. The detailing, fabrication, erection and protection cover almost 60% cost of the project [ix]. The structural optimization in steel can be widely categorized into design and construction optimization. Furthermore, fabrication also makes a bridge in between design and construction. Recent researches in optimizing steel structures mainly focus on the concept of optimization during design process which is based on mathematical programming. Often used methods of design optimization are: Adaptive Random Search, Completive Evolution, Controlled Random Search, Simulated Annealing, Genetic Algorithms, Differential Evolution, and Particle Swarm Optimization [x]. Though, compared with construction optimization techniques, design optimization has more advantages because it does not require differential information other than the objective function, however, it is more difficult to be implemented as it depends on the gradient information about the objective function. Additionally, the involvement of Genetic Algorithms (GA) makes it more complex and lengthy process to apply [x].

The use of GA to optimize portal frames is well established. Reference [xi] considered the cross-section sizes of the columns and rafters, and both length and depth of the haunch as discrete variables using a binary-coded GA to achieve minimum weight of a portal frame under imposed load only. Position of lateral and torsional restraints was fixed under eaves haunch. He concluded with suitable universal beam and haunch sizes for his structure. The optimization of the same model, used by Saka, was further extended by Reference [xii]. They applied distributed GAs to minimize the weight of the structure and resulted with suitable column and rafter sizes. Reference [vii] used a Real-Coded GA to optimize the topography of portal frames and presented a précised optimum solution. Significantly, they replaced the hot-rolled steel sections with cold-formed steel.

A number of researches have performed serviceability design optimization. Reference [xiii] discussed the elastic design optimization technique of a single-storey steel building. Authors of [v] adopted two criteria to determine the serviceability deflection limit of portal frames; one suggested by Steel Construction Institute (SCI) and the other by industry. Their proposed GA was useful and demonstrated that the industry deflection limits are suitable to design deflection limits of their proposed portal frame model.
The consideration about the working relationship between geometrical design of a structure and the optimization techniques during the manufacturing, fabrication and erection of the structure is rarely available. The literature reveals only a few studies applying design optimization methods to minimize the overall weight as well as cost of portal frames. Discussing the effects of geometry on portal frame optimization, reference [xiv] investigated the influence of using inclined columns in portal frames. His conclusion indicated that applying proper inclination to columns can increase the buckling load capacity of portal frames; hence, a more economical design can be achieved. Reference [xv] introduced the concept that using semi-rigid connections in portal frames considerably reduces the overall weight of structure. Authors of [xvi] also emphasized on using semi-rigid connections and performed design optimization operations focussing serviceability conditions in portal frames. Reference [xvii] applied design algorithms to achieve the minimum weight design of steel frames.

II. Model Details

2.1. Layout

Two different types of layouts were selected for design purpose with different spacing. The span is 15 m for Structure 'A' and 30 m for Structure 'B'. The spacing of frames for both structures (bay width) varies as 5m, 6m and 7.5m, as shown in Figure 1, 2, 3, 4, 5 and 6 respectively, to achieve the optimum design of proposed steel portal frame. Eaves height is 7m and roof pitch is considered as 6°. The bases were assumed as pinned. The length of the haunch was measured from the centre of the column to the end of haunch and limited to 10% of the frame span in each case as illustrated in Figure 7. The depth of haunch was considered from underside of the rafter till its end. Light weight metal sheeting rails spanning between the columns of portal frame were used to counter adverse environmental impacts.

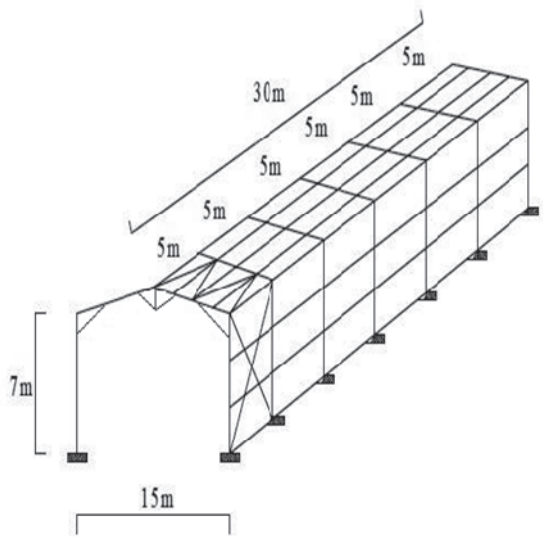

Fig.1. 5m Bay spacing in structure - A

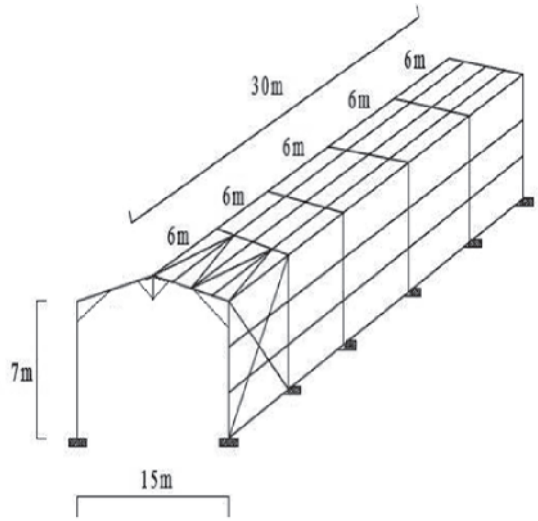

Fig.2. 6m Bay spacing in structure - A

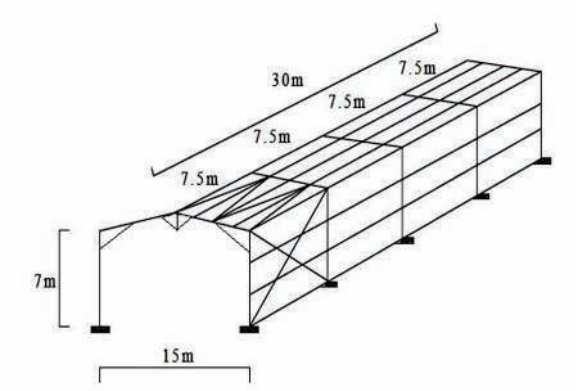

Fig.3. 7.5m Bay spacing in structure - A

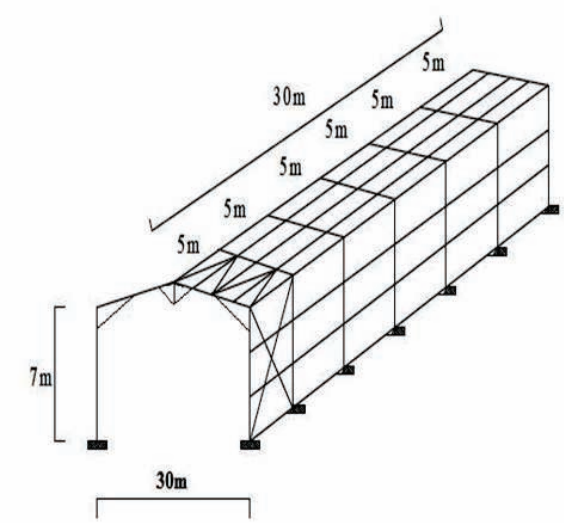

Fig.4. 5m Bay spacing in structure - B

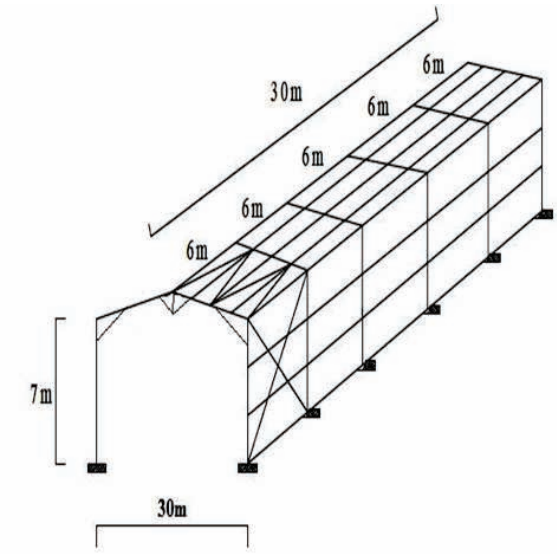

Fig.5. 6 m Bay spacing in structure – B

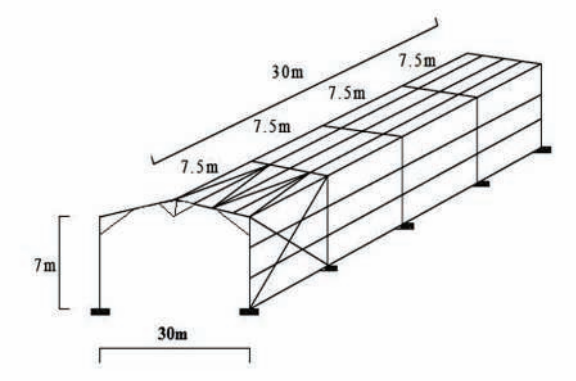

Fig.6. 7.5m Bay spacing in structure – B

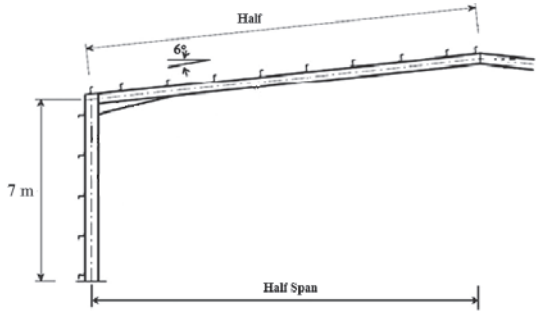

Fig.7. Eaves and haunches details

2.2. Section properties

Universal column (UC) and universal beam (UB) steel sections were proposed as columns and rafters respectively. The material properties were selected according to the most commonly used sections in the portal frames in the Malaysian construction industry and are given in Table I. Eaves haunch was designed following typical plastic design of portal frames. The haunches were supposed to be fabricated from the same section size of the rafter. Cold-formed C-section purlins were assumed at the roof. The weight of purlins is not considered in this study.

TABLE I
BASIC SECTION PROPERTIES

Connecting member	Steel grade (MPa)	Young's Modulus (GPa)	Poison's ratio	Yield strength f_y (MPa)	Ultimate strength f_u (MPa)
Column	275	205	0.3	255	410
Rafter					
Purlin C-Section	-	210	0.3	305	550

2.3. Loading and design

The building is assumed to be located in Kuala Lumpur, Malaysia and data for wind loading and site distance from the sea was assumed according to the location [xviii]. The dead load and live load were considered as 0.66 kN/m2 and 0.60 kN/m2 respectively. BS 5950 [xix] was referred to assign section sizes and loading combinations and frame was checked for ultimate limit state and serviceability limit state. The frame is assumed to fulfil the criteria for in-plane stability of the sway check method and does not take into account the second order effects for analysis and design purpose. A plastic analysis was performed by using software named Quiksoft programme [xx]. The frames are analysed and designed through QuikPort analysis and design. The connections between columns and rafters were considered as moment resisting connections. All the connections were analysed and designed through QuikJoint program.

2.4. Optimization technique

A simple optimization technique based on trial of different geometries was adopted to optimize the structure. Keeping the total width of frames constant, the parameters considered for investigation are: (i) span of frames and (ii) variable bay widths.

II. RESULTS AND DISCUSSION

Table II summarizes the results obtained by the plastic analysis of single bay portal frame with different bay spacing and varied span. Spacing of 5m and 6m does not have much difference in the cases of both structure A. The weight of columns for 7.5m spacing is slightly greater than for 5m and 6m bay spacing. Consequently, the total weight also has small difference for all the types of spacing. Therefore, for overall cost of frame, it may be possible that there would be less cost require for fabrication and connection material and construction for higher bay spacing and overall cost may be equivalent to 5m bay spacing.

TABLE II
DIMENSIONS AND WEIGHT INFORMATION OF MEMBERS DESIGNED FOR ALL THREE FRAMES FOR STRUCTURES-A AND THREE FOR STRUCTURES-B

Structures	Total width (m)	Details		Spacing		
			-	5 m	6 m	7.5 m
"A"	15	Columns (2 bars per frame)	Dimensions	305*305*97UC	305*305*97UC	305*305*118UC
			Weight (tonnes)	1.163	1.163	1.415
		Rafters (2 bars per frame)	Dimensions	356*171*57UB	406*178*67UB	457*191*74UB
			Weight (tonnes)	0.873	1.030	1.139
		Total weight (tonnes)		2.036	2.193	2.554
"B"	30	Details		Spacing		
			-	5 m	6 m	7.5 m
		Columns (2 bars per frame)	Dimensions	305*305*240UC	305*305*283UC	356*406*340UC
			Weight (tonnes)	2.881	3.395	4.079
		Rafters (2 bars per frame)	Dimensions	610*305*179UB	610*305*179UB	610*305*238UB
			Weight (tonnes)	5.491	5.491	7.303
		Total weight (tonnes)		8.372	8.388	11.382

The effect of larger span greatly influenced on total weight of structure. The weight of columns with 7.5m bay spacing in structure B is almost twice of the weight of frame with 5m bay spacing. Comparison of 5m and 6m bay spacing exhibited that there is no change in rafter sizes for both frames, however, the column sizes slightly increased in 6m bay spacing. The overall weight of 7.5m bay spacing frame is highest again and it can be said that 5m bay spacing is the optimized spacing in terms of overall weight.

Figure 8 illustrates slight changes in overall weight of structure A with all types of spacing. However, increase in span influenced with higher weight members for all bay spacing choices. The weight of frame with 7.5m bay spacing in structure B is almost 4.5 times greater than the same frame in structure A. This shows that larger span has greatly affected the weight of the frame.

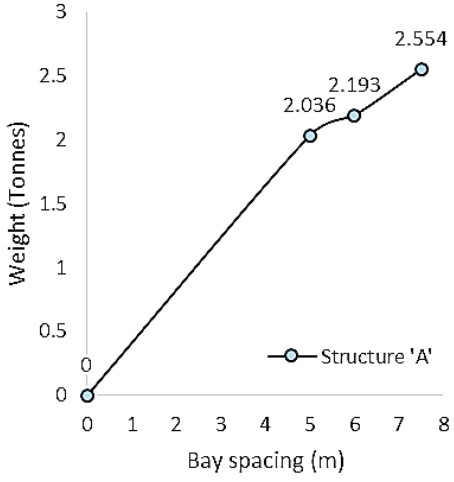

(a)

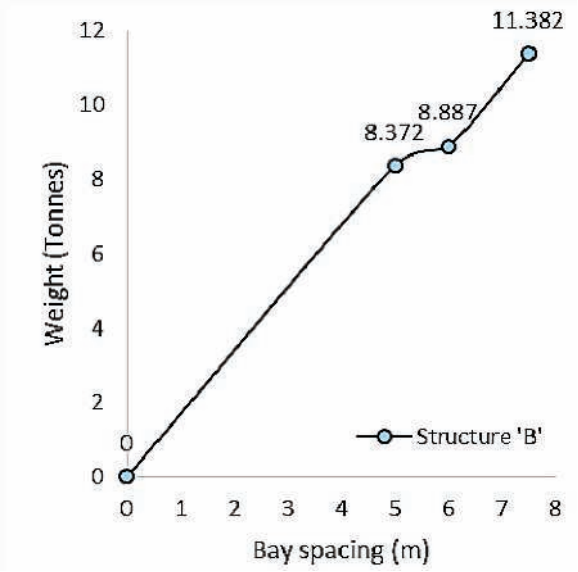

(b)

Fig.8. Variation in Total weight of Columns and Rafters according to change in spacing; (a) Structure 'A',
(b) Structure 'B'

IV. Finite Element Analysis

A FE model using Abaqus software was developed for all of the portal frames. A linear FE shell idealization of the cold-formed steel portal frame has been used to determine frame deflections. This employed shell elements for the I-sections. Both the columns and rafters were modelled using a feature

BEAM ELEMENT using a two-noded beam in plane. Beams are directly connected to the column, considering the connections as tie constraints instead of contact. Eaves and apex haunches were not modelled in order to estimate the bending stiffness of the members only. No initial imperfections are modelled in either the columns or the beams. The models were prepared for all six frames, however, only the results of the optimum structure (Structure 'A' with 5 m bay spacing) are presented in this study.

A lateral load of 15 kN was applied at the left column and that of 10 kN on the right column. A load of 2 kN acting on the left rafter in download direction and in upward direction on right rafter was applied. Pinned bases are simulated to apply practical field conditions.

Following assumptions were considered during the FE modelling of the frames:

1. Shear deformation is ignored;
2. Lateral-torsional and local buckling of the frame is not considered;
3. Only doubly symmetric sections are considered;
4. Local buckling and local failure of components in the base connections is neglected
5. Elastic-perfectly plastic steel behaviour is considered at member ends.

V. FE Results

The frame deflection can be considered to be comprised of three components: (i). Deflection due to bending of the column and rafter members; (ii) Deflection due to bolt-hole elongation in the connections; and (iii). Deflection due to in-plane bracket deformation. This study considers the deflection due to the bending of the columns and rafters. Figure 9 shows the deflection of the members.

The suitability of the optimum structure was determined by applying the equal amount of lateral load on all frames and all six frames were tested. Only the deflection in the frame due to lateral load was considered as a result of FE analysis since the purpose of this study is to propose an optimum design of portal frames in terms of members' sizes, consequently the total weight of the frame. The model prepared for the based on the geometry of structure 'A' with 5 m bay spacing exhibited the same results which were predicted by other frames. Thus, it was validated that a bay spacing of 5 m for structure A is suitable for both design and construction purposes as it can sustain the same load and exhibit performance similar to the other tested frames with minimized weight and overall cost of fabrication and construction.

The major deflection occurred in the left column which is at its maximum at the point of intersection of column and rafter. The effect of absence of eaves haunch is clearly visible. This right rafter has also been bent due to the absence of apex haunch. Moreover, the insufficient bending stiffness of the section selected for rafter caused the bending in the member. For practical field conditions, either both the haunches should be fabricated from higher strength material as compared to the material used for rafters and columns.

The FE analysis could be further extended and the same model can be modified for various types of sections, locations and loading conditions and can be used for the design of portal frames in anywhere in the world. Moreover, the material properties can also be amended in the output. However, the investigation performed for geometrical optimization is general in nature and the philosophy can be applied in its present form.

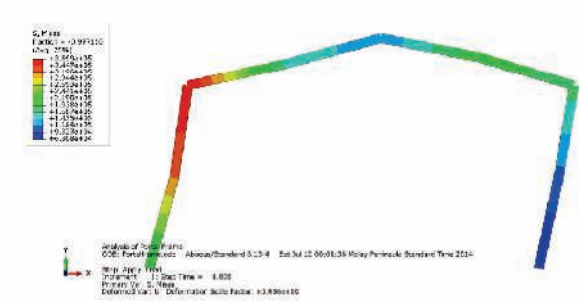

Fig.9. Finite Element Analysis of Structure 'A'

VI. Conclusions

This study emphasize on determining the effects of change in geometry of portal frames on overall cost of the structure in terms of self-weight. The total width of portal frame was kept constant and change of bay width between portals and influence of shorter and larger span on portal design was investigated by performing a plastic analysis using Quiksoft program. BS5950 was referred to apply loading combinations and selection of member sizes.

The results exhibited that keeping the total width constant, the change of spacing between the portal has varying effects upon the size of members and, consequently, on the total weight of frames. As more as the spacing of frames increases, the size of members increases. Minimizing the spacing of portals will minimize the overall cost of portal frames. Transportation and erection of low-weight member may decrease the cost of transportation and labour. However, the cost of assembly construction may be less in case of less number of members required for the structure.

It should be noted that the larger spans may greatly affect the weight of structure. The further study comparing the effect of a single bay larger and multi-bay span equal to the same as single bay span accompanied with different bay spacing may further elaborate the effects of change of span on overall cost of the structure. Furthermore, the research can be further expanded to study the cost reduction by comparing the

welded and bolted connections, by including study about the variation in foundation of each of the six models or by having the market survey about labour costs for each of the proposed structure.

REFERENCES

[i] Y. Kwon, H. Chung and G. Kim, "Experiments of cold-formed steel connections and portal frames", Journal of Structural Eengineering., vol. 132, SPECIAL ISSUE, pp. 600-607, 2006.

[ii] S. N. R. Shah, N. H. R. Sulong, R. Khan, M.Z. Jumaat and M. Shariati, "Behavior of Industrial steel rack connections", Mechanical Systems and Signal Processing., vol. 70-71, pp. 725-740, March 2016.

[iii] S. N. R. Shah, N.H. R. Sulong, M. Shariati and M. Z. Jumaat, "Steel Rack Connections: Identification of Most Influential Factors and a Comparison of Stiffness Design Methods", PLOS ONE, vol. 10, no. 10, e0139422. doi:10.1371/journal.pone.0139422, 2015.

[iv] S. N. R. Shah, N. H. R. Sulong, M. Z. Jumaat, "Effect of column thickness on the strength and stiffness of steel pallet rack connections", In: Proceedings of 7th Young Researchers and Graduates Symposium, 20-21 August, Kuala Lumpur, Malaysia.

[v] D. T. Phan, J. B. P. Lim, T. T. Tanyimboh, R. M. Lawson, Y. Xub, S. Martin and W. Sha, "Effect of serviceability limits on optimal design of steel portal frames", Journal of Constructional Steel Research., vol. 86, pp. 74-84, 2013.

[vi] J. B. P. Lim and D. A. Nethercot, "Design and development of a general cold-formed steel portal framing system", The Structural Engineer., vol. 80, no. 21, pp. 31-40, 2002.

[vii] D. T. Phan, J. B. P. Lim, C. S. Y. Ming, T. T. Tanyimboh, H. Issac and W. Sha, "Optimization of cold-formed steel portal frame topography using real-coded genetic algorithm", Procedia Engineering., vol. 14, pp. 724-733, 2011.

[viii] Abaqus 6.13.4. "SIMULIA", DASSAULT SYSTEMS, 2013.

[ix] B. Davison and G. W. Owens, "Steel designers' manual" 7th Edition. John Wiley & Sons, USA, 2011.

[x] I. G. Tsoulos, "Modifications of real code genetic algorithm for global optimization", Applied Mathematics and Computation. , vol. 203, no. 2, pp. 598-607, 2008.

[xi] M. Saka, "Optimum design of pitched roof steel frames with haunched rafters by genetic algorithm", Computers & Structures., vol. 81, no. 18, pp. 1967-1978, 2003.

[xii] H. K. Issa and F. A. Mohammad, "Effect of mutation schemes on convergence to optimum design of steel frames", Journal of Constructional Steel Research., vol. 66, no. 7, pp. 954-961, 2010.

[xiii] S. Kravanjaa, G. Turkalj, S. Šilih and T. Žula, "Optimal design of single-story steel building structures based on parametric MINLP optimization", Journal of Constructional Steel Research., vol. 81, pp. 86-103, 2013.

[xiv] J. Pietrzak, "Effect of geometrical factors on stability characteristics of portal frames", Civil Engineering Systems., vol. 7, no. 2, pp. 76*86, 1990.

[xv] E. Machaly, "Optimum weight analysis of steel frames with semi-rigid connections", Computers & Structures, vol. 23, no. 4, pp. 461-474, 1986.

[xvi] A. Wrzesien, J. B. P. Lim and D. A. Nethercot, "Optimum Joint Detail for a General Cold-Formed Steel Portal Frame", Advances in Structural Engineering; vol. 15, no. 9, pp. 1623-1640, 2012.

[xvii] F. Erbatur and M. Al-Hussainy, "Optimum design of frames", Computers & Structures., vol. 45, no. 5, pp. 887-891, 1992.

[xviii] MS 1553. "Malaysian Standards", Code of practice on wind loading for building structures. Department of Standards, Malaysia, 2002.

[xix] BS 5950. "British Standards", Structural use of steelworks in building. Part 1. Code of practice for design- rolled and welded sections. British Standards Institution, London, 2011.

[xx] Quikport XP Software, GTS Cadbuild Limited, Loughborough, United Kingdom

Effect Of Shape Of Shear Wall On Performance Of Mid-Rise Buildings Under Seismic Loading

Q. U. Z. Khan[1], A. Ahmad[2], F. Tahir[3], M. Asad[4]

[1,2,3,4]Civil Engineering Department, University of Engineering and Technology, Taxila, Pakistan
[2]afaq.ahmad@uettaxila.edu.pk

Abstract-In multi-storey reinforced concrete (RC) buildings, one of most common practices to increase their lateral stiffness against earthquakes is to introduce shear walls at the critical location of the RC building. Various shapes including (e.g. Rectangular, T-Shape, L-Shape, C-Shape) are most commonly adopted for shear walls. The present study is to investigate the effectiveness of the shear walls regarding efficiency and economy to provide lateral stiffness to multi-storey buildings in a better way and hence resist seismic loads. In this study, different shapes of shear walls are selected for comparison i.e. Rectangular, C-Shape, L-Shape, T-Shape etc. A typical twenty (20) storey RC building with regular plan is selected for analysis purpose. The building is first modeled and analyzed by introducing columns only. No shear wall is provided in the first model which will be used as reference. Then all shapes of shear walls, selected for comparison, are introduced one by one in each separate models and analyzed. The results for various analysis outputs i.e. storey drifts, storey displacements, and storey shears are obtained, plotted and compared. It is seen that Rectangular and L-Shaped walls are most effective in resisting seismic forces while H & T-Shaped walls show the least resistance towards earthquake impacts.

Keywords-Shear Walls, Base Shear, Storey Drifts, Storey Displacements, Storey Shears, ACI.

I. INTRODUCTION

The use of shear wall begins with the start of 20th century. The problem for the structural engineers was to find the optimize design farming for tall RC building and location of shear wall, against earthquake disasters[i]. The solution is the strengthen and more stiffness of the critical structural member to reduce the damage effect against the lateral loads. This idea led to the usage of shear walls in tall RC buildings.

This research is conducted to find the most optimize shape of the shear wall that is able to resist lateral loads in a much better and economical way. Hence, the output of this research will provide a guideline to solve the problem of selection of a suitable and safe shape of shear wall.

The methodology involves modeling and analysis of a typical twenty (20) storey building with regular plan, for which a suitable architectural plan of the building is selected, as shown in fig.1. For this investigation well known building analysis and design software, ETABS (Extended Three Dimensional Analysis of Building Systems) is used.

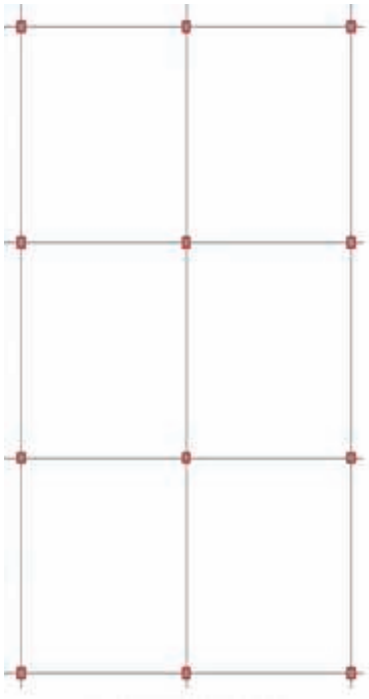

Fig. 1. Typical Building Plan

The seismic zone assumed is Zone-III which is the seismic zone for most of the developed areas of Pakistan, as per BCP-07 [ii]. Fig.2 shows the all possible shapes of the shear wall i.e. L-shape, T-shape, C-shape, H-shape and Rectangular shape, which used in the design procedure. Then these wall are added in the typical tall RC building plan one by one. For the reference ,first the RC building has been analyzed without using any shear wall. The results of this reference building then used for the comparison. Then, different shapes of shear walls are used in the same plan and different results are then compared. The area of shear wall is kept constant for all the shapes in order to

compare them in terms of economy and effectiveness. The results of various building parameters i.e. storey shears, storey displacements and storey drifts. have been compared and checked for all types of shear walls.

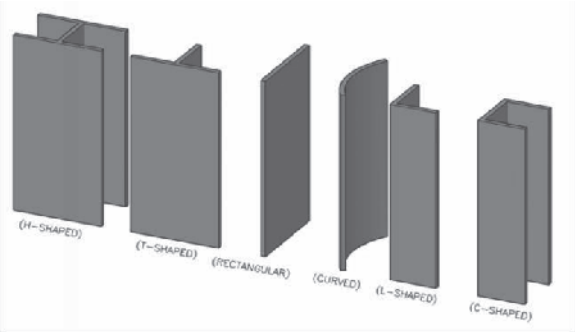

Fig. 2. Typical Shapes of Shear Walls

II. Literature Review

Burak investigated the shear wall area against the floor area under the seismic loading [iii]. Wallace presented research on seismic design of RC structural walls as per US codes and introduced various criteria to design different shapes of shear walls [iv]. Designers worked on strengthening of existing buildings for seismic forces by introducing shear walls into the old structure [v]. They suggested that external shear wall application will be a practical and economical solution for the detached buildings. There will be no changes made to the interior architecture of these buildings. Moreover, it was also observed by them that the strengthening and system improvement performed through adding external reinforced concrete shear wall to the reinforced concrete buildings will enhance behavior, strength and rigidity to the system with its low cost besides ease of construction and application. This methodology was developed for the existing reinforced concrete primary school buildings constructed as typical projects in Turkey, and was applied in most of the primary school buildings without any problems [v]. Paknahad along with his researchers worked to analyze Shear Wall Structures using optimal membrane triangle element [vi]. Wallace and Kutay Orakcal made a critical study for the provisions for seismic design of shear walls used by ACI 318-99 and prior codes and concluded that Major changes to the provisions for proportioning and detailing of structural walls were incorporated into ACI 318-99 to take advantage of displacement-based design, as well as to address shortcomings associated with prior ACI 318-99 codes [vii]. Kazimi performed analysis of Shear-Wall buildings and concluded that the shear wall buildings were evidently the most economical structural form for tall buildings. He also included a few methods to facilitate stress calculations as well as other analysis parameters through simple methods [viii]. Oztorun et al, worked on "Three-Dimensional Finite Element Analysis of Shear Wall Buildings" and concluded that "An improved simplified method for the analysis seems to be inappropriate. Three dimensional finite element analysis as presented in his study is the proper method of solution. The increasingly high speed of computers together with the use of appropriate software will make the finite element approach as a convenient design tool" [ix]. Computers and Structures Inc. provides several useful software manuals for Etabs, Sap2000, Safe etc. to aid the computerized analysis of shear walls as well as various civil structures [x,xi]. McCormac provided useful literature on design of shear walls for seismic forces [xii]. Kyaw and Thiha conducted a useful research on performance of existing buildings using ordinary moment resisting frames and concluded that most critical force for columns is bending moment which should properly be dealt with. Hence, shear walls satisfy the criteria for resisting the bending moments to a large extent [xiii].

III. Structural Analysis Parameters

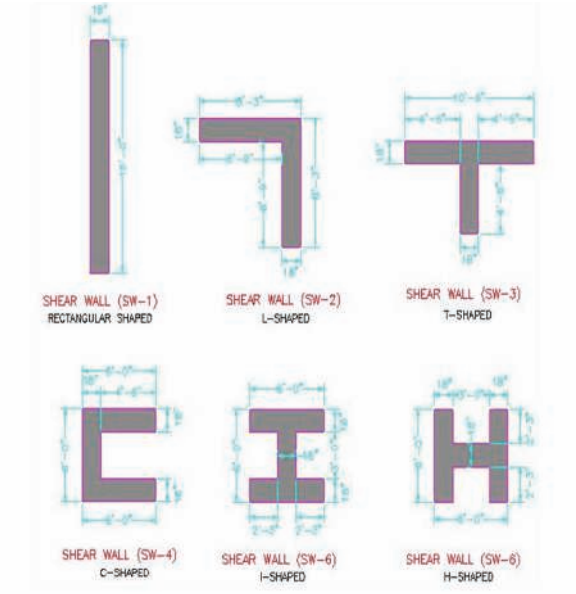

Fig. 3. Cross Sections of Various Shear Walls

Various structural analysis parameters used in the design and analysis of the model building are detailed below:

TABLE I . PROPERTIES OF SHEAR WALL

Unit weight of concrete	= 150 pcf
Modulus of elasticity of concrete	= 2850 ksi
Poisson's ratio	= 0.2
Coefficient of thermal expansion	= 5.5 x 10e–6
Conc. Compressive Strength, f'c	= 2500 psi
Yield strength of rebars fy	= 40000 psi
Shear strength of shear rebars fys	= 40000 psi

Fig.3 shows the six different shapes of the shear walls with the following cross-sections. Area of each shape of shear wall is assumed to be constant. Moreover, different structural properties, moment of inertia (I) in both axes, length (L) of walls in both axes, tensional constant (T) and polar moment of inertia (J) are calculated for each shape of shear wall as shown in the fig. 4 to 9.

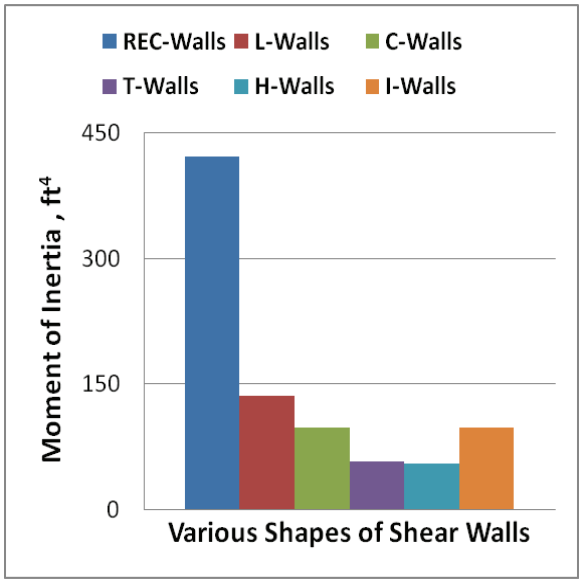

Fig. 4. Moment of Inertia of Shear Walls along X-Axis

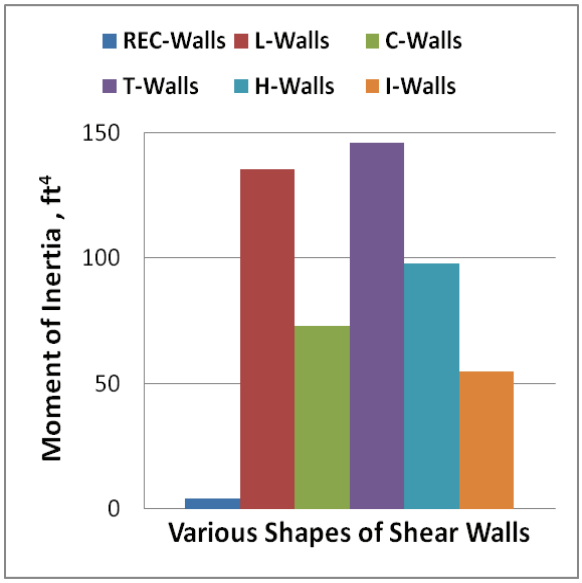

Fig. 5. Moment of Inertia of Shear Walls along Y-Axis

Fig.4&5 show the values of moment of inertia, I in x and y axes for all six different shapes of the shear walls. The rectangular shape gives the maximum value of I in the direction of x-axis and gives the minimum value in y-axis, due to the size of shape along that axis. While the T-shape gives the totally opposite values of moment of inertai along both the axes. All other shapes are also give different values depending upon the size along that axis. Fig.6&7 describe the values of length, L in x and y axes for all six different shapes of the shear walls. The I-shape gives the maximum value of length in x-axis and minimum value in y-axis, due to the size of the shape at that axis.While H-shape gives the oppposite of values for length in both axes as compare to the I-shape shear wall.

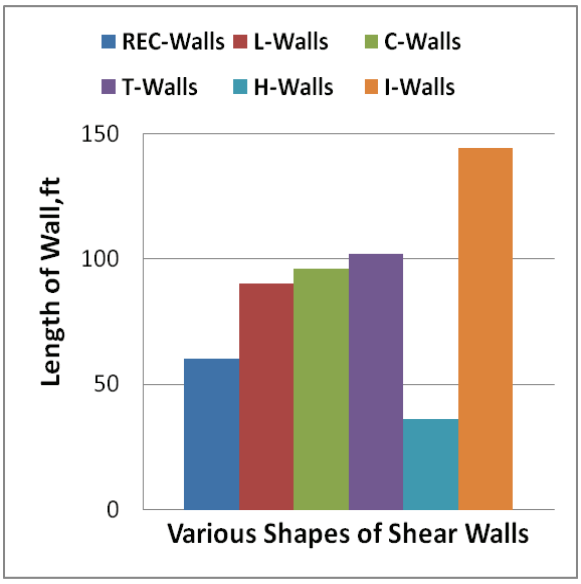

Fig. 6. Lenghts of Shear Walls along X-Axis

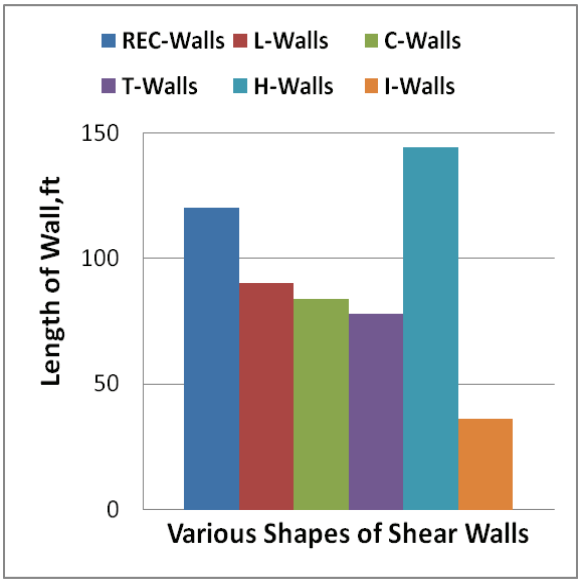

Fig. 7. Lenghts of Shear Walls along Y-Axis

Fig.8 shows the values of torsional constant, T for all six different shapes of the shear walls. This is the only structural propoerty for which all shapes give the nearly same value.

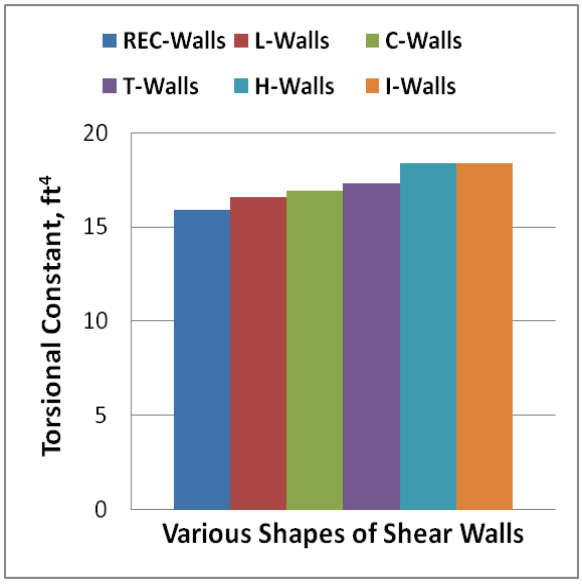

Fig. 8. Torsional constant for Shear Walls

Fig.9 shows the values of polar moment of inertia, J for all six different shapes of the shear walls. For this property, again the rectangular shape gives the maximum value.

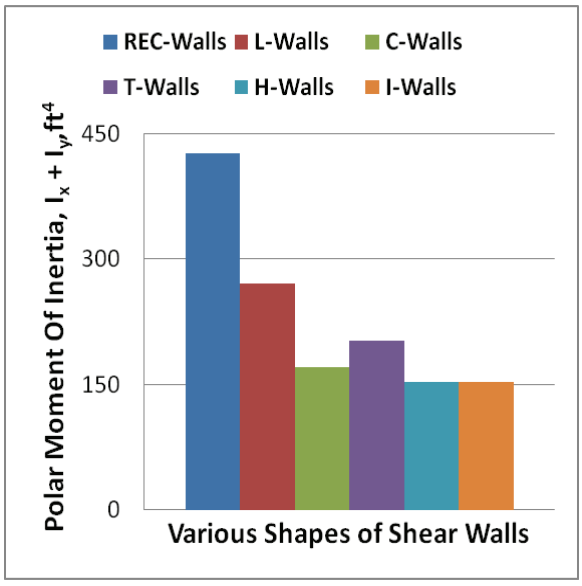

Fig. 9. Polar Moment of Inertia for Shear Walls

IV. Loading Conditions

Dead loads are defined as gravity loads that will be accelerated laterally with the structural frame under earthquake motion. Live loads are defined as gravity loads that do not accelerate laterally at the same rate as the structural frame when the structure undergoes earthquake motion. Two different values of live loads are used for first nineteen storey and for the top one as shown in the fig.10.

Dead Loads	
Unit weight of concrete	= 150 pcf
4½ inches thick brick wall weight	= 45 psf
9 inches thick brick wall weight	= 90 psf
Superimposed dead load	= 50 psf
Live Loads	
Live load on 1st to 19th floor	= 50 psf
Live load on roof (20th floor)	= 20 psf

Earthquake load consists of the inertial forces of the building mass that result from the shaking of its foundation by a seismic disturbance. Other severe earthquake forces may exist, such as those due to land sliding, subsidence, active faulting below the foundation, or liquefaction of the local sub grade as a result of vibration. Whereas earthquakes occur, their intensity is relative inversely proportion to their frequency of occurrence; severe earthquakes are rare, moderate ones more often, and minor ones are relatively frequent.

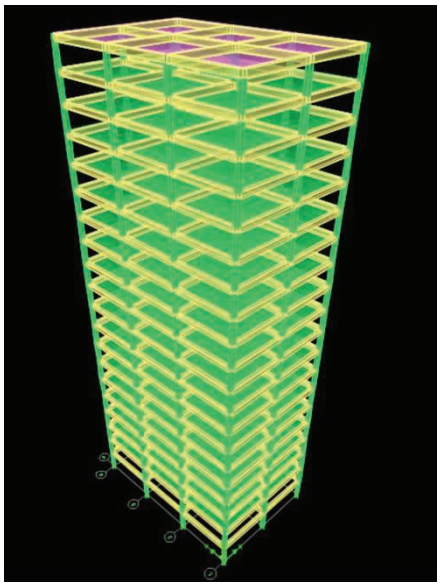

Fig. 10. Model of 20 storey building with different live load at roof

V. Modeling & Analysis

The building has been modeled in Etabs software. Fig.11 &12 show the deformed shape of the building under gravity loads. Seven separate models have been prepared with each shape of shear walls at the locations of all columns 9 (as in fig.1) as a separate model. Then analysis of each model in separate Etabs file has been run. Finally, results for various seismic parameters have been obtained and discussed for each case.

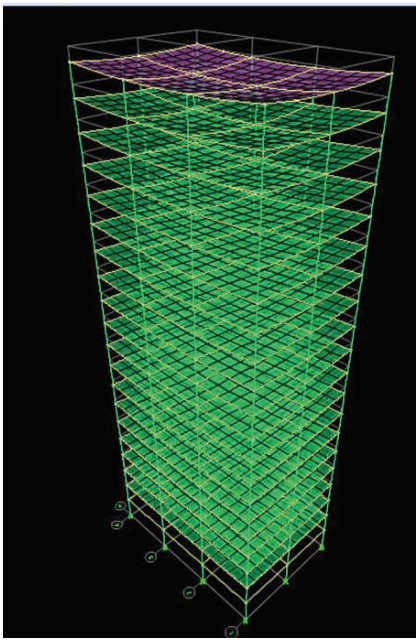

Fig. 11. 3-D view of deformed shape of 20 storey building under gravity loads

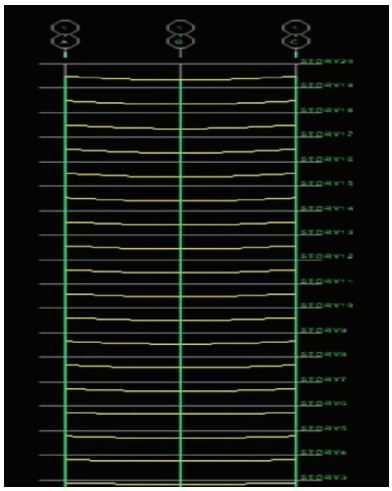

Fig. 12. Sideview of deformed shape of 20 storey building under gravity loads

I. Results And Discussions

Results for various seismic parameters; storey drifts, storey displacement and storey shears are obtained and plotted for each shape of shear wall.

A. Storey Drifts

Storey drifts is computed against lateral forces along both x and y axes and then plotted against each shape. The comparisons are plotted for each shape of shear wall, when introduced separately into the frame and are highlighted one by one in the subsequent section.

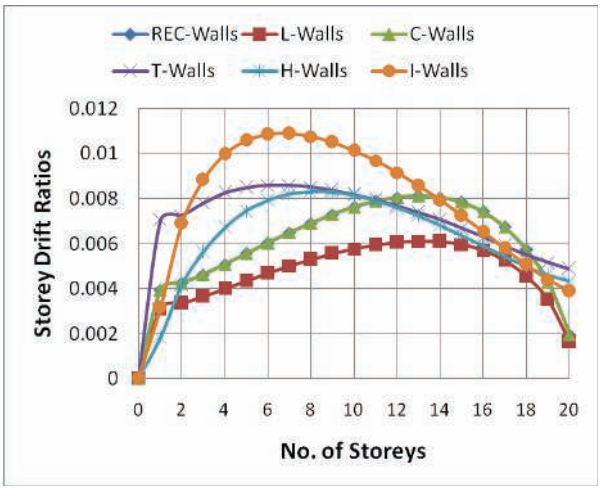

Fig. 13. Storey Drifts along X-Axis (EQ in X-Direction)

Fig.13 compares storey drifts for all shapes of shear walls and describes the response of storey drifts along x-axis against the same direction of lateral loading. I-shape shear wall gives the maximum value for the storey drift in x-axis. The storey drift has maximum value for the 8th floor. After 10th floor, the storey drift response in x-axis for all shapes start decreasing. The H-shape gives the middle response for storey drift in x-axis. While, L-shape shear wall gives the minimum value for storey drift in x-axis against the lateral loading in same axis.

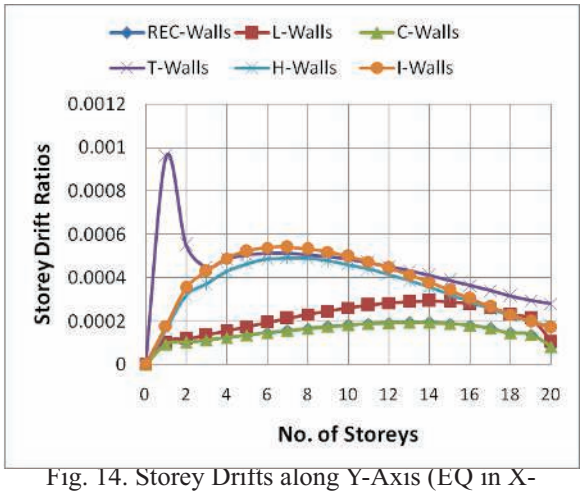

Fig. 14. Storey Drifts along Y-Axis (EQ in X-Direction)

Fig.14 shows storey drifts response along y-axis against the lateral loading in opposite x-axis. In this case, again H- shape gives the middle values almost for every floor of RC building. I-shape shear wall gives the maximum values like the previous case but for the storey drift in y-axis against lateral loading in x-axis, the C-shape shear wall gives the minimum values for all floors of RC building.

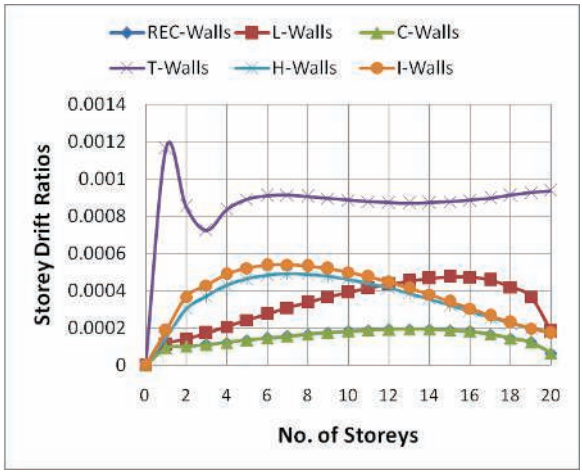

Fig. 15. Storey Drifts along X-Axis (EQ in Y-Direction)

Fig.15 shows storey drifts along x-axis due to lateral loading applied in the opposite y-axis. Like the previous two cases, in this case again H-shape shear wall gives the middle values for storey drift in y-axis for all floors. T-shape shear wall gives the maximum values and and C-shape shear wall gives the minimum values for all floors reduce as compared to the other shear wall shapes,

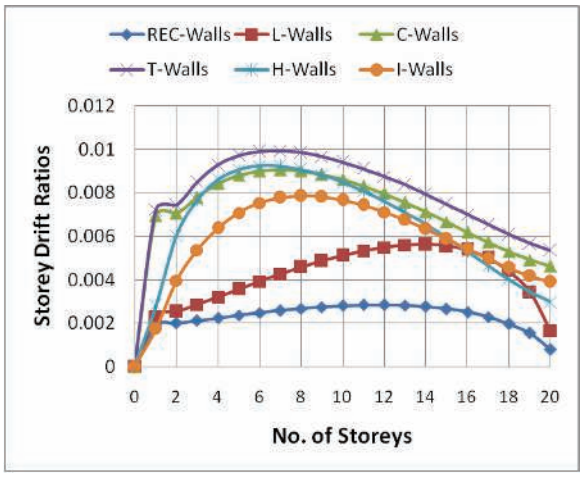

Fig. 16. Storey Drifts along Y-Axis (EQ in Y-Direction)

Fig.16 shows storey drifts along y-axis due to lateral loading applied in the same y-axis. Unlike the previous three cases, in this case H-shape shear wall gives the higher values for storey drift in y-axis for all floors. T-shape shear wall gives the maximum values and Rectangular shape shear wall gives the minimum values for all floors reduce as compared to the other shear wall shapes.

A. Storey Displacements

Since columns are extremely less stiff as compared with the stiffness of RC shear walls, therefore, they permit enlarge displacements at all floors of tall RC buildings, when compared with the displacements allowed by the shear walls. It is also proved that Rectangular and L-Shape wall restrict displacements to lower most values.

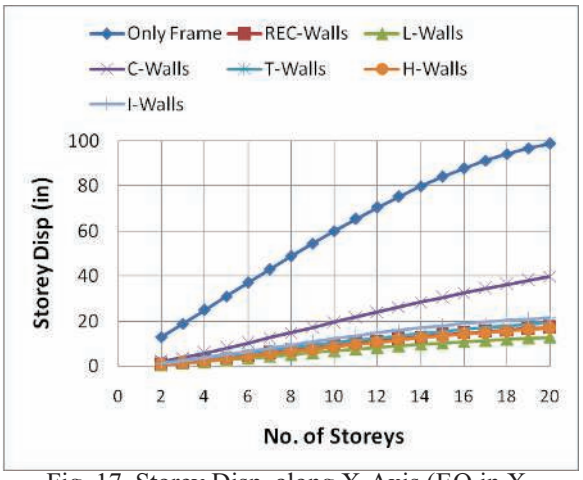

Fig. 17. Storey Disp. along X-Axis (EQ in X-Direction)

Fig.17 shows storey displacement along x-axis due to lateral loading applied in the same x-axis. The framing of RC building without any shear wall gives the maximum value for the storey displacement. All framing of RC building with any type of shear wall gives much low value, due to the stiffness of the vertical load carrying members. L-shape shear wall gives the most minimum value of storey displacement in x-axis.

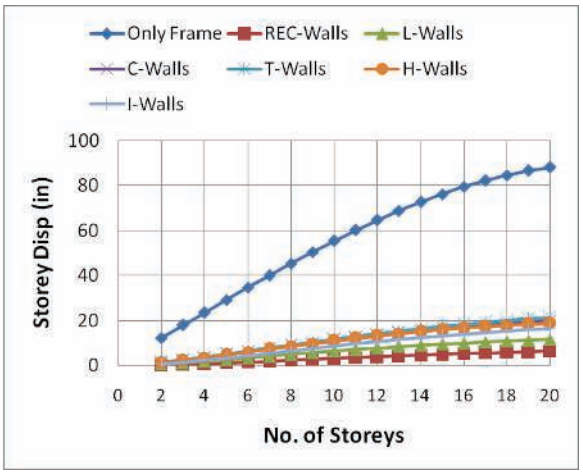

Fig. 18. Storey Disp. along Y-Axis (EQ in Y-Direction)

Same trend can be observed in fig.18, which shows storey displacement along y-axis due to lateral loading applied in the same axis. Like the previous case, building without shear wall gives the maximum value of storey displacement in y-axis as compare to the other cases. Rectangular shape shear wall gives the minimum value of storey displacement for all floors as compared to the other shear wall shapes.

A. Storey Shear

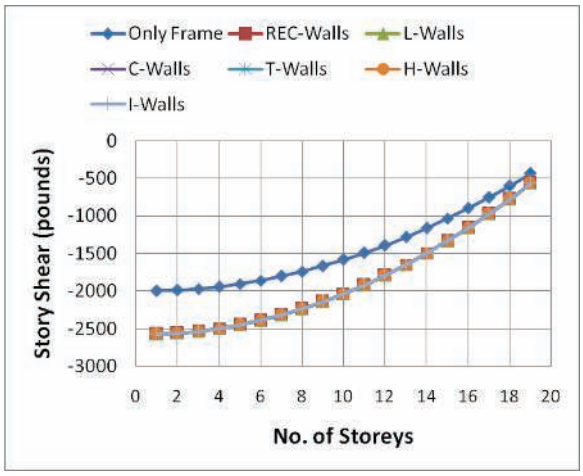

Fig. 19. Storey Shears along X&Y-Axes

As per BCP-07 formulas, base shear is mainly dependent upon the gravitational loading i.e. fixed and service dead loads. Since dead loads of columns are less than those of shear walls, they allow reduced storey shears as compared with shear walls. Also, storey shears are seen to have constant values for all shapes of shear walls due to the same x-sectional area assumed for each type of shear wall shape. Fig.19 shows the storey shear response against different shapes of shear wall in both x & y axes. The framing without any shear wall gives the less negative values as compare to the other cases.

VII. CONCLUSIONS

In this study, various shapes of shear walls i.e. Rectangular, L, T, C, H and I are incorporated in the structural farming of 20 storey tall RC building. In order to find the optimize structural framing with respect to the safest, economical and desirable shape of shear wall. Following are the conclusions of the present investigation:

1. Shear walls play an important role in reducing the enlarged seismic parameters i.e. storey drifts, storey displacements and storey shears with respect to the code specified values/limitations.
2. The higher the moment of inertia of a shear wall along a plane perpendicular to the direction of lateral loading, the higher is its tendency towards resisting seismic impacts and vice versa.
3. Rectangular and L-shaped walls are most effective in resisting seismic forces along both orthogonal directions and reduce seismic forces remarkably.
4. H-shaped and T-shaped walls show less resistance towards lateral loading.
5. Each shape of shear wall produces the same amount of storey shears in both axes (Shear force at each storey level) which clearly concludes that shape of shear wall has no impact on reduction of storey shears.
6. Since dead load of shear walls is greater than that of columns, therefore, storey shears are enlarged after inclusion of shear walls in building frame but this effect is tolerated by enlarged stiffness of shear walls as compared with columns.

REFERENCES

[i] K. O. Lakshmi, 2014 ,"Effect of shear wall location in buildings subjected to seismic loads", Journal of Engineering and Computer Science, V. 1, No. 1, pp. 07-17.

[ii] Building Code of Pakistan (Seismic Provisions-2007),Government of Pakistan, Ministry of housing and work Islamabad.

[iii] B. Burak, H. K.Comlekoglu, "Effect of Shear Wall Area to Floor Area Ratio on the Seismic Behavior of Reinforced Concrete Buildings" Journal of Structural Engineering, Vol. 139, No. 11, pp. 1928-1937, 2013.

[iv] J. W. Wallace, "Seismic Design of RC Structural Walls, Part I: New Code Format," Journal of Structural Engineering, ASCE, V. 121, No. 1, pp. 75-87, 1995.

[v] M. Y. Kaltakci, M. H. Arslan, U. S.Yilmaz, H. D.Arslan, "A New Approach on the Strengthening of Primary School Buildings in Turkey: An Application of External Shear Wall," Science Direct, Building and Environment, 43, 983–990, 2008.

[vi] M. Paknahad, J. Noorzaei, M. S. Jaafar, W. A. Thanoon, "Analysis of Shear Wall Structure Using Optimal Membrane Triangle Element," Science Direct, Finite Elements in Analysis and Design, 43, 861- 869, 2007.

[vii] J. W. Wallace, and K.Orakcal, , "ACI 318-99 Provisions for Seismic Design of Structural Walls," ACI Structural Journal, 99, No. 4. 499-508, 2002.

[viii] J. W. Wallace, and K. Orakcal, (2002), "ACI 318-99 Provisions for Seismic Design of Structural Walls," ACI Structural Journal, 99, No. 4. 499-508

[ix] N.K. Oztorun, E. Citipitioglu, N.Akkas, "Three-Dimensional Finite Element Analysis of Shear Wall Buildings," Computers and Structures, 68, 41-55, 1998.

[x] CSI, 2005, "Analysis Reference Manual for SAP2000, ETABS, and SAFE," Computers and Structures, Inc., Berkeley, CA.

[xi] E. L. Wilson., A. Habibullah. (1995), "Structural analysis programs," Computers and Structures Inc., Berkeley, CA.

[xii] McCormac, C. Jack, and J. K. Nelson. (2006), "Walls, Design of Reinforced Concrete," River Street, Hoboken, John Wiley & Sons, Inc., 558-560.

[xiii] Kyaw, M. Thiha, (2007), "Preparation for Structural Analysis and Design, A Study on Performance of Existing Building using Ordinary Moment-Resisting Frame in Seismic Zone 2A," 14-20.

Effects of Orientation and Glazing Material on Heat Gain in Semi-Arid Climate of Lahore

M. Rashid[1], T. Ahmad[2], A. M. Malik[3], M. Z. Ashraf [4]

[1, 3] *Architecture and Planning Department, University of Management and Technology, Lahore*
[2] *School of Architecture, University of Lahore*
[4] *Architecture Department, College of Art and Design, Punjab University, Lahore*
[1]memoona.rashid@umt.edu.pk

Abstract-Lahore falls in the region of semi-arid zone having long and extremely hot summer and comparatively short and mild winter. The extreme temperature in summer that spans from March to October is responsible for high solar radiation, which causes heat gain in buildings. Sun light obstruction by a horizontal shade at west, due to the low altitude of sun in summers, is not possible. This emphasizes the need of windows with high energy performance. This paper describes a simulated study conducted to test the impact of two parameters of window design i-e orientation and glazing material used, on the heat gain in semi-arid climate. The major component of window is glazing material, which is an important parameter for study regarding heat gain. The orientation is studied as it is one of the fundamental design parameter.

The significance of this study is quantitative evaluation, with the acquisition of measurable data, generated through a software named as "comfen" specifically designed to investigate the window design parameters regarding solar heat gain. In testing both parameters, results show that with the gradual decrease in heat gain, the daylight entering the room is also reduced, which is also not desireable.

Keywords-Heat Gain, Window, Orientation, Glazing Material, Semi-Arid Climate, Daylight

I. Introduction

The primary function of a building is to provide shelter. The building acts as a barrier between the indoor and outdoor climate conditions. The building envelope, like a filter, must allow the favorable climate conditions inside and obstructing the unfavorable ones. The penetration of solar radiation in the indoor can be desirable or not depending upon the climate of that particular area or region, function of the building and its orientation. Ultra violet rays should be avoided by obstructing sun's heat in the interior, in semi arid climate like that of Lahore, to prevent greenhouse effect. [i]

Window is weakest part of the building envelope thermally and are responsible for increasing the indoor temperature. The artificial cooling systems have been widely used in the buildings to counter this temperature effect and also to achieve the required level of thermal comfort. It is also observed that with the constant increase in cooling loads, there is also an increase in the lighting loads on the buildings. [ii]

According to a research conducted in India, air conditioning and lighting constitutes over 80% of energy use in commercial buildings. (Fig. 1) [iii]

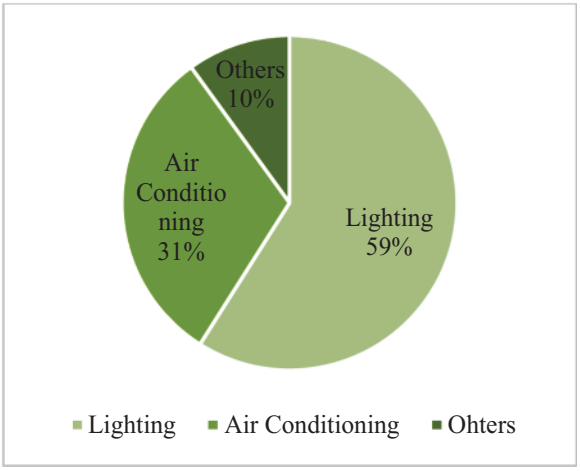

Fig.1. Energy Use Breakdown in commercial Buildings India

There are four factors which control the solar gain entering through windows. These factors are window orientation, window size, Thermal properties of glazing material used and shading devices. [ii] This study is focused to measure the impact of two factors only i-e window orientation and thermal properties of glazing material used.

A. Glazing

Glazing constitutes comparatively a larger part of window design. The transparent materials like glazing are selectively transparent to radiations. Such materials allow short wave radiations which are absorbed by the internal surfaces. These internal surfaces, in return, emit long wave radiations. The glazing material acts as opaque to such long wave radiations and in this way the interior of a building becomes hot in hot climate like that of Lahore. This phenomenon is known as

"Greenhouse Effect" and is responsible for heat gain in the buildings. [i]

The glazing affects the heat gain in a building to a huge extent. A research carried out in India for a building can be taken as a base study. The building of Energy Systems Engineering IIT Mumbai has fully glazed south façade(Fig. 2). The monthly energy demand graph of the building (Fig. 3) shows that there is only cooling load in Mumbai and no heating load. This is because the climate of Mumbai is warm and humid. But the noticeable thing is that due to excessive use of glass on the façade, there is a constant cooling load on the building throughout the year. The cooling loads dominate in the region like India and also there is a constant increase in the lighting loads on the buildings. [iii]

Fig. 2. Fully glazed South façade ofEnergy Systems Engineering IIT, Mumbai [viii]

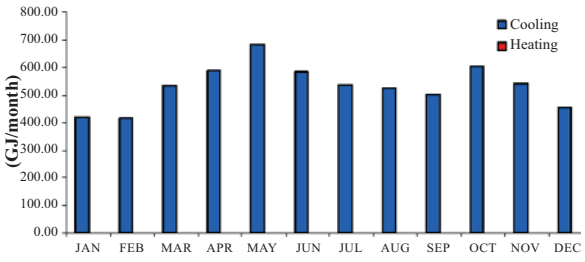

Fig.3 Monthly Energy Demand Graph [viii]

Glass was formed accidently some 4000 years ago in Eastern Mediterranean. [iv] Thin sheets of glazing material became available 2000 years after invention of glass, which were appropriate to be used in windows. It marked the beginning of the relationship between glazing material and windows, though the use of glazing in buildings being limited [v]. The trend in Architecture was changed entirely after Industrial revolution. Vertical expansion became possible with the invention of Iron / steel as construction material and frame structure. Further the invention of artificial heating and cooling systems made the architects free from the constraints that had ever determined the form of building. The larger windows or windows with larger part of glass and entire glazed wall became a trend due to all these advancements. [vi]

There are some factors through which the thermal performance of a glazing material can be assessed/ checked. These factors are Solar Heat Gain Co efficient (SHGC), U-Factor, Shading Co-efficient (SC), and Visible Light Transmittance (VLT). [vii].

B. Orientation

Heat gain can be reduced to an appreciable limit if the windows are oriented in right direction especially in hot climate. In this way, desired level of comfort can be attained. Large windows facing wrong direction can be responsible for excessive solar gains in summer and huge heat loss in winter. Excessive solar gains in summer and huge heat loss in winter is the result of in appropriate design of the windows e.g large windows facing East and West. The reason is that the amount of solar radiation received by the window on North and South is less than that received on East and West. For this reason, these orientations are considered critical and can be handled only through appropriate window design. [i].

II. Objectives

This aim of this work is to study the role of some transparent materials and orientation regarding the solar heat gain, through computer simulation. The role of orientation is studied by measuring the performance of different glazing materials on all orientations. Further, the performance of a single window at varying orientations is studied.

The research is conducted for the climate of Lahore, located between 31 degree North to 33 degree North Latitudes and, 73 and 75 degrees East longitudes. The Climate of Lahore falls in the semi-arid (Steppe) with hot summer and mild winter zone [viii]. It has hot climate for 8 months and has mild winter for the rest of 4 months. Hence the hot season predominates the whole year.

III. Methodology

A. Computer Simulation

In order to conduct this research, computer software is used. The name of the software is "Comfen". Comfen is a tool which investigates key parameters of windows which affect the thermal and visual comfort. According to different books and research publication, the key variables of window design that affect the heat gain through windows are Window Size, Glazing Type, Shading Device, Window shape, Orientation etc. But in this study, we are

focusing the two parameters i-e Thermal properties of glazing material used and Orientation.

Comfen requires some information at the start of each project before conducting the simulation. Every project requires a name, location, building type and vintage. Location includes weather data for energy plus simulation. Building type includes the lighting and occupancy. The building type can be set to office, Mid-rise Residential, Hotel, Hospital etc. Each type controls its specific occupancy and lighting along with equipment schedules. Vintage is restricted to new ASHRAE 90.1 2004. Four different types of windows are analyzed to conduct this study.

B. Description of Windows Analyzed

The four different types of windows have been analyzed in the software having the same area and frame and having 4 different types of glass materials. The windows analyzed are explained in Table I.

TABLE I
U FACTOR, SHGC VALUE AND VT VALUES FOR THE WINDOWS INVESTIGATED

	Window 219	Window 233	Window 234	Window 235	Window 236
Glazing	Single Clear	Double Clear	Triple Clear	Double Low solar Low-E Clear	Double Low solar Low-E Tinted
Frame	Al/with Break	Al/with Break	Al/with Break	Al/with Break	Al/with Break
U-Factor	1.09	0.48	0.36	0.24	0.16
SHGC	0.81	0.70	0.67	0.26	0.1
VT (% daylight)	89	79	74	64	58

Solar Heat Gain Co efficient (SHGC) : ratio of solar heat gain through glass to the incident solar radiation

U-Factor : heat flow through glazing from warmer side to cooler side. It is inversely proportional to R value which is thermal resistance whereas U value is thermal conductance.

Shading Co-efficient : **SC** = SHGC/ heat gain through 3mm clear glass.

Visible Light Transmittance : is the percentage of visible light striking the glazing that will pass through. Visible transmittance values account for the eyes' relative sensitivity to different wavelengths of light. Glazing with a high visible transmittance appear relatively clear and provide sufficient daylight and unaltered views; however, they can create glare problems. It determines the visual performance of glazing. . Higher VLT, high will be the light penetration [ix]

By putting the weather file of Lahore, the above mentioned windows have been analyzed in comfen. The five windows have been analyzed on 4 different orientations in order to observe the thermal performance of different glass types with reference to heat gain and light.

IV. RESULTS

A. Thermal Performance of Glazing Material Used

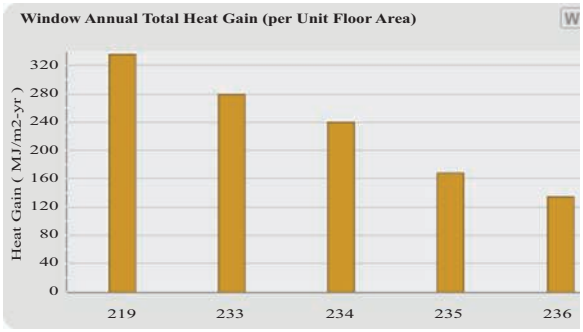

(a)

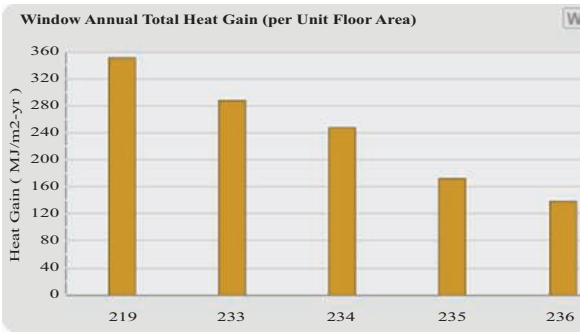

(b)

Fig. 4. Comparison Charts of Annual Heat Gain through (a) East and (b) West facing windows

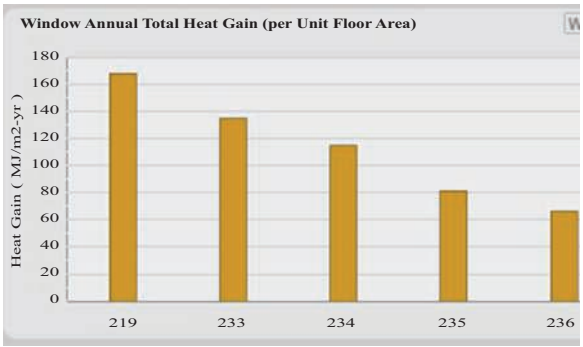

(a)

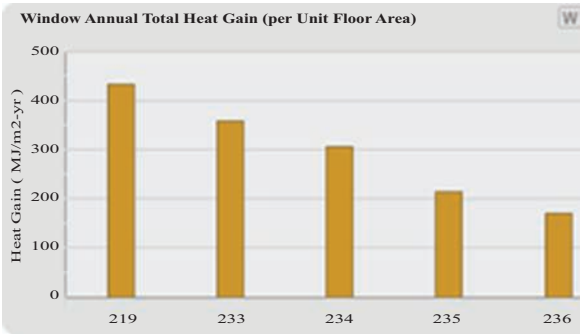

(b)

Fig. 5. Comparison Charts of Annual Heat Gain through (a) North and (b) South facing windows

Now the four selected windows are compared to analyze for daylight. The windows that have been compared for daylight area as mentioned in Table II.

TABLE II
U-FACTOR, SHGC AND VT VALUES OF THE WINDOWS INVESTIGATED

	Window 233	Window 234	Window 235	Window 236
Glazing	Double Clear	Triple Clear	Double Low solar Low-E Clear	Double Low solar Low-E Tinted
Frame	Al/ Break	Al/ Break	Al/ Break	Al/ Break
VT	0.79	0.74	0.64	0.58
U-Factor	0.48	0.36	0.24	0.16
SHGC	0.70	0.67	0.26	0.1

The results generated for comparison of daylight are as under.

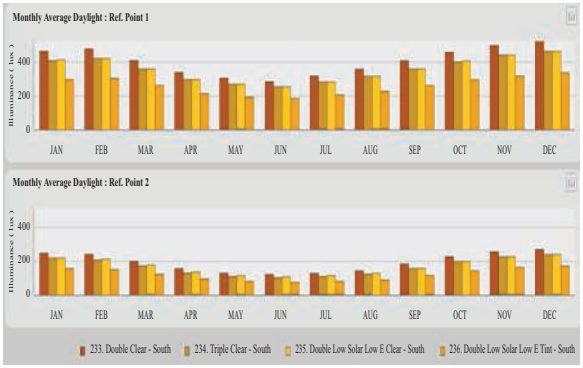

Fig. 6. Comparison charts of Monthly Average Daylight through South facing windows

B. Orientation

The effect of orientation is studied in the software by orienting the same window on all the 4 sides. The window of the same area having aluminium frame with thermal break and having Low Solar Low E Tinted glass is analyzed on 4 sides and graph (Fig 5) is obtained.

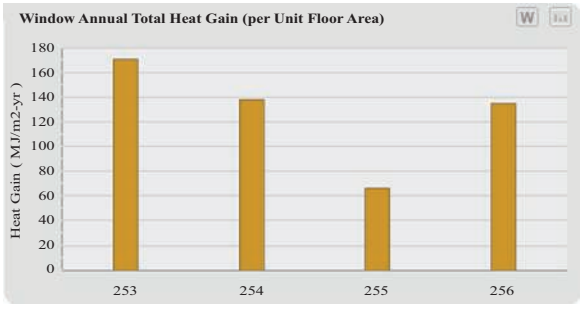

Fig. 7.Comparison graph of window facing 4 sides
Scenario 253: Window facing South,
Scenario 254: Window facing West
Scenario 255: Window facing North
Scenario 256: Window facing East

V. DISCUSSION

A gradual decrease in solar heat gain is observed on all orientations by varying the glass type in the same window from single clear to Low Solar Low E Tinted glass. The heat gain is largest when single clear glass is used and is lowest when double Low solar Low E tinted glass is used. It is however observed that on east and west orientations, the amount of solar gain is higher (up to 360 MJ / m2-yr) than on north orientation (up to 170 MJ / m2-yr). The solar heat gain is highest at south orientation i-e up to 400 MJ / m2-yr Fig 3. This shows that in the hot climate like that of Lahore, it is preferable to have more surface area of the building oriented towards north and south and lesser surface area or window opening towards east and west.

Four windows have been selected for the comparison of daylight. Results generated are contrary to those generated comparing the heat gain. The window having the Low Solar Low E tinted glass allow minimum daylight to enter i-e up to 300 lux. And the window having double clear glass (with comparatively larger heat gain) allow larger amount of daylight i-e more than 400 lux. These results are calculated by orienting the windows towards south. It can be stated, on the basis of results that by controlling the heat gain through different types of high performance glass, the daylight entering the buildings is also controlled. The big challenge therefore is to reduce the heat gain through the window glazing without compromising the daylight coming inside the building.

Orientation can be studied by the results generated previously. The heat gain is highest on south. The range of heat gain on south for the selected windows is approximately from 200-400 MJ / m2-yr. This range varies on the other orientations. On the North orientation, it is lowest i-e 70-170 MJ / m2-yr. On East and West, this range is approximately 140-370 70-170 MJ / m2-yr. The Orientation is studied further when a selected window is analyzed on 4 orientations for heat gain. The window is energy efficient and Low Solar Low E tinted glass is used. It is observed that heat gain is minimum when oriented towards North Fig 5.

VI. CONCLUSION

The heat gain and daylight are the two phenomenon that go simultaneously and cannot be separated. The need is to control the heat gain in the buildings and also to incorporate natural light efficiently. In this way the cost on the artificial systems of cooling and lighting can be reduced. Orientation factor can be tackled easily by giving windows on the recommended orientation (preferably North and South) in hot climate of Lahore. And windows on every orientation should be dealt separately keeping in view

the sun angle and the quality and magnitude of light coming inside. The most important parameter in this context is the glazing material in the window as it covers a larger part of the window opening. The effective way to do this is to use a combination of glass types in the windows. And windows on every orientation should be dealt separately keeping in view the sun angle and the quality and magnitude of light coming inside.

REFERENCES

[i] A. P. Castro, L. C. Labaki, G. C. Gutierrez, R. M. Assis. Thermal performance of different glazing surfaces in a hot climate. International conference Passive and low energy cooling for the built environment, Santorini, Greece 2005 May.

[ii] H. Dabboor, Studying the Principles of Window Design for Energy-Efficient Buildings in the Gaza Strip, Islamic University of Gaza, November, 2011.

[iii] S. Seth, Energy Efficiency Initiatives in Commercial Buildings, Energy Economist Bureau of Energy Efficiency Government of India, 2010

[iv] Slessor, Catherine, Glass Evolution, Magazine article from The Architectural Review, Vol. 203, No. 1215, May 1998

[v] F. M. Butera, Glass Architecture; is it sustainable? International Conference "Passive and Low Energy Cooling for the Built Environment", Santorini, Greece, May 2005

[vi] N. K. Garge, Guidelines for the use of Glass in Buildings, New Age International (P) Ltd., Publishers, 2007

[vii] F. K. Khan, a Geography of Pakistan; Environment, People and Economy, Oxford University Press, 1991.

[viii] J. Prajapati, Designe guidelines for Energy Efficient Bulidings, Mumbai 2006.

[ix] D. Paulus, U-factor, SHGC, CR, VT, Air Infiltration – What does this stuff mean? 2014 Source:http://www.wascowindows.com/wp-content/uploads/2014/12/U-factor-etc-v3.0.pdf

Section B

ELECTRICAL ENGINEERING & ELECTRONICS

Bandwidth Enhancement through Fractals and Stacking of Microstrip Antenna for Ku-Band Applications

[1]T. A. Khan, [1]G. Ahmad, [1]M. I. Khattak and [2]R. M. Edwards
[1]Department of Electrical Engineering, University of Engineering and Technology, Peshawar, Pakistan
[2]Department of Electrical Engineering, Loughborough University, UK
m.i.khattak@uetpeshawar.edu.pk

Abstract-One of the major constraints of a microstrip antenna is its narrow bandwidth. This paper demonstrates the influence of a dual layer staked configuration with the effect of fractal designs on a microstrip square patch antenna, for attaining both wide bandwidth and high gain properties. The proposed design of the antenna in stacked structure shows a total impedance bandwidth for S11<-10dB of 2.56GHz (18.97%) in Ku-band for satellite communication and has dual frequency bands from 11.53GHz to 13.15GHz (1.62GHz) and 15.63GHz to 16.57GHz (0.94GHz) around the resonant frequencies of 12.31GHz and 16.19GHz respectively. The intended design exhibits a 6.39dB gain whereas the radiation efficiency is up to 93.60%.These qualities of wide bandwidth and higher efficiency make the proposed antenna an excellent candidate for satellite based applications.

Keywords-Stacked, Bandwidth, Gain, Radiation Effeicieny.

I. INTRODUCTION

In view of the growing importance and development in wireless communication system, high gain microstrip antennas with broad bandwidth are in great demand for commercial, military and domestic applications. These microstrip patch antennas when compared with other conventional antennas, has great advantages and are associated with improved prospects due to their appealing features like low profile, conformal shape, smaller in dimension, low volume, very lighter in weight and being easy to manufacture [i]. Besides this, these antennas can provide high radiation efficiency, operation in multiband frequencies, flexibility in selecting feed network and can give dual and circular polarization.

Besides all of the advantages mentioned, microstrip antennas have major limitations of low gain and very low impedance bandwidth [ii]. To overcome and tackle these limitations of microstrip antenna, the parameters like length, width, thickness, feeding network configuration of the patch and overall antenna design must be reconfigured in terms of dimensions, structure and material.

A profound understanding and literature survey has been done on the existing information related to the topic. The review of the related literature survey comprises of three major areas of reading which includes; the design of antenna, methods of improving antenna gain, bandwidth and overall performance, and the operation of microstrip antenna in satellite communication bands.The recent efforts by the researchers around the globe is to increase the bandwidth, gain and radiation efficiency of the patch antenna and keeping the fabrication process easy and cost effective.The solution for improving these constraints include several methods like the use of multiple resonators [iii], employing stacking structure configuration [iv], using array configurations [v], increasing the thickness of dielectric substrate [vi], using slots in the antenna geometry [vii], selecting low dielectric constant of the substrate [viii], employing fractal designs [ix] and by improving the impendence matching of microstrip patch antenna [x].

The concept of introducing fractals and multilayer stacking structure in the proposed design is to enhance the gain and the bandwidth and to improve the overall performance of the patch antenna.In dual layer stacking structure configuration, a second parasitic patch is created in front of the feeding patch and both the patches are coupled electromagnetically at certain distance resulting a dual frequency band which results in bandwidth enhancement [xi].The geometry of fractal antenna possesses recursive self-similar fragmented design pattern that is reduced or subdivided by certain mathematical relation. This fragmented self-similar geometrical pattern enhances the total effective electrical length of antenna which provides better prospects in terms of high gain and enhanced bandwidth [xii].

In this work, a microstrip patch antenna with the effect of fractal patches and influence of dual layer staked structure, for achieving high gain and wide bandwidth properties, is proposed and analyzed for the operating frequency in Ku-band of satellite communication using the CST microwave studio.

II. ANTENNA CONFIGURATION

The proposed antenna design has been created on a "loss-free preperm 255" having relative dielectric constant $\varepsilon_r = 4.5$ with substrate thickness of 1.60mm. The ground plane material is made up of pure copper having dimensions as follows; ground plane length g-L=60.00mm, ground plane width g-W=60.00 mm and copper thickness t=0.035mm. The antenna is fed with a 50Ω coaxial cable 3.35mm along x-axis from the center of the patch. The 15GHz has been chosen as the center frequency for the proposed design to work in the Ku-band of satellite communication bands.

A. Basic Square Patch

The design specifications of the basic square patch antenna are specified in Table I.

TABLE I.
DESIGN DESCRIPTION OF SQUARE PATCH ANTENNA

Parameter Description	Description	Value
g-L	Length of ground plane	60 mm
g-W	Width of ground plane	60 mm
t	Thickness of copper	0.035 mm
h	Substrate thickness	1.6 mm
L	Antenna Length	12.52 mm
W	Antenna width	12.52 mm
Coax-x	Coaxial distance from the center along x-axis	3.5 mm
Coax-y	Coaxial distance from the center along y-axis	0.0 mm
Coax-L	Coaxial length along z-axis	-5.0 mm
epsilon	Dielectric constant value	4.5

The Figure 1 illustrates the dimensions of the basic square patch which are 12.52x12.52x0.035 mm.

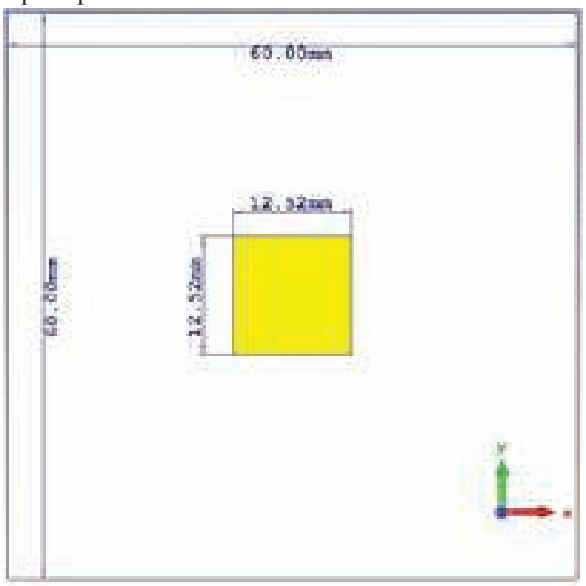

Fig. 1: Square patch antenna

B. Design Specification of Fractal structure

The idea of fractal design employed in the proposed antenna is to improve the bandwidth and gain of the proposed antenna. The geometry of fractal design describes irregular shape reduced or subdivided by certain mathematical relation. An arithmetic algorithm is used in the proposed design to produce effective fractal structure which is created iteratively by cutting every corner side of the patch in a specific span ratio of 1:5 about its parent segment, and so on.

1) 1st Iteration of Fractal Patch: In 1st fractal iteration, the length of four sides of the square patch is cutoff in the ratio of 1:5 and is detached from the parent patch. A specific length of 2.50mm is cutoff and etches out from every corner of each side of length of 12.52mm so a volume of 4x(2.50x2.50x0.035) mm is reduced in first level of iteration. The first iteration of fractal antenna is depicted in figure 2.

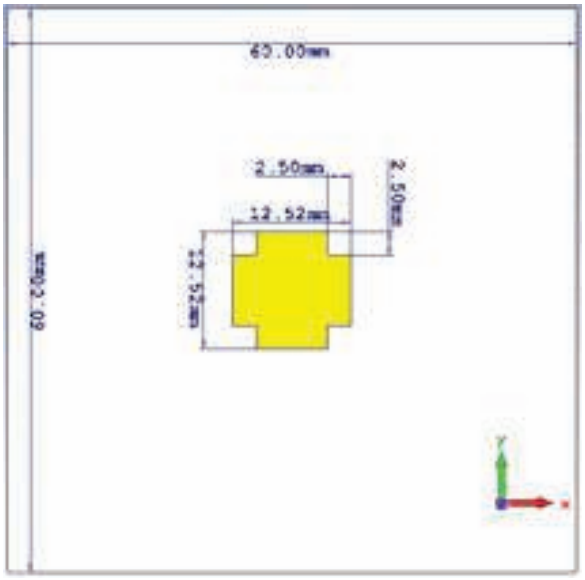

Fig. 2: 1st iteration of fractal patch

2) 2nd Iteration of Fractal Patch: The arithmetic algorithm used in 1st iterated fractal patch is also used in second level of iteration to further reduce the fractal patch by cutting each corner of every side in a specific ratio of 1:5. All the parameters and design specifications of the 2nd iteration are set to be the same as the first one. The figure 3 illustrates the second iteration of fractal patch which shows that a length of 0.5mm is further etched out from every corner side of first iterated fractal patch, that is, a total volume of 8x(0.50x0.50x0.035) mm is further cut off from its parent patch (first iterated fractal patch).

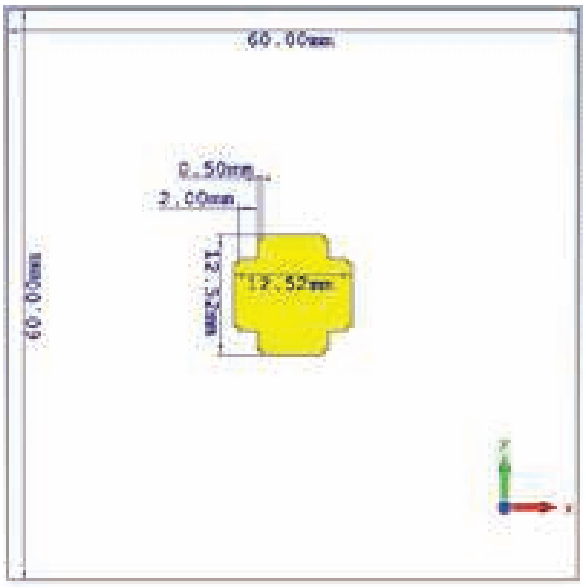

Fig. 3: 2nd iteration of fractal patch

C. Design Specification of Stacking Structure

The stacking structure configuration used in the proposed antenna design is for the improvement in the performance of antenna especially to further increase the impedance bandwidth of the antenna. The proposed design applies a two layer stacking structure containing the radiation patch and the parasitic patch which is coupled electromagnetically at a distance of fh_z=2.65mm as shown in the figure 4.

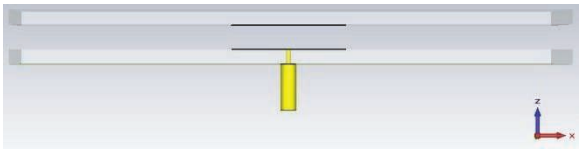

Fig. 4: Side view of stacked configuration

III. Results And Discussion

In this section, the simulated results of proposed antenna are analyzed and discussed. All the three geometrical designs, which is basic square patch, 1st iterated patch and the 2nd iterated patch with/without the influence of dual layer staked configuration has been simulated and discussed in this section.

A. Basic Square Patch

Figure 5 illustrates the simulated frequency response of the square patch at 15GHz and the far-field gain pattern is shown in figure 6. The result demonstrates that the impedance bandwidth for S11<-10dB is 0.50GHz (3.38%) from 14.66GHz to 15.16GHz, At the working frequency 15GHz, the square patch antenna gives a gain of 9.88dB and radiation efficiency of 94.84%.

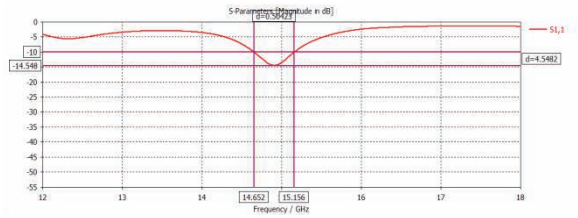

Fig. 5: Frequency response of square patch antenna

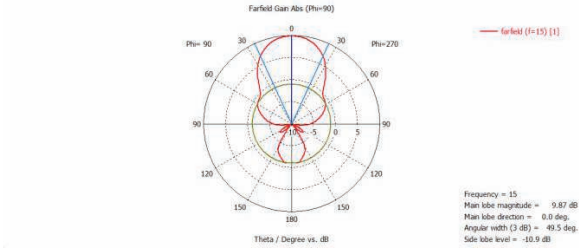

Fig. 6: Gain of square patch antenna

1) Effect of Stacking:As illustrated in figure 4, in order to apply the impression of stacking structure, a parasitic patch of same dimensions and material properties as that of radiated square patch has been introduced and are coupled electromagnetically at a distance of 2.65mm for bandwidth enhancement. Figure 7 demonstrates that the basic square patch when employed in stacking configuration exhibits dual frequency bands from 11.70GHz to 12.50GHz and 14.95GHz to 15.54GHz. The antenna has the total bandwidthof 1.97GHz (10.36%) in Ku band. The dual frequency bands have a bandwidth of 0.79GHz (6.49%) and 0.59GHz (3.87%) around the resonant frequencies of 12.09GHz and 15.19GHz respectively and the impedance bandwidth has been increased from 0.50GHz (3.38%) to 1.98GHz (10.36%). This configuration gives a gain of 7.37dB and 93.56% radiation efficiency as shown in figure 8.

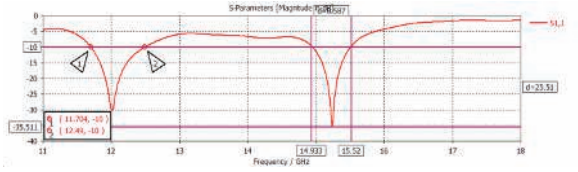

Fig.7: Frequency response of stacked square patch antenna

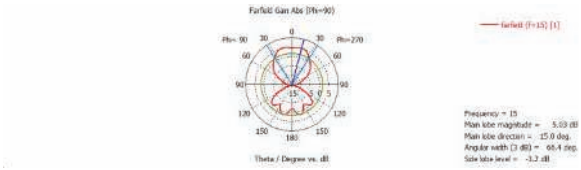

Fig. 8: Gain of stacked square patch antenna

b. 1st Iteration of Fractal Patch

The results in figure 9 and 10 illustrates the effect of 1st fractal level of iteration on the square patch and it is observed that impedance bandwidth of the fractal

antenna is improved to 0.75GHz (4.66%), which is 0.25GHz (1.27%) wider than the bandwidth achieved with basic square patch where as the gain of the fractal iterated patch is increased to 10.10dB from 9.89dB.

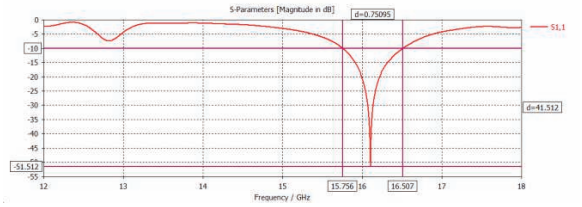

Fig. 9: Frequency response of 1st iterated fractal patch

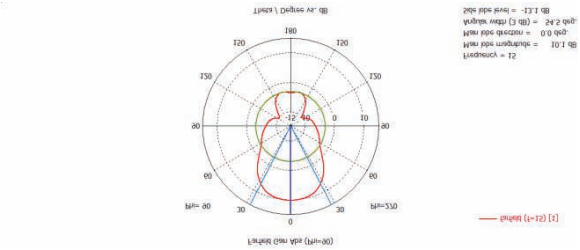

Fig. 10: Gain of 1st iterated fractal patch

1) Effect of Stacking: The 1st iterated parasitic and radiation patch of same fractal design (1st iterated) has been gap coupled in stacking configuration at a distance of 2.65mm. This antenna in stacked structure shows a total bandwidth of 2.56GHz (18.97%). The figure 11 shows that this configuration exhibits two bands of operation from 11.53GHz to 13.15GHz (1.62GHz) and 15.63GHz to 16.57GHz (0.94GHz) around the resonant frequencies of 12.22GHz and 16.21GHz respectively. It is observed that impedance bandwidth for S11<-10dB is 18.98% which is much wider than that achieved in 1st iteration of fractal patch without stacking structure whereas, the gain and radiation efficiency is decreased to 6.38dB and 93.58% respectively.

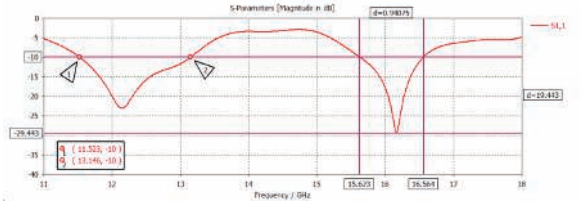

Fig. 11: Frequency response of 1st iterated fractal patch in stacked structure

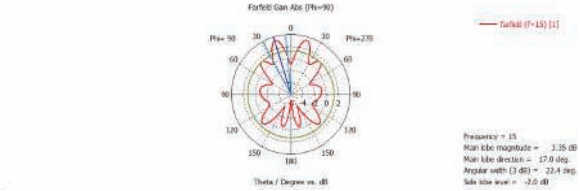

Fig. 12: Gain of 1st iterated fractal patch in stacked structure

C. 2nd Iteration of Fractal Patch

The arithmetic algorithm used in 1st iterated fractal patch is also used in second level of iteration and all the parameters and design specifications of the 2nd iteration are set to be the same as the first one. The figure 13 demonstrates the variation of return loss with frequency for 2nd iterated fractal patch. The result shows that the gain of the antennais increased to 10.13 dB whereas the bandwidth achieved is 0.80GHz (4.89%) which is 0.30GHz wider than that achieved for basic square patch.

The comparison of figure 5, figure 6, figure 9, figure 10, figure 13 and figure 14 demonstrates that the change in radiation patterns that comes from the fractal iteration is almost negligible whereas significant increase in impedance bandwidth is observed as the number of iteration increases. However, for iterations greater than two levels, the antenna design becomes relatively complex and its fabrication process becomes very complicated.

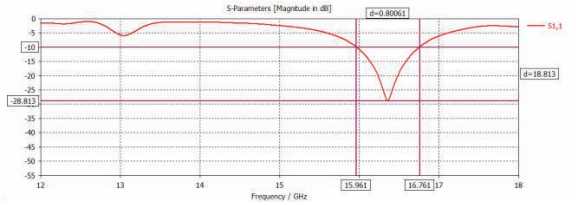

Fig.13: Frequency response of 2nd iterated fractal patch

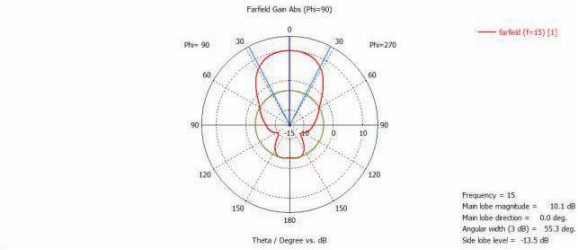

Fig.14: Gain of 2nd iterated of fractal patch

1) Effect of Stacking:A 2nd iterated radiated patch and parasitic patch has been introduced at a distance of 2.65mm in stacking configuration which gives the total bandwidth of 2.44GHz (17.96%) with a gain of 6.32dB in Ku band. This antenna has dual frequency bands from 11.78GHz to 13.41GHz (1.63GHz) around the resonant frequency of 12.55GHz and 15.72GHz to 16.53GHz (0.81GHz) around the resonant frequency of 16.24GHz respectively. It is observed that impedance bandwidth for S11<-10dB is 17.96% which is much wider than that achieved in 2nd iteration of fractal patch without stacking structure and slightly lesser than 1st iterated stacked fractal antenna.

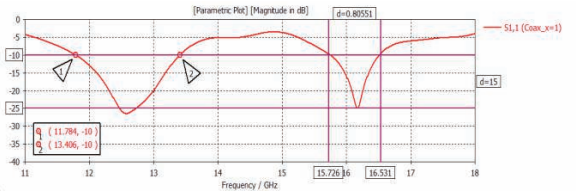

Fig. 15: Frequency response of 2nd iterated fractal patch in stacked structure

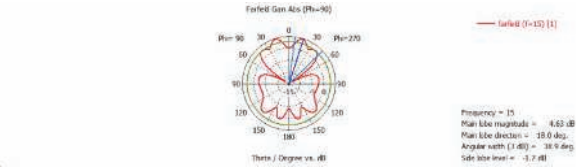

Fig.16: Gain of 2nd iterated fractal patch in stacked structure

IV. Comparison of Results

Table II demonstrates a comparative examination between various geometrical configurations of single microstrip patch.

TABLE II.
COMPARATIVE ANALYSIS BETWEEN VARIOUS PROPOSED CONFIGURATIONS

Geometry	Bandwidth	Radiation Efficiency	Gain
Basic square patch	15.16GHz - 14.66GHz = 0.50GHz =3.38%	94.84%	9.87dB
Basic square patch in stacked structure	12.49GHz - 11.70GHz = 0.78 GHz =6.50% 15.52GHz - 14.93GHz = 0.58GHz =3.85%	93.56%	7.36 dB
1st iteration of fractal patch	16.50GHz - 15.75GHz = 0.75GHz=4.65%	95.40%	10.10 dB
1st iteration of fractal patch in stacked structure	13.15GHz - 11.53GHz = 1.62GHz =13.15% 16.57GHz -15.63GHz = 0.94GHz =5.84%	93.60%	6.39 dB
2nd iteration of fractal patch	16.76GHz -15.96GHz = 0.80GHz =4.89%	94.63%	10.11 dB
2nd iteration of fractal patch in stacked structure	13.41GHz - 11.78GHz = 1.63GHz =12.94% 16.53GHz - 15.72GHz = 0.81GHz =5.02%	96.99%	6.32 dB

V. Conclusions.

The effect of a dual layer staked structure configuration with the influence of fractal designs on a microstrip square patch antenna fed with 50Ω coaxial cable, for attaining both wide bandwidth and high gain properties, is proposed and analyzed for Ku-band of satellite communication.

It is observed that using the stacked configuration and fractal patches in microstrip antenna, it has great impact on the impedance bandwidth, gain and efficiency of the proposed antenna. The result reveals that with the increase in fractal iteration level, the impedance bandwidth of the antenna also increases. The arithmetic algorithm used in the proposed design which is created iteratively by cutting every corner side of the patch in a specific length ratio of 1:5 about its parent segment, provides a high flexibility to achieve wide bandwidth and high gain properties while maintaining the radiation efficiency high in the operating frequency band. Moreover, the concept of stacked configuration used in the proposed design is for the improvement in the performance of antenna especially to further improve the impedance bandwidth.

The result shows that 2nd iteration of fractal patch is the optimum design among un-stacked configuration, whereas in stacked configuration the 1st iterated fractal patch gives optimum results in terms of gain, impedance bandwidth and radiation efficiency.

The results of 2nd iterated fractal patch demonstrates that the gain of the antennais 10.13 dB with 94.64% radiation efficiency whereas the impedance bandwidth for S11<-10dB achieved is 0.80GHz (4.89%) which is 0.30GHz wider than that achieved for basic square patch. The 1st iterated fractal antenna in stacking structure shows a total impedance bandwidth of 2.56GHz (18.97%) and exhibits dual band of operation from 11.53GHz to 13.15GHz (13.12%) and 15.63GHz to 16.57GHz (5.86%) around the resonant frequencies of 12.31GHz and 16.19GHz respectively, whereas the gain is 6.38dB, and the radiation efficiency is up to 93.60%.

References

[i] C. Balanis, Antenna theory. Hoboken, N.J.: John Wiley, 2005.

[ii] D. M. Pozar, “Microstrip antennas,” Proc. IEEE,vol. 80, pp. 79–91,Jan. 1992.

[iii] M. Alam, M. Islam and H. Arshad, "Gain Enhancement of a Multiband Resonator Using Defected Ground Surface on Epoxy Woven Glass Material", The Scientific World Journal, vol. 2014, pp. 1-9, 2014.

[iv] R. Rana, N. Vyas, R. Verma, V. Kaushik and A.K.Arya, “Dual Stacked Wideband Microstrip Antenna Array for Ku-Band Applications”, Int. Journal of Engineering Research and Applications, Vol. 4, Issue 6 (Version 1), Pp 1-4, June 2014.

[v] S. Preeti and S. Gupta, "Bandwidth and gain enhancement in microstrip antenna array for 8GHz frequency applications", Engineering and Systems (SCES), 2014 Students Conference on. IEEE, 2014.

[vi] C. S. Lee, V. Nalbandian, and F. Schwering, “Gain enhancement of a thick microstrip antenna by suppressing surface waves”, in Proc. IEEE Int. Conf. Antennas and Propagation, vol. 1, Jun. 1994, pp. 460–463.

[vii] K.-L. Lau, K.-M. Luk, and K.-F. Lee, "Design ofa circularly-polarizedvertical patch antenna",IEEE Trans. Antennas Propag., vol. 54, no. 4, pp. 1332–1335, Apr. 2006.

[viii] R. Chair, K. F. Lee, and K. M. Luk,"Bandwidth and cross-polarization characteristics of quarter-wave shorted patch antennas. "Microwave and Optical Technology Letters 22.2, 1999, pp. 101-103.

[ix] X. Ren, X. Chen, Y. Liu, W. Jin and K. Huang, "A Stacked Microstrip Antenna Array with Fractal Patches", International Journal of Antennas and Propagation, vol. 2014, pp. 1-10, 2014.

[x] D. M. Pozar, "A review of bandwidth enhancement techniques formicrostrip antennas," in Microstrip Antennas, D. M. Pozar and D. H.Schaubert, Eds. New York: IEEE Press, 1995, pp. 157–166.

[xi] H. Parikh, S. Pandey, and K. Modh, "Wideband and high gain stacked microstrip antenna for Ku band application," 2012 Nirma University International Conference on Engineering (NUiCONE). 2012.

[xii] N.M. Sahar, M.T. Islam and N. Misran, "Analysis of Fractal Antenna for Ultra Wideband Application",Research Journal of Applied Sciences, Engineering and Technology 7(10): 2022-2026, 2014.

Design of High Performance IIR Filter Using Vedic Multiplication Method

Y. A. Durrani
Electronics Engineering Department, UET, Taxila, Pakistan
[1]yaseer.durrani@uettaxila.edu.pk

Abstract-Digital filters can be found in most of the electronic circuits. One major application of these filters involve an input signals that are sampled and converted to the real-time signal to the modern computers. This paper describes the high performance infinite impulse response (IIR) filter using Vedic multiplication method due its low round-ff noise and low quantization errors. It reduces the computational delay and hardware to minimize the number of iterations and enhances the performance of the DSP processor. Vedic method enables the parallel processing stages of intermediate products and removes the unnecessary multiplication steps with zeros. The filter is designed on Xilinx software and different frequency responses are evaluated in Matlab at different filter orders.

Keywords-Digital Filter, Vedic Multiplication, Frequency Responses, Cascaded Structure

I. INTRODUCTION

The design of digital filter is entirely different from analog filters. Digital filters process signals in time domain and if a specific frequency domain response is needed, it is highly desirable to convert it into the equivalent time domain response. Normally, the digital signals are in parallel form and these are more binary-coded version of analog signals. These filters perform mathematical operations on a sampled, discrete-time signal to enhance or reduce signal. It is simply a discrete-time, discrete-amplitude convolver [i].

A large percentage of digital filters are implemented in finite and infinite impulse response (FIR) and (IIR) filters. The FIR filters are used over a wide range of sample rates in electronic design automation (EDA) tools, and DSP-based systems. The IIR filters normally have low-order than FIR filters with same performance due to low sample rates (less than 200KHz), sharpness of cutoff, and pass-band ripples etc. Due to low-order, IIR filters tend to require efficient digital multipliers with less computation and less delay elements. The IIR filter, known as a recursive filter, uses feedback to compute outputs. These are very effective in several applications such as low-power communication transceivers, routers, etc. Furthermore, they require less number of parameters in designing, lower memory requirements and lower computational cost. IIR filter do not provide linear phase within its pass-band and more feasible to designers [ii].

High performance is most critical issue in very-large-scale integrated (VLSI) technology. For many DSP applications the hardware involves in actively multi-tasking computations and it increases large amount of delay. On the other hand, the sophisticated and portable wireless devices are very power conscious. We can attenuate these dependences by tuning complexity according to the given criteria and altering the behavior of the signal [iii]. A higher order sequential IIR filter can be realized by cascading the multiple stages of 2nd order filter as they known as biquads. Each biquad section can be turned off when they are not needed in order to improve the performance. Every biquad is designed so that it can satisfy the overall required specifications with stability, and amplitude response [iv].

The bi-linear transformation technique is the earlier technique that has been developed [v]. This technique adopts the digital filter with the transformation of the corresponding analog filter, and then known filter design methods, such as Chebyshev type I and II, or Butterworth are used to develop the design of related filter. The accomplished analog filter is again inter-transformed back to digital filter by using the bi-linear transformation. However, this method requires lot of related information and in many cases demonstrates the poor results [vi]. Recently more accurate techniques have been introduced with higher performance with lesser knowledge of the filter [vii]. Apart of this area of research, several other more advanced techniques have been proposed such as impulse invariance approach, matched Z-transformation, fixed-point representation, and evolutionary algorithm [viii], [ix].

Multiplication can be performed in DSP system through different types of operations such as convolution, fast fourier transform or the filter design. The processor performance can be dependent on the speed of the multipliers. Hence, the speed of the multiplication is crucial component in DSP system. The commonly used application in any DSP system is the design of the digital filter. The IIR filter is also known as convolution filter due to the sequence of time domain multiplication is same as the convolution is

implemented in frequency domain [x]. The focus of this paper is the design of high speed IIR filter by using Vedic multiplier method. These types of the multipliers increase the performance of the processors by reducing the number of iterations. Recently few methods [xi], [xii] have been proposed using Vedic multiplication structure. Their work with the reduction of number of bits in multiplication process gives reasonable performance but more average execution time as compared with Matlab built-in function.

The paper is organized as follows. In Section II, the detailed background of digital IIR filter is discussed. The proposed architecture of IIR filter is described in Section III. The experimental results are demonstrated IV. Finally, the Section V summarizes the work.

II. IIR Filter Background

The IIR filter is a linear-time-invariant discrete time system characterized by difference equation in (1):

$$y[n] = \sum_{k=0}^{\infty} h(k)x(n-k) = \sum_{k=0}^{N} b[k]\,x(n-k) - \sum_{k=1}^{M} a[k]y(n-k) \quad (1)$$

where $h[k]$ is the impulse response of the filter with infinite in duration, $a[k]$ and $b[k]$ are coefficients of the filter, $x(n)$ and $y(n)$ are the input/output (I/O) of the filter respectively. The transfer function of IIR filter can be expressed in z-domain of (1) is given in difference equation in (2):

$$H(z) = \frac{b_0 + b_1 z^{-1} + \cdots + b_N z^{-N}}{1 + a_1 z^{-1} + \cdots + a_M z^{-M}}$$

$$H(z) = \frac{\sum_{k=0}^{N} b_k z^{-k}}{1 + \sum_{k=1}^{M} a_k z^{-k}} \quad (2)$$

Using equation (2), the IIR digital filter realization needs feedback as shown in Fig. 1. The n_{th} order filter transfer function of II filter can be characterized as $2n + 1$ coefficients. Generally it requires $2n$ two adders and $2n + 1$ multipliers for the hardware implementation.

Different type of realization structures can be obtained by difference equation of the filter named as direct-form realizations. The most common realizations are: direct form-I, direct form-II and transposed direct form-II. These all forms are functionally equivalent but there is a difference in their architecture, such as [vii]:

- *Direct form-I* has $n + m + 1$ multipliers, $n + m$ adders and $n + m$ memory locations (or delay components). The coefficients of the multiplier are accurately the coefficient of the transfer function.
- *Direct form-II* architectures uses $n + m$ adders, $n + m + 1$ multipliers, and maximum of $\{n, m\}$ locations of memory. Such architectures use minimum locations of memory than the direct form-I architecture, it known as canonic.
- *Transposed direct form-II* realization architecture also uses same amount of adders, multipliers, and locations of the memory as direct form-II structure. It uses less number of delay elements in its design compared to direct form-I.

III. Proposed Architecture of IIR Filter

In this section, a *cascaded form* of digital IIR filter design methodology is proposed. The recursive system of filter architecture exhibits high performance, low computational complexity and minimum memory requirements. As the filter order increases, the complexity of the hardware implementation is increased and the range of the precision decreases. In this paper, for better attenuation the 4th order IIR filter is implemented by cascading two stages of 2nd order IIR filter or biquads (two poles and two zeros). The 2nd order architecture is not very sensitive to the quantization of coefficient and several bits are not required to identify the values of the coefficients. The IIR filter uses more than one cascaded biquad architecture. For higher-order filters, many biquads are cascaded such as:

$$H(z) = \prod_{i=1}^{n} \left(\frac{b_{i0} + b_{i1} Z^{-1} + b_{i2} Z^{-2}}{1 + a_{i0} Z^{-1} + a_{i1} Z^{-2}} \right) \quad (3)$$

where n is the number of biquads. The cascaded of biquads can be re-ordered to minimize the round off noise. However, the n biquads gives n possible options.

Analyzing fig. 1, each biquad structure is comprised of two feedback paths (a_1 and a_2) and two feed-forward paths (b_1 and b_2). The operation of the filter is summarized by the set of recursive equations in (4) and (5):

$$p(n) = x(n) - a_1.p(n-1) - a_2.p(n-2) \quad (4)$$

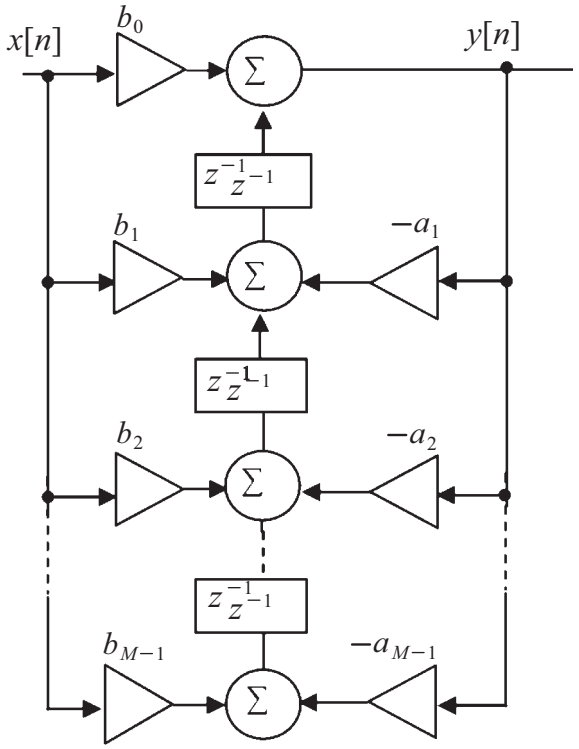

Fig. 1. Block diagram of transport-direct form II IIR filter

$$y(n) = b_0.p(n) + b_1.p(n-1) + b_2.p(n-2) \quad (5)$$

Analyzing (4) and (5), to implement a biquad filter, only four addition and five multiplication blocks are required. In the design of the IIR filter, the traditional array or Booth multiplier is not used, instead Vedic multiplier is implemented due to the fast switching ability and low-computational complexity. The transposed-direct form II structure is used for the reduction of round-off errors. This type of error is due to the coefficient quantization and truncation of bits. Every biquad section implements a 2nd order filter by using the equation of difference in (6) using (7) and (8):

$$y[n] = b_0 * x[n] + p_1 \quad (6)$$
$$p_1 = b_1 * x[n] + a_1 * y[n] + p_2 \quad (7)$$
$$p_2 = b_2 * x[n] + a_2 * y[n] \quad (8)$$

where p_1 and p_2 are the two state value *s*, b_0, b_1, and b_2. The coefficients multiply the input signal $x[n]$ as referred to the feed forward coefficients. The a_1 and a_2 coefficients multiply the output signal $y[n]$ is the feedback coefficients. The output not only depends on the present input but also on the previous values of outputs i.e., it has a recursive structure. The use of transpose-direct realization structure reduces the necessary number of adders and delay lines.

A. Vedic Multiplication

High-speed parallel multiplication is very significant in digital signal processing (DSP) system. Vedic multiplication method is used in many DSP applications such as digital IIR filter, FET, convolution and Fourier transform etc. The Vedic multiplication method [xiii] enables to reduce the traditional processing steps. It uses 16 formulae and 16 sub-formulae, which deals with the several basic and complex mathematical computational operations. It performs multiplication through crosswise and vertically steps. The numeric digits on the two different ends of the each line are multiplied and their result can be added with previous value of the carry. If there are more lines in one single step, all results can be added to the previous carry value. The least-significant digit is obtained and acts as one of the result that takes the carry for the next step. Initially the carry value is considered as zero.

The Vedic multiplication process is performed through the generations of all possible partial products with the concurrent addition of these partial products. Parallel partial products are calculated with their sum. Let the product of N x N-bit binary numbers P and Q where $P = p_1 p_2 p_3 ... p_n$ and $Q = q_1 q_2 q_3 ... q_n$. The multiplication process may be viewed by two steps: The evaluation of partial products and the accumulation of shifted partial products can be described in the following steps:

Step 1: Divide the multiplicand P and multiplier Q into two equal lines, each consists of $[1 + n \ to \ (n/2)]$ bits and $[n \ to \ 1]$ bits, where first part represents the most-significant-bit (MSB) and other indicates least-significant-bit (LSB).

Step 2: Indicates the parts of P *as* P_{MSB} and P_{LSB} and parts of Q *as* Q_{MSB} and Q_{LSB}.

Step 3: For P x Q, the product can be obtained as:

P and Q are divided in P_a, P_b *and* Q_a, Q_b further their a and b part is divided into 4 bits. We can get the resultant product as shown in Fig. 2.

The Vedic multiplication can be performed as:

$$Q_b \ Q_a \text{ x } P_b \ P_a = R_3 R_2 R_1 R_0 \quad (9)$$

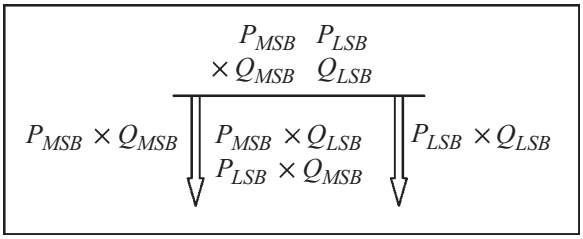

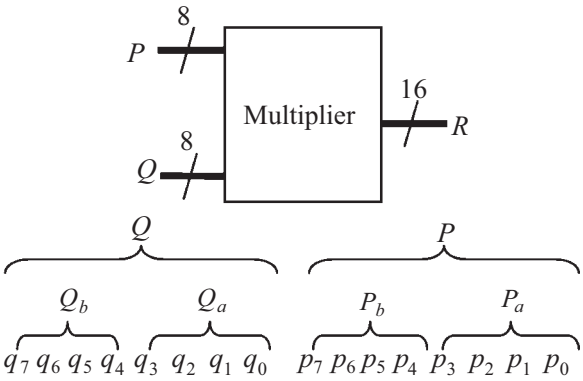

Fig. 2. 8 x 8-bit Vedic multiplication

where

$R_0 = P_a$ x Q_a, $R_1 = (P_b$ x $Q_a) + (P_a$ x $Q_b)$, $R_2 = P_b$ x Q_b (10)

The line diagram of the Vedic product of mapping in binary system is shown in Fig. 3. Each bit is encircled in the Figure and the process of multiplication is demonstrated in [xiv].

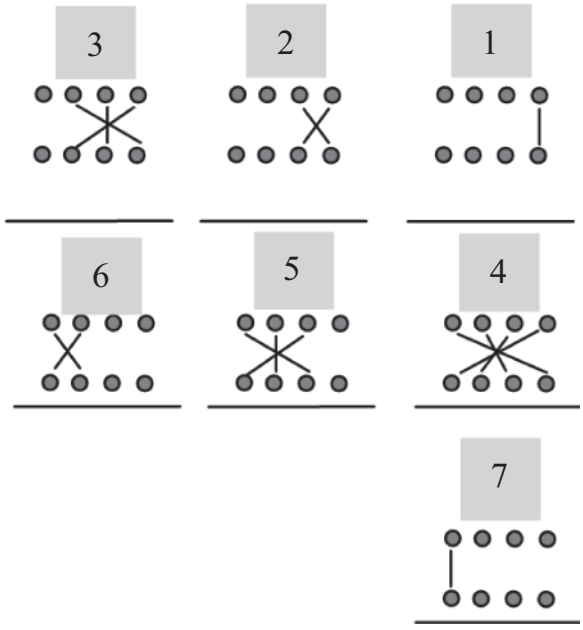

Fig. 3. Line Diagram for the multiplication of two 4 bit numbers [xiii].

B. Hardware Implementation

Binary multiplication consists of following basic operations:

0 x 0 = 0, 1 x 1 = 1, 0 x 1 = 0, 1 x 0 = 0

As hardware, two *n*-bit numbers *p* and *q*, can be expressed as in (11) and (12):

$$p = 2^x \pm \alpha_1 \quad (11)$$

$$q = 2^x \pm \alpha_2 \quad (12)$$

where x is the exponent, a_1 and a_2 of p and q respectively. Assuming the product Z of both numbers is:

$$Z = p \times q = (2^x \pm \alpha_1)(2^x \pm \alpha_2) \quad (13)$$

The bases of multiplier and multiplicand can be assumed same, thus (14) can be expressed as:

$$Z = pq = 2^x(p \pm \alpha_2) \pm \alpha_1\alpha_2 \quad (14)$$

The large multiplication can be decomposed into a small multiplication, shifting addition, and subtraction. Hence, the power, delay, and cost factors can be improved by the reduction of hardware. Similarly, if we multiply two bits *p* and *q*, then logical AND operation produces the same result as shown in Fig. 4.

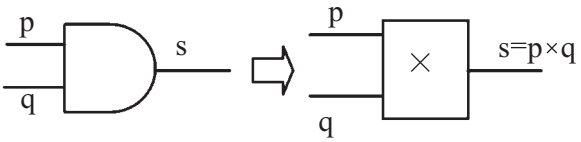

Fig. 4. Bit-level multiplier

The logic synthesis is performed at register transfer level (RTL). Initially 2x2-bit Vedic multiplication is performed with four input AND gates and half-adders (HA) as given in Fig. 5-(a). Similarly, the 4x4-bit Vedic multiplication uses same 2x2-bit multiplier as the basic building module and the 8x8-bit multiplication uses 4x4-bit module and similarly for *n* x *n*-bit multiplication. The 8-bit multiplicand *P* splits into two 4-bit sub-multiplicands P_a and P_b. Similarly for 8-bit multiplier *Q* also splits into two 4-bit sub-multiplier Q_a and Q_b. The results of this product would be more than 4-bits $R_3R_2R_1R_0$ are given in (10). To implement 8x8 multiplications, we need four 2x2-bit Vedic multipliers and three 4-bit full adders. Multiplication minimum hardware architecture and low-computational complexity is shown in figure 6. Here the partial product and addition is performed concurrently. The ripple carry adder (RCA) consist two parts:

- Sum and carry selector
- Sum and carry generator

The second part consumes the most of the logic sources of RCA and creates the critical path. The RCA design in the multiplier is with the minimum hardware. It effectively eliminates all redundant operations and the logical sequences are performed according to the data dependence.

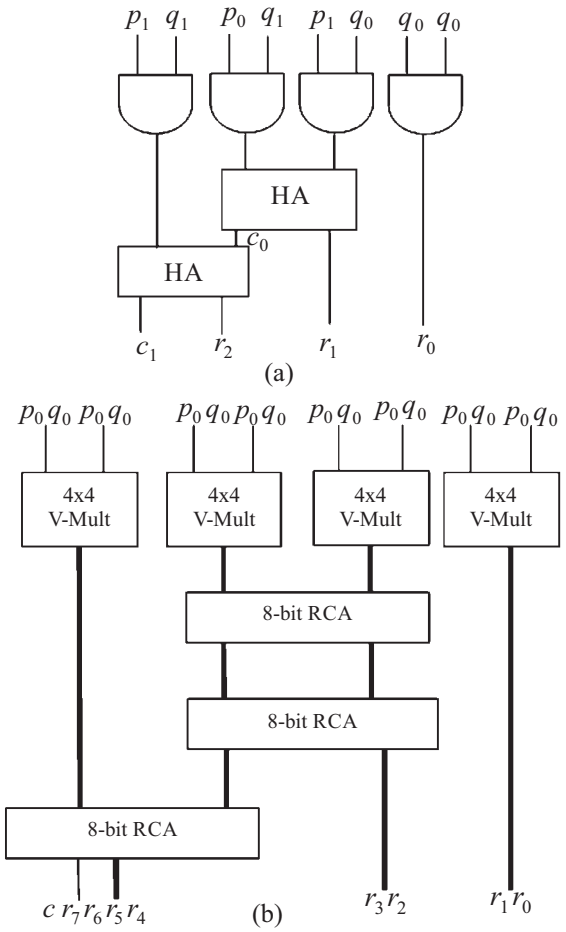

Fig. 5. Hardware implementation of (a) 2x2-bit Vedic multiplication (b) 8x8-bit Vedic multiplication

IV. Experimental Results

In this section, we evaluate the performance of 8-bit IIR filter through Vedic multiplication method. The logic synthesis and simulation is performed in Xilinx EDA (Electronic Design Automation) tool. The extensive simulations are performed for accurate results through various test benches. To verify the digital outputs of the filter, several waveforms are generated as shown in Fig. 6. The figure demonstrates accurate waveforms obtained from Xilinx EDA tool.

The 2nd order IIR filter of direct-form II, with band-pass Butterworth response is implemented in Matlab to find the coefficients of the filter. The magnitude, phase and impulse responses are shown in Fig. 7. The filter response has wider range during the lower order with low-computational complexity, good linearity and insensitive to the parasitic capacitances. The filter has band-pass sampling and cut-off frequencies of 8400Hz and 1320Hz respectively. The experimental result shows that the responses of the complex filter are very similar with the commercial software plots and shows accurate results in terms of

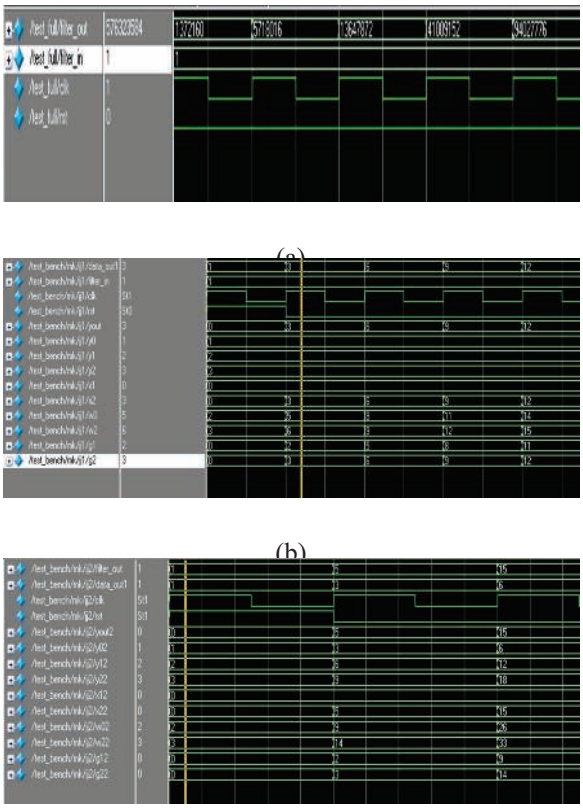

(a)

(b)

(c)

Fig. 6. (a) Filter output (b) Section-II simulation (c) Section-II simulation

The proposed Vedic multiplication method is analyzed for performance and well-know multiplication approaches. Table 1 demonstrates the comparison of the results in term of the basic design requirements. Table clearly shows the power consumption, memory usage and delay of the Booth, array and Vedic multipliers respectively. The Vedic multiplier has minimum hardware utilization and consumes almost equal power with Booth and Array multipliers as given in third and fourth column. In fifth and six columns, the Vedic multiplier occupies minimum memory usage and achieves highest performance with minimum gate delay.

TABLE I
Comparison of Different Multipliers

Multiplier	No. I/O	No. of Slices (Area)	Power (mW)	Memory Usage (KB)	Delay (ns)
Vedic	32	436	19.12	181233	18.12
Booth	32	770	19.06	230331	25.33
Array	32	856	21.88	250206	29.28

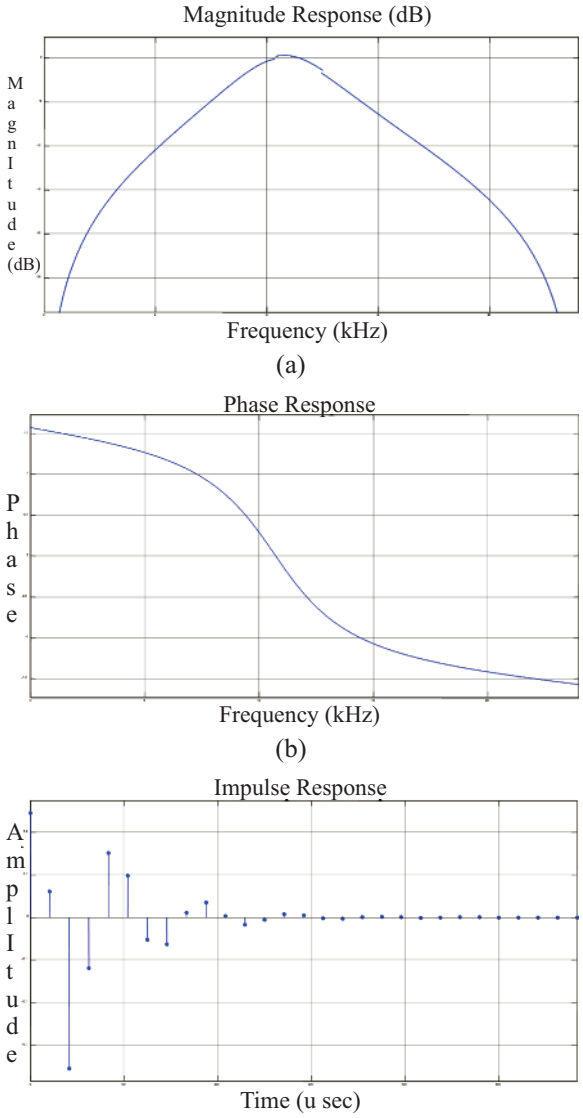

Fig. 7. Frequency responses of IIR band-pass filters with (a) Magnitude response (b) Phase response (c) Impulse response

V. Conclusions

The IIR filter is designed with Vedic multiplier method is proposed in this paper. The Vedic multiplier architecture is used due its low round-ff noise and low quantization errors. The results demonstrate that it reduces the computational delay and hardware to minimize the number of iterations and enhances the performance of the DSP processor. Vedic method enables the parallel processing stages of intermediate products and removes the unnecessary multiplication steps with zeros. The filter coefficients and frequency responses are found in Matlab. The magnitude and phase responses of the filter are very similar to the Multisim software.

References

[i] P. E. Danielson, "Serial-parallel convolvers", *IEEE Transaction on Computers*, vol. 33, no. 7, pp. 652-667, 1984.

[ii] R. Dutta, "Power efficient VLSI architecture for IIR filter using modified-Booth algorithm", *International Journal of Advanced Research in Technology*, vol. 2, no. 1, pp. 27-34, 2012.

[iii] K. Yeo, and Kaushik Roy, "Low-voltage, low-power VLSI subsystems", *McGraw-Hill companies publisher*, USA, 2005.

[iv] E. Singhal, "Performance analysis of FIR filter design using various window methods", *International Journal of Scientific Research Engineering & Technology*, vol.1, no. 5 , pp. 018-021, 2012.

[v] A. Gupta, U. Malviya, and V. Kapse, "Design high speed arithmetic logic unit based on ancient Vedic multiplication technique", *International Journal of Modern Engineering Research*, vol. 2, no.4, pp. 2695-2698, 2012.

[vi] S. Gupta, and A. Panghal "Performance analysis of FIR filter design by using rectangular, hanning and hamming windows methods", *International Journal of Advanced Research in Computer Science & Software Engineering*, vol. 2, no.6, pp. 334-347, 2012.

[vii] S. K. Mitra, "Digital Signal Processing: A computer based approach", *Mc-Graw Hill Higher Education Publisher*, 3rd Edition, 2006.

[viii] Y. Wang, and B. Li, "Two-stage based ensemble optimization for large-scale global optimization" *Proceeding of the IEEE Conference on Evolutionary Computation*, Spain, pp. 4488-4495, 2010.

[ix] Y. Wang, B. Li, and Y. B. Chen, "Digital IIR filter design using multi-objective optimization evolutionary algorithm" *Journal of Applied Soft Computing*, vol. 23, pp. 45-53, 2010.

[x] Y. Yu, and Y. Xinjie, "Cooperative co-evolutionary genetic algorithm for digital IIR filter design" *IEEE Transactions on Industrial Electronics*, vol. 54, pp. 1811-1819, 2007.

[xi] Y. Wang, B. Li, and W. Thomas, "Two-stage ensemble memetic algorithm: Function optimization and digital IIR filter design", *Journal of Information Sciences*, vol. 220, pp. 408-424. 2013.

[xii] H. Choo, K. Muhammad, and K. Roy, "Complexity reduction of digital filters using shift inclusive differential coefficients", *IEEE Transactions on Signal Processing,* vol. 52, pp. 1760-1772, 2014.

[xiii] P. Puri, and U. Patil, "High Speed Vedic Multiplier in FIR Filter on FPGA", *Journal of VLSI & Signal Processing*, vol. 4, no.3, pp. 48-53, 2014.

[xiv] K. Padma, Z. Sameena, S. Ankita, "16-order IIR filter design using Vedic mathematics technique", *International Journal of Engineering Innovation and Research*, vol. 3, no. 2, pp. 138-145, 2014.

Thermography as Automatic Diagnostic Tool For Electrical Substations: A Review

J. Amjad[1], M. Abrar[2]

[1,2]Electrical Engineering Department, UCE & T, Bahauddin Zakariya University, Multan
[1]jawadamjad93@gmail.com

Abstract-Temperature and resulting heat signatures are pragmatic indicators of the healthiness of electrical equipments employed in substations. The thermal heat, resulting due to losses induced by square of current flowing through switchgear and any irregular pattern, can be appropriately measured and detected by infrared based non-destructive and non-contact type thermographic technique to detect any anomaly present in the electrical substation. Thermographic process can detect any irregular and abnormal conditions in the substation without having need to impede productivity thus enhancing the overall reliability, safety, availability of power system along with reducing maintenance costs by predicting the fault in the electrical substation. The different kinds of problems encountered in the substation equipment along with the constraints of thermography have been presented. The main focus of this paper is on review of image processing methods which essentially automate the process of fault detection in substation. These image processing methods augment the thermographic process with advantages of negating the possible effects of human errors, suppressing the external noise signals and also speeding up process of pinpointing the faulty area in the target image which is core objective of thermography of substation because manual analysis is laborious and error prone. In addition, due to its widespread usage as a condition monitoring tool, the applications of thermography in different fields of life have also been discussed.

Keywords-Pragmatic, Thermographic, Productivity, Image Processing, Automate.

I. INTRODUCTION

The infrared thermography (IRT) is a technique of measuring the temperature of materials by inspecting them with the help of some thermal imaging means. This inspection is performed to make a thorough observation and inspection about the operating condition and service life of the material. These thermal imaging devices actually measure the radiations emitting from the surface of the material upon which the inspection is being performed. These thermal imaging devices are designed to measure the radiations and convert them into useful observations. As the name implies they measure the infrared energy emitting from the material. Every material above absolute zero (0 Kelvin) releases heat in some form of radiations.

Thermography has emerged to be an excellent technique for monitoring and diagnosis of substation equipment. In order to make a correct and thorough diagnosis of substation equipment, it is imperative to have knowledge about the component identification and thermal signatures to be obtained from different substation equipment [i].

One of the main advantages of thermal infrared thermography is that all the electrical equipments in a substation get heated to unbearable extent before they become permanently damaged, that's what thermography works on. Its process, advantages in the rural utility have been discussed such as immediate bottom line results, reduced outage costs, less downtime, good customer relationships and increased overall revenues to utility, improved and effective maintenance, pinpointing the fault location, reduced operational costs, reduced power losses in system [ii]. It can help avoiding the duration and frequency of outages, along with detecting the quality of material, work performed as well as rectifying bad work practices [iii]. The causes of abnormal temperature detected by thermal means help to increase the life cycle of the equipment along with avoiding any other related hazard [iv].

In this paper, different image processing techniques have been discussed to augment thermography process of substation which are based on different kinds of algorithms for automatically and speedily locate the faults and hotspots. All these techniques are refining the results of thermographic inspections. Multiple technology trends of thermography like Robotics inspection, HD thermal detectors, efficient fault detection algorithms, pulse and modulation thermography are being implemented in the diverse fields like power systems, substations, detecting faults in pipe lines, wood deformations, concrete defects, inspection of machineries, corrosion monitoring, welding process inspection, bruise detection in fruits etc. due to its usefulness of applications in different fields.

II. Background of Infrared Thermography Instruments

The infrared (IR) radiations were discovered by William Hershel during his experiment which revealed that the some of the radiations refracted from the prism onto thermometers showed high temperatures which for first time showed that there are some forms of energy which are invisible to human [vi]. The concept of thermal imaging can be made clearer by understanding the concept of the black body radiation. The term black body was introduced by Gustav Kirchhoff in 1960. The black body radiation is an electromagnetic radiation for a material that is thermal equilibrium with the surrounding environment. The type of radiations emitted by the materials can be considered as the black body radiation. The radiations emitted by a perfect black body lies in the infrared spectrum which is not visible to the human eye as it is not sensitive to observe such low wavelengths. The black body absorbs all the radiations thrown at it and also has an emissivity of one. The black body has a frequency spectrum depending upon the temperature of the body known as Plank's Spectrum or Plank's Law [vii].

$$M_\lambda(\lambda,T) = \frac{c_1}{\lambda^5}\frac{1}{e^{\frac{c_2}{\lambda T}} - 1} \quad (1)$$

where M (W/m^2) is spectral radiant exitance, λ (m) is wavelength of radiation, T (K) is absolute temperature of body , c_1 and c_2 are the first and second radiation constants respectively.The interpretation of the formula produces a series of curves corresponding to various temperatures. The exitance is zero near λ=0 and increases to a maximum value at λ_{max} and then again becomes zero at higher wavelengths. As the temperature of the black body keeps on increasing above 500^{o}C, the infrared emissions convert into reddish and radiations appear to the human eye in the visible spectrum. By differentiating Plank's law with reference to λ to find maxima, we get Wien's Displacement Law[viii].

$$\lambda_{max} = b/T \quad (2)$$

where T (K) is absolute temperature and b is the constant of proportionality and is called Wien's Displacement constant having value equal to 2898x10^{-6} which explains the fact why colors change from red to orange as with increase of temperature. By further integrating the Plank's law from λ=0 to λ=infinity, we get Stefan-Boltzmann's Law, which is given as[ix]:

$$W = \sigma T^4 \quad (3)$$

where W (W/m^2) is spectral intensity, T (K) is absolute temperature; σ is Stefan-Boltzmann constant of proportionality. From this law, one can determine the power radiated from anybody in terms of its temperature.

A. Thermal Radiation Principles

In real word applications, no material perfectly behaves as a black body which has property to exhibit perfect emissivity. There are three parameters for real world materials when radiation energy impinges on it: a fraction of it is absorbed α, some of it is reflected γ and remaining of it is transmitted τ. From these parameters, a law named Total Radiation Law is derived which is given by formula[x]:

$$W = \alpha W + \gamma W + \tau W \quad (4)$$

On further simplification, the formula is reduced to following form:

$$1 = \alpha + \gamma + \tau \quad (5)$$

These parameters absorption coefficient (α), reflection coefficient (γ) and transmission coefficient (τ) depend upon the material properties and may have a value anywhere between zero and one. Another important parameter encountered while making thermal inspection is emissivity (ε) which is the property of the material to radiate the amount the energy which is absorbed by it. In general terms, the spectral emissivity is the ratio of radiant energy emitted from the material to that of a perfect black body at same temperature and wavelength conditions.

B. Instruments for Temperature Detection

Different Types of equipments are employed to measure the temperature of materials. These instruments are: glass thermometer, thermocouple, resistance temperature detector (RTD), thermistor, pyrometer, infrared thermography. Only infrared thermography will be discussed here.

1) Infrared Thermography

The thermographic inspections work on principles of detection of infrared radiations and convert these radiations into a visible thermal image. The radiations measured through the lens of thermographic devices are in fact coming from different sources which are to be interpreted correctly. In infrared thermography system, two kinds of infrared detectors are used to detect the radiations in infrared spectrum i.e. mid wave (MW) and long wave (LW) having measuring ranges of 2–5 μm and 8–14 μm of the electromagnetic spectrum band, respectively[xi]. It is interesting to note that these detectors are not designed to detect very low range infrared waves in electromagnetic spectrum because of the effect of atmosphere to infrared radiations, there are uncertainties introduced in the measurements due to cause of blocking of some of radiations by atmosphere [xii].There are two kinds of thermographic instruments being used for condition monitoring:

1. Infrared thermometer (thermographic gun)

2. Infrared camera (focal plane area)

The infrared thermometer has a serious drawback that it focuses at only one point at a given surface area and provides temperature reading of that point and it is prone to missing the hotspots that exist. Some thermal line detectors are also there which have a somewhat better field of view coving a larger area. On the other hand, with the recent advancement in technology, electronics laced thermographic camera has revolutionized the field of thermography. It provides more flexibility and accurate results although cost is downside of it [xiii]. The specifications of the infrared thermographic camera FLIR T440 is described in Table I as:

TABLE I
TECHNICAL DATASHEET OF FLIR T 440

Sr. No.	Features	Details
1	Temperature Range	-20 ºC to 1200 ºC
2	Zoom	8X continuous
3	Multi spectral Dynamic imaging	IR image with enhance detail presentation
4	Frame Rate	60 Hz
5	Field of view (FOV)	25˝x 19˝
6	Focus	Manual/automatic
7	Thermal sensitivity (N.E.T.D)	<0.045 ºC at 30 ºC
8	Detector Type	320x 240 pixels
9	Spectral Range	7.5 µm to 13 µm
10	Image modes	Thermal/visual
11	Lens	25º
12	Measurement Range	40m to 200m

III. THERMOGRAPHY IN ELECTRICAL SUBSTATION

The application of thermography in electrical substation brings vital importance for the effective maintenance of substation. In this section, measurement approaches in thermography, type of faults in substation equipment, the constraints in thermal inspections and finally thermal image processing techniques will be discussed.

A. Measurements Approach

There are two criteria defined for deciding the level of criticality so that necessary maintenance action may be performed.

1. Quantitative Approach
2. Qualitative Approach

In quantitative measurement [xiv], the exact temperature of the point of interest is taken for evaluation. The quantitative measurements require accurate data extraction methods because of lot of variable factors to be accounted for during thermographic inspection. The Fig.1 shows an example of quantitative approach of thermography in which abnormal condition of 220kV current transformer is diagnosed.

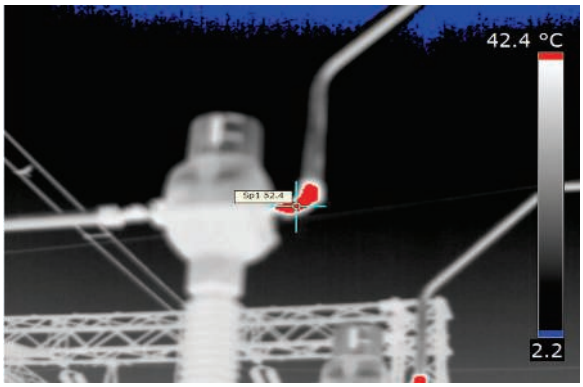

Fig. 1: Quantitative thermographic diagnostic approach

The Fig.1 above shows that the current transformer with abnormal heating pattern. Because of various external factors influencing the quantitative measurements, the exact temperature obtained through thermal imaging means is error prone thus the image has to be processed and accurate results have to be calculated based on the extrapolation methods. The quantitative approach for fault diagnosis is tabulated in Table II.

TABLE II
QUANTITATIVE APPROACH OF FAULT DIAGNOSIS

Sr. No.	Temperature of Equipment	Severity level of fault	Remarks
1	Temp. >130 ºC	Serious	Emergent shutdown of equipment for necessary repair and maintenance.
2	100ºC≤Temp. ≤130ºC	Mild	Perform repair and maintenance as soon as possible.
3	75ºC≤Temp. Rise<100ºC	Incipient	Monitor continuously until possible

The Fig. 2 shows an example of qualitative thermography [xv] which is more robust technique in a way that different components of same nature in a similar environment are compared with each other to find any problems. In qualitative approach, the difference of temperature (ΔT) between the similar phases is used for fault analysis. It is also known as comparative thermographic technique.

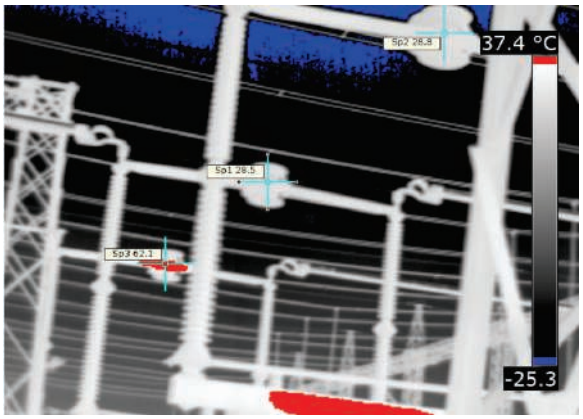

Fig. 2: Qualitative Approach of Fault Diagnosis

Here, one can observe that three phases of 220kV isolators are investigated in a single field of view to diagnose any anomalies present. It is clear from above figure that the red phase (farther) down the picture has an absolute temperature of 62.1 ºC as compared to other two phases, yellow and blue, having almost similar temperatures. Thus it indicates clear fault in red phase. This thermal view explains the importance of qualitative measurements and its easy apprehension. Now the fault must be attended in accordance to some criteria to perform necessary maintenance activity without any loss of equipment or productivity. Therefore, qualitative approach of fault diagnosis is tabulated below in table 3, which is divided into four categories according to condition of equipment and a priority is devised to investigate the fault [xvi]. This method is also called **ΔT** method [xvii].

TABLE III
QUALITATIVE APPROACH OF FAULT DIAGNOSIS

Sr. No.	Temperature Rise (ΔT)		Remarks
	Over Similar Phases	Over Ambient	
1	ΔT >15ºC	ΔT >40ºC	Indicates Major discrepancy which should be attended immediately
2	-------	20ºC≤ ΔT <40ºC	Monitor continuously until corrective measures can be taken
3	4ºC≤ ΔT <15ºC	11ºC≤ ΔT <20ºC	Indicates possible deficiency which must be attended during planned shutdowns
4	1ºC≤ ΔT <4ºC	0ºC≤ ΔT <10ºC	Indicates probable deficiency which warrants investigation

B. Thermographic Inspection of Joints

During the thermographic inspection, most of the problems that are encountered are at the joints. The joints are where two similar or dissimilar materials are connected together are usually the weakest link in the product design so a special attention is to provided to assure that joint is strongly bonded and has a life time of product. Infrared thermography technique can be applied to monitor different types of bonds which are mechanical linked joints, welded joints and adhesively bonded joints [xviii]. All the connecting surfaces are rough on micro scale, in fact the coupling between the two solid surfaces is where the roughness of one surface meets the roughness of the micro peaks of the other mating surface so in actual the contact area is very little. The corrosion and oxidation are responsible for the connector degradation [xix]. During the initial stages of degradation the coolness of the surface might not be detected through thermography. The inspection not only helps in rooting out defects but also helps in detecting design defects and its operation in a certain environment. Hence a technique has been suggested by author where a computerized model is used to describe the relation between temperature of electrical connection and surface temperature to find accurate results. A general rule of thumb is during thermographic inspection the load current should be more than 30% as load less than this leads to inaccurate results [xx]. The electrical anomalies found at the contact junctions having equation of equilibrium of contact junctions[xxi] which is as follows:

$$0.24.I^2.(R_k-R_l) = \alpha_{ef}(T_k-T_l).F_k \qquad (6)$$

Where

I = Electric current in the busbar, A;

R_k, R_l = Contact resistance and resistance of bus bar (without contact), Ω;

T_k, T_l = Temperature of contact & the Busbar, K;

F_k = Square of contact radiating surface, m^2;

α_{ef} = Radiation intensity of contact & bus surface , W/m^2.

The infrared thermography has redefined the criteria of maintenance. Instead of performing preventive maintenance on the equipments, the utilities are urged to perform predictive maintenance courtesy of infrared thermography. The equipment maintenance is prioritized based on the permissible temperature limits. The author experience shows that most of the hotspots are due to the bolted connections and isolator contacts deformation with time [xiv]. The measurements taken in a substation are prone to variable loading conditions, so in order to estimate an accurate result of the inspection even at loads less than 30%, a method has been proposed by Tommie M. Lindquist [xxii] to determine the probability of time to failure of a large number of electrical contacts in a substation. The Fig. 3 shows some of the measurements of thermographic inspection in which problems are encountered in joints at substation.

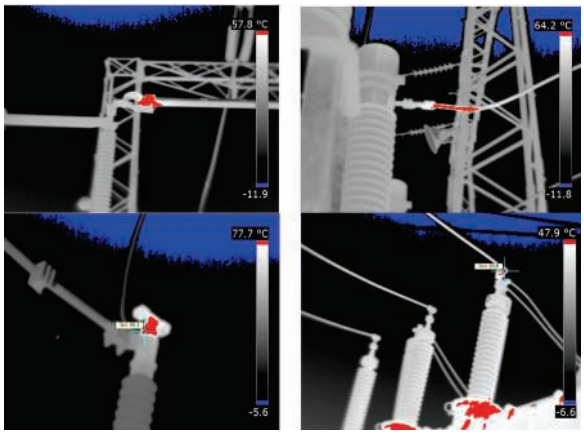

Fig. 3: Thermal analysis of electrical joints in substation

The temperature rise at the joints calculated for different loading conditions is equated as[xxiii]:

$$T_r = T_m (I_n / I_{load})^2 \quad (7)$$

where T_r=temperature rise, K;
T_m=temperature measured, K;
I_n=nominal load, A;
I_{load}= load current, A.

A probability density function is mapped to determine the rate of failures and maintenance programs for the suspicious contacts. As more measurements over the years are performed the overall results accuracy is increased.

C. In Sight and Out of Sight Faults

Infrared thermography helps in monitoring the electrical stresses on the substation equipments due to which timely preventive intervention could be made to avoid system failures. During diagnosis of high voltage equipments with faults, it was found there were two types of faults;

(i) External faults
(ii) Internal faults

The external faults are simpler to interpret but it takes some going to extrapolate the causes of internal faults in the equipments[xxiv]. The loose connection of circuit breaker contacts, current transformer contacts, inferior insulation of CCVT, low oil in Current transformer, ingress of moisture in the surge arrester, leading to breakdown of these high voltage equipments, are some examples of faults discovered during thermographic inspection. The external faults are shown in Fig. 4.

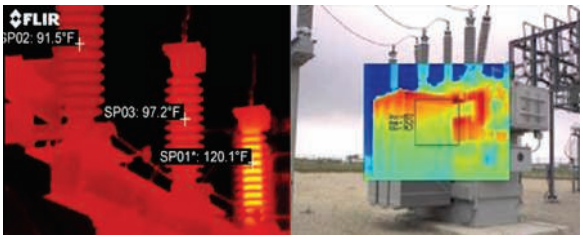

Fig. 4: Thermal View of Internal Inspection of Substation equipments

D. Anomalies in Power Substation Equipments

There are different types of equipments employed in substation for controlling, voltage regulation and protection of power system. As these are in large number employed in a large substation, it requires their proper maintenance plan and equipments knowledge. The thermographers must have knowledge about the component identification and thermal signatures to be obtained from different substation equipments. Different components behavior must be thoroughly studied like power transformers, instrument transformers, surge arresters, insulators, on load tap changer before inspecting these equipments [i]. The faults in a substation can be classified into loose connections, open or short circuit, overload, unbalanced load and improper component installation [iii]. The poor connections are base of faults most of the time [ii]. The different anomalies occurred in a power substation equipments are given below:

1) Transformer

The following types of faults can occur in transformer.

Oxidation in contacts, loose and deteriorated connection, load unbalancing, blocked or chocked radiator tubes, overloading, poor ground connection, unleveling of transformer tank, unbalanced load, low level of oil.

2) Circuit Breaker, Disconnector, Lightening Arrester, Cables

The following types of faults can occur in above mentioned.

Poor electrical connection, oxidation in contacts, misaligned breaker and isolator contacts, overheated lightening arrester, overloading, Failure of metal oxide discs of lightening arrester, improper connection at splices of cables, insulation breakdown in cables.

3) Bus Bar, Capacitor Banks, Fuses

The faults are: Overloading conditions, poor electrical connections, overloading conditions, corrosion.

4) Motor and Generator

The faults are: Blocked Rotor, harmonics, poor connections of connectors, poor heat dissipation, slip rings and commutators overheating.

E. External Factors affecting thermal inspections

There are some constraints regarding the

thermography which should be addressed to obtain error free results. These factors if neglected can cause influence during IR inspections in an air insulated substation (AIS) and consequently leading to erroneous condition evaluation of the equipment under analysis. Since this research is based on air insulated substations, so the stress has been on these factors. Such factors of influence can be characterized as procedural, technical or environmental factors [xxv] which will be discussed one by one.

1) Emissivity

During the thermographic inspection, one of most important factors to be counted for, to make accurate readings, is emissivity of materials to be inspected. Actually the readings recorded by the thermal means fall in the infra red region in the electromagnetic spectrum where the luminance have maximum value. The emissivity is the ability of a body to emit the infra red radiations. The black body is ideal with respect to emitting the absorbed energy. For a black body the emissivity is one but emissivity of electrical equipments varies between the vales of 0.1 to 0.95 depending upon material characteristics. As the thermographic camera measures the surface temperature of the objects so if emissivity factor is not correctly compensated, wrong temperature readings would be recorded as the temperature measured would not account for the reflections as well as refractions which would compromise the inspection process [xxvi]. Another important consideration during thermal inspection of substation is the angle of view. The angle of view of measurement also affects the emissivity values because the apparent temperature depends upon the angle of view along with thermal camera field of view. Thus these important facts must be taken into account [xxvii]. The emissivity of various materials are given in Table IV below [xxviii-xxix].

TABLE IV
EMISSIVITY OF SOME COMMON MATERIALS

Sr. No.	Description of Material	Temperature °C	Emissivity
1	Aluminum anodized	70	0.97
2	Aluminum weathered	17	0.87
3	Asphalt	4	0.96
4	Asbestos	20	0.96
5	Brass oxidized	100	0.61
6	Brick	20	0.93
7	Bronze powder	25	0.78
8	Carbon graphite	20	0.98
9	Clay	70	0.91
10	Concrete rough	17	0.97
11	Copper oxidized	20	0.88
12	Fiber board	20	0.85
13	Gold polished	100	0.02
14	Iron cast	1000	0.95
15	Lead oxidized	200	0.63
16	Magnesium	538	0.18
17	Nichrome oxidized	500	0.98
18	Nickel oxidized	1227	0.85
19	Paint different colors	70	0.93
20	Paper black dull	20	0.94
21	Plastic glass fiber	70	0.94
22	Platinum	538	0.12
23	Rubber	20	0.95
24	Sand	20	0.90
25	Skin human	32	0.98
26	Water ice	0	0.97

2) Reflected apparent temperature

When inspecting substation components, there may be other sources of radiation between thermal imaging device and electrical equipment. If the emissivity is low and there is any other source reflecting, then this factor must be adjusted for correct measurements.

3) Humidity

The rain, fog or snow may cause cooling and mask incipient faults in electrical equipments during inspection. Any potential faulty point may be cooled to temperature where it seems to be normal. Thus humidity factor must be fed to device to get accurate results. However for short distances, the humidity factor does not appreciably affect the measurements.

4) Distance/Object size

Another factor is the distance to the equipment from the inspection point. If distance to object is very large object is too small, then error is introduced which must be accounted for. This factor if neglected can take the priority into serious nature so it is imperative proper attention is made.

5) Wind

The wind at the outdoor substations has a significant impact on the thermographic inspections as it produces a reduction in the temperature effect as given by equation:

$$F_R = 1 - k.(1 - e^{-v/V}) \quad (8)$$

where k and V are the coefficients which depend upon the equipment and v (km/hr) is the velocity of wind [xxx]. As wind affects the temperature significantly and the substations are located all over the world having variable wind velocities throughout the year, so some correction factor must be applied to get accurate measurements. This correction factor at different wind speeds has been calculated experimentally and is tabulated in Table V below:

TABLE V
CORRECTION FACTOR FOR WIND SPEEDS

Wind Speed (m/s)	Wind Speed (knots)	Correction factor
1	2	1
2	4	1.36
3	6	1.64
4	8	1.86
5	10	2.06
6	12	2.23
7	14	2.40
8	16	2.54

6) Solar Irradiation

Solar heating raises the temperature of the equipments above the ambient temperature so a reference temperature must be calculated to negate the effect of sun's heating and used in measurement process.

F. Significance of Image Processing Techniques

As discussed above, numerous factors affect the measurements, so images obtained after the inspections are in raw form which may be erroneous so if action proposed to be taken according to non-dependable measurements could result in a significant revenue loss to a utility due to wrong interpretations. Most of the IR camera also has software applications, so that after capturing thermal images, they can be further analyzed. But the analysis requires qualified personnel having experience in the field of thermal inspection and along with that it is time consuming. Hence automated techniques are proposed to expedite the process and analysis of thermal images to minimize the operator dependence thereby enhancing the reliability of thermographic inspection. Generally in the image processing initially the thermal image is preprocessed, after that it is segmented from the background, then feature extraction algorithm is applied to extract the requisite features from the image, then image is classified for decision making

Different approaches or methods have been proposed earlier to investigate the faults through image processing means and they will be discussed in the following.

An automatic diagnostic method based on infrared thermography has been proposed using the statistical method based image processing and morphological processed image techniques, also collectively give rise to infrared thermography anomaly detection algorithm (ITADA) [xvii], are utilized to detect the presence of any problems in the system. In order to expedite the process of thermography, this algorithm is used to perform inspection effectively and accurately countering the effects of human errors during inspection. In this technique, the image is separated from the background using Otsu's statistical threshold selection algorithm [xxxi] and then morphological means are used to extract the hotspot in the image.

The thresh holding image obtained A (x,y) from the original image B (x,y) is defined as:

$$A(x,y) = \begin{cases} 1 \text{ if } B(x,y) > T \\ 0 \text{ if } B(x,y) \leq T \end{cases} \quad (9)$$

Where T is thresh holding value obtained by Otsu method. In order to determine the reference temperature, the average grey value of the picture other than the hotspot point will be computed. Then the hotspot temperature will be compared with the reference value computed.

In another technique, instead of using grey level images, the original image is processed. Only the points around the fault will be extracted while the non-relevant points are set to zero. In this method Zernike Moment is used to find feature vector and all those non-faulty points will be flushed out in this phase. After that the image is classified by designing image classifiers such as Support Vector Machine (SVM) [xxxii]. SVM uses the kernel to convert the feature vectors into high dimensional feature space in linear form. Surge arresters are important equipment for safety of power system to divert the surges safely to ground. A new image processing method, Watershed Transform, has been applied to segment the thermal image accurately. Then the computational results are used to train a neuro-fuzzy logic networks having three layer topology by using the thermographic results databases having hundreds of points of interest [xxxiii]. The results of digital signal processing and neuro-fuzzy networks have been validated to be within 10% to classify the operational performance of arresters as faulty, normal, light and suspicious.

The original RBG data is captured by the help of thermographic camera and it is a straight forward image processing method in which pixel region tool for the target image is derived [xxxiv]. The information deduced is then used to train a three layer artificial neural network (ANN) using Levenberg Marquardt algorithm. This method has a major drawback that the processing time is very high being calculated by ANN. A software based program, SIDAT also called integrated system for automatic diagnosis, has been proposed for automatic fault diagnosis of transformer which includes infrared thermography, Chromatography, Chemical and Electrical Tests to confirm the operation of power transformers. It is based on Finite State Machines (FSMs) which takes into account the above testing procedures to describe the time life of transformer to analyze accordingly. In this module, thermography has been designed to substitute the high cost thermovision cameras as all the processing is performed by the thermography module. Hence it is clear that thermography has evolved one of the dependent technologies to count on for maintaining

the substation [xxxv].

A new fault diagnosis method is suggested to root out the electrical problems. There are in general a total of four steps in sequence for the thermal image processing:

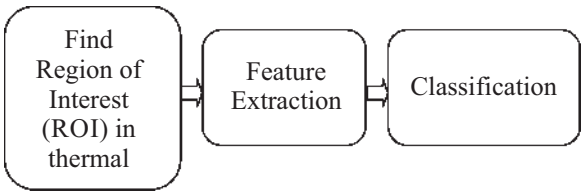

The above hierarchy has been utilized by the author by using K means algorithm as feature extraction process by dividing the thermal image into five clusters and applied SVM (parameter optimization) as the classifier to final optimal final result. Thus a better and accurate result has been obtained for automatic fault detection [xxxvi]. This technique is shown in the Fig.5 whereby original images are shown and the resultant clustered images are shown in Fig. 6.

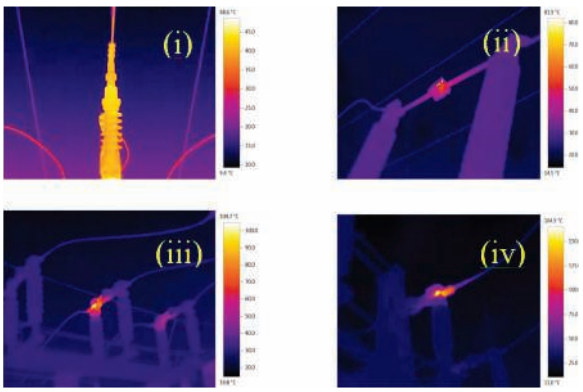

Fig. 5: Original infrared images, from left to right are (i) normal (ii) general failure (iii) serious failure (iv) emergency breakdown.

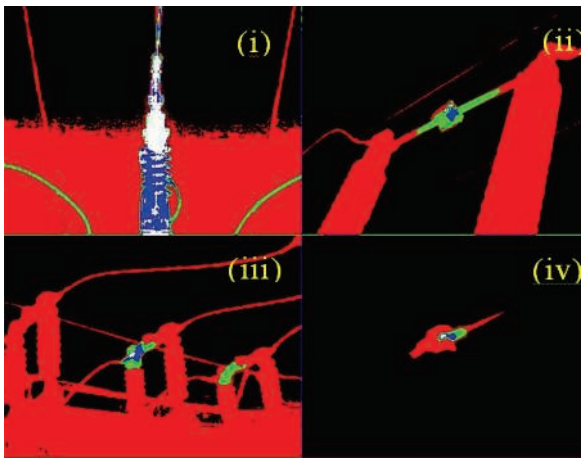

Fig. 6: Cluster results, from left to right are (i) normal (ii) general failure (iii) serious failure (iv) emergency breakdown.

The transmission lines faults can be effectively diagnosed with the help of thermal image processing. As transmission lines are prone to fault due to the environmental factors, early fault detection is the key for maintaining the reliability. Due to the exposedness of the transmission line system to the environmental impacts the thermography is a key predictive maintenance tool for the proper operation of power systems.

The infrared thermography has been applied for fast detection of the transmission lines automatically through preprocessing the thermal image by converting the RGB image into grey level histogram to enhance the contrast and eliminate noise. Then cellular automation is then applied to segment the preprocessed image. After that, the transmission line is detected using Hessian matrix, then temperature information is used to find the fault if temperature is above threshold value. This method has an accuracy of above 90% to detect power transmission lines faults accurately [xxxvii]. The below Fig. 7 illustrate this process.

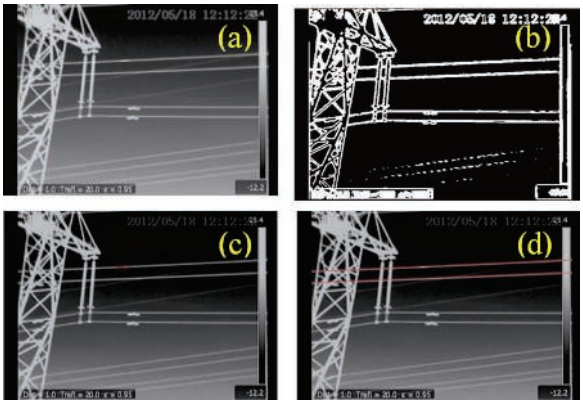

Fig. 7: (a) Grey scale image (b) Segmented image (c) Detection of T/Line (d) Detection of Hotspot (From left to right)

1) Thresholding Technique

In Image processing thresholding technique is very accepted way of automatically detecting the hotspots [xxxviii]. This technique is commonly used to extract the target image from the background [xxxix]. If only one value is used as thresholding value, then it is known as global thresholding and technique involves segmenting sub-images inside target image, it is called local threshold. In that regard, some thresholding techniques have been discussed here.

a) OTSU Thresholding Technique

In this technique, it involves finding the optimal thresholding value by discriminant criterion. It maximizes the between class scatter by minimizing sum of within class variants of foreground and background pixels. This is excellent method to apply if number of pixels are likely similar to one another [xxxi].

b) *Kapor Thresholding Technique*
Another technique for thermal image processing has been proposed in which the image foreground and background are considered as two separate class signal sources whose entropies have been summed to obtain maximum entropy image. From this thresh holding value T is obtained called Kapur Thresh holding Technique [xl].

c) *Hamadani Thresholding Technique*
In this technique, the first order statistical features have been utilized to find the hot region in the target image[xli].

d) *Kittler and Illingworth Thresholding Technique*
In this technique, the pixel classification error rate is optimized based on minimum error thresholding (MET) algorithm [xlii].

e) *Iterative Thresholding Algorithm*
Iterative thresholding algorithm is suitable application for IR images where image does not provide deep valley histogram to segment the image. Thus an arbitrary threshold value is chosen and image is segmented into foreground and background. A new threshold value is calculated from the average pixel intensities and then new and old threshold values are iteratively compared with each other unless a minimum is found[xliii].

In the preceding section, different techniques have been presented to segment the images such as thresholding, clustering based, boundary/ edge based, active contour based. All these techniques are based on the quantitative measurements of pixel intensity. However in electrical equipments, load imbalance or fault in only one phase could occur, so qualitative measurement is always preferred approach. In this method , the image segmentation is done by local key point detection which results in better performance with respect to find Region of Interest (ROI)[xliv].

A new method namely recursively constructed fuzzy systems (RCFS) is presented to determine the electrical faults in equipments. This method automatically realizes the hotspots by recursive application of proposed algorithm. This method has sets the priority levels, normal, warning and critical to establish the maintenance program [xlv]. In another approach, the thermal images are automatically identified by another technique based on Maximally stable extremal region (MSER) algorithm to find out the region of interest. To find similar equipment within the thermal image, Euclidean Distance method is used. The similar equipments are then grouped together for segmentation process then by using qualitative approach , the thermal faults are accurately calculated [xlvi].

In another fault detection technique, two systems Non-invasive Off line Visual Inspection system (NIOLVIS) and Non-invasive Real Time Visual Monitoring system (NIRTVMS) have been proposed. The images obtained through thermographic inspection are segmented color wise to detect the hot regions in the image, features are extracted and matched. Afterwards, an algorithm based on redness of region is applied to find out the severity of problem to generate the tripping, alarming and controlling signals. This method of diagnosis presented is robust in the presence of humid, extreme hot and cold temperature variations [xlvii]. Another Image processing tool namely Region growing method has been effectively used for the segmentation of IR image. In this technique, some seed point is selected and region around the seed point grows according to some predetermined criteria like pixel intensity. If the intensity falls comparable to seed point then region grows. This method has a key advantage that it does not cause over-segmentation of the image thus the accuracy is better[xlviii].

Another infrared software tool based on MATLAB is presented where the thermal measurements are taken without direct comparison method as it suffers from different external factors. In fact same objected when inspected at different times may yield different thermal trends as accurate qualitative analysis results are quite challenging [xx]. The Invariant coefficient method is used to find the hotspots. The thermal ratios defined in test object are determined which represents a robust model with respect to load variations and external factors. The similar components temperature ratios in an object need to close to one under normal conditions while the other component ratios need to be normalized. In another method, instead of using the conventional grey level histograms, the thermal images of electrical equipments are converted to HSI (hue, saturation and intensity) color model for processing. Then edge detection technique is used for finding hotspots in thermal image[xlix].

The high voltage substation risk assessment has been evaluated by thermographic inspection by using neuro fuzzy controller [l]. The approach is used to determine the urgency of intervention for maintenance decision. The age, voltage level, temperature of hotspots, DGA result, Dielectric breakdown strength of oil etc. are fed to the fuzzy controller to be used in risk maps for appropriate decision making. This helps in maintaining the system as the decision is based on the many different input parameters on which system is being operated.

The above mentioned techniques of image processing for automatically finding hotspots are summarized in the form of table which shows what

hotspot detection technique as well as fault classification tool are being applied for the operation and maintenance of power system.

TABLE VI
AUTOMATIC DIAGNOSTIC TECHNIQUES FOR HOTSPOT DETECTION

Sr. No.	Authors	Hotspot Detection Technique & Fault Classification Method
1	Y.-C. Chou and L. Yao	OTSU thresholding method and morphological image processing technique [xvii]
2	A. Rahmani, J. Haddadnia, and O. Seryasat	Zernike Moment and SVM method [xxxii]
3	C. A. L. Almeida, A. P. Braga, S. Nascimento, V. Paiva, H. J. Martins, R. Torres, *et al.*	Watershed Transform and Neuro Fuzzy Logic [xxxiii]
4	M. A. Shafi and N. Hamzah	RGB value comparison and Artificial Neural Network (ANN) [xxxiv]
5	A. M. Carneiro, A. Pasquali, M. E. R. Romero, E. M. Martins, R. Santos, J. M. Silva Filho, *et al.*	SIDAT based on Finite State Machines (FSMs) [xxxv]
6	Z. Hui and H. Fuzhen	K means algorithm and SVM image classification [xxxvi]
7	S. He, D. Yang, W. Li, Y. Xia, and Y. Tang	Grey level histogram threholding and Hessian matrix to detect transmission line [xxxvii]
8	M. M. Ahmed, A. Huda, and N. A. M. Isa,	Recursively constructed Fuzzy systems (RCFS) [xlv]
9	M. S. Jadin, S. Kabir, and S. Taib	Maximally stable extremal region (MSER) and Eucladian Distance [xlvi]
10	Z. A. Jaffery and A. K. Dubey	Colour Wise segmentation and Algorithm based on redness of region of interest [xlvii]
11	Z. Korendo and M. Florkowski	Invariant Coefficient Method [xx]
12	M. Žarković and Z. Stojković	ANN based fuzzy controller [l]

G. Robotized Inspection of Power Lines

To further automate the process of thermography, robots have been utilized for on-line monitoring of the power transmission lines. The fault in power transmission lines can be automatically diagnosed using thermovision technique carried out via robot due to this; the human errors are rectified as process is automated. The image extracted by robotic mounted thermographic camera, acting as a server, after capturing the images in resolution of 320x240 sends the packets of raw data to client image processing software, where the image is processed to extract hotspots from power cable [li]. In another robotic thermographic inspection, the thermal camera records a stream of video and then sends data to the software which process the images for fault detection. The real time monitoring of power system utilizing thermography reaps high benefits for early fault detection in transmission lines[lii].

H. Economic Aspect of Thermal Inspections

One thing should be kept in mind the conventional thermographic approach will require experienced personals to carry out detail inspections and root out the external problems which are visible as well as internal equipment problems which are invisible which requires experienced and skilled personnel. The costs due to external inspections will be high keeping in view the contracted staff, more detailed inspections as equipment depreciates with the time requiring more expenditure eventually if analyzed over the life time of equipment, the cost related to these inspections come out as high running costs overall. In a method proposed by author known as internal inspection, the MATLAB Based GUI program is developed having a database of all the equipment on the plant, the personnel dealing with the software will have easy method to apply thermographic process automatically with overall less cost. The overall time in evaluating the fault analysis will be quite reduced by the software. The cost saved by internal inspection is about 6.3% with reference to external inspection process which could save a significant amount of capital to the owner[liii].

I. Applications of Infrared thermography

There are many applications of infrared thermography in different fields of life some overview of these applications will be discussed here.

The presence of leakage currents on the structure of power transformer causes localized overheating on the screws of the transformer which bind the upper cover and body together. This overheating is detected by thermographic camera. These stray eddy currents can tear of the paint on the body, cause the gas kits to soften up contaminating the oil and also ultimately be a cause of major failure. The author proposed a solution to this problem by installing a copper sill around the screws to provide a bridge to the stray fields directly to the earth and also greater surface for heat dissipation thus reducing the temperature of the hotspots on the screws thus enhancing the life of transformer[liv].

The electrical and thermal characteristics of Metal oxide varister (MOV) under power frequency have been discussed where the thermal runaway property of MOV is related to its maximum temperature limit. The surge arrester leakage current consists of two components, from which resistive current is main indicator of the healthy condition of metal oxide surge arrester. As the resistive current increases due to any defect, the heat generation becomes more than the heat dissipation that's the point where surge arrester becomes thermally unstable. With the help of thermography on can predict the leakage current of

varister by the image processing of the thermal image extracted thus keeping a close watch on the performance of varister [lv]. In another study on the surge arresters, a series of experiments conducted on surge arresters due to its operation in variable external environmental factors like variable wind, humidity, reflected temperature, increased voltages than rated to determine the relation of change of resistive current and the temperature of surge arrester during all the set experiments was determined by thermography to relate the effect of leakage current with the results of thermography thus to improve the validity of thermal inspections. The thermographic parameters needed to be tuned keeping in view these variable external effects [lvi].

As all the substations or plants contain the panels for the wiring for control, protection, regulation, indications, metering and various other purposes, the proper maintenance of these panels is important to keep the availability of substation or plant. The thermographic monitoring technique is quite successful in maintaining these panels. The qualitative approach is applied to probe any anomalies in the panels thus increasing the efficiency, life time of panel equipments [lvii]. The induction motors are important equipment in the industrial environment. A new intelligent method has been proposed for condition monitoring of three phase induction motor. The color based segmentation technique is used to determine the hot regions in the motor along with red color intensity algorithm to find and declare the healthiness of motor [lviii].

One of the important applications of thermography is in the field of PV systems. As demand for clean energy is growing day by day, a need has arisen how to maintain these panels efficiently and effectively It helps to determine the defects of the PV panels so it helps in the detection of defects even during the production stage thus avoiding losses to production company. It helps in identifying mismatched cells, bypassed diodes fault, high resistance soldering joints, packing material degradation and resistive shunts in the PV panels. All these defects give rise to hotpots which is readily detected by thermal imaging thus enhancing the overall efficiency of PV systems [lix]. Aerial solar thermography is used to find the condition of the solar panels in the large arrays of solar (PV) power plant. As a damaged cell in a panel not only causes the electrical output to reduce but if that damage cell persists over longer periods of time it also spread the damaging effect to the cells around it and eventually the panel becomes unserviceable hence in that regard solar thermography has been very useful for proper maintenance of solar panels [lx]. In another research, the PV array consisting of series and parallel combination of panels diagnosed for faults using thermography to find maximum power point tracking to examine the problem of partial shading condition. If against such problem is not acted upon, then along with reduced output power , hotspot occur producing maximum power points (MPPs) which can affect the neighboring cells in the PV array producing increased losses. The PV panels with complete faulty rows, mixed and healthy cells were thermally inspected to find global maximum power point (GMPP) of the PV array by comparing their power output [lxi]. The Fig. 8 shows short circuited PV module [lix].

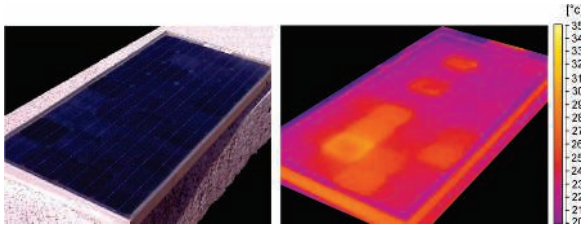

Fig. 8: (a) photovoltaic modules; (b) IR image of module short-circuited under fine weather in outdoor conditions.

Thermal imaging application in food industry has revolutionized the conservation and quality of food. Due to its non-invasive analytical nature of measurement than the contact type thermometers and thermocouples, the scope of food safety, pasteurization, sterilization, cooking has reached new levels. The drying of foods for long period of conservation is now more quality oriented by its application by modeling the dehydration kinetics thus the determining final drying temperature and to develop the efficient control system. The products can be verified for standard packing by monitoring the ingress of bad contaminated air or in other words the whole packing methods can be verified [lxii].The Fig. 9 shows the difference of temperature between sound and defected tissues in apple [lxiii].

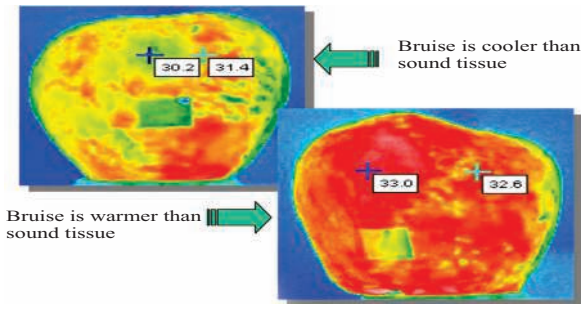

Fig. 9: Temperature variation for bruise tissue and sound tissues in red

The application of thermography in the field of art work has enabled to detect any sub-surface level defects with the help of determining the temperature distribution across the art work. The non-contact type appliance is required to investigate the problems hence thermography fits the requirement. The method of non-destructive heating to the specimen is applied which is

used to determine the temperature signals based on the uniformity of the model by creating a test duration and optimum sampling interval [lxiv].The Fig. 10 shows the application of thermography in art works[lxv].

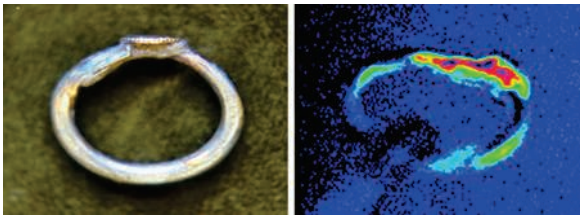

Fig.10: (a) Photograph (b thermogram of a Phoenicians ring revealing the material used to weld the collet to the support.

Wood is material used in all forms of buildings and materials. The preservation of wood is vital for long endurance. Thermography is utilized to inspect the decay detection of wood. Firstly, with the varied levels of moisture content, the thermal inspection is performed and found out the moisture level is in direct relation to temperature difference. Then the defects with varied depthless has been inspected to determine the problems and found out that as depth increases the temperature difference decreases but still it is possible to get a sniff about the defect for long duration inspections[lxvi].

In inspecting the welded joints, the joints where two similar or dissimilar materials are connected together are usually the weakest link in the product design so a special attention is to be provided to assure that joint is strongly bonded and has a life time of product. Infrared thermography technique has been applied to monitor different types of bonds which are mechanical linked joints, welded joints and adhesively bonded joints. The pulse and modulation thermography techniques have been deployed to check the bond between surfaces. The later technique was particularly stressed because of less variation due to non-uniform surface heating and emissivity factor[lxvii].The Fig. 11 shows the defects in wood detected by IRT[lxviii].

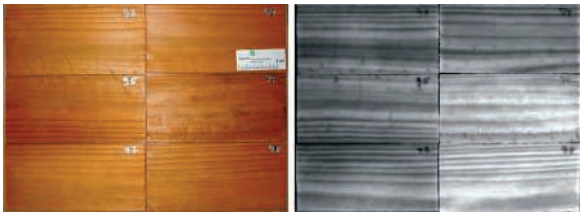

Fig. 11:The photo (left) shows a small wood panel and the thermographic image (right) the compressed wood as white (hot) area within the material.

The ball bearings are used within every rotational machines and it is imperative to inspect the condition of ball bearing as it has a direct impact on rotational performance of machines. The machine with little loss of lubricating oil showed increased levels of temperature as compared to normal due to higher force of friction. Also by vibration spectral analysis, the results were confirmed but it has a disadvantage that it is contact type method so extra experimental arrangements have to be made. The damaged, loss and normal samples have been segregated[lxix].

The pipelines are being used in many industrial as well as power sectors. The defects in the pipe line affect the performance of the system. With the help of thermography, both the internal as well as external defects of pipe line heat insulation layer (PHIL) can be probed into non-intrusively. The maximum temperature can be determined and the depth and dimensions of the leakage can also be analyzed comprehensively so as to conserve the system operation[lxx].

IV. Challenges and Future Scope

It has been clear that the thermography has emerged to be one of the effective diagnostic tools in different fields of the world as explained in the preceding sections. Like any other field, the research in this field also requires constant up gradation and improvement with the passage of time. One of the improvements needed in the electrical substation thermography is to carry out the inspections of unmanned substations through robots with real time image processing capabilities. This can be achieved with artificial intelligence based programming to automatically adapt to the system loading conditions and make appropriate measurements and decisions accordingly with varying loading conditions. In such cases the decisions will be very important regarding the system stability as less loading conditions up to 30% do not reveal right results by the existing thermographic methods.

One of the much needed improvements can be to integrate the thermography with the Substation Automation system (SAS) to speedily discover any anomalies in the substations. This can be achieved by implementing robotic based continuous surveillance of substation equipment. Additionally, such surveillance efficiency and reliability can be further enhanced by deploying fast fault classification methods having redundant combination of Artificial Neural Networks (ANN) and support Vector Machine (SVM) to feed their combined results to SAS system which can help in improving the reliability of the substation system and overall power system. Also The economy is also a major constraint especially for third world countries to implement thermographic based fault detection techniques, this field must be globally invested in by manufacturers to help the performance of power systems.

V. CONCLUSION

Infrared thermography has emerged as one the excellent condition monitoring technique which helps in on line monitoring of a process and non-intrusive way of inspection. It helps in predicting the faults thus preventing breakdowns or catastrophes at a later stage thus reducing the maintenance costs and down time consequently resulting in massive savings both from the operational point of view as well as asset safety. The inspection of electrical installations by infrared thermography poses challenges due to non-homogeneity of the thermal images extracted. Thus, the augmentation of image processing tools has revitalized the field of thermography as the thermal images are automatically investigated by fault detection algorithms. The image processing methods also have eliminated the possibility of most likely human errors, the external environmental impacts and other noise signals to provide an accurate results of analysis of thermal images thus a lot of savings could be effected that would have to be invested in outsourcing the substation inspection to experts. Due to the diversified nature of thermography technology, it has applications not only in field electrical substation and power system but also wood inspection, PV systems, food industry, pipelines, art works and other fields as briefly reviewed in this paper. These different applications of thermography as reviewed in this paper can be quite helpful for successfully implementing and producing the desired results in temperature measurement and heat signature based processes.

REFERENCE

[i] J. L. Giesecke, "Substation component identification for infrared thermographers," in AeroSense'97, 1997, pp. 153-163.

[ii] Z. Azmat and D. J. Turner, "Infrared thermography and its role in rural utility environment," in Rural Electric Power Conference, 2005, 2005, pp. B2/1-B2/4.

[iii] M. A. Kregg, "Benefits of using infrared thermography in utility substations," in Defense and Security, 2004, pp. 249-257.

[iv] I. Garvanov, I. Zarev, and B. Rakovic, "The influence of temperature to the regularity of life cycle," in Electrical Apparatus and Technologies (SIELA), 2014 18th International Symposium on, 2014, pp. 1-4.

[v] R. A. Botelho and A. Calente, "Follow-up of failures in electrical equipment and installations using thermography," in Aerospace/Defense Sensing, Simulation, and Controls, 2001, pp. 297-306.

[vi] C. Hellier, "Handbook of nondestructive evaluation," 2001.

[vii] M. Planck, Eight Lectures on Theoretical Physics: Delivered at Columbia University in 1909: Columbia University Press, 1915.

[viii] W. Wien, "XXX. On the division of energy in the emission-spectrum of a black body," The London, Edinburgh, and Dublin Philosophical Magazine and Journal of Science, vol. 43, pp. 214-220, 1897.

[ix] G. B. Rybicki and A. P. Lightman, Radiative processes in astrophysics: John Wiley & Sons, 2008.

[x] J. R. Howell, M. P. Menguc, and R. Siegel, Thermal radiation heat transfer: CRC press, 2010.

[xi] W. Minkina and S. Dudzik, Front Matter: Wiley Online Library, 2009.

[xii] D. Wretman, "Finding regions of interest in a decision support system for analysis of infrared images," Master of Science Thesis, Royal Institute of Technology, Stockholm, Sweden, 2006.

[xiii] R. A. Epperly, G. E. Heberlein, and L. G. Eads, "A tool for reliability and safety: predict and prevent equipment failures with thermography," in Petroleum and Chemical Industry Conference, 1997. Record of Conference Papers. The Institute of Electrical and Electronics Engineers Incorporated Industry Applications Society 44th Annual, 1997, pp. 59-68.

[xiv] J. Martínez, R. Lagioia, and S. Edenor, "Experience performing infrared thermography in the maintenance of a distribution utility," in 19th International Conference on Electricity Distribution, Vienna, 2007, pp. 21-24.

[xv] I. E. T. Association, Acceptance Testing Specifications for Electrical Power Distribution Equipement and Systems: InterNational Electrical Testing Association, 2007.

[xvi] T. Lindquist, L. Bertling, and R. Eriksson, "Estimation of disconnector contact condition for modelling the effect of maintenance and ageing," in Power Tech, 2005 IEEE Russia, 2005, pp. 1-7.

[xvii] Y.-C. Chou and L. Yao, "Automatic diagnostic system of electrical equipment using infrared thermography," in Soft Computing and Pattern Recognition, 2009. SOCPAR'09. International Conference of, 2009, pp. 155-160.

[xviii] C. Meola, G. M. Carlomagno, A. Squillace, and G. Giorleo, "The use of infrared thermography for nondestructive evaluation of joints," Infrared physics & technology, vol. 46, pp. 93-99, 2004.

[xix] C. Wilson, G. McIntosh, and R. S. Timsit, "Contact spot temperature and the temperature of external surfaces in an electrical connection," in Electrical Contacts (ICEC 2012), 26th International Conference on, 2012, pp. 12-17.

[xx] Z. Korendo and M. Florkowski, "Thermography based diagnostics of power equipment," Power Engineering Journal, vol. 15, pp. 33-42, 2001.

[xxi] N. Dorovatovski and O. Liik, "Results of thermographic diagnostics of electric grid contact junctions and generators of oil shale power plants," Oil shale, vol. 22, pp. 243-258, 2005.

[xxii] T. M. Lindquist and L. Bertling, "Hazard rate estimation for high-voltage contacts using infrared thermography," in Reliability and Maintainability Symposium, 2008. RAMS 2008. Annual, 2008, pp. 231-237.

[xxiii] T. Lindquist and L. Bertling, "A method for calculating disconnector contact availability as a function of thermography inspection intervals and load current," in CIGRE Symposium Osaka 2007: System Development and Asset Management under Restructuring, 1 November 2007 through 4

November 2007, Osaka, Japan, 2007.
[xxiv] N. Hou, "The infrared thermography diagnostic technique of high-voltage electrical equipments with internal faults," in Power System Technology, 1998. Proceedings. POWERCON'98. 1998 International Conference on, 1998, pp. 110-115.
[xxv] L. dos Santos, E. da Costa Bortoni, L. C. Barbosa, and R. A. Araújo, "Centralized vs. decentralized thermal IR inspection policy: Experience from a major Brazilian electric power company," in Defense and Security, 2005, pp. 121-132.
[xxvi] E. W. Neto, E. Da Costa, and M. Maia, "Influence of emissivity and distance in high voltage equipments thermal imaging," in Transmission & Distribution Conference and Exposition: Latin America, 2006. TDC'06. IEEE/PES, 2006, pp. 1-4.
[xxvii] P. R. Muniz, R. da Silva Magalhães, S. P. N. Cani, and C. B. Donadel, "Non-contact measurement of angle of view between the inspected surface and the thermal imager," Infrared Physics & Technology, vol. 72, pp. 77-83, 2015.
[xxviii]R. P. Madding, "Emissivity measurement and temperature correction accuracy considerations," in AeroSense'99, 1999, pp. 393-401.
[xxix] W. L. Wolfe, "Handbook of military infrared technology," DTIC Document1965.
[xxx] E. C. Bortoni, G. S. Bastos, L. dos Santos, and L. E. Souza, "Wind-influence modeling for outdoor thermographic surveys," in SPIE Defense, Security, and Sensing, 2010, pp. 766107-766107-6.
[xxxi] N. Otsu, "A threshold selection method from gray-level histograms," Automatica, vol. 11, pp. 23-27, 1975.
[xxxii] A. Rahmani, J. Haddadnia, and O. Seryasat, "Intelligent fault detection of electrical equipment in ground substations using thermo vision technique," pp. V2-150.
[xxxiii]C. A. L. Almeida, A. P. Braga, S. Nascimento, V. Paiva, H. J. Martins, R. Torres, et al., "Intelligent thermographic diagnostic applied to surge arresters: a new approach," Power Delivery, IEEE Transactions on, vol. 24, pp. 751-757, 2009.
[xxxiv]M. A. Shafi and N. Hamzah, "Internal fault classification using artificial neural network," in Power Engineering and Optimization Conference (PEOCO), 2010 4th International, 2010, pp. 352-357.
[xxxv] A. M. Carneiro, A. Pasquali, M. E. R. Romero, E. M. Martins, R. Santos, J. M. Silva Filho, et al., "SIDAT-integrated system for automatic diagnostic on power transformers," in Industry Applications (INDUSCON), 2012 10th IEEE/IAS International Conference on, 2012, pp. 1-6.
[xxxvi]Z. Hui and H. Fuzhen, "An intelligent fault diagnosis method for electrical equipment using infrared images," in Control Conference (CCC), 2015 34th Chinese, 2015, pp. 6372-6376.
[xxxvii]S. He, D. Yang, W. Li, Y. Xia, and Y. Tang, "Detection and fault diagnosis of power transmission line in infrared image," in Cyber Technology in Automation, Control, and Intelligent Systems (CYBER), 2015 IEEE International Conference on, 2015, pp. 431-435.
[xxxviii]H.-F. Ng, "Automatic thresholding for defect detection," Pattern recognition letters, vol. 27, pp. 1644-1649, 2006.
[xxxix]J. S. Weszka and A. Rosenfeld, "Threshold evaluation techniques," Systems, Man and Cybernetics, IEEE Transactions on, vol. 8, pp. 622-629, 1978.
[xl] A. N. Huda, M. S. Jadin, and S. Taib, "Extracting electrical hotspots from infrared images using modified Kapur thresholding technique."
[xli] N. A. Hamadani, "Automatic Target Cueing in IR Imagery," DTIC Document1981.
[xlii] J. Kittler and J. Illingworth, "On threshold selection using clustering criteria," Systems, Man and Cybernetics, IEEE Transactions on, pp. 652-655, 1985.
[xliii] A. Perez and R. C. Gonzalez, "An iterative thresholding algorithm for image segmentation," IEEE Transactions on Pattern Analysis & Machine Intelligence, pp. 742-751, 1987.
[xliv] M. S. Jadin, S. Taib, and K. H. Ghazali, "Finding region of interest in the infrared image of electrical installation," Infrared Physics & Technology, vol. 71, pp. 329-338, 2015.
[xlv] M. M. Ahmed, A. Huda, and N. A. M. Isa, "Recursive construction of output-context fuzzy systems for the condition monitoring of electrical hotspots based on infrared thermography," Engineering Applications of Artificial Intelligence, vol. 39, pp. 120-131, 2015.
[xlvi] M. S. Jadin, S. Kabir, and S. Taib, "Thermal imaging for qualitative-based measurements of thermal anomalies in electrical components," in Electronics, Communications and Photonics Conference (SIECPC), 2011 Saudi International, 2011, pp. 1-6.
[xlvii] Z. A. Jaffery and A. K. Dubey, "Design of early fault detection technique for electrical assets using infrared thermograms," International Journal of Electrical Power & Energy Systems, vol. 63, pp. 753-759, 2014.
[xlviii] R. C. Gonzalez and R. E. Woods, "Digital image processing," 2002.
[xlix] T. Dutta, J. Sil, and P. Chottopadhyay, "Condition monitoring of electrical equipment using thermal image processing," in 2016 IEEE First International Conference on Control, Measurement and Instrumentation (CMI), 2016, pp. 311-315.
[l] M. Žarković and Z. Stojković, "Artificial intelligence based thermographic approach for high voltage substations risk assessment," Generation, Transmission & Distribution, IET, vol. 9, pp. 1935-1945, 2015.
[li] J. H. E. De Oliveira and W. F. Lages, "Robotized inspection of power lines with infrared vision," in Applied Robotics for the Power Industry (CARPI), 2010 1st International Conference on, 2010, pp. 1-6.
[lii] W. F. Lages and V. Scheeren, "An embedded module for robotized inspection of power lines by using thermographic and visual images," in Applied Robotics for the Power Industry (CARPI), 2012 2nd International Conference on, 2012, pp. 58-63.
[liii] F. Selim, A. M. Azmy, and H. El Desuoki, "Economic Investigation of High Quality Thermal Inspections," Journal of Electrical Systems (JES), J. Electrical Systems, vol. 9, pp. 39-51, 2013.
[liv] J. Olivares-Galván, S. Magdaleno-Adame, R. Escarela-Perez, R. Ocon-Valdéz, P. Georgilakis, and G. Loizos, "Experimental validation of a new

methodology to reduce hot spots on the screws of power transformer tanks," in Electrical Machines (ICEM), 2012 XXth International Conference on, 2012, pp. 2318-2322.

[lv] C. Srisukkhom and P. Jirapong, "Analysis of electrical and thermal characteristics of gapless metal oxide arresters using thermal images," in Electrical Engineering/Electronics, Computer, Telecommunications and Information Technology (ECTI-CON), 2011 8th International Conference on, 2011, pp. 677-680.

[lvi] W. A. Ursine, J. L. Silvino, L. G. Fonseca, and R. M. de Andrade, "Metal-oxide surge arrester's leakage current analysis and thermography," in Lightning Protection (XII SIPDA), 2013 International Symposium on, 2013, pp. 297-303.

[lvii] U. M. Ferreira, M. Z. Fortes, B. H. Dias, and R. S. Maciel, "Thermography as a Tool in Electric Panels Maintenance," Latin America Transactions, IEEE (Revista IEEE America Latina), vol. 13, pp. 3005-3009, 2015.

[lviii] D. Chaturvedi, S. Iqbal, and M. P. Singh, "Intelligent health monitoring system for three phase induction motor using infrared thermal image," in Energy Economics and Environment (ICEEE), 2015 International Conference on, 2015, pp. 1-6.

[lix] G. S. Spagnolo, P. D. Vecchio, G. Makary, D. Papalillo, and A. Martocchia, "A review of IR thermography applied to PV systems," in Environment and Electrical Engineering (EEEIC), 2012 11th International Conference on, 2012, pp. 879-884.

[lx] H. Denio III, "Aerial solar thermography and condition monitoring of photovoltaic systems," in Photovoltaic Specialists Conference (PVSC), 2012 38th IEEE, 2012, pp. 000613-000618.

[lxi] Y. Hu, W. Cao, J. Wu, B. Ji, and D. Holliday, "Thermography-based virtual MPPT scheme for improving PV energy efficiency under partial shading conditions," Power Electronics, IEEE Transactions on, vol. 29, pp. 5667-5672, 2014.

[lxii] A. Gowen, B. Tiwari, P. Cullen, K. McDonnell, and C. O'Donnell, "Applications of thermal imaging in food quality and safety assessment," Trends in food science & technology, vol. 21, pp. 190-200, 2010.

[lxiii] J. Varith, G. Hyde, A. Baritelle, J. Fellman, and T. Sattabongkot, "Non-contact bruise detection in apples by thermal imaging," Innovative Food Science & Emerging Technologies, vol. 4, pp. 211-218, 2003.

[lxiv] E. Grinzato, P. Bison, S. Marinetti, and V. Vavilov, "Nondestructive Evaluation of Delaminations in Fresco Plaster Using Transient Infrared Thermography," Research in Nondestructive Evaluation, vol. 5, pp. 257-274, 1994/01/01 1994.

[lxv] F. Mercuri, U. Zammit, N. Orazi, S. Paoloni, M. Marinelli, and F. Scudieri, "Active infrared thermography applied to the investigation of art and historic artefacts," Journal of thermal analysis and calorimetry, vol. 104, pp. 475-485, 2011.

[lxvi] A. Wyckhuyse and X. Maldague, "A study of wood inspection by infrared thermography, Part I: Wood pole inspection by infrared thermography," Journal of Research in Nondestructive Evaluation, vol. 13, pp. 1-12, 2001.

[lxvii] B. Lahiri, S. Bagavathiappan, T. Saravanan, K. Rajkumar, A. Kumar, J. Philip, et al., "Defect detection in weld joints by infrared thermography," 2011.

[lxviii] P. Meinlschmidt, "Thermographic detection of defects in wood and wood-based materials," in 14th International Symposium of Nondestructive testing of Wood, Honnover, Germany (May 2nd-4th 2005), 2005.

[lxix] D.-Y. Kim, H.-B. Yun, S.-M. Yang, W.-T. Kim, and D.-P. Hong, "Fault Diagnosis of Ball Bearings within Rotational Machines Using the Infrared Thermography Method," Journal of the Korean Society for Nondestructive Testing, vol. 30, pp. 558-563, 2010.

[lxx] C. Fan, F. Sun, and L. Yang, "Investigation on nondestructive evaluation of pipelines using infrared thermography," in Infrared and Millimeter Waves and 13th International Conference on Terahertz Electronics, 2005. IRMMW-THz 2005. The Joint 30th International Conference on, 2005, pp. 339-340.

Designing Wideband Patch Antenna by Fusion of Complementary-Split Ring Resonator, Inter-Digital Capacitor and Slot Cutting Technique

[1]S. Anwar, [1]S. A. Niazi, [2]M. I. Malik, [1]A. Aziz
[1]Department of Electrical Engineering, University College of Engineering and Technology, Islamia University of Bahawalpur.
[2]Department of Electrical Engineering, University College of Engineering and Technology, Bahauddin Zakariya University, Multan
[1]summeya_anwar@yahoo.com

Abstract-An electrically small wideband patch antenna loaded with meta-material unit cell is proposed in this thesis. Meta-material unit cell is constructed by inter-digital capacitance (IDC) and rectangular slot on the patch and complementary split ring resonator (CSRR) etched on ground plane. The parametric analysis reveals that the electrical size of antenna becomes small by increasing inter-digital finger length, due to increase in series capacitance. The circulating current distribution across CSRR slot induces second radiation mode. The radiation modes resulting due to CSRR and inter-digital capacitor, overlaps by introducing rectangular slot, without any pattern distortion. This yields a wideband property regardless of small electrical size of the proposed antenna. We achieved a wide bandwidth of 780MHz, directional radiation pattern and moderate gain.

Keywords-Wideband antennas, Microstrip Patch Antennas, Metamaterials, Inter-digital Capacitance (IDC), Complementary Split-Ring Resonators (CSRR).

I. INTRODUCTION

Meta-material based patch antenna have attracted many researchers as it offers certain desirable characteristics such as increase in bandwidth and reduction in electrical size [i] as compared to conventional patch antenna. In 1968, the innovative theoretical model claiming negative permittivity and permeability of material that results in negative index medium was proposed by [ii]. After 30 years of experimentation it is verified that medium with artificial negative index exists [iii]. The materials with negative refractive index were categorized as Left-handed materials [iv]. Meta-materials are specifically engineered to produce electromagnetic properties that are unavailable in natural resources [v] . Meta-materials have drawn broad interest in many electromagnetic applications both in microwave and optical regime [vi,vii] due to permittivity, permeability, and index of refraction [viii-ix].

Antennas are used to increase radiation efficiency [x]. Meta-material based antennas can enhance radiation efficiency quite appreciably. Microstrip patch antennas are low profile antennas that are compatible with integrated circuitry due to their small size, simple structure and low cost. Theoretically, the size of patch antenna can be less than half of its resonance frequency. Therefore, many schemes have been proposed for the reduction of size [xi] and enhancement of radiating bandwidth of patch antenna [xii] . These schemes involve modification of geometry [xii, xiv], using multilayered substrate [xv] and cutting slots of different shaped on ground plane and patch [xvi, xvii]. Moreover, composite right/left handed (CRLH) properties of meta-materials can be achieved by coupling transmission line or waveguides with CSRR [xviii].

An electrically small wideband patch antenna which is loaded with planar meta-material unit cell is proposed and simulated. For shunt admittance, the unit cell consists of complementary split-ring resonators (CSRR), for series capacitance inter-digital capacitors [xix] are used and a rectangular slot for wide bandwidth characteristic. For small antenna applications, its dispersion characteristics are analyzed. Increase in inter-digital finger length results in TM01 radiations due to circular current distribution around CSRR. The wideband can be achieved by combining TM10 and TM01 mode without any pattern distortion. As compare to conventional antenna the proposed antenna have wide bandwidth characteristic, small electrical size and reasonable gain.

II. MATERIALS AND METHODS

An electrically small wideband microstrip patch antenna which is loaded with planar metamaterial unit cell is proposed. The proposed antenna is designed and simulated in Computer Simulated Technology (CST) Microwave studio. In this section the design geometry of proposed antenna is discussed.

Choice of Substrate

Choosing a substrate is as critical as the configuration itself. The substrate itself is a part of the antenna and contributes altogether to its radiative properties. A wide

range of components are considered in choosing a substrate, for example, dielectric constant, thickness, firmness and in addition loss tangent. The dielectric constant must be as low as could reasonably be expected to energize bordering and radiation. A thicker substrate is additionally picked as it expands the impedance bandwidth. In any case, utilizing a thick substrate would bring about a loss in accuracy since most microstrip antenna models utilize thin substrate estimation in the analysis. Substrates which are lossy at higher frequencies should not be utilized for clear reasons. The decision of a hardened or soft board essentially relies on upon the current application.

III. MODELING

Basic Geometry

The proposed antenna is designed in CST Studio Suit based on Finite Integration Technique (FIT). The radiating element is constructed on 1.57mm thick Teflon substrate, with relative permittivity (εr=2.1) and loss tangent (tan δ = 0.001). Following steps are involved in the designing of proposed wideband patch antenna.

Designing a Simple Patch Antenna:

The first step in designing the proposed antenna is to design a simple patch antenna. Figure 1 shows the design geometry of patch antenna. A 19mm × 19mm patch is constructed on Teflon substrate of dimensions 40mm × 35mm and the thickness of substrate is 1.57mm.

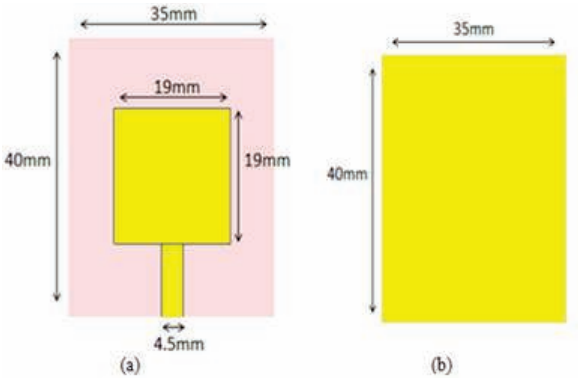

Fig. 1: Structure of Simple Patch Anteena
(a) Top view and (b) Bottom view

A square radiating patch is constructed on the top of Teflon substrate. The radiating element is excited by a 4.5 mm wide microstrip feed line having a reference impedance of 50 Ω.

Inserting Inter-digital Capacitor in Patch:

Inter-digital capacitor is inserted in patch to introduce the capacitive effect. Capacitance increases as the finger length increases and gaps decreases. The inter-digital finger length is optimized to 6.5mm. Figure 2 shows the top view of patch antenna after insertion of IDC of optimized finger length of 6.5mm.

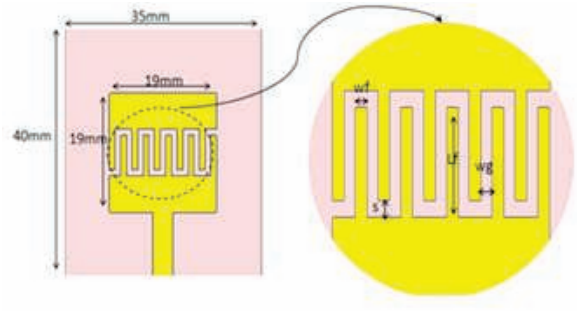

Fig. 2: Inter-digital capacitor loaded patch antenna

Dimension of IDC loaded patch antenna is given in Table I. Inter-digital finger length is denoted by Lf, width of inter-digital finger is wf and wg is the gap between two fingers.

Table I
DIMENSIONS OF IDC LOADED ANTENNA

Lf	6.5mm
wf	1mm
wg	1mm
s	1mm

By varying inter-digital finger length, electrical size of antenna can be varied. Our goal is to design an antenna that have wideband characteristics and electrically small in size as compare to the conventional patch antenna. By increasing inter-digital finger length, capacitance increases thus the resonance frequency is decreased. By adding capacitance, resonance frequency is reduced by keeping antenna size same. So actually, the size of antenna is reduced for low resonance frequency by adding capacitance.

Etching CSRR in Ground plane:

Ground plane is loaded with CSRR for shunt admittance. Figure 3 shows the ground plane of proposed antenna that is loaded with inter-digital capacitor. List of all the dimensions is given in Table 2.

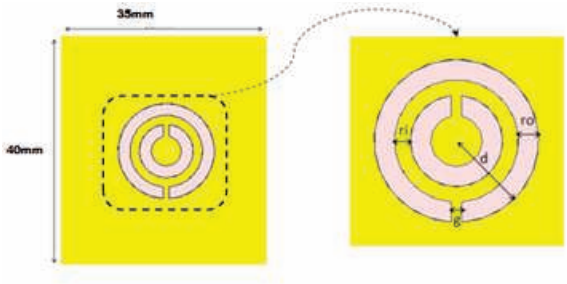

Fig. 3: CSRR etched on ground plane

Table II
DIMENSIONS OF CSRR

d	8mm
ro	2mm
ri	1.5mm
g	1mm

As shown in Figure 3, CSRR is pair of enclosed loops. These loops have splits at opposite ends in them .These splits supports resonant wavelength. These wavelengths are much higher than the diameter of the rings. These splits in the rings are responsible for excitation second resonant mode. To get required device performance they are electrically coupled with different microstructures.

Design of Proposed Antenna:

Figure 4 shows design of proposed antenna. In addition to inter-digital capacitor, patch is also loaded with rectangular slot. This rectangular slot is responsible for wideband characteristic in patch antenna. Different shapes of slots are cut on the surface of a path in antenna for enhancement of bandwidth. A rectangular slot is incorporated to the patch to perturb surface current. Complete dimensions of proposed antenna are given in Table 3.

Table III
DIMENSIONS OF PROPOSED ANTENNA

L	40mm	W	35mm
lp	19mm	wp	19mm
ws	14mm	ls	14mm
Lf	6.5mm	wm	4.5mm
d	8mm	g	1mm
ro	2mm	ri	1.5mm

It is interesting to note that when a rectangular slot is inserted in the patch, operating frequency bands which results due to inter-digital capacitance and CSRR overlaps. Because of phase difference they do not interfere with each other. Therefore wide bandwidth is achieved for proposed antenna.

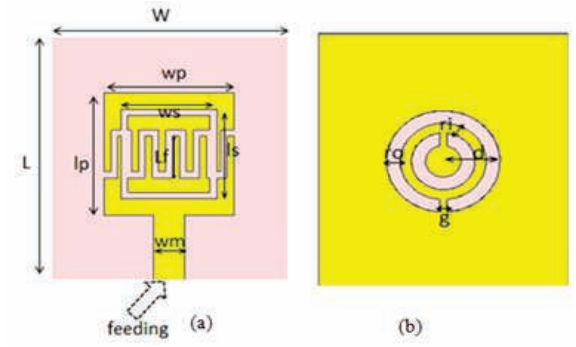

Fig.4: Geometry of proposed antenna
(a) Top view and (b) Bottom view

IV. RESULTS AND DISCUSSIONS

The parametric analysis and simulation of designed antenna is done in the CST Microwave Studio in order to get the following parameters.

Return loss (S11) Parameter:

In a system, the relationship between input- output terminals (ports) is represented by its S-parameters. S11-parameter is also known as return loss or reflection coefficient as it describes amount of power that is reflected by antenna. If the value of S11= 0 dB, it means that all of the power is reflected by antenna and no power is radiated. And if the value of S11=-10 dB, this infers power delivered to antenna is 3dB and then the reflected power will be -7dB.

Figure 5 shows S11-parameter of simple patch antenna of dimensions (40mm × 35mm × 1.57mm). Bandwidth of simple patch antenna of given dimension is 310MHz. The resonant frequency occurs at 6.7GHz. The plot below shows the return loss or S11-parameter (dB) vs frequency (GHz) curve.

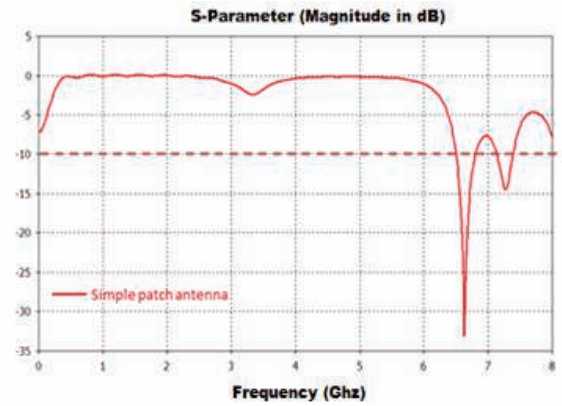

Fig. 5: S11-parameter of simple patch antenna

Figure 6 shows S11-parameter of antenna when it is loaded with IDC. The resonant frequency occurs at 4.6GHz, when an inter-digital capacitor is loaded in the patch.

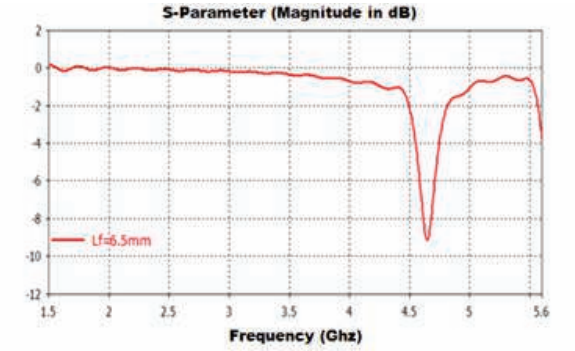

Fig. 6: S11 parameter of IDC loaded antenna when Lf=6.5 mm

Parametric study reveals that by varying finger length (Lf) electrical size of the antenna can be varied. Figure 7 shows the parametric study of antenna by varying Lf. It can be seen, by increasing Lf resonance frequency decreases as the capacitance increases. Thus the

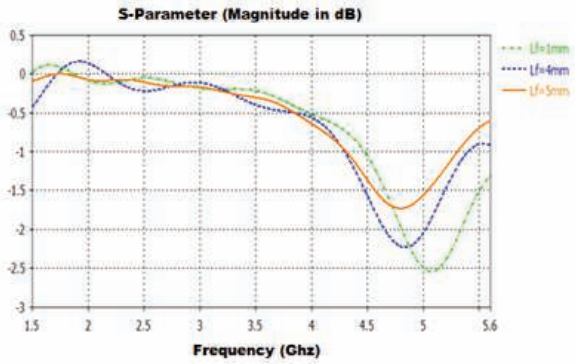

Fig. 7: S11 performance comparison by varying LF

After etching CSRR in ground plane another resonance frequency appears. This resonance frequency appears due to circulating current distribution across CSRR. Figure 8 shows the S11-parameter after inserting CSRR in the ground plane. First resonance frequency appears at 4.05GHz having 103MHz bandwidth and second resonance frequency appears at 5.7GHz having bandwidth of 155MHz.

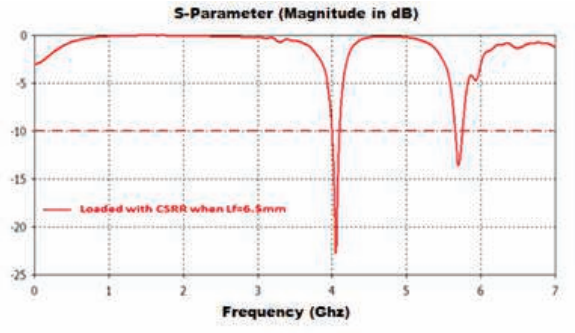

Fig. 8: S11 parameter ofAntenna loaded with CSRR

Figure 9 shows the parametric study of antenna loaded with CSRR by varying Lf. It can be seen, by increasing Lf resonance frequency decreases. The first resonance frequency decreases from 4.9GHz to 4.05GHz as Lf increases from 1mm to 6.5mm.

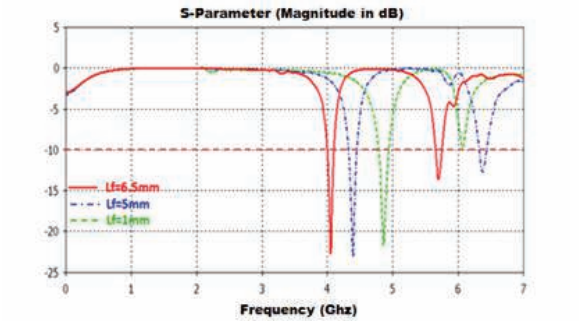

Fig.9: S11 performance comparison by varying Lf with CSRR loading

Figure 10 shows the simulated S11 parameter of proposed antenna. Bandwidth of proposed antenna extends from 5.2GHz to 6.02GHz. As compare to conventional patch antenna operating at same frequency, proposed antenna bandwidth is approximately three times wider because of combination of two radiation modes. Because when a rectangular slot is inserted in the patch, frequency bands which results due to inter-digital capacitor and CSRR overlaps. Bandwidth of designed antenna is 780MHz.

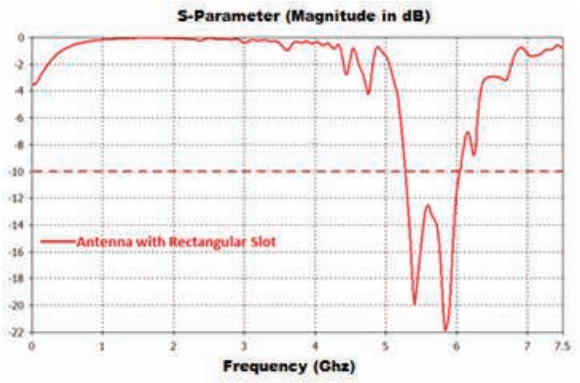

Fig. 10: S11 parameter of Proposed Antenna

To see the impact of rectangular slot on the bandwidths and resonant frequencies, a parametric study is performed for proposed antenna. Figure 11 shows the effects of variation in the width of the rectangular slot. As ws (width of slot) is decreased from 3mm to 1mm, two modes are overlapped efficiently and the bandwidth is increased but after it at ws = 0.5mm there is decrease in bandwidth.

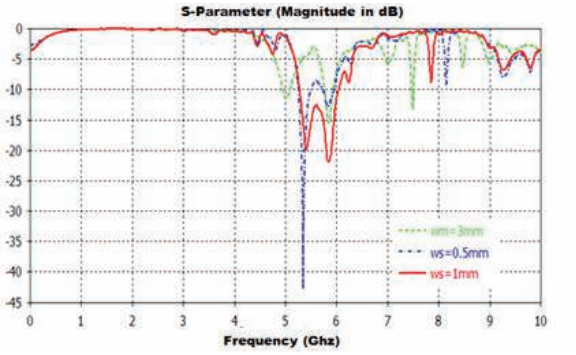

Fig. 11. S11 performance comparison of proposed antenna by varying ws

Surface Current Distribution:

An antenna is a structure conveying or carrying an electrical current and the electrical properties of the antenna relies on the distribution of that current in size (magnitude) and phase. At the point when the current distribution of the antenna is transformed, it likewise changes its attributes.

From Figure 8 it can be seen that another resonant frequency appears after etching CSRR in ground plane, one at 4.05GHz and the other at 5.7GHz. Figure 12 shows the current distribution at 4.05GHz and 5.7GHz respectively.

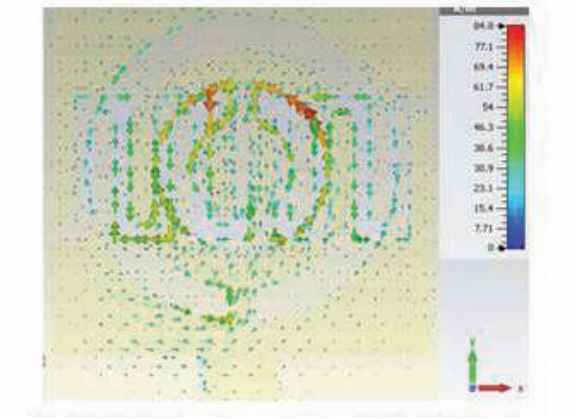

Fig 12 (a): Surface current distributions at 4.05 GHz

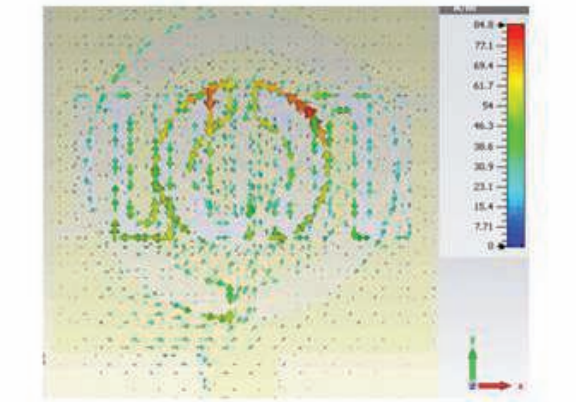

Fig. 12 (b): Surface current distributions at 5.7GHz

It can be seen from Figure 12 that maximum current distribution at 4.05GHz and 5.7GHz is across CSRR and IDC respectively. Figure 13 shows the surface current distribution of proposed antenna at the central frequency of 5.6GHz. It can be seen that maximum current is distributed across the rectangular patch which is responsible for widening bandwidth.

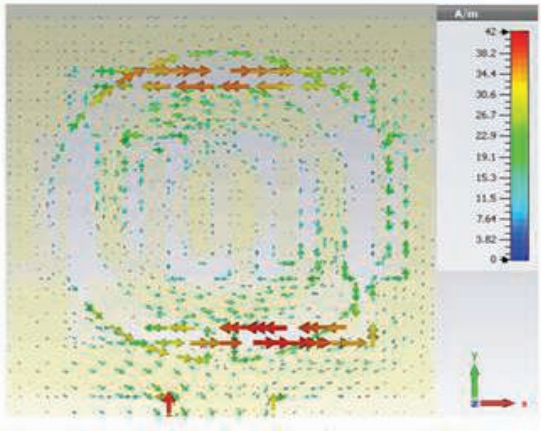

Fig. 13: Surface current distribution at 5.6 GHz

Radiation Pattern:

Figure 14 shows 2-D radiation patterns in polar E-plane and H-plane at the resonant frequency 5.6GHz. The radiation pattern shows that the antenna is directional with directivity (7.43dBi).

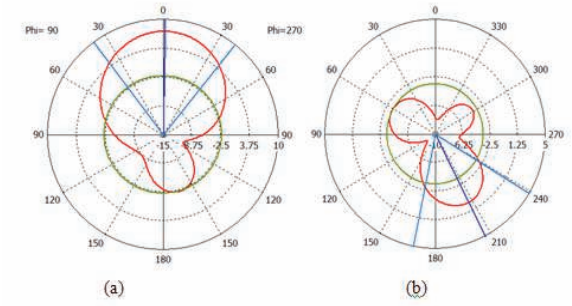

Fig. 14 2-D Radiation patterns of proposed antenna (a) Azimuth or H-Plane (b) Elevation of E-plane

VSWR vs Frequency plot

Figure 15 shows Voltage Standing Wave Ratio (VSWR) vs frequency plot of proposed antenna. Curve below VSWR=2 represents the bandwidth of antenna. It can be seen for proposed antenna the value of VSWR is less than 2 for frequency range 5.2GHz to 6.02GHz. Thus bandwidth of proposed antenna is 780MHz.

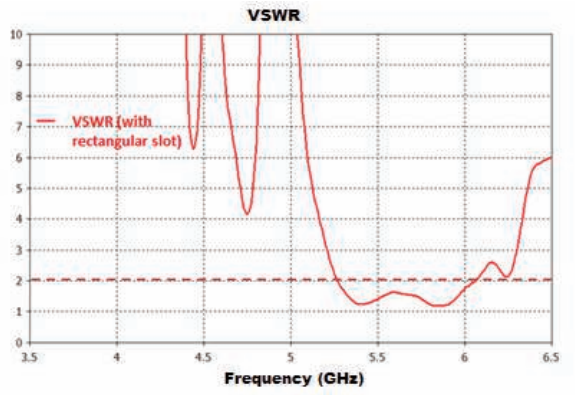

Fig. 15: VSWR vs frequency curve
(antenna with rectangular slot loading)

CONCLUSION

A novel wideband antenna loaded with CRLH unit cell is proposed. In proposed antenna, CRLH unit cell consists of inter-digital capacitor and rectangular slot on patch and CSRR etched on ground plane. By increasing inter-digital finger length series capacitance increases due to which electrical size of proposed antenna is reduced. 30% reduction in patch size of proposed antenna is achieved as compare to conventional patch antenna. Due to circulating current distributing along CSRR, resonance frequency is observed which generates TM01 mode. Rectangular slot on patch combines the TM01 mode generated by circulating current across CSRR and normal TM10 mode. A wider bandwidth from 5.2 GHz – 6.05 GHz is achieved by combination of these two modes.

The proposed antenna has a wide bandwidth and moderate gain regardless of its size as compare to that of conventional patch antenna of same dimensions, operating at same frequency. Based on performance of proposed antenna such as moderated gain and wide bandwidth of 780MHz. Due to wide bandwidth characteristic proposed antenna can be used in WLAN and due to directional radiation patterns it can be used in RFID applications.

REFERENCES

[i] S. K.0 Sharma, R. K. Chaudhary. A compact zeroth-order resonating wideband antenna with dual-band characteristics. IEEE Antennas and Wireless Propagation Letters. 2015;14:1670-2.

[ii] V.G. Veselago, "The electrodynamics of substances with simultaneously negative values of E and p". Soviet physics uspekhi 10(4): 509 – 514, 1968.

[iii] R. A. Shelby, D. R. Smith and S. Schultz , "Experimental Experimental verification of a negative index of refraction". Science 292: 77–79, 2001.

[iv] N. Engheta and R. W. Ziolkowski. "A Positive Future for Double-Negative Metamaterials". IEEE Transactions on Microwave Theory Technology 53(4): 1535-1556, 2005.

[v] Ian Hunter, D. Rhodes and D. Snyder, "Continued Discussion About "Propagation and Negative Refraction"[Backscatter], IEEE Microwave Magazine 15(5): 18 – 20, 2014.

[vi] S. Genovesi, F. Costa and A. Monorchio, "Wideband Radar Cross Section Reduction of Slot Antennas Arrays", IEEE Transaction on Antennas and Propagation 62: 163 – 173, 2014.

[vii] Z.Y. Pan, P. Zhang, C.Z. Chen, G. Vienne, M.H.Hong, "Hybrid SRRs Design and Fabrication for Broadband Terahertz Metamaterials", IEEE Photonics Journal 4:1267–1272, 2012.

[viii] D. R. Smith, W. J. Padilla, D.C. Vier, S. C. Nemat-Nasser and S. Schultz , "Composite Medium with Simultaneously Negative Permeability and Permittivity", Physical Review Letter 84: 4184-4187, 2000.

[ix] R. Marques, F. Martin, and M. Sorolla, "Metamaterials with Negative Parameters: Theory, Design, and Microwave Applications", John Wiley & Sons. Vol. 183, 2011.

[x] M. I. Khattak, M. Shafi, N. Khan, R. Edwards, Nasim Ullah, M. Saleem, "Variations in Return Loss of Patch Antennas in the Close Proximity of Human Body and Rectangular and Cylindrical Phantoms at 1.8 GHz", Technical Journal, University of Engineering and Technology (UET) Taxila, Pakistan Vol. 19 No. III, 2014.

[xi] J. Saranya and S. Thankachan. "Size miniaturization and bandwidth amelioration in microstrip antenna with metamaterials", IJSETR-International Journal of Science Engineering and Technology Research. Vol 5, 2016.

[xii] K. Saurav, D. Sarkar and K.V. Srivastava, "CRLH Unit-Cell Loaded Multiband Printed Dipole Antenna", IEEE Antennas and Wireless Propagation Letters 13: 852 – 855, 2014.

[xiii] M. Obaid Ullah, E. Alsusa, "A Virtually Blind Spectrum Efficient Channel Estimation Technique for MIMO OFDM Systems", Technical Journal, University of Engineering and Technology (UET) Taxila, Pakistan Vol. 20 No. III, 2015.

[xiv] W. Hu, Y. Z. Yin, P. Fei and X. Yang, "Compact triband square-slot antenna with symmetrical L-Strips for WLAN/WiMAX applications", IEEE Antennas Wireless Propagation Letters 10: 462 -465, 2011.

[xv] Y.F. Cao. S.W. Cheung and T.I. Yuk, "A Multiband Slot Antenna for GPS / WiMAX / WLAN Systems", IEEE Transactions on

Antennas and Propagation 63: 952 – 958, 2011.

[xvi] S. Kaushik, S.S. Dhillon and A. Marwaha, "Rectangular Microstrip Patch Antenna with U-Shaped DGS Structure for Wireless Applications", Computational Intelligence and Communication Networks (CICN):27 – 31, 2013.

[xvii] Y. Liu, L. Shafai and C. Shafai, "Gain and bandwidth enhancement of stacked H-shaped patch-open ring antenna". ANTEM-International Symposium on Antenna Technology and Applied Electromagnetics :1-2, 2016.

[xviii] H. P. Li, G. M. Wang, X. J. Gao, and L. Zhu, 2015. CPW-fed multiband monopole antenna loaded with DCRLH-TL unit cell. IEEE Antennas and Wireless Propagation Letters, 14, pp.1243-1246.

[xix] J. Ha, K. Kwon, Y. Lee, J. Choi , Young ki Lee, and Jaehoon Choi, "Hybrid Mode Wideband Patch Antenna Loaded With a Planar Metamaterial Unit Cell", IEEE transactions on Antenna and Propagation 60(2): 1143-1147, 2012.

Section C

MECHANICAL, INDUSTRIAL, MATERIAL, ENERGY ENGINEERING AND ENGINEERING MANAGEMENT

Mathematical Modeling of Low Velocity Impact on Hybrid CNG Cylinder

N. Mohsin[1], R. Khan[2], S. A. Masood[3]

[1,2,3]Mechanical Engineering Department, Islamic International University, Islamabad
[1]engr_nabeel99@hotmail.com

Abstract-In this paper a comparison was studied between mathematical modeling of CNG hybrid cylinder under impact. Impact resistance of hybrid material is analyzed using analytical modeling. Impact resistance against applied force is studied using Hertzian law which relates contact stiffness of wooden block and composite. Finite Element Analysis (FEA) for Low velocity impact (LVI) of wooden block on hybrid CNG cylinder is done for finding structural response parameters. 2 degree of freedom (2DOF) spring mass system is used for mathematical modeling of impact of wooden block on hybrid CNG cylinder. Stiffness values by analytical modeling are used in mathematical modeling for comparison with FEA. Results further show that values found by FEA and mathematical modeling are closely comparable.

Keywords-Hybrid Material, FEA, CNG Cylinder, Ansys Workbench

I. Introduction

Composite material is an alternate choice for pressure vessel than metals as they are lighter, stronger and cheaper. Composite material is a preferable choice for manufacturing of the pressure vessel. The pressure vessels made from the composite materials are lighter with higher burst pressure. [i].

Use of (Compressed Natural Gas) CNG as a fossil fuel has provided advantage for the automotive industry. Hybrid cars are made with idea of fewer emissions and highly efficient. CNG cylinders is made of storage in automotive. Pressure vessels are critical to impact loading during service life. Human safety has high and strict standards for safety throughout world. High safety standards need designer to increase thickness and consequently gain weight. Fiber metal laminates can be appropriate choice with considering safety and weight constraints.

The paper is structured as follows: Section I: introduction to composite and hybrid composite CNG cylinder in automobiles. Section II: literature introduction of Fiber metal laminates (FML), its application and latest research work in impact resistance. Section III current system description, its analytical modeling, FEA simulation and mathematical modeling of impact. In Section IV: comparison is made FEA simulation and mathematical modeling results.

II . Literature Review:

Combining suitable properties of material and fiber reinforce composite as an idea behind for development of new type of material called fiber metal laminate (FML). Fiber metal laminates (FML) [ii] are light weights hybrid metal and composite material or multi layered heterogeneous material. It consists of alternating layers of metal bonded with composite laminates. FML demonstrate outstanding damage tolerance capabilities in combination with excellent impact resistance when compared with composite and metal separately. FML is providing impact resistance under impact. Composite has properties of heterogeneous combination of different materials. Composite has high localized densities due to fiber immersed in Epoxy and high specific strength than single material. It has also improved fatigue resistance. In FML, it is composed of alternately stacked metal with composite such that the superior fatigue and fracture characteristics associated with fiber reinforce composite material may be combined with plastic behavior and durability offered by many metal [xvi] . These laminates consist of thin (0.3mm ~ 0.5 mm) metal strip bonded together with alternating unidirectional composite prepeg. These prepeg are Aramid or glass fiber in epoxy resin as shown in Fig. 1.

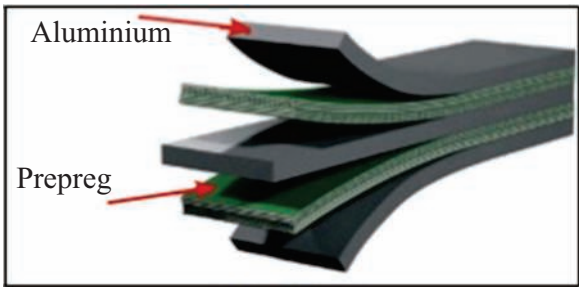

Fig. 1. FML materials layup

FML has significant characteristics of high specific strengths, better damage tolerant, blunt notch strengths, formability, and reparability.

Impact is force transferring phenomena that have to be considered in the design process for safety

reasons [iii]. Impact damage is an important type of failure in modern structures. However no available method can predict the perforation behavior of FML under impact loading due to different material combination. Multiple studies have resulted in the theoretical prediction of the impact response of FML under various loading conditions but the methodologies focus mainly on the elastic response which represents a minor portion of the perforation response. The impact resistance and damage tolerance should be determined. The development of impact resistance is limited because of scatter experimental data. New technique is necessary to assess impact performance of FML.

We are concentrating attention in this paper to develop some method for theoretical study of FML. In study of impact on FML require modeling of FML . Two improve model have been developed energy based model and spring mass model for calculating impact force and duration during low velocity impact of composite plate. Both model include contact deformation of impactor ,and plate as well as bending , transverse shear, membrane deformation of plate. Energy based model is based on conservation of energy. It is need of modeling that we use conservation law for imparting impact force on contact. Conservation of energy method assumes that impactor becomes stationary when structure reaches its maximum deflection and initial kinetic energy consumes in deforming structure. This approach is beneficial that deformation energy is quantified and identified separately. It determines maximum impact force .In spring mass approach spring is used to represents effective structural stiffness of system.

This model is effective for finding impact force load time history which is required for damage tolerance design studies [ix]. 2DOF spring mass model caters membrane, flexural and transverse stiffness. It contains mass of impactor and plate. In this spring mass model composite orthotropic nature of plate is considered. Spring mass model consider contact of impactor with plate and consider contact force duration for plate deflection [ix].

III. System Under Study

Geometry of CNG Cylinder:

Hybrid CNG cylinder is used for the storage of CNG at high pressures. Hybrid CNG cylinder consists of metal liner wrapped in composite cylinder. In this paper, CNG cylinder is made of 30CrMnSiA annealed Metallic liners with the thickness of 0.5 mm. It is wrapped by Epoxy glass fiber composite having thickness of 4.4 mm for making it light weight with high strength as shown in Fig. 2.CNG cylinder simulation is done according to safety standards of FMV404 i.e. American automobile safety. CNG cylinder is pressurized to 360 bars. Impactor is wooden block having mass 18 kg and velocity of 12 m/sec as shown in Fig. 2.

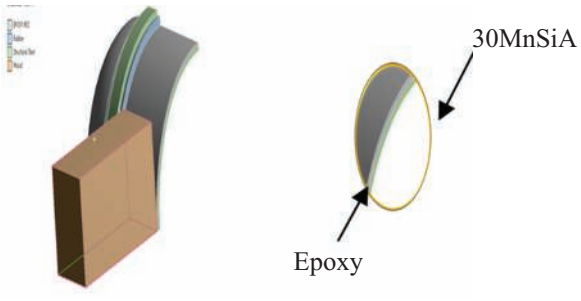

Fig. 2. Hybrid Cylinder and Impact Object

Many models used to study impact dynamics are classified according to impact velocity of projectile. There is not any generic model for describing impact of composite as well as hybrid structure. In order to understand mechanics of composite and hybrid structures it is desirous to study impact response of composite and hybrid structures [iv].

This paper is concerned about modeling of impact on CNG hybrid cylinder. Analytical modeling of composite and metal determine stiffness and deformation values of composite.

Impact phenomena broadly can be divided into three categories based on velocity at time of impact. Low velocity impact (LVI) range from (0~12m/sec). Global plate motion is established in LVI [v]. LVI induce mild damage in composite laminates. This invisible damage caused by mild impact was found to decrease residual strengths. Intermediate velocity impact regimes ranges from (12 ~50 m/sec). Hurricane debris collision on runway or roads lies in this category. High velocity impact (Ballistic impact) is usually results of explosive blasts, bullet strike[vi-viii] .

Considering mechanics of impact produce shear wave, flexural wave and tension or compression waves are produce in plate [ix]. In LVI impact stress wave propagation is slow and shear wave rebounds after reaching boundary condition [x]. Shear wave changes into flexural waves as more time of impact passes. Tensile or compressive strength at point of impact becomes dominant for composite [xi].

In our study case composite material in CNG hybrid cylinder bears impact directly. After damage in composite layer impact is transferred on metal liner. Metal liner deformation is produced after composite laminate damage. In this paper using analytical equations we modeled composite and metal separately. All symbols used in analytical modeling are described in Table 1 in Appendix A at end of paper.

Analytical Modeling

Contact within composite laminates and metal is essentially important parameter for transferring of impact force on both materials. During LVI

composite deforms more easily so contact area between impactor and composite changes non -linearly. Transient deformation of the panel as shear wave propagate from the point of impact is approximated by spring mass system. Local deformation in the contact zone is not modeled with beam, plate or shell theories usually assume that the structure is inextensible in the transverse direction. However in many cases local indentation has a significant effect on the contact free history and must be accounted for in the analysis. During loading phase contact force P is related to indentation α by Hertzian law [xii] expressed in equation 1,2,3.

$$P = k\alpha^{1.5} \quad (1)$$

$$P = \left(\frac{5}{4}\right)^{\frac{3}{5}} [M^3 V^6 k^2]^{1/5} \quad (2)$$

$$T_c = 3.1245[\frac{M^2}{Vk^2}]^{1/5} \quad (3)$$

Where $\mathbf{T}_c$= contact time (sec)

Basically stiffness in glass epoxy composite is calculated using material properties of Glass epoxy given in Table II.

TABLE II
ORTHOTROPIC PROPERTIES OF GLASS/EPOXY

Material properties	Glass Epoxy
E_1	38.6 Gpa
$E_{zz} = E_{rr}$	8.27 Gpa
$G_{\Theta z} = G_{\Theta r}$	4.14 Gpa
G_{rz}	4.14 Gpa
$V_{\theta r} = V_{\theta z} = V_{rz}$	0.26
ρ	1800 kg/m^3

A11, A22 and A12 are extensional stiffness parameter in longitudal, transverse and shear direction respectively for glass epoxy composite. The contact stiffness is given by equation 4, 5, 6, 7, 8, 9 & 10.

$$K_1 = 1 - \frac{\vartheta_1^2}{\pi E_1} \quad (4)$$

$$K_2 = \frac{\sqrt{A_{22}[(A_{11}*A_{22}+G_{zr})^2-(A_{12}+G_{zr})^2]^{1/2}}}{2\pi\sqrt{G_{zr}(A_{11}A_{22}-A_{12}^2)}} \quad (5)$$

$$A_{11} = E_z(1-\vartheta_r)\beta \quad (6)$$

$$A_{22} = \frac{E_r\beta(1-\vartheta_{zr}^2\delta}{(1+\vartheta_r)} \quad (7)$$

$$A_{12} = E_r\vartheta_{zr}\beta \quad (8)$$

$$B = \frac{1}{1-\vartheta_r-2\vartheta_{zr}^2\delta} \quad (9)$$

$$\delta = \frac{E_r}{E_z} \quad (10)$$

$$\lambda = k_c^{2/5}\, V^{1/5} M^{3/5}/[8\sqrt{m}^{-} D^*] \quad (11)$$

Using equation 1, 2 , 3 & 11 we get following parameters in Table III.

TABLE III
CONTACT FORCE PARAMETERS

Contact parameters	Glass Epoxy
P	1665 N
T_c	0.148 sec
λ	614.2e6

λ Inelasticity parameter comes out by putting values in equation (11) which shows that most of portion of kinetic energy is absorbed by glass epoxy composite.

Contact area of composite increases with penetration as shear wave interacts with bending waves. This material behavior can be approximated with two degree of freedom spring mass system.

Energy Based Model

Energy based modeling is based upon the principle of conservation of total energy of plate impactor system [xiii]. Total energy is sum of energies due to contact, bending, shear and membrane deformations and plastic energies petaling of aluminum layers. All energy which is equivalent to impactor kinetic energy [xiv] as shown in equation 12.

$$E_{impactor} = E_c + E_{bs} + E_m + E_p \quad (12)$$

$\mathbf{E_c}$= Contact Energy
$\mathbf{E_{bs}}$= Energy due To bending and shear
$\mathbf{E_m}$= Membrane Energy
$\mathbf{E_p}$= Plastic Deformation Energy

Contact energy is based upon on integral of contact force producing indentation α using equation 13.

$$E_C = \frac{\frac{2}{5}P^{5/3}}{n^{2/3}} \quad (13)$$

Reactive force can be resolved into two components using equation (14)

$$P = P_{bs} + P_m \quad (14)$$

$\mathbf{P_{bs}}$ is reactive force which is due to bending and shear deformation. $\mathbf{P_m}$ is reactive force associated with membrane deformation. Equation of 15 can be further elaborated as

$$P = K_{bs}w + K_m w^3 \quad (15)$$

$$K_{bs} = \frac{K_s K_b}{K_b + K_s} \quad (16)$$

$$K_b = \frac{4\pi E_r h^3}{3a^2*1-\vartheta_r^2} \quad (17)$$

$$K_s = 1.33\pi G_{zr} h \left(\frac{E_r}{E_\theta} - 4\vartheta_{rz}G_{zr}\right) * \frac{1}{1.33+\frac{\log a}{a_c}} \quad (18)$$

$$E_{bs} = \frac{1}{2K_{bs}w^2} \quad (19)$$

$$E_m = \frac{1}{4K_m w^4} \quad (20)$$

$$E_p = \frac{n_p(\sigma_o \pi^2 R h_{steel}{}^2)}{4} \quad (21)$$

where K_b, K_s, K_m are bending, shear, membrane stiffness of composite respectively. Energy absorption during impact can be elaborated in Table IV.

TABLE IV
ABSORBED ENERGY PARTITION

Energy	Glass Epoxy	% energy absorbed
E_m	4.67e-5 J	3.60e-6 %
E_c	753.19 J	58.1 %
E_{bs}	3.024 J	0.23 %
E_P	544.768 J	42.0
E_{tot}	1296 J	100 %

Using energy balance equation

$$\mathbf{M_1 V_o^2 = K_{bs} w^2 + \left[\left(\frac{K_m w^4}{2} + \frac{\frac{4}{3}\left|\left(K_{bs} w + K_m w^3\right)\right|}{n2}\right)\right]^{1/3}} \quad (22)$$

By putting values K_b, K_s, K_m in above equation and using Newton Raphson numerical technique the deflection w is calculated, w is **25.9** mm by finding roots of above equation. The deflection is crossing over material thickness. This value is indication of deflection which is bearing by composite only. This deflection is reduced by using metal liner along with composite absorbing 42 % of total energy.

Finite Element Simulation

CNG cylinder in simulation is carried by following American standards of automobile safety FMV404. CNG cylinder is pressurized to 360 bars when filled. Impactor is wooden block having mass 18 kg and velocity of 12 m/sec. In FEA simulation ANSYS EXPLICT is used for impact simulation. For impact simulation we used proximity based body algorithm in ANSYS Explicit dynamics module. From impact simulation basically target is to calculate impact penetration in composite and metal liner. Material properties of Wood is used in ANSYS is given in Table V.

TABLE V
MATERIAL PROPERTIES OF WOOD

Material properties	Glass Epoxy
E	0.9 Gpa
E	8.27 Gpa
ν	0.45
ρ	666 kg/m^3

In ANSYS Explicit dynamics hybrid CNG cylinder is modeled having impact by wooden block. Hybrid layup has 4.4 mm thick composite layup made in ANSYS ACP and 0.5 mm metallic liner. CNG cylinder is pressurized on 360 bars. For holding cylinder metallic strips and rubber bands are used for simulation. It has been observed that deflection stress in composite metal laminate. It has shown in Fig. 3.

Fig. 3: Strains in the pressure vessel

Mathematical Modeling in MATLAB

Applying Newton second law of motion, equation of equilibrium of two degree of freedom spring mass system are written as in equation 22 & 23 [xv]

$$M_1\ddot{x} + \lambda n[(x_1 - x_2)]^{1.5} = 0 \quad (22)$$

$$M_p\ddot{x} + K_{bs}x_2 + K_m x_2^3 - \lambda n[(x_1 - x_2)]^{1.5} = 0 \quad (23)$$

Mathematical modeling of composite laminate using spring mass system which is governed by equation 24

$$F = M\ddot{x} + C\dot{x} + Kx \quad (24)$$

When contact behavior follows Meyer's law and overall deflection are negligible a (single degree of freedom) SDOF model including damping is given in equation 25.

$$F = M\ddot{x} + C\dot{x} + Kx^n \quad (25)$$

Spring mass system has two degree of freedom. It is dealing with rigid body of impactor and plate. This model is extension of Lee's spring mass model for impact of beams. The spring combination below the plate mass satisfy the following conditions impact force is shared by bending shear and membrane deformations of plate; for thin plate the spring combination reduced to thin plate theory due to relatively low bending stiffness.

Let $X_1(t)$ and $X_2(t)$ as shown in Fig. 4 represents the displacement responses of the two masses at any time t after impact. The corresponding velocities were represented by differential of displacement of each mass individually. The contact deformation is given by

$\dot{x}_1(t)$-$\dot{x}_2(t)$ (26)

Throughout the analysis the impactor mass was assumed to be in contact with the plate. Initial conditions for equation are X_1 (0) = 0 and X_1 = V_o for impactor mass and X_2 (0) = 0 and X_2 (0) = 0 for plate mass. The coupled numerical equation is solved in MATLAB. Simulink model is shown in Fig. 5.

In graph of MATLAB simulation in Glass epoxy is 1.27mm as shown in Fig. 6. In this simulation metallic plate is not consider.

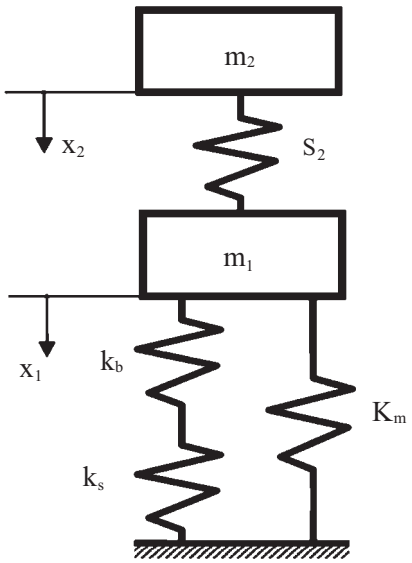

Fig. 4. Graphical description of 2 DOF spring mass model

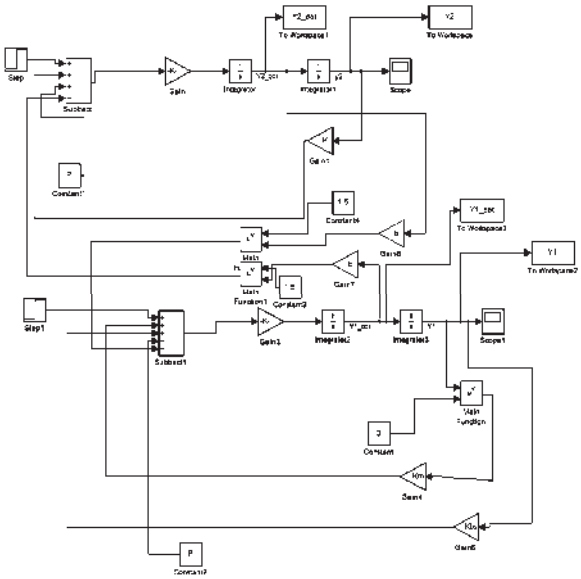

Fig. 5. 2DOF Spring Mass Model in MATLAB SIMULINK

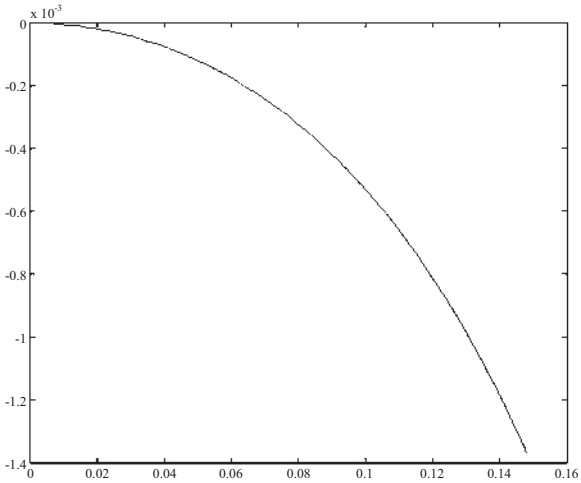

Fig. 6. Displacement time history in Glass/Epoxy plate after impact of wooden block by using spring mass model

IV. Conclusion

Comparing all methods in this paper we consider discretization of differential equation of impact on composite cylinder. This equation has given deformation of composite cylinder i.e. 1.27 mm. In FEA this simulation deformation in hybrid structure deformation is 0.44 mm. The difference is due to pressurized CNG cylinder. In paper energy based simulation reveals differentiation of energy distribution in different mechanisms in impact. Metallic liner takes 42 % impact energy which is less than plastic deformation energy .i.e. 1665.49 J from equation 21. From analytical equation deformation comes is 25.4 mm because considering only composite in equation 22.

Concluding all methods give impact dynamics depends upon different methods mentioned in analytical, energy, mathematical modeling method. In FEA simulation it is able to get actual boundary conditions. Results haves shown close relation to each method.

References

[i] Abrate Serge. "Modeling of impacts on composite structures." *Elesvier-Composite structures*, 1998: PP 130-138.

[ii] CAJR, Vermeeren. "A historic overview if the developement fiber metal laminates ." *applied Composite materials*, 2003 vol 10 No. 4: pp 189-205.

[iii] E. H. LEE. "Impact of mass striking a beam." *Applied mechanics* . Dec 1940. 1-129 to A138.

[iv] F. D. Moriniere R. C. Alderliesten, R. Benedictus. "energy distribution in Glare and 2024-T3 aluminum during low velocity

impact." *ICAS 2012.* Delft , The Netherlands: delft techonolgies, 2012.

[v] G. Caprino, Spataro S. del Luongo. "Low velocity impact behavior of fiber glass aluminum laminates ." *compos part A*, 2004: 605-615.

[vi] Hoo Fatt MS, Park KS,. "Modeling low velocity impact damage of composite sandwich panels." *J sandwich struct Material* , 1985,23: : 442-9.

[vii] Iaccarino P, Langella A and Caprino G. "A simplified model to predict the tensile and shear stress strain behavior of fiber glass aluminum laminates." *Composite science and technology* , 2007: 1784-1793.

[viii] J. W., Vlot A. and Gunnink. *Fiber metal laminates an introduction.* Klyuwer Academic publisher, 2001.

[ix] K. N. Shivaku, ar, W.Elber and W.Illg. *Prediction of Impact force and duration during low velocity impact on circular composite laminates.* NASA Technincal memorandum, Hampton Virginia 23665: NASA Langley research center, October 1983.

[x] Logan, D.J. *Applied Mathematics* . Jhon Wiley & Sons, second edition 1997.

[xi] "Mettalic materials and elements for aerosapce vehicle structures." In *MIL HDBK-5H*. 1998.

[xii] Payeganeh GH, Asshenai Ghasemi F and Malekzadeh. "Dynamics response of fiber metal laminates subject ti low velocity impact." *thin walled structure*, 2010: pp 62-70.

[xiii] Vadori, G.Belingardi R. "Low velocity impact tests of laminates glass fiber epoxy matrix composite material plates." *Interantion journal impact Eng.*, 2002: 213-229.

[xiv] Vlot A, Kroon E and La Rocca G. "Impact response of fiber metal laminates." *Key engineering material* , 1998: pp 235-276 .

[xv] W. J. Strong. *Impact Mechanics.* Cambridge university Press UK, 2000.

[xvi] Remmers JC .Discontinuities in material and structures: a unified computational approach , PhD thesis , Delft university of technology , 2008

[xvii] M. Sadighi. impact resistance of fiber metal laminates a review , international journal of impact engineering 49 (2012) 77-90

[xviii] C.C FOO, A modified energy balance approach model to predict low velocity impact response for sandwich composite, composite structures 93 (2011) 1385 - 1393

Appendix A

TABLE I
LIST OF SYMBOLS

α =Indentation in Composite Panel	K_m =Membrane Stiffness
A_{deb} =De-bonding Area	L =Length of Indenter
A_{del} =Delamination Area	R_o =Equivalent Projectile Radius
A_{ij} =Membrane Stiffness	t =Time
D_{ij} =Bending Stiffness	U =Strain Energy
E =Young's Modulus	V_o =Projectile Initial Velocity
Ep =Plastic Modulus	w =Transverse Plate Deflection
E_{ay} =Average Panel Stiffness	W =Work done by External Force
E_{bm} =Bending and Membrane Energy	z =Through Thickness Co-ordinate
E_{deb} =De-bonding Energy	ϵ =Strain
E_{del} =Delamination Energy	ϵ_{cr} =Fracture Strain
E_{ij} =Laminate Stiffness	ϵ_{Al} =Fracture Strain in Aluminum
E_p =Petaling Energy	$\epsilon_{G/E}$ =Fracture Strain in Glass Epoxy
e_t =Energy density for tensile failure	ν_{ij} =Poisson's Ratio for Laminate
E_t =Tensile fracture energy	ν =Poisson's Ratio for Panel
E_{tot} =Total Energy	Π =Total Potential Energy
F =Impact Load	ρ_{av} =Average Density
G_{ij} =Laminate Stiffness	ρ =Density
h =Laminate Thickness	σ_f =Tensile Fracture Strength
h_{AL} =Aluminum Ply Thickness	σ_o=Yield Strength
$h_{G/F}$ =Glass Epoxy Ply Thickness	ξ =Deformation Zone
K_b =Bending Stiffness	

Common Vertical Axis Savonius-Darrieus Wind Turbines for Low Wind Speed Highway Applications

Z. Anjum[1], L. A. Najmi[2], A. Fahad[3], R. Ashraf[4], S. Ehsan[5], W. Aslam[6]

[1-6]*Mechanical Engineering Department, Swedish College of Engineering and Technology, Wah Cantt, Punjab*
[1]zeeshan.anjum@scetwah.edu.pk

Abstract-Wind energy is considered to be the fastest growing alternative of fossil fuel and a clean energy source. In this research work a combination of common vertical axis wind turbine is designed and tested specifically for the sites having low wind speed availability. This combination of Savonius and Darrieus rotor blades on a common shaft provides the benefits of both the starting at very low wind speeds and good efficiency. This combination has been used to recapture the wind power available on the highways due to the movement of the vehicles. Savonius rotor blades being self-starting at low wind speeds help the Darrieus rotor blades to rotate which have greater efficiency than Savonius. Average wind speed available at the highway during this study is taken to be 4.8 m/s. Up to 37% efficiency is achieved by using this combination at a tip speed ratio of 0.9 and with no overlap conditions. With the increase in tip speed ratio, the overall efficiency and power coefficient increases. At high wind speeds, the tip speed ratio and power coefficient decreases.

Index Terms—wind energy; Savonius; Darrieus; self-starting; tip speed ratio; power coefficient

I. Introduction

Shelter is globally recognized as a basic need of human being. Under the Universal Declaration of Human Rights and the UN Habitat Conference 1996, all the governments are responsible to make diligent efforts for providing affordable housing to their citizens [i-ii]. Affordable housing means the housing facility that low to median income households can avail within their resources without compromising their other basic necessities for living such as food, clothing, children education and medical facility [iii]. For housing to be affordable in metropolitan areas, it is

NOMENCLATURE

Abbreviations

VAWT	Vertical Axis Wind Turbine
HAWT	Horizontal Axis Wind Turbine
FOWTs	Floating Offshore Wind Turbines
TSR	Tip Speed Ratio
NWT	Numerical Wind Tunnel
CFD	Computational Fluid Dynamics
RPM	Revolutions per Minute

List of Symbols

D	diameter of Savonius rotor blade
H	height of Savonius rotor blade
R	radius of Darrieus rotor blade
L	length of Darrieus rotor blade
A_s	swept area of Savonius rotor blade
A_{sd}	swept area of Darrieus rotor blade
ω	angular speed of the rotor
λ	blade tip speed ratio
V_b	blade tip speed
V_a	average ambient wind speed
P_{th}	theoretical power to drive the turbine
P_{act}	actual available power
η_{th}	theoretical efficiency
η_{act}	actual efficiency
T	actual torque
T_w	theoretical torque
I	current
V	voltage
A	total swept area
ρ	density of the air
P	turbine output power/ shaft power
C_P	power coefficient

I. Introduction

Wind energy being environmental friendly and abundantly available in the earth's atmosphere is considered as a potential alternative source of fossil fuels. Dependency on fossil fuels can be reduced by the help of such a potential alternative energy source and its importance is being recognized in many developing countries.

A well designed wind rotor machine like vertical axis wind turbine can help to meet the desired power by utilizing the available wind energy to its maximum. Generally horizontal axis wind turbines (HAWT) are considered as more suitable in terms of their efficiency as compare to vertical axis wind turbines (VAWT) but later ones are considered to be more advantageous in terms of safety, compact design, cost and operation in urban environments. Moreover even at low blade speed ratios and with zero net mas flux actuation, better robust power output can be achieved [i]. Common VAWTs are shown in Fig. 1.

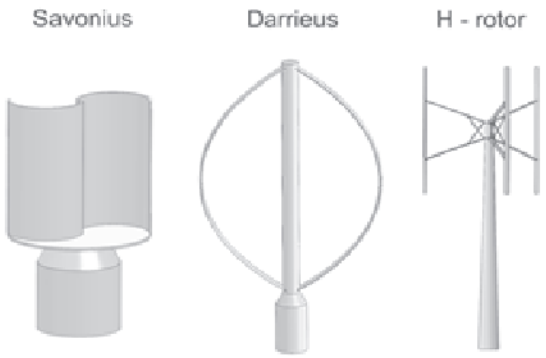

Fig. Common VAWTs

VAWTs can be easily installed on building rooftops and areas of turbulent flow with more success than HAWTs and thus find wide use in domestic, private and commercial applications where turbine placement and wake effects are the major concern [ii]. VAWTs are well suited for offshore wind energy exploitation as floating offshore wind turbines (FOWTs) using suitable mooring line models [iii]. A more suitable hydrodynamic model for floating offshore wind turbines is Cummins equation with number of modifications. Moreover fixed support structures are not technically suited for offshore wind applications so floating support structures are necessary for deep offshore wind turbines to become economically viable [iv]. Savonius rotor vertical axis wind turbine is a drag type VAWT, initially developed in late 1920s by dividing a cylinder into two equal semi-cylindrical surfaces and then moving them sideways along their cutting plane [v]. Savonius rotors with two blades, end plates and with no overlap give better performance [vi]. The aerodynamic noise of Savonius rotor can be predicted by applying FW-H equation. S-shaped Savonius turbine with a twist angle of 200 was found to provide the maximum reduction in the noise [vii]. Creating wind jets towards the concave side of advance and return rotors of Savonius turbine rotor can significantly enhance its performance, however the wide wake produced around and behind the rotors must be considered [viii]. Bronzinus is a novel type of VAWTs which gives better coefficient of performance as compare to the classical Savonius turbines [ix]. Darrieus wind turbine being a lift type of a VAWTs that was invented by a French inventor, George Darrieus, having two or three curved shaped blades with airfoil type cross section having constant chord length [x]. Adaption of accurate blade Reynolds number (Re) in case of Darrieus wind turbine is necessary to predict correct information at high tip speed ratios [xi]. The most commonly used mathematical models for performance prediction of Darrieus turbine are: vortex model, cascade model, double multiple stream line model and blade element momentum (BEM) model [xii, xiii]. Increasing the tilt angle of Darrieus wind turbine causes reduction in power production and coefficient of performance and hence it must not exceed the angle at Troposkien root which is at 300 [xiv]. Improvement in power coefficient up to 51% had been observed in combined Darrieus-Savonius rotor with no overlap and reduction in power coefficient was observed with the increase in overlap [xv]. The main contribution of Savonius rotor in Darrieus-Savonius rotor is to provide the starting torque at different intensities and directions of inlet air [xvi]. The net power output of VAWT can be improved by properly positioning it behind the deflector plate [xvii]. Optimum hybrid H-Savonius rotor shows improved performance in terms of its self-starting ability at all azimuthal angles and better output as compare to other existing H-type vertical axis wind turbine rotors [xviii]. Numerical wind tunnel (NWT) technique is commonly used to study the performance of VAWTs by analyzing the flow around and inside the multistage VAWTs surrounded by stator vanes [xix]. Computational Fluid Dynamics (CFD) gives a good insight to study the aerodynamics of VAWTs as compare to computational aerodynamics and can analyze the flow patterns around the airfoils [xx].

In this experimental work, a combination of combined vertical axis Savonius-Darrieus rotor wind turbine is proposed and successfully implemented for extracting the wind energy available from the high speed moving vehicles on the highways. The wind turbines are designed to be placed in high traffic areas on the medians to utilize the maximum amount of available wind energy and hence fluid flow from both sides of the highway is considered in this design. Up to 37% efficiency has been achieved by the proposed setup.

II. Design Of Savonius-Darrieus Wind Turbine

In present experimental work a hybrid Savonius-Darrieus rotor VAWT is designed and tested for highway applications with both turbines on the same common shaft. Savonius rotor being self-starting but less efficient at low wind speeds is used to start straight bladed Darrieus rotor which has greater efficiency than Savonius [xxi]. The aim is to combine both types of turbines to increase overall efficiency of the system and to convert maximum available wind energy into useful work with less complexity in design and cost effectiveness.

A. Blades

The blades designed for Savonius-Darrieus rotor in this study are of aluminum alloy, Al-2024 due to its light weight, low cost and good mechanical properties.

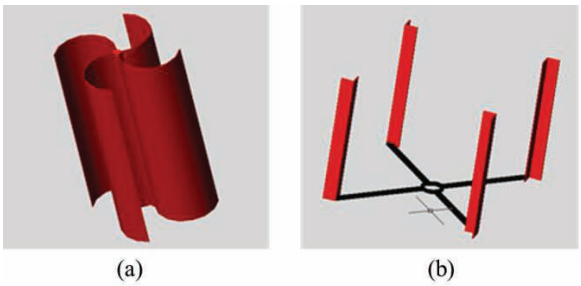

(a) (b)

Fig. 2: (a) Savonius rotor blades (b) straight bladed Darrieus rotor blades

Number of blades selected during the current study are 4 as they produce more torque than 3 blades at low TSR [xxi]and at an angle of 900 to each other as shown in Fig. 2.

These blades are obtained by bending and rolling aluminum sheets having a height of 2 feet and 1mm thickness as shown in Fig. 3. The zero overlap condition has been used.

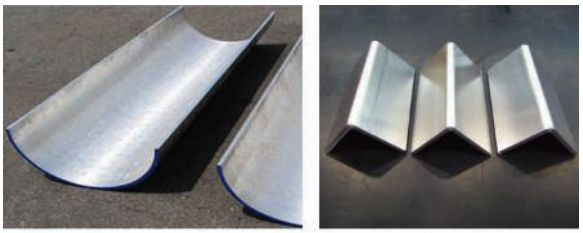

(a) (b)

Fig.3: (a) Savonius rotor blades (b) Darrieus rotor blades

Properly fitted hollow aluminum shaft having diameter of 1 inch and total length of 3.5 feet is used to transfer rotational energy obtained from hybrid Savonius-Darrieus rotor blades to the generator. Partition plates made of aluminum are used between the Savonius-Darrieus rotors and cast iron flanges are used to attach spoke arms to the shaft. Complete 3D model of hybrid Savonius-Darrieus rotor VAWT is shown in Fig. 4.

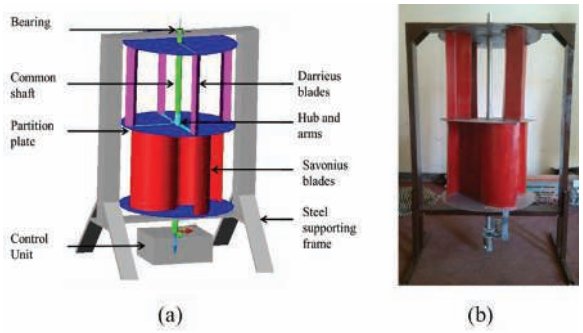

(a) (b)

Fig. 4: (a) 3D model of Hybrid Savonius-Darrieus rotor VAWT (b) fabricated model

Control units consisted of gear box having gear ratio of 1:13 to increase the available rpm, ammeter, voltmeter, DC to AC converter, fuse and battery for power storage.

VAWT has a rectangular shaped swept area given by (1) & (2) for Savonius and Darrieus rotors respectively [xxii]:

$$A_s = \pi \times D \times H \quad (1)$$

$$A_{sd} = 2 \times R \times L \quad (2)$$

Swept area limits the volume of the air passing by the turbine and power output directly depends upon the swept area. Total swept area in this study is 0.8 m2. For stability the diameter to height ratio (D/H) is kept to 1.2.

Different designs are being proposed by different researchers [viii] to utilize the input power of the wind to its maximum. Wind diverter is one of the techniques that can be applied to get maximum power from the wind available by converging it towards the turbine rotor as shown in Fig. 5.

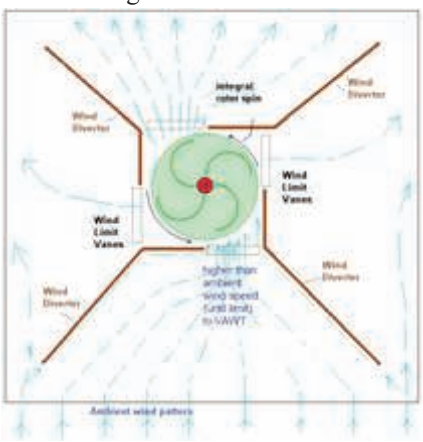

Fig. 5: Wind diverters to increase the input wind power

The function of wind diverters is to harvest the wind power by converging it to high velocity jet which strikes on the concave side of Savonius blade and a guide mechanism designed to limit the wind flow on convex side. Hence it helps to increase the positive torque and reduction in drag. Several configurations have been investigated for obtaining maximum torque and reducing drag.

A. Tip Speed Ratio (TSR)

The power coefficient depends upon the blade tip speed ratio (λ) which is the ratio of blade tip speed (Vb) and average wind speed (Va) available, in our case it is 0.99 and average available wind speed measured by anemometer is 4.8 m/s. The number of revolutions as measured by tachometer is 180.

$$\lambda = \frac{V_b}{V_a} \quad (3)$$

where,

$V_b = \omega \times R$

For different tip speed ratios, the theoretical efficiency for ideal VAWTs can be calculated using following relations as provided in Table I

TABLE: THEORETICAL EFFICIENCY RELATIONS FOR IDEAL VAWT [xxii]

1	For $0.5 \leq \lambda \geq 1$	$\eta_{th}=0.196 \times \lambda+0.23233$
2	For $1 \leq \lambda \geq 1.5$	$\eta_{th}=0.104 \times \lambda+0.32433$
3	For $1.5 \leq \lambda \geq 2.5$	$\eta_{th}=0.055 \times \lambda+0.399$
4	For $2.5 \leq \lambda \geq 4$	$\eta_{th}=0.022 \times \lambda+0.481$
5	For $\lambda \geq 4$	$\eta_{th}= 0.078369\times\lambda^2+ 0.92146 \times \lambda$

Power and efficiency of the VAWTs can be calculated by the following equations [xxi, xxiii,xxv]:

$$P_{th} = \frac{1}{2} \times \rho \times A \times V_{a^3} \quad (4)$$

$$P_{act} = I \times V \quad (5)$$

$$\eta_{th} = \frac{2\times T\times \omega}{\rho\times {V_a}^3 \times A} \quad (6)$$

$$\eta_{act} = \frac{Output}{Input} \quad (7)$$

$$P = P_{th} \times \eta_{th} \quad (8)$$

Efficiency of conversion of available energy can be represented by power coefficient (Cp) which is the ratio of turbine output power to the power of wind [xxi, xxiv] as in (9):

$$C_p = \frac{P}{P_{th}} \quad (9)$$

Whereas, coefficient of torque (C_t) is given by (10):

$$C_t = \frac{T}{T_w} = \frac{4T}{\rho\, A_s\, d\, {V_a}^2} \quad (10)$$

III. Results And Discussion

The hybrid Savonius-Darrieus rotor VAWT is designed for highway applications. The average speed of air available at the installation site from the movement of vehicles as measured by anemometer is 4.8 m/s. It can vary depending upon the traffic, vehicle speed and weather conditions. This design of combining the Savonius and Darrieus rotor on a common shaft helps to increase the overall efficiency of the system and wind energy from the both sides of moving vehicles is used as input which helps the turbine rotors to rotate smoothly and speedily. The wind power available to a single unit to drive the turbine, refer to (4) is 54.6 watt and hence the theoretical efficiency for an ideal VAWT with tip speed ratio of 0.9 is 42%,refer to (6). Theoretical power output is 23 watt calculated as in (8).

A number of such units can be installed on the highways which are grid connected to obtain maximum power from this clean alternative energy source and this addition is quite useful in meeting the fastest growing electricity demand.

Numerical simulation using standard finite element software is an important tool applied nowadays [xxvi, xxvii]. Numerical simulation using ANSYS resulted that the turbine with 4 blades produces more torque at low TSR while turbine with 3 blades show optimum performance at TSR [xxi].

The actual power output of turbine has been compared with the theoretical power output at various wind powers in the Fig.6. With the increase in tip speed ratio,both actual as well as theoretical powers are reduced.

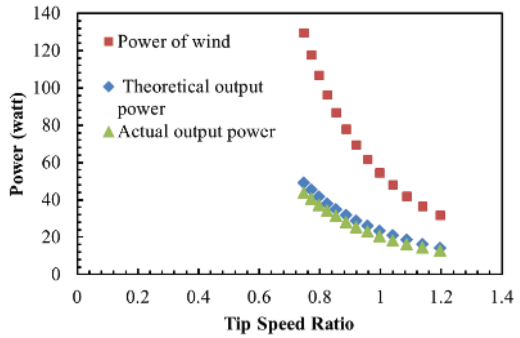

Fig. 6: Actual and theoretical power outputs at various TSRs and available wind powers

TSR is found to have an inverse relation wind speeds as shown in Fig. 7. On the other hand TSR is found to have a direct relation with the overall efficiency as shown in Fig. 8.

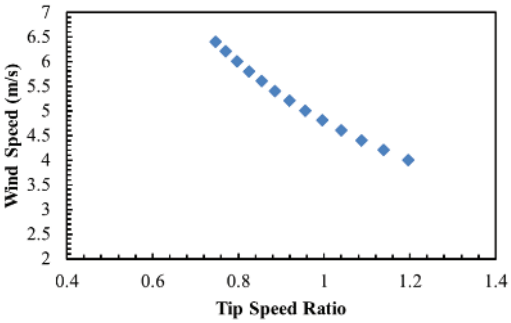

Fig. 7: Variation in TSR at various wind speeds

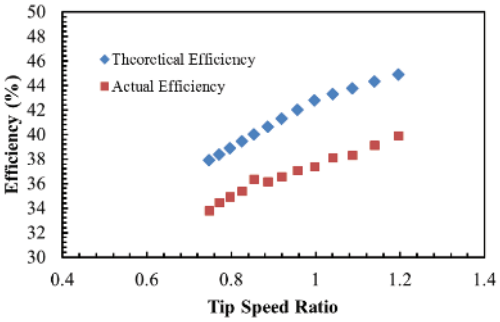

Fig. 8: Increase in efficiency with increase in TSR

Also it is found that with the increase in tip speed ratio the power coefficient increases while it has an inverse relation with the wind speed as shown in Fig. 9.

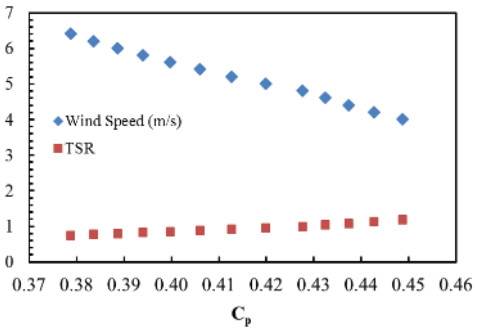

Fig. 9: Change in power coefficient at various wind speeds and TSR

The actual power output available as calculated by using (5) at the average wind speed of 4.8 m/s is 20.4 watt and the actual efficiency achieved is 37% which is very acceptable in comparison with the theoretical efficiency of 42% considering several factors like weight of the assembly etc.

IV. Conclusions

The proposed design of hybrid Savonius-Darrieus turbines for highway applications is very useful as an alternative energy resource. Installing a number of such units increase the overall power output thus utilizing the maximum amount of available wind energy. The average available wind speed during the current study is 4.8 m/s and the hybrid configuration of Savonius-Darrieus VAWT has an efficiency of 37%. Up to 20 watt power output is obtained. Also with the increase in TSR, the overall efficiency and power coefficient increase. At high wind speeds, the TSR and power coefficient decreases.

References

[i] J. Yen and N. Ahmed (2012). Improving safety and performance of small-scale vertical axis wind turbines. Procedia Engineering, 49: p. 99-106.

[ii] H. Chowdhury et al. (2015). Adjacent wake effect of a vertical axis wind turbine. Procedia Engineering, 105: p. 692-697.

[iii] M. Borg, M. Collu, A. Kolios. Offshore floating vertical axis wind turbines, dynamics modelling state of the art. Part II: Mooring line and structural dynamics. Renewable and Sustainable Energy Reviews. 2014 Nov 30;39:1226-34.

[iv] M. Borg and M. Collu (2015). Offshore floating vertical axis wind turbines, dynamics modelling state of the art. Part III: Hydrodynamics and coupled modelling approaches. Renewable and Sustainable Energy Reviews, 46: p. 296-310.

[v] S.J. Savonius (1931). The S-rotor and its applications. Mech. Eng, 53: p. 333-338.

[vi] N. H. Mahmoud, A. A. El-Haroun, E. Wahba, M. H. Nasef. An experimental study on improvement of Savonius rotor performance. Alexandria Engineering Journal. 2012 Mar 31;51(1):19-25.

[vii] S. Kim and C. Cheong (2015). Development of low-noise drag-type vertical wind turbines. Renewable Energy, 79: p. 199-208.

[viii] W. A. El-Askary, M. H. Nasef, A. A. AbdEL-hamid, H. E. Gad. Harvesting wind energy for improving performance of Savonius rotor. Journal of Wind Engineering and Industrial Aerodynamics. 2015 Apr 30;139:8-15.

[ix] G. G. Muscolo and R. Molfino (2014). From Savonius to Bronzinus: a comparison among vertical wind turbines. Energy Procedia, 50: p. 10-18.

[x] G. Darrieus (1931). Turbine Having its Rotating Shaft Transverse to the Flow of the Current United States Patent No. 1. 835. 018.

[xi] F. Z. Tai, K. W. Kang, M. H. Jang, Y. J. Woo, J. H. Lee. Study on the analysis method for the vertical-axis wind turbines having Darrieus blades. Renewable energy. 2013 Jun 30;54:26-31.

[xii] N. C. Batista, R. Melício, V. M. Mendes, M Calderón, A. Ramiro. On a self-start Darrieus wind turbine: Blade design and field tests. Renewable and Sustainable Energy Reviews. 2015 Dec 31;52:508-22.

[xiii] M. Islam, S. K. David, Ting, A. Fartaj. Aerodynamic models for Darrieus-type straight-bladed vertical axis wind turbines. Renewable and Sustainable Energy Reviews. 2008 May 31;12(4):1087-109.

[xiv] G. Bedon, S. De Betta, E. Benini. A computational assessment of the aerodynamic performance of a tilted Darrieus wind turbine. Journal of Wind Engineering and Industrial Aerodynamics. 2015 Oct 31;145:263-9.

[xv] R. Gupta, A. Biswas, K. K. Sharma. Comparative study of a three-bucket Savonius rotor with a combined three-bucket Savonius–three-bladed Darrieus rotor. Renewable Energy. 2008 Sep 30;33(9):1974-81.

[xvi] J. Gavalda, J. Massons, F. Diaz. Experimental study on a self-adapting Darrieus—Savonius wind machine. Solar & Wind Technology. 1990 Jan 1;7(4):457-61.

[xvii] D. Kim and M. Gharib (2013). Efficiency improvement of straight-bladed vertical-axis wind turbines with an upstream deflector. Journal of Wind Engineering and Industrial Aerodynamics, 115: p. 48-52.

[xviii] S. Bhuyan and A. Biswas (2014). Investigations on self-starting and performance characteristics of simple H and hybrid H-Savonius vertical axis

wind rotors. Energy Conversion and Management, 87: p. 859-867.

[xix] M. Burlando, A. Ricci, A. Freda, M. P. Repetto. Numerical and experimental methods to investigate the behaviour of vertical-axis wind turbines with stators. Journal of Wind Engineering and Industrial Aerodynamics. 2015 Sep 30;144:125-33.

[xx] X. Jin, G. Zhao, K. J. Gao, W. Ju. Darrieus vertical axis wind turbine: Basic research methods. Renewable and Sustainable Energy Reviews. 2015 Feb 28;42:212-25.

[xxi] F. Wenehenubun, A. Saputra, H. Sutanto. An experimental study on the performance of Savonius wind turbines related with the number of blades. Energy Procedia. 2015 Apr 1;68:297-304.

[xxii] A. T. Zhuga, B. Munyaradzi, C. Shonhiwa. Design of alternative energy systems: A self-starting Vertical Axis Wind Turbine for stand-alone applications (charging batteries). SPONSORS. 2006 Jul 12:72.

[xxiii] S. Chaitep, T. Chaichana,P. Watanawanyoo H. Hirahara. Performance evaluation of curved blades vertical axis wind turbine. European Journal of Scientific Research. 2011;57(3):435-46.

[xxiv] U. K. Saha, S. Thotla, D. Maity. Optimum design configuration of Savonius rotor through wind tunnel experiments. Journal of Wind Engineering and Industrial Aerodynamics. 2008 Sep 30;96(8):1359-75.

[xxv] M. M. A. Bhutta, N. Hayat, A. U. Farooq, Z. Ali, S. R. Jamil, Z, Hussain. Vertical axis wind turbine–A review of various configurations and design techniques. Renewable and Sustainable Energy Reviews. 2012 May 31;16(4):1926-39.

[xxvi] F. Qayyum, M. Shah, O. Shakeel, F. Mukhtar M.Salem, F. Rezai-Aria. Numerical simulation of thermal fatigue behavior in a cracked disc of AISI H-11 tool steel. Engineering Failure Analysis. 2016 Apr 30;62:242-53.

[xxvii] Z. Anjum, F. Qayyum, S. Khushnood, S. Ahmed, M. Shah. Prediction of non-propagating fretting fatigue cracks in Ti6Al4V sheet tested under pin-in-dovetail configuration: Experimentation and numerical simulation. Materials & Design. 2015 Dec 15;87:750-8.

Diffusion of e-Government System in Pakistan; Analysis of Adoption by Government Employees of Pakistan

J. Riaz[1], M. T. Nawaz[2], F. Shakeel[3], S. A. Raza[4]

[1,2,3,4]*Engineering Management Department, College of Electrical & Mechanical Engineering, NUST, Islamabad, Pakistan*

[1]jawadriaz@gmail.com

Abstract-Governments around the globe are switching to electronic government (e-Government), which is the usage of Information and Communication Technology (ICT) for information sharing, delivering better and faster public services and various types of transactions with citizens, government institutions and businesses. Hence, it is crucial to investigate adoption of e-Government system among public employees which is an aspect of this area not much explored in Pakistan although likely to influence positively other stakeholders.

The study validates leading technology theory i.e. Diffusion of Innovation (DOI) in order to explore the diffusion trends of e-Government system among government employees' of Pakistan in terms of five significant determinants i.e. Relative Advantage, Complexity, Compatibility, Trialability and Observability.

Survey strategy is employed for this research using simple random sampling. Sampling frame consists of government organizations in Federal Government of Pakistan which are functioning on the e-Government system. By employing statistical analyses over the captured responses, it was found that Relative Advantage, Compatibility, Complexity and Trialability have a positive association with intention to adopt/ diffusion of e-Government system among government employees' whereas Observability has no significant relationship.

This research is expected to contribute through investigations regarding determinants influencing e-Government adoption and diffusion in Pakistan's scenario as a developing nation and recognize the attributes which practitioners need to tackle in their endeavor to promote the adoption and diffusion of e-Government.

Keywords-Government, Government to Employee (G2E), Diffusion of Innovation, Intentions to Adopt, Relative Advantage, Compatibility, Complexity, Trialability, Complexity, Observability, Behavioral Intention.

I. INTRODUCTION

Governments around the world whether in industrialized or developing countries are switching from traditional functioning through manual working to e-Government systems. e-Government has improved the cumbersome nature of work to a more efficient one thus facilitating citizens in a true sense and also helped in improving the negative image of governments by making its processes transparent and effective. e-Government employs the latest information and communication technologies (ICTs) to revolutionize government dealings, facilities, democracy and enabling citizens' access to valuable information. It is the transformation of government to a more citizen centered one [i]. ICT provides an efficient and effective e-Government mechanism as it is the main driving force of e-Government technology [ii].

Diffusion of Innovation (DOI) theory was established in 1963 [iii]. DOI theory explains that at what pace an innovation is diffused in a population over time. Roger also explained that different innovations can follow different rate of adoptions owing to their characteristics. The main attention of the DOI theory is on the attributes of the innovation which directly affect its adoption [iv]. This model is widely used to determine the intention to adopt/ rate of diffusion of e-Government in many other countries like Nigeria, Mauritius, South Africa, Lorraine, Netherlands etc. The results of one country cannot be held true for another due to different conditions such as political, cultural values, ICT literacy and so on. Research is needed to conclude the aspects responsible for slow rate of diffusion of e-Government in Pakistan.

This model used in this research is the most suitable concerning the scenario of e-Government in Pakistan. It is the only model whose main focus is on characteristics of the innovation rather than users' perspective. DOI model is validated in this research to predict factors contributing towards diffusion of e-government in Pakistan by analyzing the government to employee perspective (G2E). Establishment of an

effective e-Government infrastructure and services among government departments will greatly improve the image of e-Government through enhanced transparency and efficiency. The goal of this research paper is to investigate the primary attributes which are accountable for influencing diffusion/ adoption of e-Government in Pakistan thus may be analyzed and manipulated according to findings

II. Rationale and Significance

In many developing countries, citizens distrust their government due to political instability, large scale corruption or history of dictatorship. Pakistan is one of the developing country facing many obstacles for efficient e-Government deployment such as political instability, fraud, poor educational systems and policies, low ICT literacy and uneven distribution of technology [i]. Pakistan started e-Government implementation in October 2002 by laying down foundations of Electronic Government Directorate (EGD) under Ministry of Information technology (MOIT) [v]. The United Nations Electronic Government Readiness Index (EGRI) for Pakistan in 2002 was 0.104 with a global ranking of 120 [ii]. EGRI and world ranking for e-Government of Pakistan has been going through many ups and downs owing to different factors e.g. political instability, low ICT literacy, lack of infrastructure etc. The UN ranking for Pakistan in 2014 is 158 with an EGRI of 0.2580 [vi].

The main objective of this research paper is to explore the key parameters responsible for the downfall of e-Government in Pakistan thus influencing the progress of Pakistan at many levels. It identifies various gaps in government to employees' (G2E) perspective which need to be addressed for smooth e-Government employment as when the foundations are strong, better structure will be provided resulting in satisfied stakeholders. DOI model can be considered to be the most suitable for analyzing the scenario of e-Government in Pakistan as it is the only model focusing upon characteristics of the innovation rather than users' perspective. This research will benefit the Government of Pakistan to a great extent in remedies of key hurdles which will pave the way for efficient and effective e-Government establishment.

III. Literature Review

World is advancing day by day and governments all around the globe are taking measures to switch to electronic services which is the employment of Information and Communication Technology for information sharing and various types of transaction among government and citizens, businesses, and other government organizations.

A. e-Government

The government has obligation to deliver better and faster public service through Electronic Government (e-Government). The key basic principle of electronic government can be regarded as the improvement of government operations effectively and efficiently and improving communication and interaction within itself, citizens, businesses and other stakeholders [vii]. e-Government can also be regarded as a socio-technical system which is greatly influenced by the capabilities of the institution, their concerned policies and socio-cultural suggestions [viii]. It aids in reducing cost [ix] and lays down the foundations for trustworthy and efficient communication among all levels and sub-branches of e-Government [x]. e-Government can also be regarded as change in old-fashioned practices and switching to electronic ways of facilitating the citizens' in a true sense [xi].

A lot of mistrust issues have been seen among the citizens and governments of developing nations and it has been mainly attributed to illiteracy, corruption and lack of communication mediums [xii]. The world is advancing day by day with the adoption of new technological revolutions and increased levels of literacy, an awareness has been created and governments are re-engineering themselves to be more alert, reliable and as efficient as possible [xiii]. A need for re-structuring of government has arisen in the perspective of organization, practices and methods of service supply to approach the standard that e-Government truly offers [xiv].

1) Importance of ICT in e-Government

Government should identify the true importance and worth of ICT and should employ it in every field of life [xv]. ICT enables improved communication and knowledge sharing. It ensures effective and fast exchange of information among citizens and government and also within government departments, businesses and employees'. e-Government is also regarded as the efficient use of ICT to enable proficient and transparent government procedures, implementing democracy, making government operations error free and facilitating businesses and citizens in a true sense. This will aid in minimizing corruption from its roots resulting in major savings. Besides implementing ICT devices in government organizations for effective e-Government application, the ICT level of citizens, employees etc. should also be improved as ICT is the prime driving force of e-Government [ii].

2) Principles of e-Government

Following are the basic principles of e-Government which when implemented carefully will help in development of e-Government system leading to progress of country [ii].

- The main focus should always be citizens' and the applications should be developed keeping in mind their needs to facilitate them in a true sense.
- The various applications and facilities introduced by the government is made accessible to everyone so all can benefit from them.

- Social inclusion should be facilitated so that everyone takes a part in adopting and efficiently utilizing e-Government services.
- The information provided should be accurate and up to date and it should be shared responsibly.
- Government resources should be efficiently and effectively utilized to make e-Government a success.

3) Stems of e-Government

There are four basic stems of e-Government which are employing ICT to assist relationship between government and other stakeholders. Many researchers have further divided them into further sub-types. The four basic types are [xvi]:

• *Government-to-Citizen (G2C)*

The primary concern of this branch of e-Government system is to make the files and necessary information available online for citizens' use at government portals [xvii]. A fruitful and understanding relationship is established between government and citizens' (G2C) when the citizens' also interact with the government as a member in democratic process i.e. e-Democracy and e-Voting. This area underwent a lot due to in numerable reasons such as insufficient measures, lack of Internet facility, ICT illiteracy etc. thus creating a hurdle in the success of G2C services.

• *Government-to-Business (G2B)*

The main focus of this stem of e-Government system is to interact with private division to acquire services and goods and to synchronize dealings with private corporations with the help of ICT e.g. e-Procurement. By employing G2B e-Government in the routine procedures for procurement becomes translucent and cost and time efficient [xviii]. The award of contract and provision of licenses for operating business becomes efficient and transparent which gives rise to unbiased competition among local business thus refininga country's business atmosphere [xvi].

• *Government-to-Government (G2G)*

The main focus of this branch of e-Government system is providing services to different tiers of governments by creating a harmonious relationship among all. It has the ability to bring forward stakeholders from all levels of government whether national, local or state/ provincial and is considered as the backbone of Electronic Government [xi]. e-Government implementation also ensures resource sharing among different government departments for a faster, resource efficient and quality decision making process.

• *Government-to-Employees (G2E)*

The research focuses upon this vital stem of e-government so it is explained in detail. In G2E, employees are empowered in a true sense with responsibility to facilitate citizens and business to counter their problems. G2E can be regarded as the primary stem because employees are working at back end to satisfy other stakeholders so the employees should go online before any other stakeholder [xix]. G2E is the least explored and researched branch of e-Government and some researchers also look upon it as an internal part of G2G [xx]. The success of e-Government and its diffusion hugely depends and is influenced by the procedures, readiness, the stakeholders and the employees' present in government organizations so they should be dealt intelligently [xxi].

This area if properly managed can lead to great results concerning the progress of e-Government. When the employees' will be fully equipped with the latest technologies, supported, trained by the government then a trust based relationship will exist with them which will positively affect the whole system through employees' performance. It improves efficacy and usefulness of government procedures [xxii]. G2E is considered as the most crucial stem of e-Government as its efficient working will have a direct impact on all the concerned stakeholders and without its efficient functioning, one cannot expect the successful application of other e-Government branches.

B. Electronic Government in Pakistan

Pakistan being one of the developing countries, is facing many problems in adoption and diffusion of information technologies. This shift towards the information and communication technologies (ICT) was initially focused by Ministry of Science and Technology (MOST) and a new IT and Telecommunication (IT & T) division was formulated under MOST in March 2000. e-Government was considered to be most important part of first National IT Policy and Action Plan which was agreed upon by the Federal Cabinet in 2000 [xxiii]. Originally e-Government implementation was handled by Pakistan Computer Bureau (PCB). In 2002, an independent ministry for Information Technology was formulated by the Government of Pakistan and IT &Telecommunication Division as made portion of Ministry of Information Technology (MOIT).

The primary goal of MOIT is to boost ICT capability of Pakistan in the 21st century. One of the major objectives of MOIT was Transformation to Electronic Government which has revolutionized the government processes all around the world. In October 2002, Electronic Government Directorate (EGD) was formulated by MOIT to specifically focus on successful implementation of Electronic Government [v]. In August, 2014 EGD and PCB have been merged under National Information Technology Board (NITB) as an attached department of MOIT for more efficient and successful implementation E-Government technology. Pakistan Government also signed an agreement with Pakistan Telecommunication

Company Limited (PTCL) in 2013 for ensuring transparent and effective E-Government [xxiv]. Electronic Government in Pakistan is still at a developing stage and despite much effort it has not been able to cope up with the demands of citizens.

C. UN e-Government Readiness Index (EGRI)

The e-Government readiness index shows the development pace of a country with respect tovarious factors which affect the e-Government development. e-Government Readiness Index also shows the ability and inclination of a country to switch to e-Government for ICT led development. The more established countries have given priority to their e-Government program whose success also shows their political, social and economic composition. To make e-Government services a success, minimizing the digital divide should also be focused as merely an access to the World Wide Web (WWW) will not solve the issue of poor acceptability of e-Government services. Table I below, shows the UN Global Ranking and EGRI of Pakistan from year 2002 to 2014:

TABLE I
PROGRESS OF E-GOVERNMENT IN PAKISTAN

Year	EGRI	Global ranking
2002 [ii]	0.104	120
2003 [xxiii]	0.247	137
2004 [xv]	0.3042	122
2005 [xxiv]	0.2836	136
2008 [xxv]	0.3160	131
2010 [xxvi]	0.2755	146
2012 [xxvii]	0.2823	156
2014 [vi]	0.2580	158

It can be seen clearly that there are regular ups and downs in the progress phase of e-Government in Pakistan from 2002 to 2008. Thereafter, EGRI and world ranking of Pakistan has been going down the road. It indicates insufficient support by governments and thus demands considerable amount of attention towards employees' perspective which will in turn influence other stakeholders.

D. Diffusion of Innovation (DOI) Theory

This theory given by Everett M. Rogers in 1963, is one of the initial theories concerning innovation diffusion [iii]. It was modified with time keeping in mind the continuously changing technological advancements [xxx, iv, xxxi]. The main emphasis of the DOI theory is on the attributes of innovation which directly affect its adoption [iv]. The main difference between DOI theory and other models that predict adoption is that DOI focuses on the characteristics of an innovation which can be improved to increase rate of adoption while the main focus of other models is on user's attitude and feeling about an innovation. According to Roger, there are five variables which determine rate of adoption/ diffusion (D) of innovation [iv] comprising Perceived Attributes of Innovation, Types of Innovation Decision, Communication Channels, Extent of Change Agents' Promotion Efforts and Nature of Social System. Rate of Adoption is effectively explained (49 to 87% of Variance) by the Perceived Attributes of Innovation. [xxx]. Hence these Attributes are focused in research.

IV. RESEARCH FRAMEWORK

The main objective of this research is to explore theG2E perspective of e-Government through investigating key attributes which are influencing the diffusion of system in Pakistan. Diffusion of Innovation (DOI) theory proposed by Roger is used as reference model to identify various gaps which need to be addressed in G2E perspective for successful diffusion of e-Government. The corresponding research question that is drawn out is as follows: The theoretical framework explained above is shown in Fig. 1.

"How does attributes of innovation affect the Intention to Adopt/ Diffusion of e-Government (Employee perspective G2E) in Pakistan (ministries / divisions of federal government)?"

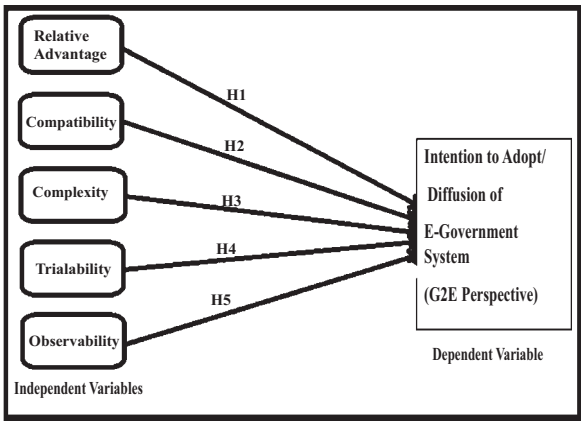

Fig. 1. Theoretical Framework.

A. Operational Definitions and Research Hypotheses

Operational definitions for the various constructs considered in the proposed theoretical framework are as follows:

• *Relative Advantage*

Relative Advantage (RA) is the extent to which the proposed invention is more useful than the concept or an innovation which it replaces. The advantage offered by the new innovation can be of any type e.g. reliability, time sharing, economic benefit, social status etc. The type of relative advantage offered can differ from an innovation to an innovation as it mainly depends upon the nature of an innovation and characteristics of the

adopters under concern. Customers want to know than that what kind of advantage the innovation offers and thus this information can be regarded as the heart of diffusion process. So relative advantage can result in decrease of discomfort and found to have a positive relationship with the rate of diffusion thus following hypotheses are formulated.

Ho1: *"No relationship exists between Relative Advantage and intention to adopt/ diffusion of E-Government system (G2E Perspective)".*

H1: *"Relative Advantage will have a positive direct effect on intention to adopt/ diffusion of E-Government system (G2E Perspective)"*

• *Compatibility*

Compatibility (Compat) can be regarded as the extent to which the proposed invention matches with the existing practices, past principles and requirements of the customers. The high degree of compatibility reduces the unforeseen threats related to an innovation in the minds of the potential adopters as it is perceived to be familiar. The innovation should be well-matched with sociocultural beliefs and values, previous ideas and requirements of the customer. Compatibility may be regarded as a less important construct than relative advantage but its effect is large and it is found to be positively related to the rate of adoption thus following hypotheses are formulated:

Ho2: *"No relationship exists between Compatibility and intention to adopt/ diffusion of E-Government system (G2E Perspective)".*

H2: *"Compatibility will have a positive direct effect on intention to adopt/ diffusion of E-Government system (G2E Perspective)".*

• *Complexity*

Complexity (Complex) is the extent to which the invention is thought to be ambiguous, hard to comprehend and use. Any new innovation can be categorized into two types i.e. either complex or simple. An innovation should be simple enough to the extent that customers shall be able to comprehend its advantage, usefulness and learn how to use it which will in turn yield high rate of adoption. Complexity of an innovation was found to have a negative relationship with the rate of diffusion as it creates difficulty and a major obstacle for innovation usage in the eyes of the adopter whereas a less complex innovation appears to the adopter as more useful thus achieving high rates of adoption. Following hypotheses are formulated to explain this phenomenon:

Ho3: *"No relationship exists between Complexity and intention to adopt/ diffusion of E-Government system (G2E Perspective)".*

H3: *"Complexity will have a negative direct effect on intention to adopt/ diffusion of E-Government system (G2E Perspective)".*

• *Trialability*

Trialability (T) is the extent to which the new innovation should be tested for a limited period of time before its widespread launch. In this way the ideas or innovations are launched step by step or in installments which increases its chance of achieving high rate of adoption. It removes any form of ambiguity in adopters mind and it also gives a meaning to the innovation that how it works under different conditions and environments thus improving rate of adoption. Trialability of an innovation was found to have a positive relationship with the rate of diffusion and is more important for the early adopters. Following hypotheses are formulated to explain this phenomenon:

Ho4: *"No relationship exists between Trialability and intention to adopt/ diffusion of E-Government system (G2E Perspective)".*

H4: *"Trialability will have a positive direct effect on intention to adopt/ diffusion of E-Government system (G2E Perspective)".*

• *Observability*

Observability (O) is the extent to which the positive outcome of an innovation is easily noticeable to everyone. The results or usefulness of some innovations is easily observed by everyone whereas the results of some innovations are not clearly visible, no matter how useful they actually are. If an innovation is useful but its results are hard to observe than it can be regarded as a useless innovation which hinders its rate of adoption. The software base innovations have a slow rate of adoption generally as its usefulness is not clearly observable. Observability of an innovation was found to have a positive relationship with rate of diffusion of an innovation and thus following hypotheses were formulated.

Ho5: *"No relationship exists between Observability and intention to adopt/ diffusion of E-Government system (G2E Perspective)".*

H5: *"Observability will have a positive direct effect on intention to adopt/ diffusion of E-Government system (G2E Perspective)".*

B. Research Design

- Research setting for this research is non-contrived as interference from the researcher is minimal and natural setting is used.
- The data has been collected at a single point of time making the study cross-sectional [xxxii] making it convenient to identify and analyze the relationships between the various determinants involved [xxxiii].
- The population to be considered for this research study was Government Employees of Pakistan. But due to budget and time constraints, sampling frame has been restricted to employees' of ministries and departments under Federal Government of Pakistan.
- Probabilistic sampling (simple random) linked with survey based strategies has been used to make deductions from the sample related to the population and conclude the research. A

confidence level of 95% with 5% error margin, the minimum size of sample should be 384 to achieve reliable results [xxxiii]. In order to achieve true results, the questionnaires were distributed among 633 employees of Federal Government of Pakistan. Around 517 questionnaires were filled and received back, from which 28 were ineligible. Therefore an overall response rate of 81.67 % was achieved.

- Survey strategy has been adopted to carry out this research. Research Choice is quantitative as various statistical analyses have been performed on numerical data to extract useful results [xxxiv]. Moreover, quantitative research comprises of specifying precisely both dependent and independent variables under study, making the interpretations and results more reliable [xxxv].
- The questionnaire used to collect primary data comprises of two main parts, with the opening section comprising six (6) questions related to the demographic details and the second part containing twenty four (24) questions measuring employee's adoption/ diffusion level of e-government system on five point Likert Scale. The questionnaire for Relative Advantage and Compatibility has been adopted from [xxxvi], Complexity from [xxxvii], Observability and Trialability from [xxxviii] and intention to adopt/ diffusion of e-Government system (G2E Perspective) from [xxxix].
- The questionnaire was verified by a number of subject and language experts to validate language and comprehensiveness of questionnaire and then it was followed by a pilot study though reliability was ensured by calculating Cronbach alpha shown below in Table II.

TABLE II
CRONBACH ALPHA FOR PILOT TESTING

Constructs	Cronbach's Alpha	No. of items
Relative Advantage	0.813	5
Compatibility	0.701	3
Complexity	0.798	4
Observability	0.737	4
Trialability	0.781	5
Diffusion	0.827	3

The items were found reliable and consistent as the results of the pilot tests were acceptable for further continuing the research. Therefore the questionnaire was further distributed for responses.

V. DATA ANALYSIS

In order to extract some useful inferences, data analysis is necessary which is now much easier to perform with the help of latest software such as Statistical Package for the Social Sciences (SPSS).

A. Descriptive Analysis

The table III refers to the results of descriptive analysis showing minimum, maximum values and the mean values of the dispersion in the data measured by standard deviation and the value of skewness to check whether the data is skewed within the range +1 to -1 to be considered as normal distribution. The values of kurtosis have also been mentioned, which depicts the peakedness of the curves, of the series of values used in the study.

TABLE III
DESCRIPTIVE STATISTICS

	Min	Max	Mean	Std Dev.	Skew ness	Kurt osis
RA	1	4	1.75	.457	.474	3.07
Compat	1	4	1.88	.495	.548	1.68
Complex	1	5	3.10	.982	.025	-.98
O	1	4	2.21	.598	.191	.21
T	1	4	2.14	.550	.689	1.59
D	1	4	1.88	.463	.314	2.06

Fig. 2 below shows the normal Q-Q plots for the collected data against each construct of the model. It's very obvious from these plots that quantile values of the observations are mostly lying close astride the strait line with few outlier observations. Hence the sample data set for all the constructs is pretty normal to carry out the analysis through performing parametric statistical tests.

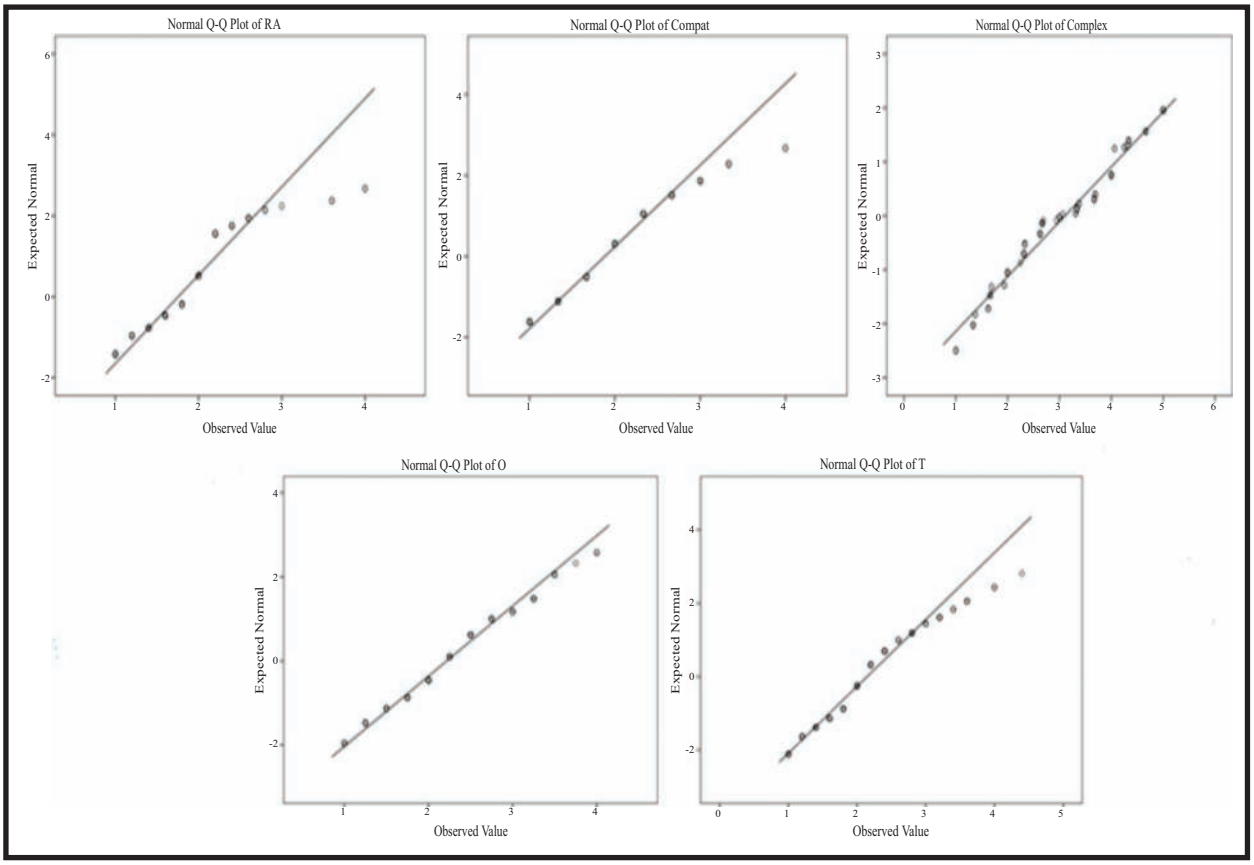

Fig. 2. Descriptive Statistics-Normality Tests Through (Q-Q Plots).

B. Inferential Analysis

Inferential data analysis using various statistical techniques to test the hypothesis mainly comprises two parts. The first part encompasses the assessment of association among the variable whether the relationship exists or not. The second part is more deliberate over the predictability of the dependent variable by the independent variables.

• *Correlation Analysis*

Statistical Correlation is the measure of association among different constructs, identifying whether the relationship is weak or strong and positive or negative. At this point in the research the null hypothesis will be accepted or rejected based upon the r values and sig levels

Table IV below illustrates the relationship between the variables. All the independent variables are showing moderate strength of positive relationships with the criterion variable i.e. BI and also showing moderate positive association amongst each other with $0.7 > r > 0.3$ and $sig < 0.05$ resulting in rejection of null hypotheses.

TABLE IV
CORRELATION ANALYSIS – DOI CONSTRUCTS

		RA	Compat	Complex	O	T	D
RA	Pearson Correlation						
	Sig. (2-tailed)						
Compat	Pearson Correlation	.554**					
	Sig. (2-tailed)	.000					
Complex	Pearson Correlation	-.226**	-.085				
	Sig. (2-tailed)	.000	.090				
O	Pearson Correlation	.160**	.148**	.282**			
	Sig. (2-tailed)	.001	.003	.000			
T	Pearson Correlation	.229**	.225**	.210**	.631**		
	Sig. (2-tailed)	.000	.000	.000	.000		
D	Pearson Correlation	**.608****	**.573****	**-.425***	**.384****	**.524****	
	Sig. (2-tailed)	.000	.000	.012	.000	.000	

• *Regression Analysis*

Table-V, the model summary of regression model shows value of R, known as multiple correlation coefficient, defined as the correlation among predicted and observed values of dependent variable,. The value of R > 0.7 indicates a strong positive association of the predictors with the criterion variable. Moreover the value of R Square which is coefficient of determination indicates that 60% of the variance in Behavioral Intention measured outcome can be accounted for by the model used for this research. The adjusted R Square narrates the predictive loss in R square value if the same model is applied to other similar samples.

TABLE V
MODEL SUMMARY OF REGRESSION MODEL

Model Summary				
Model	R	R Square	Adjusted R Square	Std. Error of Estimate
1	.777[a]	.604	.598	.29410
a. Predictors: (Constant), RA, O, Complex, Compat, T				

In the ANOVA Table VI below, the null hypothesis is that the model has no explanatory power and only if the sig < 0.05 of the F value then it lets rejection of the null hypothesis and allows to proceed further with regression analysis. Table-VI shows that F = 99.500 with sig = 0.000 which means that the model has sufficient explanatory power with regards to variance in Intention to adopt/ diffusion of e-government system (G2E Perspective) explained and accounted for by the predictors, hence the model is fit to proceed further with the results of regression analysis and conclude the hypothesis testing process.

TABLE VI
ANALYSIS OF VARIANCE

ANOVA[a]						
Model		Sum of Squares		Mean Square	F	Sig.
1	Regression	51.636		8.606	99.5	.000[b]
	Residual	33.905		0.086		
	Total	85.541				
a. Dependent Variable: D						
b. Predictors: (Constant), RA, O, Complex, Compat, T						

In Table VII T-value with its sig level is important which validates the predictability of dependent variable by the independent variable only if sig < 0.05.The overall tests and analysis performed predicted that, an instrumental relationship exists among independent and the dependent variables except for observability because the results of e-government during its launching and deployment phase are not much visible to the stakeholders: in this case employees working with conventional system, no matter how useful they actually are. If an innovation is useful but its results are hard to observe than it can be regarded as a useless innovation which hinders its rate of adoption. The software base innovations have a slow rate of adoption generally as its usefulness is not clearly observable.

TABLE VII
COEFFICIENTS FOR REGRESSION ANALYSIS

Coefficients[a]						
Model		Unstandardized Coefficients		Standardized Coefficients	T	Sig.
		B	Std Err	Beta		
1	Constant	.157	.098		1.603	.110
	RA	.334	.040	.330	8.268	.000
	Compat	.249	.037	.266	6.749	.000
	Complex	-.063	.017	-.134	-3.643	.000
	O	-.043	.033	-.056	-1.332	.184
	T	.357	.036	.424	9.956	.000
a. Dependent Variable: D						

• *Summary of Inferential Analysis*

The results obtained for the concerned hypotheses are listed below in Table VIII.

TABLE VIII
SUMMARY OF INFERENTIAL ANALYSIS

Hypotheses	Results
Ho1	Not Supported
H1	Supported
Ho2	Not Supported
H2	Supported
Ho3	Not Supported
H3	Supported
Ho4	Not Supported
H4	Supported
Ho5	Not Supported
H5	Not Supported

VI. RESULTS AND DISCUSSION

To investigate the employees' intentions to embrace e-Government technology, this study was conducted using the Diffusion of Innovation model from which Perceived Attributes of Innovation were considered and this model was validated considering the scenario of e-Government (G2E perspective) in Pakistan. According to the results achieved, all the constructs influence Intention to Adopt/ Diffusion of e-Government system (G2E perspective) but when the combined effect was noticed Relative Advantage, Compatibilty and Trialability were positively related to Intention to Adopt/ Diffusion of e-Government technology. Complexity was seen to have a negative relationship with Intention to Adopt/ Diffusion of e-Government technology (G2E perspective) while Observability were seen to have no profound association with Intention to Adopt/ Diffusion of e-Government technology. The outcome obtained from this study revealed several important findings for the fruitful acceptance and employment of e-Government technology among Government employees of Pakistan.

If the technology is perceived to be useful by the government employees, then they will be more inclined to use/ adopt e-Government system. Thus government employees are ready to accept and adopt e-Government system because they believe that it offers a valuable advantage and usefulness in their work as it increases their efficiency. It was confirmed that if the technology is perceived to be complex by the government employees, then their willingness to use/ adopt e-Government technology will decrease. It shows that government employees are ready to accept and adopt e-Government system if it is easy to use and understand, in other words if it offers less complexity. Government should make the technology less complex for its efficient adoption. It was also seen that if the technology is well recognized by the employees' and its importance is already known to them so observability plays no major role in polishing their intention to adopt/ diffusion of e-Government systems. Trialability and Compatibility are considered to be very important constructs in DOI model and strong determinants for any technology. Trialability and compatibility are significant determining factors of Intention to Adopt/ Diffusion of e-Government in Pakistan's context, as the employees do realize its importance and it is compatible to their beliefs and trial usage also enhances their desire to use e-Government systems.

VII. CONCLUSION

This study was conducted to analyze Intention to Adopt/ Diffusion of e-Government system among government employees, through investigating the influence from Attributes of innovation basedupon DOI theory and the previous literature. According to the results obtained, **60%** of variance in Intention to Adopt/ Diffusion of e-Government system is explained/ influenced by the Perceived Attributes of Innovation investigated in this research. According to Roger (1983), Perceived Attributes of Innovation may explain 49-87% of variance in intention to adopt/ diffusion, hence considering the scenario of e-Government (G2E perspective) in Pakistan the theoretical framework stands validated with results falling within the prescribed range. Accordingly, Relative Advantage, Trialability, and Compatibility) were found to be positively associated with the Intention to Adopt/ Diffusion of e-Government system. Observability was not found to be an important determinant which means whether the e- government system advantages are visible to the employees' or not does not hold much importance as compared to other determinants and Complexity shows a negative relationship for Intention to Adopt/ Diffusion of e-Government system.

VIII. Recommendations and Future Work

Based on the statistical inferences and hypothesis testing carried out, promotion indiffusion of e-Government system among government employees of Pakistan is possible through extensive trainings on e-Government systems to acquaint the employees of its working. As e-Government is not yet fully implemented and is still in its initial phases, so to increase the awareness and acceptance, different seminars and workshops may be conducted for motivating users' to integrate the new trends in working lifestyle. The future researchers can include various government departments, citizens and businesses in order to diversify the research sample. The perception of employees will certainly change and alter with passage of time especially in case an awareness campaign is launched for the employment of e-Government system. Therefore the future research can be done as a longitudinal study in which researchers can identify all the changes and improvements in the perspective of employees after successful implementation of e-Government. Different moderating variables e.g. ICT knowledge, government policies etc. can be considered in future research. Future research work can employ other technology acceptance/ diffusion models to investigate the determinants affecting the efficient organization of e-Government systems in Pakistan.

References

[I] International Telecommunication Union, "Roadmap for E-Government in the Developing World", Pacific Council on the International Policy, 2002.

[ii] UN Report,"Benchmarking E-Government: A Global Perspective...Assessing the UN Member States", United States Division for Public Economics and Public Administration, American Society for Public Administration, 2002.

[iii] E. M. Rogers,"Diffusion of Innovations (2nd ed.)",New York: The Free Press, 1963.

[iv] E. M. Rogers, "Diffusion of Innovations (4th ed.)",New York: The Free Press, 1995.

[v] Higher Education Commission. (2004). E-Government: A Detailed Perspective.

[vi] UN Report, "United Nations E-Government Survey 2014...E-Government for the future we want", Department of Economics and Social Affairs, 2014.

[vii] Y. Kitaw, "African e-Governance – Opportunities and Challenges", Lausanne: Swiss Federal Institute of Technology, 2006.

[viii] D. Sarantis, Y. Charalabidis,&D. Askounis, "A goal-driven management framework for electronic government transformation projects implementation",*GovernmentInformation Quarterly*, pp 117-128, 2011.

[ix] I. Holliday, "Building E-Government in East and Southern Asia: Regional Rhetoric and National (In) Action",Public Administration and Development, pp 323-335, 2002.

[x] A. T. K. Ho, "Reinventing Local Governments and the E-government Initiatives",Public Administration Review,Vol 62,No 4, pp. 434-444, 2008.

[xi] N. Nkwe, "E-Government: Challenges and Opportunities in Botswana", International Journal of Humanities and Social Science, Vol. 2 No. 17, 2012.

[xii] R. Heeks, "E-Governmentin Africa: Promise and Practice",Information Policy, pp 97-114, 2002.

[xiii] W. Wong,&E. Welch, "Does e-Government Promote Accountability?", An International Journal of Policy, Administration, and Institutions, pp 275–297, 2004.

[xiv] K. Kraemer, & J. L. King, "Information Technology and Administrative Reforms; Will e-Government be Different?", In D. Norris, e-Government Research. Policy and Management, pp 12-31. Hershey. New York, 2008.

[xv] UN Report, "UN Global E-Government Readiness Report 2004...Towards Access for Opportunity", Department of Economic and Social Affairs, Division for Public Administration and Development Management, 2004.

[xvi] International Telecommunication Union,"Electronic Government for Developing Countries", 2008.Available [online] at: www.itu.int

[xvii] Z. Ebrahim, & Z. Irani, "E-Government adoption: architecture and barriers" ,Business Process Management Journal, 11(5), pp 589-611, 2005.

[xviii] M. J. Moon, "The Evolution of E-Government among Municipalities: Rhetoric or Reality?",Public Administration Review, *62*(4), pp 424-433, 2002.

[xix] V. R. Rao, "Collaborative Government to Employee (G2E): Issues and challenges to E-Government",Journal of E-Governance, Vol. 34, Issue 4, pp 214-229, 2011.

[xx] B. T. Riley, "Electronic Governance and Electronic Democracy: Living and Working in The Connected World", Commonwealth Centre For Electronic Governance, Brisbane, Australia, Vol. 2, 2001.

[xxi] M. Ahn, & S. Bretschneider, "Politics of E-Government: E-Government and the Political Control of Bureaucracy", Public Administration

Review, pp 414-424, 2011.

[xxii] S. AlAwadhi, &Z. Morris, "Factors Influencing the Adoption of E-Government Services", Journal of Software, Vol. 4, No. 6, 2009.

[xxiii] Electronic Government Directorate, "E-Government strategy and 5-Year plan for the Federal Government",Ministry of Information Technology, Government of Pakistan, 2005.

[xxiv] More Magazine,"Government signs agreement with PTCL for E-governance in Pakistan", 2013.

[xxv] UN Report,"UN Global E-Government Survey 2003",UN Department of Economic and Social Affairs, Civil Resource Group, 2003.

[xxvi] UN Report, "United Nations Global E-Government Readiness Report 2005...From E-Government to E-Inclusion", Department of Economic and Social Affairs, Division for Public Administration and Development Management, 2005.

[xxvii]UN Report,"UN E-Government Survey 2008...From E-Government to Connected Governance",Economic and Social Affairs, 2008.

[xxviii]UN Report,"United Nations E-Government Survey 2010...Leveraging e-Government at a time of financial and economic crisis", Economic and Social Affairs, 2010.

[xxix] UN Report, "United Nations E-Government Survey 2012...E-Government for the People", New York, 2012.

[xxx] E. M. Rogers, "Diffusion of Innovations (3rd ed.)", New York: The Free Press, 1983.

[xxxi] E. M. Rogers, "Diffusion of Innovations (5th ed.)", New York: The Free Press; A Division of Macmillan Publishing Co., Inc, 2003.

[xxxii]W. G. Zikmund, "Business Research Methods(7th ed.)", Ohio: Thompson South-Western, 2003.

[xxxiii]M. Saunders, P. Lewis, & A. Thornhill, "Research methods for business students", *5th ed*. Harlow, Pearson Education, 2009.

[xxxiv]M. J. Smith,"Contemporary communication research methods", National Forensic Journal, 2, pp 112-121, 1988.

[xxxv]H. R. Bernard, "Social research method: Qualitative and quantitative approaches", California: Sage Publication, Inc, 2000.

[xxxvi]G. C. Moore, &I. Benbasat, "Development of an Instrument to Measure the Perceptions of Adopting an Information Technology Innovation," Information Systems Research (2:3), pp. 192-222, 1991.

[xxxvii]Thompson, L. Ronald, Higgins, A. Christopher, Howell, &M. Jane,"Personal Computing: Toward a Conceptual Model of Utilization",MIS Quarterly, pp 124-143, 1991.

[xxxviii]T. J. Ntemana, &W. Olatokun, "Analyzing the influence of Diffusion of Innovation Attributes on Lecturers' Attitudes toward Information and Communication technologies", An Interdisciplinary Journal on Humans in ICT environment 8(2), 2012.

[xxxix]N. M. Suki, &T. Ramayah,"User Acceptance of the E-Government services in Malaysia: Structural Equation Modelling Approach" Interdisciplinary Journal of Information, Knowledge and Management, Vol. 5, 2010.

Section D

COMPUTER, SOFTWARE, TELECOMMUNICATION, COMPUTER SCIENCE

Measuring Students' Learning and Task Performance Using Semantic Multi-Modal Aids in Virtual Assembly Environments

Sehat Ullah
Department of Computer Science & IT, University of Malakand, Dir (L), Pakistan
sehatullah@hotmail.com

***Abstract*-**Learning and performance improvement during procedural task realization in Virtual Reality (VR) environments can be enhanced using different types of cognitive aids. Previous work in literature stressed on task learning (with performance drop) or vice versa. In this paper we propose the concept of semantic aids to be systematically used in virtual environments to increase user performance as well as learning, A Guided Virtual Reality Training System (GVRTS) is used for the assembly of three phase step-down transformer in the experimental study. Group1 (20 students) used direct cognitive aids (change in color of object candidate for selection, blinking arrow showing final position, a color line bar under the object pointing to its accurate placement). Group2 (20 students) are trained with GVRTS where direct cognitive aids plus visual semantic aids are provided, group3 use direct plus audio semantic aids, and group4 (20 students) use direct aids plus audio and visual semantic aids. A comparison based on task performance, resulted in less performance drop in case of group2, group3 and group4 as compared to group1. Experimental results also revealed that semantic aids considerably improved learning and knowledge transfer to the real world.

***Index Terms*—**virtual Reality, Virtual Environment, Semantic Aids, Multi-modality, Interaction Based Learning

I. Introduction

HUMAN use various sensory channels to acquire knowledge and perform different tasks on its basis during their lifetime for existence. They are always in search of how to know and interact with their environment/surrounding. Learning can be divided into two categories i.e. Task learning and Task related theory learning:

· Task learning

Task learning is related to the practical performance of a task e.g. to assemble a three phase step-down transformer, initially the user needs to identify which part to be chosen, how to pick a part, how to transfer it from source to destination, how and where to place it. The most important is the order of steps to be carried out.

- Task related theory learning

This kind of learning is related to the theoretical aspects of the task. For example to carry out the assembly of a three phase step-down transformer, the knowledge about the name, type, function of various parts of the transformer and their relationship with each other.

Regular guiding instructions of a skilled trainer are necessary in performing the task precisely and timely. This sort of training which is supervised by a trainer is always desirable for learning of cognitive and motor skills . Acquiring knowledge through real world approaches is difficult because of high cost, non-availability of devices and limited space . In addition the availability of expert trainers, time limitation and danger to human health also minimize the usefulness of real world training approaches [i]. To overcome these challenges, Virtual Environments (VEs) can be of vital importance in training and learning activities .

Virtual environments are computer generated worlds that mimic the real world situations and permit user to interact with virtual entities in real time. For training users in different areas such as medical, military and education, these environments can be efficiently used. VEs become more valuable when augmented with cognitive guidance specially multi-modal guidance which is provided to users during task realization [i-ii] . Cognitive load theories [iii-viii] and multimedia representation principles [ix] also support the same perceptions. Various types of instruction/guidance aids such as audio, visual, haptic, or simple instruction manuals may be used for this purpose. The audio aids might be the oral directions of the trainer, manual may be in the form of an instruction guide, visual aids may include a blinking arrow over the object or change in color. Similarly haptic aids may be the attractive force towards the target object. On the basis of provided information, these aids may be divided into two types: direct and indirect aids .

Indirect aids: These are implicit type of information/aids such as instruction book, manual, charts, maps, verbal/gestural instructions of a trainer, provided to assist trainees in performing a task. It does not provide any direct clue for the trainee in the training environment. In indirect aids during performance of the

task, the trainee needs mental translation of the available information which results in increased mental burden [ii]. For guiding trainees in an assembly task [i]. used instruction book.

Direct aids: These are explicit type of information/aids such as color, arrow, haptic force etc. provided by a system to assist trainee in performing a task. The use of direct aids during the task operation produces little or no mental overhead on the trainee due to straight forward nature of the guidance cues. Direct aids offer simple and valuable information in a simple style to accomplish the task. Three different types of navigational guidance aids (arrows, compass, and lighting source) were used by [x] to help users in finding the target objects in a virtual environment. Navigational guidance aids (arrow and tracer) were provided by [xi] to assist users in the exploration of a VE. [ii] argued that direct aids allow little exploration as well as it reduces transfer of knowledge in to real environment due to dependency on the training environment.

This paper investigates the hypothesis that if semantic aids are added with direct aids, it will lead to enhanced learning/exploration and higher student's performance in the virtual training environment along with improved knowledge transfer into real world environment.

The hypothesis is experimentally tested using a three dimensional (3D) guided virtual reality training system (GVRTS). GVRTS is a desktop based virtual assembly environment. The students perform the assembly task using experimental conditions i.e. direct aids and different semantic aids. Following are the objectives of the work:

- To examine the effect of using semantic aids with direct aids on students' learning.
- To investigate the effect of audio, visual and their combination with semantic aids on task performance.
- To investigate the effect of semantic aids on knowledge transfer to the real world environment.
- To investigate the effect of GVRTS on the acquisition of technical skills.
- To investigate the application of technical skills gained through GVRTS in real world environment.

In section 2 related work is presented, section 3 explains GVRTS, section 4 presents guidance, section 5 is related to experiments and evaluation and section 6 presents result analysis. Conclusion and future work is finally described in section 7.

II. Related Work

In 1980, VR started to be used in training and education.

Different VR based education projects such as Global Change, Science Space, Virtual Gorilla Exhibit, Cell Biology, Atom world, and many other being introduced in 90's . Now VR is the most attractive research area in teaching and training.

Various virtual learning environments (VLEs) have been developed in different areas such as for routing and designing of cable [xiv], power system operation [xv], mathematics [xvi-xvii], physics [xviii-xix], Radioactivity [xxi], assembly planning and training [xxvi], medical education [xxvi] and biological education [xxvii-xxviii] etc.

In educational virtual environments different researchers proposed various types of guidance techniques in literature. For guiding users in a virtual environment, [x] used three different kinds of guidance aids (lighting source, compass, and guiding arrows). They found that compass and arrows are better than lighting source [xi] compared a VLE based on navigational guidance aids (arrows and tracer) with a non-guided VLE. The results showed that VE supplemented by guidance aids (arrows and tracer) produced improved learning as compared to non-guided VE. [xxix] used an Augmented Reality (AR) image based instruction system for the assembly operations of a Fun Train on a desktop computer. Here the guidance aids were in the form of texts, labels and arrows. Assembly operations in the form of video clips were also used for guidance.

For guiding users in a path navigation task, Kuang et al. used virtual fixtures as guidance cues. They performed the task using virtual fixtures with haptic and without haptic guidance. Here virtual fixtures plus haptic guidance aids showed good results as compared to the graphics only fixtures used for path representation. In path navigational tasks virtual fixtures offers substantially good performance results on the basis of speed, accuracy, or both . Rosenberg developed a 3D teleoperation environment for peg-in-hole task in which he used haptic and aural virtual fixtures. The use of virtual fixtures improved performance by 70% as compared to no virtual fixtures in the experimental study. For guidance of surgeon's tools in tele operated coronary bypass, [xxxv] used a virtual wall on mammary vein in tomography image. The use of virtual wall removed the tours outside the preferred areas and reduced the completion time about 27%. In a collaborative virtual environment [xxxvi] examined user performance, co-presence and cooperation using haptic guides. They found better results in using haptic guides in terms of performance, awareness, and co-presence. [ii] compared verbal guiding instructions with verbal guiding instructions plus pointing of the target position on a screen using a mouse. The environment was a 3D virtual puzzle game. The use of guidance based on mouse pointing reduced cognitive load [xli] on learner but at the same time reduced performance significantly.

A 3D haptic VE is presented by Rodriguez et al. that was used for the assembly of a Lego helicopter. The assembly consisted of 75 sequential steps. Two types of guidance aids were used in the VE. In the first case indirect aids were provided using an instruction book which consisted of 75 images of all steps. In the second case direct aids were provided via changing the required object color and a copy of the object over the final position in a controlled fashion. Then the assembly was performed in real world. Experimental comparison showed that the controlled use of direct aids doesn't degrade knowledge transfer from virtual to real environment.

Gavish et al. developed IMA-VR system. The system used haptic and visual aids as guidance cues. In haptic aids attraction force towards the target point/object were used. Visual aids were provided using highlighting object, displaying copy of object at destination point, and color change of object. The next step to be taken was represented using the appearance of a blinking circle at that point. According to them it is essential to give more information to learner to produce good metal model of the task, but there is little exploration in direct aids along with dependency on the training system which reduces transfer of knowledge into real world . For building a mental model of the task which results in independent performance of the task, high exploration is very essential . It is also needed for problem solving and error dealing in 3D environments.

We will use semantic guidance to improve learning while availing the high performance of direct aids and to ensure maximum knowledge transfer to real environment. We will use GVRTS, a 3D VE for experimental purposes. ARToolKit markers [xl] (as shown in Figure 1) will be used for interaction with the system.

Fig. 1 . Example of ARToolKit markers'

III. Guided Virtual Reality Training System

GVRTS is a 3D desktop based VE for assembly. Its purpose is to train students in the assembly task of a three phase step-down transformer.

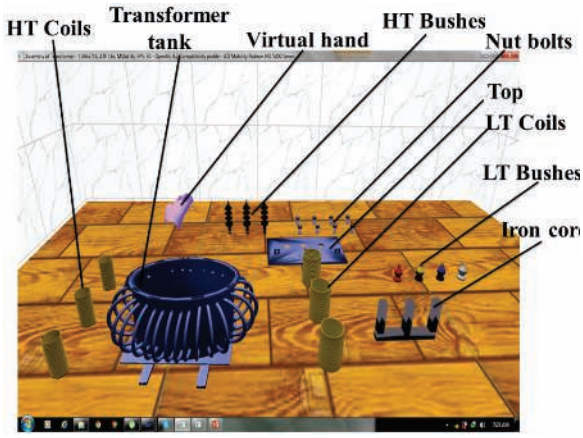

Fig. 1: GVRTS and its main components

The structure of GVRTS is shown in Fig. 2. The 3D environment along with all transformer parts are designed using 3DS Max to achieve good quality with increased realism. All the models are placed after loading in the virtual environment. The system allows user to navigate, select, and manipulate the parts in a realistic fashion.

ARToolKit markers (printed patterns) are used for interaction (with six degree of freedom) with the system. The complete system model is shown in Figure 3. The complete working mechanism of GVRTS is

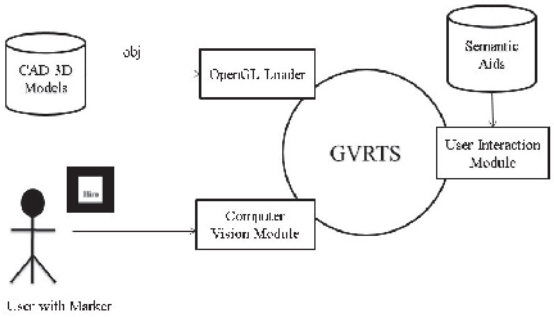

Fig. 3 . Illustration of the main modules of GVRTS

Three Dimensional Models

All the components of the three phase step-down transformer and the entire environment are designed (with high quality) in 3D Studio Max 2009. These models along with\ texture, colour, and material information are then converted to .obj file format and finally exported to OpenGL Loader software.

OpenGl Loader

This module is responsible for conversion of .obj file in to VE along with placement of objects at specific locations.

Computer Vision Module (CVM)

Interaction with GVRTS is based on computer vision system to make the system more realistic and simple

along with reduction in cost and complication. It will also ensure easy implementation of the system at various organizations. CVM has three main modules i.e. ARToolKit Markers, ARToolKit Library, and a camera. The ARToolKit Markers pare black and white patterns. A normal video camera is used to capture an input video stream, which is further analysed by an algorithm and compared with patterns of ARToolKit Library. If the pattern is matched its position and orientation is measured by the ARToolKit and sent to the VE.

User Interaction Module (UIM)

The most important prerequisite of any VE is the realistic and simple interaction. UIM controls various operations of the VE including navigation, selection, manipulation, inter-object collision detection, collision detection between object and the virtual hand and other

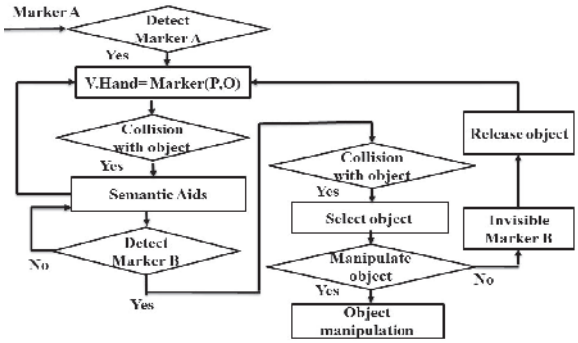

Fig. 4. Flow diagram for navigation, object selection and manipulation using markers

The system allows free 3D navigation in the VE. The user (represented by the virtual hand) can move (navigate) freely in all directions (x, y, and z) in the VR environment. The virtual hand is mapped with the marker Fig. 4, whenever user moves the marker using his hand in the real environment, the virtual hand follows its motion in the VE dynamically in real time. The camera also moves along with the virtual hand in the VE.

Many selection and manipulation tasks are performed in the VE. In this process first the object selection is performed by the virtual hand and then various manipulation operation are performed. The manipulation may be the change of behavior of an object (color change of object, and change in position etc.). Interaction (identification, selection, navigation, and manipulation etc.) in VE is made using ARToolKit markers. Free navigation and object identification is carried out using free movement and visibility of a single marker in front of camera Fig. 5(a). For the selection of an object the collision of the virtual hand with object and the visibility of second marker is required Fig. 5(b). Making the second marker invisible to the camera, simply release that object. The user can dynamically perform these operations (navigation, selection, manipulation (rotation, movement), and release) on different objects in the VEs.

Guidance in GVRTS

For assistance of students in the assembly task, GVRTS guidance system provides two types of cognitive aids. These aids are direct aids and semantic

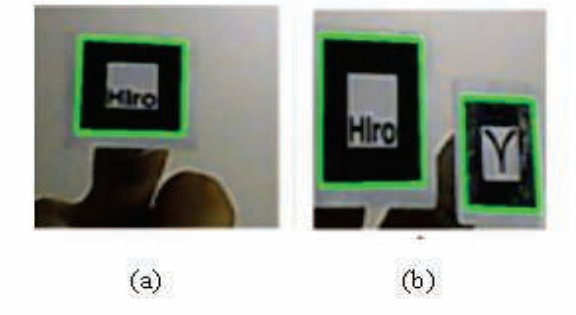

Fig. 5. Interaction via ARToolKit markers (a) Single marker (b) Two markers both visible

1) Direct Aids

The explicit information/aids such as color change, arrow above an object, haptic force towards target/object, lighting or shadow above a position etc., provided by the system to assist trainee in performing the task. Direct aids provide direct and straightforward clues for the trainee which results in error free task operations. They are easy to use and follow/interpret instructions during task operation . GVRTS system offers directs aids in the following forms:

- Object color change
- Guiding arrow using color change or blinking
- Guiding arrow using movement (up-down)
- Appearance of line bar (color) below the selected object

As the user (virtual hand) navigates inside the VE, the system changes the color of the object to be selected. In this way the system leads the user to select only the specified object in the assembly task. As the user selects (picks) an object, the system displays a blinking arrow just above the specified target location. The arrow moves up-down while frequently changes color to red and yellow which guides the user towards the final position of the selected object Fig. 6. To help the user to place the selected object at precise position, a vertical color line bar below that object is used Fig. 6.

1) Semantic Aids

Direct aids help trainee to perform an action easily and accurately, but there is no exploration i.e. they give no information/knowledge related to objects (object name, type, and function) or task (sequence of steps involved in assembly task, relationship between parts etc.). Semantic aids are short meaningful (information

rich) cognitive aids offered by the system to the user. These aids are used to improve students learning (exploration) related to objects and assembly task in the VE. These aids are provided in the following two forms i.e. visual semantic aids and verbal/audio semantic

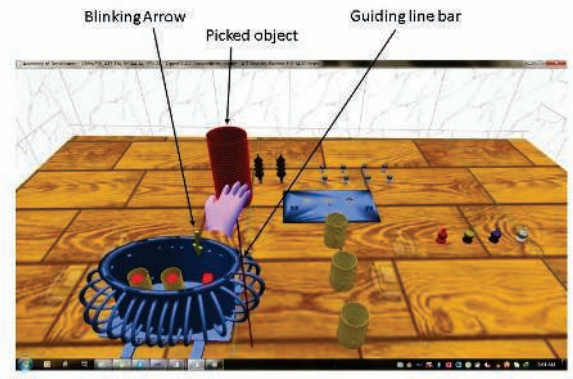

Fig. 6. Transformer assembly realization through various direct aids

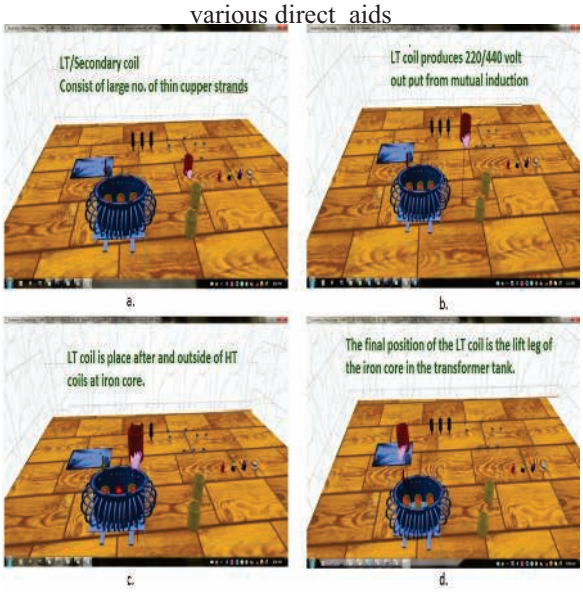

Fig. 7. Provision of semantic aids for selected object (a) name plus structure (b) Function (c) Sequence of placement (d) Target (destination) position.

a. Visual semantic aids

The system provides semantic aids visually (textually). These aids (information) are provided to user step by step to enhance their learning gradually during the assembly task. As the user picks the object, the system provides semantic aids related to object's name and structure Fig.7a, which improve students learning related to parts identification.

In the next step, the system provides information concerning the object's function Fig. 7b. These information are used to increase students' learning regarding working and function of transformer objects. After that semantic aids concerning the relationship between objects in the assembly task are delivered by the system Fig. 7c. These aids increase students' learning related to different steps in the assembly task as shown in Fig. 7c. Finally information related to object's target location are delivered to students. This will improve the knowledge concerning objects' final position in the assembly Fig. 7d.

b. Verbal semantic aids

In this type of semantic aids, the system provides information (semantic aids) related to each step (as discussed in the previous subsection) to users verbally or in audio form.

IV. Experiments And Evaluation

We performed experimental (objective and subjective) evaluation to examine the effect of semantic multi-modal and direct aids in GVRTS on students learning, task performance and knowledge transfer to real

Fig. 8. A user performing the assembly task experiment on GVRTS.

Protocol and task

To evaluate the GVRTS we used 80 participant in the experimental setup. We selected male students from different polytechnic institutions. They were students of 3rd year and they had ages from 19 to 22 years. The subject of three phase step-down transformer was contained within their course. Four groups (i.e. G1, G2, G3, and G4) were made. Each group contained 20 students. Students of G1 used GVRTS with direct aids Fig. 6. G2 used the system (GVRTS) with direct plus visual semantic aids as shown in Fig. 7a-d. Direct plus audio semantic aid are used with GVRTS for G3 while that of G4 used direct aids with combined audio visual semantic aids. All the students were briefly demonstrated about the usage of the system. They were also educated about how to perform different operations in the VE i.e. how to navigate, select, and

manipulate different objects in the GVRTS. After that each participant performed the assembly task of transformer in the GVRTS using their specified aids Fig. 8. After performing the task each student filled a questionnaire. After completion all the questionnaires were collected for analyses.

In the second phase all the students (G1, G2, G3, and G4) had to perform the assembly operation of a real world transformer in a workshop.

V. Result Analysis

This section presents objective (task execution time) and subjective (questionnaire) analysis of all the four groups (G1, G2, G3, and G4). After that, analysis of transfer of knowledge in real environment is carried out.

Objective analysis (Task execution time)

In the objective analysis, the execution time of G1 is 802.2 seconds (STD=9.95), whereas that of G2 is 826.9 seconds (STD=12.03), for G3 it is 815.9 seconds (STD=10.82), and for G4 is 815.4 seconds (STD=9.25), as shown in figure Fig. 9. The direct aids which were used by G1 achieved good performance (short task execution time) among all groups. As direct aids involve little cognitive processing so students completed the task in less time. The task execution time of G2 was greater than G3 and G4. The reason for the high task completion time is the loss of control in performing the task as the users were looking and reading the textual information during task operation. While completion time for G3 and G4 is approximately the same. So it means that providing semantic aids in audio and visual plus audio form gives the same good performance results as compared to visual aids only.

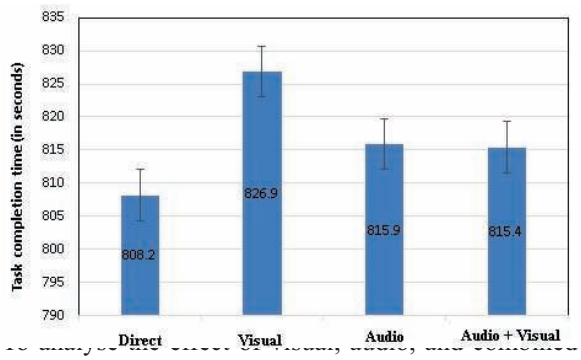

To analyse the effect of visual, audio, and combined audio/visual semantic aids in addition to direct guidance aids on students' learning, we used a questionnaire. The questionnaire included three questions. A scale of 1 to 5 was used to answer these questions. Where 1= low and 5 = very high level. The analysis of these answers is given below.

1) Learning in GVRTS

On the basis of the following perspective, evaluation of the students' learning in GVRTS is carried out in real environment.

- Parts identification
- Steps in assembly task
- Function of transformer parts

Following were the questions:

Q1. Up to what extent did you learn about the name of each part of transformer?

Q2. Up to what extent did you learn about the functions of various parts?

Q3. Up to what extent did you learn about the steps involved in the assembly?

To achieve best quality along with realistic view, 3D Studio Max 2009 was used for the development of all parts of the step-down transformer. The question concerned with parts identification, 58% students of G1 voted for the very low level of learning choice, 22% for high, and 20% for higher levels Fig. 10. 40% of G2 students selected high and higher level options, 40% of G3 students opted for the high level and 60% selected the highest level, whereas 30% opted for high level and 70% for highest level in G4. From the above results, we can conclude that groups with semantic aids got more knowledge as compared to group with direct aids in the

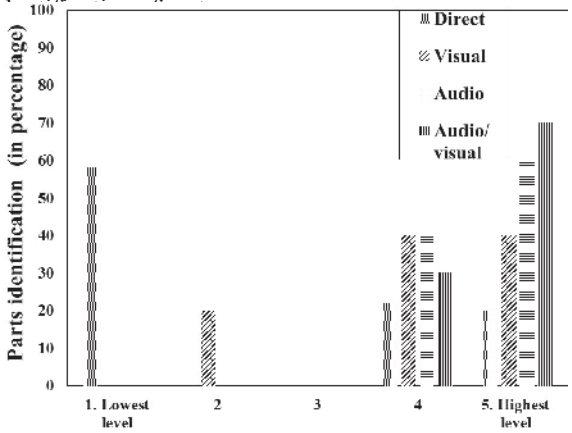

Fig. 10. Identification of transformer parts.

For the question concerned with learning the assembly steps, students of G1 responded with 40% for high level while 30% for nuetral Fig. 11. 50% students of G2 selected the highest and 40% high level learning option. Students of G3 voted 50% to highest and 30% to high level learning option while students of G4 selected 60% to highest level learning while 40% to high level option. The results showd that G1 which used direct aids got little learning as compared to other groups which have nearly the same results. The use of semantic aids in different groups got nearly the same results but combined audio/visual semantic aids used by G4 got comparabaly good results.

Question concerning to function of transformer parts, students of G1 voted 90% to lowest level as shown in figure 12, while G2 students voted 40% to high level and 20% to highest level option. Students of G3 selected 50% to both high and highest level of learning. Similarly students of G4 opted 50% to each of high and highest level option. From the above results we can conclude that students of G1 got lowest level of learning. In learning related to function of transformer parts, G4 is at the topmost position in learning while G3 is on the second position. So it can be concluded from the above results that the using both audio/visual semantic aids were better as compared to single visual, audio, or no semantic aids.

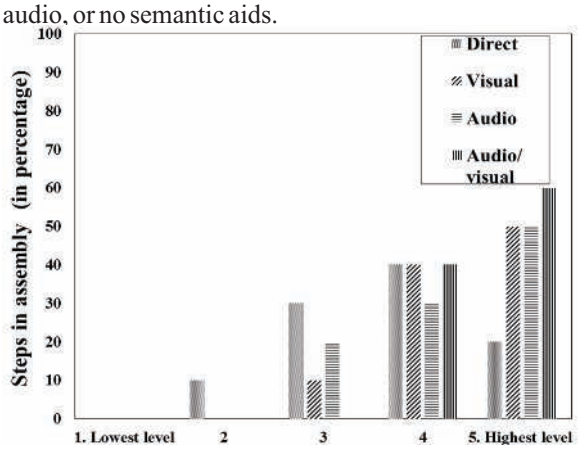

Fig. 11. Steps involved in assembly task

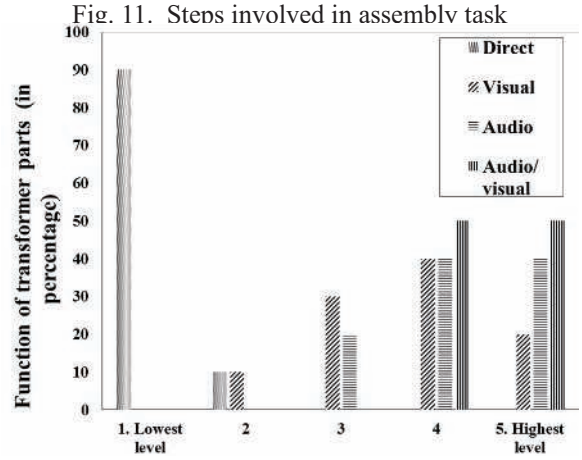

Fig. 12. Learning related to function of transformer parts.

Transfer of knowledge into real situation:

Finally we analysed transfer of knowledge in real world workshop in the final stage of our experimental study. For this purpose we brought all the groups to a physical workshop. The evaluation was done on the basis of the following perspectives:

- Identification of the real world transformer parts
- Function of transformer parts
- Order of steps in the assembly task
- Relationship of transformer parts in the assembly task

Each part of transformer in the GVRTS was designed in 3D Studio Max in order to get best quality and increase realism. Due to the high quality of models and resemblance with real word transformer, they were easily identified by the students. Students of G1 responded correctly to object identification as shown in Fig. 13. While students of G2, G3, and G4 with 81%, 83% and 90% correctly identified the transformer parts. The results shows that the use of semantic aids (combined audio/visual) in GVRTS highly improved students' learning related to parts identification. As there was no great difference among students trained with audio semantic aids and visual semantic aids. There is no source for knowledge improvement using direct aids, the 43% of correct responses came due to physical appearance of some transformer parts in real world such as transformer tank, nut bolts, and bushes etc.

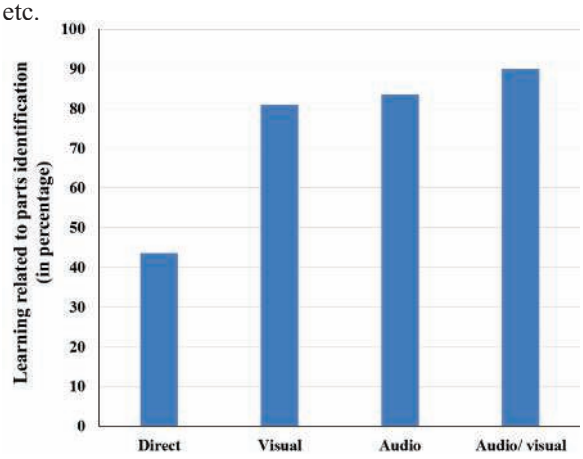

Fig. 13. Learnig associated with parts identification.

Learning associated with the steps involved in the assembly task, the response from studetns of G1 was 38.5%, whereas 78.5% of G2, 82.2% of G3, and 96.1% of G4 Fig. 14. So it means that there is a low level learnig of students who used the system with only direct aids as compared to those who used semantic plus direct aids. While the combined audio/visual semantic aids have better resluts as compared to only visual or audio semantic aids.

For the learning concerned with transformer parts' final position, the correct response of G1, G2, G3 and G4 was 46.7%, 83.5%, 82.3%, and 89.6% respectively Fig. 15. The above results revealed that the use of combined (audio/visual) semantic aids outperformed as compared to others.

VI. Conclusion And Future Work

In this paper we proposed semantic aids with direct

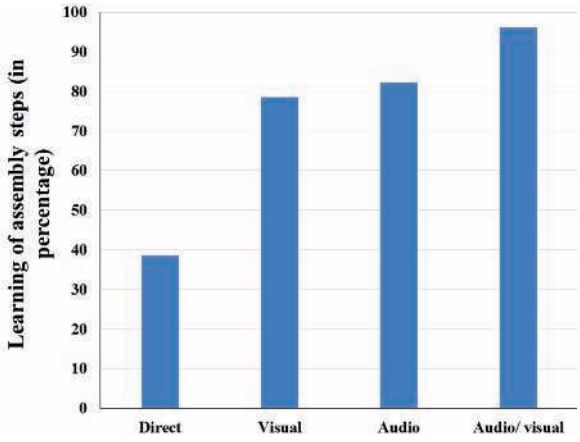

Fig. 14. Learning related to steps in assembly task.

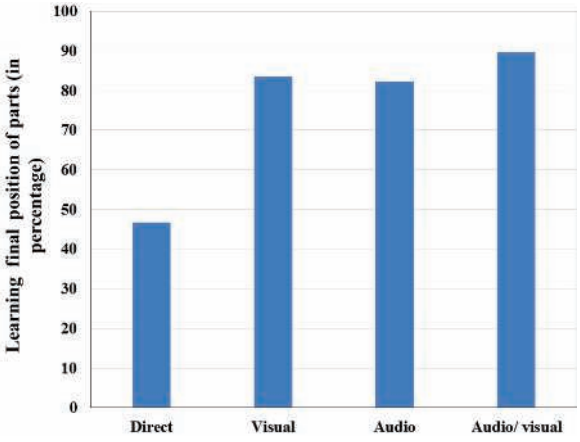

Fig. 15. Learning associated with transformer parts final position.

aids in order to get the benefits (high performance) of direct aids while to decrease its low learning effects. For the experimental study we used Guided Virtual Reality Training System (GVRTS), a desktop based VE. Fiducial markers were used for interaction with the system. A comparison based on task performance, resulted in less performance drop in case of the use of semantic (audio, visual, and combined) with direct aids as compared to simple direct aids. Experimental results also revealed that semantic aids considerably improved learning and knowledge transfer to the real world.

REFERENCES

[i] J. Rodríguez, E. J. Sánchez, I. Aguinaga, S. Casado, and T. Gutiérrez. (2012). Training of Procedural Tasks Through the Use of Virtual Reality and Direct Aids: INTECH Open Access Publisher.

[ii] N. Yuviler-Gavish, E. Yechiam, and A. Kallai. (2011). Learning in multimodal training: Visual guidance can be both appealing and disadvantageous in spatial tasks. International journal of human-computer studies. 69(3), pp. 113-122.

[iii] R. E. Mayer. (2002). Multimedia learning. Psychology of Learning and Motivation. 41, pp. 85-139.

[iv] R. E. Mayer. (1989). Systematic thinking fostered by illustrations in scientific text. Journal of Educational Psychology, 81(2), pp. 240.

[v] R. E. Mayer and R. B. Anderson (1991). Animations need narrations: An experimental test of a dual-coding hypothesis. Journal of educational psychology. 83(4), pp. 484.

[vi] R. E. Mayer and R. B. Anderson (1992). The instructive animation: Helping students build connections between words and pictures in multimedia learning. Journal of educational Psychology. 84(4), pp. 444.

[vii] J. Sweller, J. J. Van Merrienboer, and F. G. Paas (1998). Cognitive architecture and instructional design. Educational psychology review. 10(3), pp. 251-296.

[viii] J. J. Van Merrienboer and J. Sweller (2005). Cognitive load theory and complex learning: Recent developments and future directions. Educational psychology review. 17(2), pp. 147-177.

[ix] R. E. Mayer and R. Moreno. (2002). Aids to computer-based multimedia learning. Learning and instruction. 12(1), pp. 107-119.

[x] T. T. H. Nguyen, T. Duval, and C. Fleury, "Guiding techniques for collaborative exploration in multi-scale shared virtual environments," in Proc. of GRAPP ICCGTA, pp. 327-336, 2013.

[xi] C. J. Chen, W. Ismail, and W. M. Fauzy. (2008). Guiding exploration through three-dimensional virtual environments: A cognitive load reduction approach. Journal of Interactive Learning Research. 19(4), pp. 579-596.

[xii] Hawkins, D. G. (1995). Virtual reality and passive simulators: The future of fun.Communication in the age of virtual reality, 159-189.

[xiii] C. Youngblut. (1998). Educational uses of virtual reality technology. in IDA Document D-2128, i. o. d. analysis, Ed., ed Alexandria, VA.

[xiv] F. M. Ng, J. M. Ritchie, J. E. L. Simmons, and R. G. Dewar. (2000). Designing cable harness assemblies in virtual environments. Journal of Materials Processing Technology. 107(1), pp. 37–43.

[xv] A. N. Angelov and Z. A. Styczynski, "Computer-aided 3D Virtual Training in Power System Education," in Power Engineering Society General Meeting, 2007., Tampa, FL, June 2007, pp. 1 - 4.

[xvi] Y. Wang, S. Cui, Y. Yang, and J.-a. Lian. (2009).

virtual reality mathematic learning module for engineering students. Technology Interface Journal, 10(1), pp. 1-10

[xvii] A. Pasqualotti and C. M. d. S. Freitas. (2002). MAT3D: a virtual reality modeling language environment for the teaching and learning of mathematics.CyberPsychology & Behavior, 5(5), 409-422.

[xviii] H. Kaufmann and B. Meyer, "Simulating educational physical experiments in augmented reality," in SIGGRAPH Asia '08 ACM SIGGRAPH ASIA 2008 educators programme, ACM New York, NY, USA ©2008., 2008.

[xix] C. Dede, M. C. Salzman, R. B. Loftin, and D. Sprague, "Multisensory Immersion as a Modeling Environment for Learning Complex Scientific Concepts," in Modeling and Simulation in Science and Mathematics Education Modeling Dynamic Systems, W. Feurzeig and N. Roberts, Eds., Springer New York, 1999, pp. 282-319.

[xx] M. E. Loftin R. Bowen, Robin Benedetti, "Applying virtual reality in education: A prototypical virtual physics laboratory," in Proceedings, IEEE-RFVR, IEEE Computer Society Press, San Jose, CA, USA, 1993, pp. 67 - 74.

[xxi] J. K. CROSIER, S. V. G. COBB, and J. R. WILSON. (2000). Experimental comparison of virtual reality with traditional teaching methods for teaching radioactivity. Education and Information Technologies. 5(4), pp. 329–343.

[xxii] Y. X. Yao, P. J. Xia, J. S. Liu, and J. G. Li. (2006). A pragmatic system to support interactive assembly planning and training in an immersive virtual environment (I-VAPTS). International Journal of Advance Manufacturing Technologies. 30(9-10), pp. 959 – 967.

[xxiii] C. J. R. Dunne and C. L. McDonald. (2010, July Supplement) "Pulse!!: A Model for Research and Development of Virtual-Reality Learning in Military Medical Education and Training " MILITARY MEDICINE, 175(7S), pp. 025-027.

[xxiv] K. C. Shim, J. S. Park, H. S. Kim, J. H. Kim, Y. C. Park, and H. I. Ryu. (2003). Application of virtual reality technology in biology education. Journal of Biological Education. 37(2), pp. 71-74.

[xxv] T. A. Mikropoulos, A. Katsikis, E. Nikolou, and P. Tsakalis. (2003). Virtual environments in biology teaching. Journal of Biological Education. 37(4), pp. 176-181.

[xxvi] M. Yuan, S. Ong, and A. Y. Nee. (2005). Assembly Guidance in Augmented Reality (AR) Environments Using a Virtual Interactive Tool, International Journal of Production Research. 46(7), pp. 1745-1767.

[xvii] Kuang, A. B., Payandeh, S., Zheng, B., Henigman, F., & MacKenzie, C. L. (2004, March). Assembling virtual fixtures for guidance in training environments. In Haptic Interfaces for Virtual Environment and Teleoperator Systems, 2004. HAPTICS'04. IEEE Proceedings. 12th International Symposium on. pp. 367-374.

[xxviii] P. Marayong, A. Bettini, and A. Okamura. (2002). Effect of virtual fixture compliance on human-machine cooperative manipulation. In Intelligent Robots and Systems, 2002. IEEE/RSJ International Conference on. 2, pp. 1089-1095. IEEE.

[xxix] L. B. Rosenberg. Virtual fixtures: Perceptual tools for telerobotic manipulation," in Virtual Reality Annual International Symposium, 1993, 1993 IEEE, 1993, pp. 76-82.

[xxx] A. Bettini, S. Lang, A. Okamura, and G. Hager. (2004). Vision assisted control for manipulation using virtual fixtures: Experiments at macro and micro scales, in Robotics and Automation, 2002. Proceedings. ICRA'02. IEEE International Conference on, 2002, pp. 3354-3361.

[xxxi] S. Payandeh and Z. Stanisic, "On application of virtual fixtures as an aid for telemanipulation and training," in Haptic Interfaces for Virtual Environment and Teleoperator Systems, 2002. HAPTICS 2002. Proceedings. 10th Symposium on, 2002, pp. 18-23.

[xxxii] S. Park, R. D. Howe, and D. F. Torchiana, "Virtual fixtures for robotic cardiac surgery," in Medical Image Computing and Computer-Assisted Intervention–MICCAI 2001, 2001, pp. 1419-1420.

[xxxiii] M. A. Peshkin, J. E. Colgate, W. Wannasuphoprasit, C. A. Moore, R. B. Gillespie, and P. Akella. (2001). Cobot architecture. Robotics and Automation, IEEE Transactions on. 17(4), pp. 377-390.

[xxxiv] S. Ullah, P. Richard, S. Otmane, M. Naud, and M. Mallem, "Haptic guides in cooperative virtual environments: Design and human performance evaluation," in Haptics Symposium, 2010 IEEE, 2010, pp. 457-462.

[xxxv] J. Rodríguez, T. Gutiérrez, E. J. Sánchez, S. Casado, and I. Aguinaga, "Training of Procedural Tasks Through the Use of Virtual Reality and Direct Aids." Training of procedural tasks through the use of virtual reality and direct aids. INTECH Open Access Publisher, 2012.

[xxxvi] N. Gavish, T. Gutierrez, S. Webel, J. Rodriguez, and F. Tecchia, "Design guidelines for the development of virtual reality and augmented reality training systems for maintenance and assembly tasks," in BIO Web

of Conferences, 2011, 1, pp. 00029.
[xxxvii] U. Neisser, Cognition and reality: Principles and implications of cognitive psychology: WH Freeman/Times Books/Henry Holt & Co, 1976.
[xxxviii] W.-T. Fu and W. D. Gray. (2006). Suboptimal tradeoffs in information seeking. Cognitive Psychology. 52(3), pp. 195-242.
[xxxix] E. Yechiam, I. Erev, and A. Parush. (2004). Easy first steps and their implication to the use of a mouse-based and a script-based strategy. Journal of Experimental Psychology: Applied. 10(2), pp 89.
[xl] H. Kato. (Nov: 2011, 2/4/15). How does ARToolKit work? , ARToolKit Documentation. Available:
http://www.hitl.washington.edu/artoolkit/documentation/userarwork.html

Optimal Techniques of Localization in Wireless Sensor Networks

[1]Y. Salam, [2]Y. Saleem, [3]M. Farooq, [4]M. Rizwan

[1, 2, 3] Department of Computer Science and Engineering, University of Engineering and Technology, Lahore
[4] Department of Mechatronics and Control Engineering, University of Engineering and Technology, Lahore

[1]yasirsalam08@hotmail.com, [2]ysaleem@gmail.com, [1]yasirsalam08@hotmail.com, [3]mfarooq152@hotmail.com, [4]mohsin_riz@yahoo.com

Abstract-Localization in wireless sensor networks is an open challenge. The work is based on the localization of mobile nodes in wireless sensor networks (WSN) by using the Received Signal Strength Indicator (RSSI) method. A trilateral localization algorithm based on RSSI has been proposed to localize the mobile sensor nodes. It is advantageous to apply RSSI based algorithm as it has solved the problems of cost, power utilization and reliability in wireless sensor networks. Furthermore, RSSI based algorithm has been compared with the existing techniques. Results shown in the paper are the evident of the situations where RSSI is considered best techniques of localization.

Keywords-WSN, RSSI, Localization, Attenuation, Beacon node.

I. INTRODUCTION

In the modern era everything is the part of wireless networks because of the universal truth that every activity of human being affects the system due to time varying nature of the channel. This effect can be analyzed in term of multi path fading, noise and Doppler Effect. Now a days there are small computing devices which have memory, processor, transceiver and battery(most important), these devices are called node [i]. Wireless sensor network will be the part of everyone's life in future because it is emerging and newly born field. A lot of work has also been done to enlarge the computing capability and sensing range of the nodes and a development for miniaturization and optimization of the hardware. At this point, there is need to learn about localization of wireless sensor nodes in a wireless sensor network, because if you want to communicate with something it is necessary to having information about its location. And in wireless sensor networks concept of getting the information about the location is called as localization[ii] . In a more sophisticated way localization can be define as, "To determine the physical coordinates of a group of sensor nodes in a wireless sensor network (WSN) is called localization" [i].Localization can be classified into two different classes;

- Distributed and Centralized
- Range-based and Range-free

In centralized approach all the calculations related to the localization are worked out at the base station[iii-iv]. There is information sharing process among the wireless sensor nodes and base station, and the information at the base station is used to calculate the coordinates of the nodes. Whereas in distributed approach all the calculations are made on the node so base station is not required . Complex mathematical algorithms in centralized approach lead to use a powerful centralized node. Main difference between centralized and distributed approach is processing. In centralized approach migration of inter-node ranging and connectivity of the data is required, which is transferred to a powerful central node. After processing the data, information about the localization is migrated to the concerning node. In range based localization algorithms are required to determine the distance among the wireless sensor nodes [iii].

Range based localization scheme requires extra hardware so it is costly as compare to range free localization scheme. Applications like missile tracking need high level accuracy. So, there is a need to implement this localization scheme because it gives us more accurate results as compare to range free localization. Some important terms related to range based localization has been defined [i- ii, v- vi]. In range based localization, received signal strength indicator (RSSI) is the most important factor that shows the relation between the distance and level of received power. Power of the transmitted signal decreases as it travels away from the base stations, called attenuation. TOA is the travel time of a radio signal from a solitary transmitter to a distant single receiver [i].

The relation between speed of light in vacuum and the carrier frequency of a signal is used to measure the time for the calculation of distance between transmitter and receiver. Time difference of arrival (TODA) uses the concept of synchronization therefore, an extra time is required. Ultrasound, Light rays, RF signal and microwaves are used in TODA approach. Accuracy of TODA depends upon the line of sight (LoS).

TODA is hardware based algorithm and mostly implemented by using the sensor which have integrated

speaker and microphone. Chirp signal concept is used here for time difference. Angle of Arrival (AoA) also used for the purpose of localization but in this approach an array microphone or radio is used but it can be implemented by using the optical communication approach [iv] .

In contrast to range based localization range technique of localization is easier. In range free localization technique there is no need of time of arrival, time difference of arrival and angel of arrival [i-ii]. The cost of implementing this technique is lower but there is a compromise over accuracy. Range free localization technique can further be classified into two categories.

A. Local Technique

Local technique works on the concept of beacon nodes. In this technique area is divided into triangular shapes and beacon nodes (whose positions are known) are placed at the edges of the triangles. When a mobile node enters in the sensing range of the beacon nodes it transmits some messages. Beacon nodes receive the messages and extract the position. Accuracy of the technique can be increased by increasing the node density.

B. Hope Counting Technique

In hop counting technique those nodes whose localization is being performed gets the value of hop size from the neighbor beacon node and try to get least hop counts by using the diverse protocols. In this way every node gets its hop count and by using this information an estimated distance is calculated from its neighbor [ii]. Node density also affects the localization results, as hop counting based localization scheme results are very accurate if there is high density of nodes is used. Thus node density is very important factor of designing an algorithm because it may charge high price to implement an algorithm with high density of nodes. From the above discussion, we can conclude that following should be considered in case of wireless sensor node,

1. For a node it is essential to avoid the complex and time consuming computations because it would reduce the energy supply rapidly.
2. The computations should consider the error (appeared in the measurements), which can be large [vii].

Section 2 describes the work related to the articles that is previously done. Section 3 provides a solution to the aforementioned problems. Section 4 gives the model of RSSI based algorithm. Section 5 includes the implementation of the system and section 6 concludes the whole work done for the wireless sensor networks.

II. Motivation And Related Work

Previous discussion shows the work that has been done. But, still there is a potential to find out more and more new techniques to localize the wireless sensor nodes. To solve the problem of localization in outdoor environment Global Positioning System (GPS) is mostly used. GPS module is used in vehicles to track the position of the vehicle. GPS is also used in wireless sensors network for localization currently, but economically it will not be a good way to use GPS module at each sensor node [viii].

Therefore, there are a lot of schemes has developed to solve the problem of localization which are very efficient and cost effective especially for the case of WSN. As we know that WSN is formed by the deployment of large number of nodes. These nodes are so small that they have a limited memory, processing and most important one limited resources of energy [i] , [iv-v]. There are different techniques such as triangular [iii], or statistical inference [v] used to calculate the coordinates of mobile node w.r.t beacons nodes.

Due to the unpredictable nature of radio propagation behavior the RSSI based localization scheme severely suffers with error . If ultrasound is used for the purpose of localization values need to be calculated ToA and TDoA and these values can further be used for the purpose of localization. For indoor localization we can use RFID tag, ultrasonic, infrared, WLAN and Bluetooth technologies. Multipath, reflections, interference and dead spots effects the localization in indoor cases [i].

To improve the localization results in indoor cases RSSI and Link Quality Indicator can be used. LQI and RSSI are used to see the effects of environment on the received signal strength. So LQI and RSSI are helpful to handle the noise effect on the received signal. In all approaches there are a lot of computations involved, such as minimum mean square error method, system of complex equation and Kalman filter.

RSSI is the most realistic model for sensor network communication. But due to the environmental effects it is unrealistic to calculate the correct result by taking on one reading from the beacon node in RSSI mode. Location prediction mechanism is an extension of multicast and multipath routing [xii].

Therefore node location is estimated by taking small number of reading [vii]. There is another approach exist which is FM Radio base localization scheme. In FM based localization the strength of the signal from the set of FM broadcasting station outdoor environment is measured [x]. If FM Radio signals and GSM signals spectrum is analyzed it is reported that both the techniques achieve the similar accuracy level. In the next session we discussed some well-known localization schemes. IR light can also be used for the purpose of localization. In this technology images are taken by the camera and after a lot of image processing on these images localization is achieved. Furthermore, power tuning anchors algorithm includes the localization of mobile nodes on the basis of minimum

power received from the neighbors [xi].

Ultrasound waves have also used for the purpose of localization [i, iv]. Ultrasonic sensors for a specific environment have a specific field pattern. If there is any obstacle then it will change the pattern and from this pattern changes information about the location of the object can be extracted. Cricket, Bats and Dolphin utilize ultrasonic wave to localize their prey.

III. Localization Techniques

Localization can be performed by using the different type of sensor nodes. A change in the sensor type technology also changes the localization. Sensors are selected according to the applications and environment. There are some constraints in every localization technology as well as merits and demerits. These technologies are shown below in Fig.1.

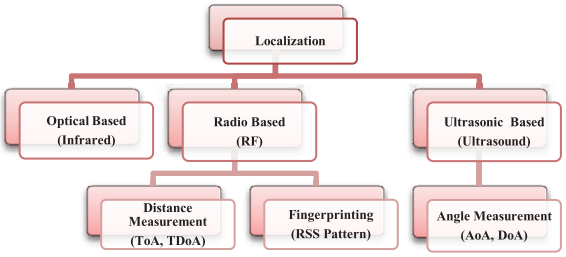

Fig. 1: Different Localization Schemes

A. Optical Based Localization

Optical based localization is also possible. In this technology light signal is used for localization purpose. Infrared light which is special type of light is used for this purpose. IR light is also used for the purpose of tracking in many applications. Sun is also an infrared light source which radiates the infrared light within similar frequency band. Therefore this localization technology can be implemented in that case if there is no sun light. In this technique a lot of image processing is required. Images are taken by special type of cameras.

B. Ultrasonic Based Localization

As everyone knows that ultrasonic wave is similar to sound wave but frequency is higher than 20 kHz. Ultrasonic sensors are used in this approach. Ultrasonic sensors are placed in such a way that they send a field pattern and then receive back these waves and the change of field pattern is used to extract the information about the object which we want to localize. Angle of Arrival (AoA) and Difference of Arrival (DoA) of these waves are used to get the coordinates of the localization.

C. Global Positioning System (GPS)

Global Position System is also used for localization purpose. There are 27 different satellites which are revolving around the earth which are used for localization. Global position system also uses radio frequency for this purposed of communication between the transmitter and receiver. GPS technology of localization is costly as compared to other localization technologies. GPS technology is mostly used for the purpose of vehicle security. GPS performance is environment dependent i.e. the localization results for outdoor and indoor are very different. When GPS is used for indoor localization error in the results is increased.

D. Radio Based Localization

In Radio based localization scheme Radio Frequencies are used between the receiver and transmitter for the purpose of communication. As we know that the received power strength decreases with the distance as shown in Fig. 3. And we also have seen a relationship between the received signal power and RSSI value which shows that RSSI value is large when power received is large and its value decreases with the decrease in received power value. In RSSI based localization technology no extra hardware is required which is the main advantage of this technology. RSSI value changes with time due to time varying nature of channel.

E. Received Signal Strength Indicator

In IEE 802.11 100mW of the power is transmitted by a base station, but in IEEE 802.15.4 52mW to 29mW power is transmitted per station. There are many IEEE 802.15.4 radios used so in such networks RSSI localization is used. This approach of localization is not good for those applications where high level of accuracy is required. Equation 1 shows a relationship between the distance and RSSI value . A graph is also shown in fig. 1 which shows the same relationship.

$$RSSI = -(10 * n * log_{10}(d_{bs}) + A_o) \quad (1)$$

Where,

n = Propagation constant and its value can vary with the environment.

d_{bs} = It is the distance from base station.

A_o = Reference value of received signal strength at one meter of distance.

In below graph value of n is considered 2 and A_0 value is- 3dbm.

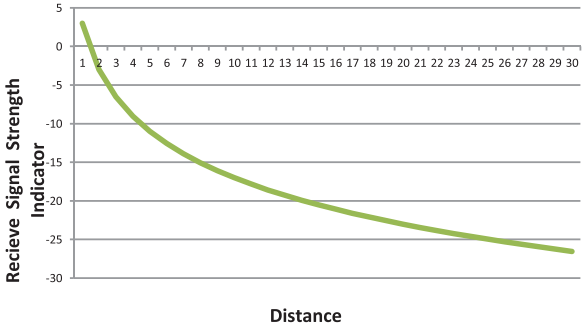

Fig.2: RSSI VS Distance

It is the basic law of propagation that the power

received Pr at a distance d is inversely proportional to the square of distance and directly proportional to the transmitted power Pt. This basic law is represented by a relationship of Pr, Pt and d which is known as Friis equation;

$$Pr = \frac{Pt\ Gt\ Gr}{1}\left(\frac{\lambda}{4\pi d}\right)^2 \quad (2)$$

Where

P_r = Received at distance d.
P_t = Power Transmitted.
G_t = Gain of Transmitting Antenna.
G_r = Gain of Receiving Antenna.
λ = Transmitted Signal Wave Length.
d = Distance between the Transmitter and Receiver.

From the above relationship it can be concluded that, the larger the distance from the transmitter the smaller power will be received. This fact is shown in below Fig. 3.

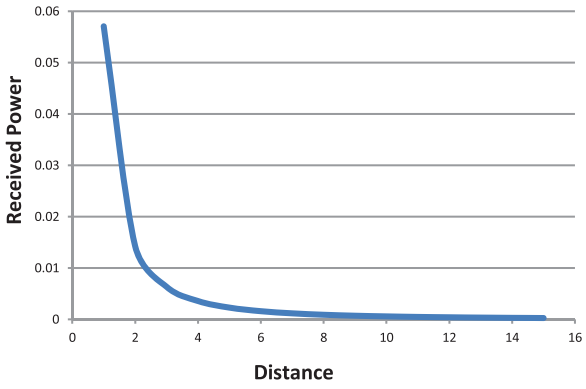

Fig. 3: Received power VS Distance

In the above graph value of Pr is calculated with the *Gt*=*Gr*=1, *Pt*=100mw and λ = 3.

IV. RSSI Based Model

Friis equation gives the relationship between the received power and the distance,

$$Pr(d) = \frac{Pt\ Gt\ Gr}{1}\left(\frac{\lambda}{4\pi d}\right)^2 \quad (3)$$

$$Pr(do) = \frac{Pt\ Gt\ Gr}{1}\left(\frac{\lambda}{4\pi do}\right)^2 \quad (4)$$

Dividing (3) by (4), we get

$$Pr(d) = Pr(do)\left(\frac{do}{d}\right)^n \qquad d > do > df \quad (5)$$

Where

$Pr(do)$ = Power received at distance do
do = reference distance
n = path loss exponent
df = Far field Region (Fraunhofer Distance)

But there are some limitations in the use of FRIIS equation that is only valid in far field region. So we can use the following equation which gives us power received at distanced in dBm instead of above equation[ix],

$$Pr(d)\ dBm = Po(do)\ dBm + n10\ log_{10}\left(\frac{do}{d}\right) \quad (6)$$

In free space the value of n path loss factor is 2, which means that the power received at distance d will decrease with the square of distance . Path loss factor n value can vary in between 2 to 6 with different environments. The value of path loss exponent changes with the environment as given below in Table I.

TABLE I
PATH LOSS EXPONENTS

Environment	Path Loss Exponent
In building line of sight	1.6-1.8
Free space	2.0
Obstructed in factories	2.0- 3.0
Inner-city area cellular radio	2.7-3.5
Shadowed urban cellular radio	3.0-5.0
Foiled in building	4.0-6.0

In wireless communication channel affects the signal power in two ways.

1. Time varying nature of the wireless channel causes fluctuations in received signal strength. These fluctuations can vary the mean value of RSSI from ±2 to ±5 dBm as shown in Fig. 4.

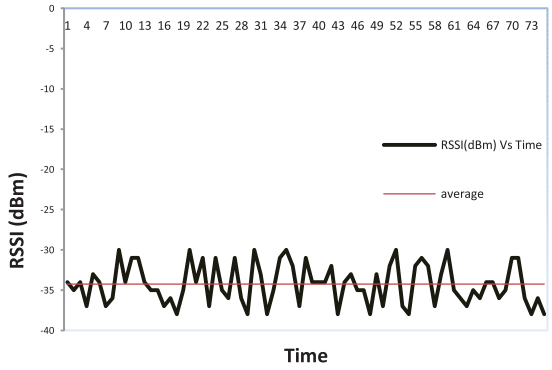

Fig. 4: RSSI VS Time

So it is necessary to minimize the effect of fluctuations in the RSSI value. To eliminate the fluctuations we take average. Hence an average 0f 20 to 30 values is taken to obtain the mean RSSI value. The mean value of RSSI is used to calculate the distance.

1. Waves traveling in the environment are diffracted, reflected and scattered that results in loss of power in radio channel. This effect can be overcome by measuring the exact value of path loss exponent n.

A. Path Loss Exponent

First step is to calculate the value of n which is used to

determine the RSSI value used for localization. For this purpose we have to measure Pr (d1) at distance d1 and Pr(d2) at d2. Both are average received powers. And value of n is calculated using the equation (7).

$$n = \frac{(Pr(d_1)\ dBm - Pr(d_2)\ dBm)}{10 * log_{10}\left(\frac{d_2}{d_1}\right)} \qquad (7)$$

From the value of n we can also calculate the distance by using the equation (8) given below.

$$Pr(d)\ dBm = Pr(do)\ dBm + n10\ log_{10}\left(\frac{do}{d}\right) + Xo$$

$$d = (do)(10^{\frac{(Pr(d) - Pr(do) - Xo)}{(10\,n)}}) \qquad (8)$$

On the basis of some important factors regarding the technologies, we can differentiate and compare them in a sophisticated way as shown in TABLE II.

TABLE II
COMPARISON of LOCALIZATION SCHEMES

Factor	Infrared	Ultrasound	GPS	RSSI
Applicable indoor	Yes	Yes	Not recommended	Yes
Need for extra Hardware	Yes	Yes	Yes	No
Cost of Extra hardware	Low	High	High	N.A
Size of extra hardware	Average	Large	Average	N.A
Average expected error	±5 meters	±10 meters	±10 meters	1-3meters

V. Implementation And Results

Triangular Localization Approach

In triangular approach the three nodes which are called as beacon nodes are placed at the three corners of the triangle whose coordinates are known and another node called anchor node is placed inside the triangle. The coordinates of the anchor node are unknown and can be calculated from special calculations. From these three nodes one node is attached with a computer and is known as base station. This triangular configuration is sh

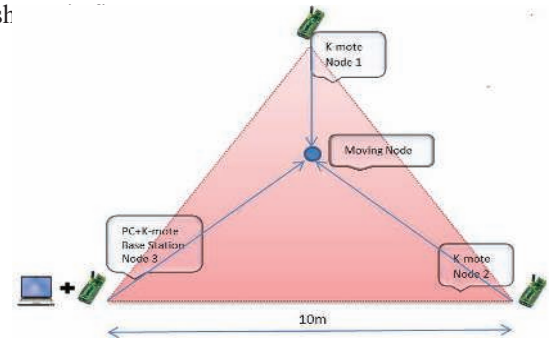

Fig. 5: Triangular Approaches

To find the location of an anchor node following steps will be adopted.

1. First, anchor node broadcast a message consisting on packets to all other beacon nodes.
2. RSSI value is calculated from the received packets at beacon nodes.
3. Calculated value of RSSI is sent to base station.
4. At the base station RSSI value is used to calculate the distance.
5. Anchor node coordinates can easily be found after calculating the three distances. Suppose l1, l2, and l3 are the three distances values from the beacon nodes 1, 2, 3 respectively. And (x1, y1), (x2, y2) and (x3, y3) are x, y coordinates for the node1, node2 and node3 respectively. Consider that x0 and y0 are the values of coordinates for the anchor node. So from all of the above information we can write three different equations by using the distance formula.

$$l_3^2 = (x_0 - x_3)^2 + (y_0 - y_3)^2 \qquad (9)$$
$$l_2^2 = (x_0 - x_2)^2 + (y_0 - y_2)^2 \qquad (10)$$
$$l_1^2 = (x_0 - x_1)^2 + (y_0 - y_1)^2 \qquad (11)$$

By expanding the above equations (9),(10) and (11)

$$l_3^2 = x_3^2 + y_3^2 + x_0^2 + y_0^2 - 2x_0x_3 - 2y_0y_3 \qquad (12)$$
$$l_2^2 = x_2^2 + y_2^2 + x_0^2 + y_0^2 - 2x_0x_2 - 2y_0y_2 \qquad (13)$$
$$l_1^2 = x_1^2 + y_1^2 + x_0^2 + y_0^2 - 2x_0x_1 - 2y_0y_1 \qquad (14)$$

After simplification we can write the above equations in matrix form as,

$$2\begin{pmatrix}(x_3 - x_1) & (y_3 - y_1)\\ (x_3 - x_2) & (y_3 - y_2)\end{pmatrix}\begin{pmatrix}x_0\\ y_0\end{pmatrix} = \begin{pmatrix}d_2^2 - x_2^2 - y_2^2 + x_3^2 + y_3^2 - d_3^2\\ d_1^2 - x_1^2 - y_1^2 + x_3^2 + y_3^2 - d_3^2\end{pmatrix}$$

(15)

Where we can assume

$$X = 2\begin{pmatrix}(x_3 - x_1) & (y_3 - y_1)\\ (x_3 - x_2) & (y_3 - y_2)\end{pmatrix}$$
$$b = \begin{pmatrix}x_0\\ y_0\end{pmatrix}$$
$$Y = \begin{pmatrix}d_2^2 - x_2^2 - y_2^2 + x_3^2 + y_3^2 - d_3^2\\ d_1^2 - x_1^2 - y_1^2 + x_3^2 + y_3^2 - d_3^2\end{pmatrix}$$

So the equation 15 becomes

$$X\,b = Y$$
$$b = X^{-1}Y$$

Where X^{-1} is the inverse of matrix X and after putting the values of (x_1, y_1), (x_2, y_2) and (x_3, y_3) we get the coordinates of anchor nodes this can be seen in below fig. 6.

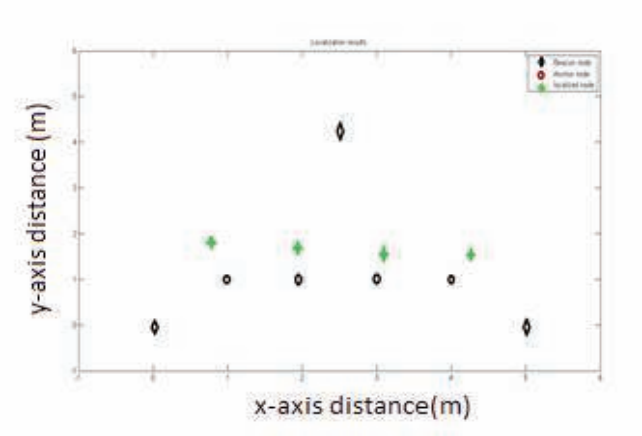

Fig. 6 Triangular Approaches

In the above diagram it can be shown that an error of 1m to 3m is possible which is smaller than other localization schemes.

VI. Conclusion

A trilateral RSSI based localization algorithm has been proposed. Analytical model of RSSI is explained and results have shown that proposed technique is more feasible and gives accurate results. RSSI based localization scheme is applicable for both static and dynamic anchor node localization. Furthermore, comparison of RSSI based method with other techniques has shown that it is superior in terms of environment, extra hardware, cost of implementation and accuracy. Satisfactory results of this technique are the evident of the situations in which RSSI performs much better that the other techniques.

References

[i] C. H. Tian He, B. M. Blum, J. A. Stankovic, T. Abdelzaher, "Range-Free Localization Schemes for Large Scale Sensor Networks1," ed, 2003.

[ii] Boudhir, A. Anouar, M. Bouhorma, and M. B. Ahmed "New Technique of Wireless Sensor Networks Localization based on Energy Consumption," International Journal of Computer Applications vol. 9, p. 4, November November 2010.

[iii] L. Lazos, R. POOVENDRAN, "SeRLoc: Robust Localization for Wireless Sensor Networks," ACM Transactions on Sensor Networks, vol. Vol. 1, p. 28, august 2005.

[iv] J. C. Taylor, "Localization in Sensor Networks," Master, Computer Science and Artificial Intelligence Laboratory Massachusetts Institute of Technology Cambridge, MA 02139.

[v] K. Yedavalli, B. Krishnamachari, "Sequence-Based Localization in Wireless Sensor Networks," presented at the IEEE TRANSACTIONS ON MOBILE COMPUTING, 2008.

[vi] M. Rudafshani, S. Datta, "Localization in Wireless Sensor Networks," p. 10.

[vii] C. Papamanthou, F.P. Preparata, R. Tamassia, "Algorithms for Location Estimation Based on RSSI Sampling," Springer-Verlag Berlin Heidelberg, p. 15, 2008.

[viii] N. Bulusu, J Heidemann, and D. Estrin,. "GPS-less low-cost outdoor localization for very small devices," Personal Communications, IEEE vol. 5, p. 7, oct 2000.

[ix] J. A. Palazon, J. Gozalvez, M. Sepulcre, G. Prieto, "Experimental RSSI-based Localization System using Wireless Sensor Networks," presented at the 17th IEEE International Conference on Emerging Technologies and Factory Automation.

[x] C. Yin, D. Lymberopoulos, J. Liuz, B. Priyantha, "FM-based Indoor Localization," 2012 ACM, vol. MobiSys'12,, p. 13, 2012.

[xi] S. Jabbar, M. Z. Aziz, A. A. Minhas, D. Hussain, "PTAL: Power Tuning Anchors Localizatio Algorithm for Wireless Ad-hoc Micro Sensor Network." (IEEE) ICESS' 2010, 29th June-2nd July 2010, Bradford, UK

[xii] Abdullah, S. Jabbar, S. Alam, A. A. Minhas, D. Hussain, "Location Predection for Improvement of Communication Protocols in Wireless Communications:Considerations and Future Directions'' International Conference on Communications Systems and Technologies 2011 (ICCST'11), Held on19th -21stOctober, 2011 in San Fransisco, USA.

Technical Journal
Website: www.uettaxila.edu.pk.
University of Engineering and Technology, Taxila-Pakistan

Researchers and Academia are invited to submit the research articles to Technical Journal of UET Taxila. It is a peer reviewed, broad-based open access journal. It covers all areas of engineering sciences and engineering management.

Technical Journal is a quarterly publication of UET Taxila recognized by HEC in "Y" category. It is published regularly with a key objective to provide the visionary wisdom to academia and researchers to disseminate novel knowledge and technology for the benefit of society. Technical Journal is indexed by well recognized international database such as PASTIC Science Abstracts, AGRIS Data Base, ProQuest Products, EBSCO Data Bases, Library of Congress and various other nineteen (19) HEC approved abstracting and indexing agencies.

For enquiries, submissions of articles or any other information please visit our website http://web.uettaxila.edu.pk/techjournal/index.html or contact the Editorial Office on the following number: +92-51-9047896
e-mail: technical.journal@uettaxila.edu.pk

Submission of paper remains open round the year. Researchers and Academia can submit their papers at any time which they deem fit. Presently there are no charges for publication of research paper in Technical Journal.

It will be highly appreciated if the information is forwarded to interested colleagues from Pakistan as well as abroad.

Looking forward to receiving the research papers on behalf of Technical Journal Editorial Office.

Dr. Hafiz Adnan Habib
Chief Editor
Technical Journal,
UET, Taxila

Instruction for authors for publishing in Technical Journal UET Taxila

General

Papers may be submitted any time throughout the year. After receipt of paper it will be sent to concerned referees, at least one from a technology advanced countries. Papers reviewed and declared fit for publication will be published in the coming issue. The journal is quarterly publication, having four issues annually. A soft copy of paper must be submitted through online submission system by using the following link:-

http://tj.uettaxila.edu.pk/index.php/technical-journal/about/submissions

Authors are required to read the following carefully for writing a paper.

Manuscript Preparation

Text should be type-written with M.S word, Times New Roman Font size 10, at single space and with margins as 1 inch top,1 inch left, 0.5 inch right, and 1 inch bottom, on an A-4 size paper. The manuscript should be compiled in following order:-

Title Page

The Title page should contain:

- Paper title
- Author names and affiliations
- Postal and email addresses
- Telephone/Cell and fax numbers
- One author should be identified as the Corresponding Author

Abstract

An abstract up to maximum of 200 words should be written in the start of paper. The abstract should give a clear indication of the objectives, scope, methods, results and conclusions.

Keywords

Include at least five keywords (Title Case) in a separate line at the end of the abstract.

Body of the Paper

Body of the paper may include introduction and literature review, materials and methods, modeling/experimentation, results-discussions and conclusions etc.

- Define abbreviations and acronyms the first time they are used in the text, even after they have already been defined in the abstract. Do not use abbreviations in the title unless they are Unavoidable.
- Use zero before decimal places: "0.24" not ".24".
- Avoid contractions; for example, write "do not" instead of "don't."
- If you are using *Word,* use either the Microsoft Equation Editor or the *MathType* add-on (http://www.mathtype.com) for equations in your paper (Insert | Object | Create New | Microsoft Equation *or* Math Type Equation). Number equations consecutively with equation numbers in parentheses flush with the right margin, as in (1). Refer to "(1)," not "Eq. (1)" or "equation (1)," except at the beginning of a sentence: "Equation (1) is ... ."
- Symbols used in the equations must be defined before or immediately after it appears.
- Use SI units only.

Originality

Only original contributions to Engineering, Science and Management literature should be submitted for publication. It should incorporate substantial information not previously published.

Length

Research paper should be consisting of 5-8 pages as per specifications given above.

Accuracy

All the technical, scientific and mathematical information contained in the paper should be checked with great care.

Figures

All figures should be at least 300 dpi in JPG format. It is to be also ensured that lines are thick enough to be reproduced conveniently after size reduction at the stage of composing. All figures (graphs, line drawings, photographs, etc.) should be numbered consecutively and have a caption consisting of the figure number and a brief title or description of the figure. This number should be used when referring to the figure in the text. Figure may be referenced within the text as "Fig. 1" etc.

Tables

Tables should be typed in a separate file using M.S. Word 'table' option. All tables should be numbered in Roman numerals consecutively. Tables should have a caption in Upper Case, must be centered and in 8 pt. consisting of the table number and brief title. This number should be used when referring to the table in text. Table should be inserted as part of the text as close as possible to its first reference.

When referencing your figures and tables within your paper, use the abbreviation "Fig." Even at the beginning of a sentence. Do not abbreviate "Table." Tables should be numbered with Roman Numerals.

Acknowledgments
All individuals or institutions not mentioned elsewhere in the work who have made an important contribution should be acknowledged.

References
Reference may be cited with number in square brackets, e.g. "the scheme is discussed in [iii]". Multiple references are each numbered with in bracket. e.g. the scheme is discussed in [iv-vii]. Do not use "Ref." or "reference" except at the beginning of a sentence: "Reference [xi] illustrates... ."

Please do not use automatic endnotes in Word, rather, type the reference list at the end of the paper using the "References" style. Reference list/bibliography and in text references, both will be cited in roman alphabet. "Within text citations must be in chronological order in the first appearance. The subsequent appearance(s) of the same may be random as per need of the paper."

Note: For template of paper please visit our journal's page:
http://web.uettaxila.edu.pk/techjournal/index.html

Check List

<table>
<tr><th>Sr. No.</th><th>Description</th><th>Yes/No</th></tr>
<tr><td>1</td><td>Undertaking signed by all authors that the research paper has not been submitted to any other journal for publishing and submitted research work is their own original contribution is required as per following format.
<table>
<tr><td colspan="4">Paper Titled:</td></tr>
<tr><td colspan="4">Authorship and Contribution Declaration</td></tr>
<tr><td>Sr.#</td><td>Author-s Full Name</td><td>Contribution to Paper</td><td>Author-s Signature</td></tr>
<tr><td>1</td><td>Mr./Dr./Prof. Alpha (Main/principal Author)</td><td>Proposed topic, basic study Design, methodology and manuscript writing</td><td></td></tr>
<tr><td>2</td><td>Mr./Dr./Prof. Bravo(2nd Author)</td><td>Data Collection, statistical analysis and interpretation of results etc.</td><td></td></tr>
<tr><td>3</td><td>Mr./Dr./Prof. Charlie (3rd Author)</td><td>Literature review & Referencing, and quality insurer</td><td></td></tr>
<tr><td>⋮</td><td>⋮</td><td>⋮</td><td></td></tr>
</table></td><td></td></tr>
<tr><td>2</td><td>Pictures are placed on paper at proper places and separate pictures in JPEG format are provided in a separate file with their caption as well.</td><td></td></tr>
<tr><td>3</td><td>Technical Journal UET Taxila follow IEEE format. Please submit your paper according to required format i.e. double column, tables and figures captions & numbers, indentation and particularly in-text citation and bibliography according to IEEE format.</td><td></td></tr>
<tr><td>4</td><td>"Time New Roman" font shall be used in legends, captions of Figures, Graphs and Tables etc.</td><td></td></tr>
<tr><td>5</td><td>Complete contact information of the corresponding author:-.
Name:_____, Designation:_____
Institute Name:_____, Email:_____
Cell:_____, Ph No. and Fax (if any)_____</td><td></td></tr>
<tr><td>6</td><td>Main area of Research paper e.g. Electrical, Mechanical etc. shall be mentioned</td><td></td></tr>
<tr><td colspan="3">Note: Ensure that all requirements have been met before submitting the paper
http://tj.uettaxila.edu.pk/index.php/technical-journal/about/submissions For any query please visit:
http://web.uettaxila.edu.pk/techJournal/index.html</td></tr>
</table>

EDITORIAL OFFICE: Correspondences should be made on the following address:
Asif Ali Editor, Technical Journal Editorial Office
Central Library, University of Engineering and Technology (UET) Taxila, Pakistan
Tel**:** +92 (51) 9047896 Email**:**technical.journal@uettaxila.edu.pk